

ORGANIC REACTIONS IN THE GAS PHASE

Part I: The Thermal Rearrangement of 3,3-Dimethylcyclopropene

Part II: Interaction of Remote Functional Groups in the Ion Chemistry  
of Bifunctional Ethers

Thesis by

Thomas Hellman Morton

In Partial Fulfillment of the Requirements

For the Degree of

Doctor of Philosophy

California Institute of Technology

Pasadena, California

1973

(Submitted 29 August 1972)

Copyright © by  
THOMAS HELLMAN MORTON  
1972

## ABSTRACT

**PART I: The Thermal Rearrangement of 3,3-Dimethylcyclopropene**

The thermal rearrangement of 3,3-dimethylcyclopropene was investigated by entering the energy surface for the reaction by two routes: thermal isomerization of the cyclopropene and pyrolysis of a diazo compound precursor, 3-methyl-1-diazo-2-butene. The products from both reactions are identical; however the proportions vary greatly. Greater than 95% of the product from the diazo compound is the cyclopropene, and the remainder of the product is isoprene and isopropylacetylene in a 5:2 ratio, with trace gem-dimethylallene. The products from isomerization of the cyclopropene are isopropylacetylene, isoprene, and gem-dimethylallene in a ratio of 500:50:1. From these data it is concluded that two intermediates exist for the isomerization, gem-dimethylvinylcarbene,  $(\text{CH}_3)_2\text{C}=\overset{\circ}{\text{C}}\overset{\circ}{\text{H}}$ , and a 90° rotamer, designated as a diradical,  $(\text{CH}_3)_2\overset{\circ}{\text{C}}\text{H}=\overset{\circ}{\text{C}}\text{H}$ . Relative rates of interconversion and cyclization and an energy surface are determined and the results are compared with Huckel and CNDO/2 calculations on vinylcarbene.

**PART II: Interaction of Remote Functional Groups in the Ion Chemistry of Bifunctional Ethers**

An Ion Cyclotron Resonance examination of bifunctional ethers of the form  $\text{CH}_3\text{O}(\text{CH}_2)_n\text{OR}$ , where  $n = 1 - 6$  and  $\text{R} = \text{H}, \text{CH}_3,$  or  $\text{C}_2\text{H}_5$ , reveals a large number of mass spectral processes and ion-molecule reactions in which the interaction of remote functional groups plays a prominent role. Chainlength effects are particularly pronounced: 6-member cyclic intermediates are inferred in rearrangements of odd-electron species, while larger cycles appear preferred in rearrangements of many even electron species.

ACKNOWLEDGMENTS

I thank my research advisors, R. G. Bergman and J. L. Beauchamp.

I am indebted to Erich Siegel, not only for his craft, but for his extraordinary patience.

I wish to express my gratitude to the Petroleum Research Fund and the Atomic Energy Commission, who, by grants to RGB and JLB, supported this research; to the California State Scholarship and Loan Commission for a tuition scholarship (1968 - 69 ); and to the Public Health Service for an NIH Predoctoral Fellowship ( 1969 - 72).

To Paco Lagerstrom

*il quale per buona sorte, era di più il suo migliore Amico*

## CONTENTS

<b>Part I: The Thermal Rearrangement of 3, 3-Dimethylcyclopropene</b>	<b>1</b>
Background	1
A. Thermal Isomerization of 3, 3-Dimethylcyclopropene	21
B. Thermal Decomposition of 3-Methyl-Diazo-2-butene	68
C. Calculations on C <sub>3</sub> H <sub>4</sub> Rotamers	82
D. Discussion	102
References	115
<b>Part II: Interaction of Remote Functional Groups in the Ion Chemistry of Bifunctional Ethers</b>	<b>123</b>
Background	124
A. Electron Impact and Chemical Ionization Mass Spectra of Bifunctional Ethers Studied by ICR	129
Tabulated ICR Mass Spectra	173
B. Ion-Molecule Reactions of Mass Spectral Fragments of Bifunctional Ethers Studied by ICR Spectroscopy	185
Experimental	215
References	220

PART I: The Thermal Rearrangement of  
3,3-Dimethylcyclopropene

*If now you desire the population of Albemarle, I  
will give you, in round numbers, the statistics, according  
to the most reliable estimates made upon the spot:*

<i>Men</i> .....	<i>none</i>
<i>Ant-eaters</i> .....	<i>unknown</i>
<i>Man-haters</i> .....	<i>unknown</i>
<i>Lizards</i> .....	<i>500,000</i>
<i>Snakes</i> .....	<i>500,000</i>
<i>Spiders</i> .....	<i>10,000,000</i>
<i>Salamanders</i> .....	<i>unknown</i>
<i>Devils</i> .....	<i>do.</i>

---

*Making a clean total of ..... 11,000,000*

*exclusive of an incomputable host of fiends, ant-eaters,  
men-haters, and salamanders.*

Herman Melville, *The Encantadas*

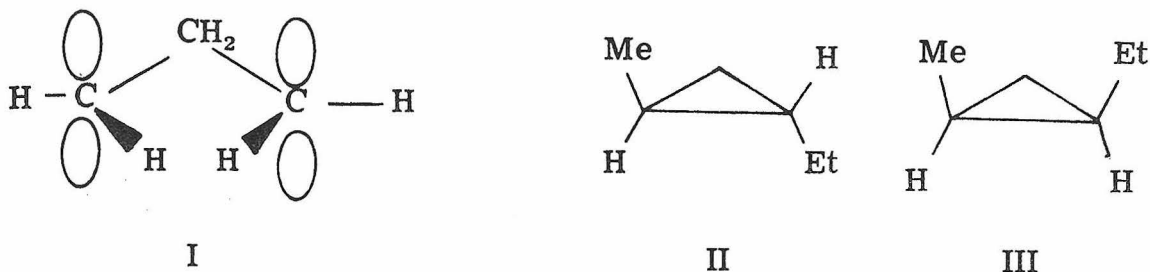
BACKGROUND

Isomers of alicyclic hydrocarbons which possess divalent or trivalent carbon have long intrigued organic chemists. In the initial paper (1882) on the synthesis of the "trimethylene" isomer of propylene from reduction of 1,3-dibromopropane with sodium, Freund specifically excluded two carbenoid structures for the product on the basis of his experimental evidence.<sup>1</sup> Having omitted from consideration the trimethylene diradical and any other structure involving trivalent carbon, Freund concluded that this  $C_3H_6$  hydrocarbon has the cyclic structure by which cyclopropane is now represented.

The possibility of the intermediacy of the trimethylene diradical (referred to below simply as trimethylene) in the thermal isomerization of cyclopropane was considered by Kistiakowsky and Chambers in 1934;<sup>2</sup> however, the necessity for this intermediate, presumed to arise from an initial ring opening step, was not admitted until 1958, when Rabinovitch, Schlag, and Wiberg determined that geometrical isomerization of cis and trans-cyclopropane- $d_2$  occurred more swiftly than structural isomerization to propylene- $d_2$ .<sup>3</sup>

Schlag and Rabinovitch were careful to point out that the diradical intermediate and the ring opening mechanism "must not be taken too literally since the opening ends of the cyclopropane structure would not be removed from each other's sphere of influence, nor are they in trimethylene."<sup>4</sup> This view was amplified by Hoffmann, who has suggested that the structure I,  $\pi$ -cyclopropane, might be stabilized

by "through-bond interaction" of the  $\pi$  lobes.<sup>5</sup> A corollary of this hypothesis is that such a structure might exhibit a preference for a conrotatory mode of reclosure to cyclopropane.<sup>6</sup>

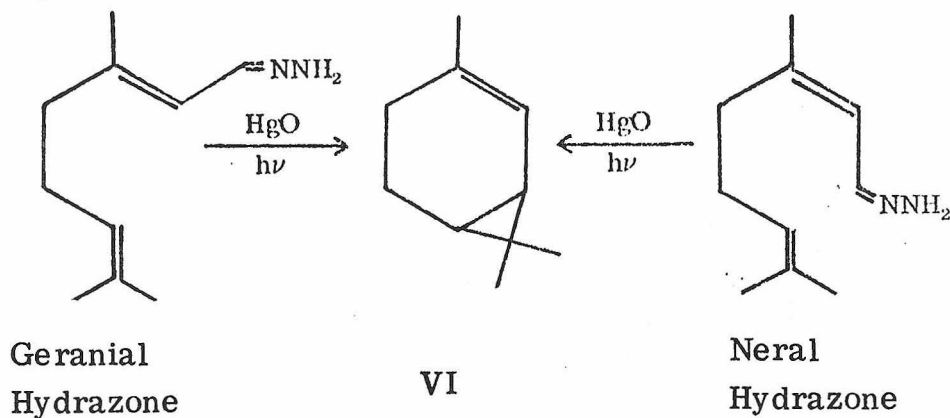


The work of Bergman and Carter on the relative rates of optical and geometrical isomerization of compounds II and III revealed no evidence for conrotatory ring closure of the intermediate structure.<sup>7</sup> This was concluded from the fact that the rates of cis-trans isomerization were within experimental error of the rates of racemization. The formation of a  $\pi$ -cyclopropane intermediate, which possesses a plane of symmetry, would be expected to lead to racemization; however, if the diradical were constrained to close in a conrotatory mode, cis-trans isomerization would not be observed.

Efforts to observe 1,3-diradicals are continuing,<sup>8</sup> as the high temperatures required for the pyrolysis of cyclopropane may be responsible for the observed lack of discrimination between disrotatory and conrotatory modes of closure of the trimethylene diradical. A diradical intermediate would be more readily formed from a more highly strained 3-membered ring if the heat of formation of the ground state reactant were raised more than the heat of formation of the intermediate. A corresponding decrease in the activation energy would



In 1964, Büchi and White observed a vinylcarbene which closes to a cyclopropene with greater alacrity than it undergoes an intramolecular addition to a remote double bond to yield the vinylcyclopropane structure of thujopsene.<sup>11</sup> Interestingly, these workers noted that the hydrazones from geranial and from neral both afford the same product, VI, when converted to the diazo compound and photolyzed, shown in Scheme B. Unfortunately, the report is fragmentary; nevertheless, this result suggests that the vinylcarbene derived from geranial is able to rotate 180° about the double bond in order to react in the same intramolecular fashion as the vinylcarbene from neral. Presumably, this means that the intermediate passes through the 90° rotamer, or diradical structure, without being entirely converted to cyclopropene.



Scheme B

In 1964, Stechl concluded from his investigations that vinylcarbenes were accessible from alkyl cyclopropenes under conditions of pyrolysis and transition metal catalysis.<sup>12</sup> Likewise, the studies of Battiste and coworkers of the thermal rearrangements of arylcyclopropenes also suggest the intermediacy of a vinylcarbene.<sup>13</sup>

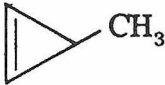
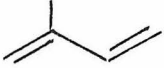
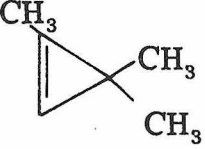
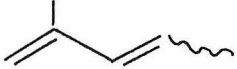
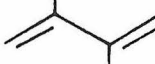
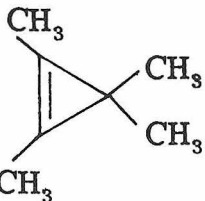
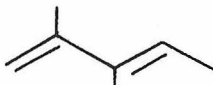
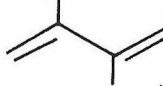
In 1969, Srinivasan published the first kinetic data on cyclopropene pyrolysis.<sup>14</sup> These data for cyclopropene and for 1-methylcyclopropene are summarized in Table 1. The small value of the pre-exponential factors for these rearrangements suggests, perhaps, the possibility that cyclopropenes might rearrange by some concerted mechanism.

In a later publication, however, Srinivasan determined kinetic parameters for alkylcyclopropenes that were more consistent with a ring opening mechanism and formation of an intermediate. These data, summarized in Table 2, show larger pre-exponential factors and higher activation energies than do the data for cyclopropene and 1-methylcyclopropene.

TABLE 1: KINETIC PARAMETERS FOR THERMAL REARRANGEMENT OF CYCLOPROPENE AND 1-METHYLCYCLOPROPENE<sup>14</sup>

	log A	Products	Activation Energy
	12.13	$\text{CH}_3\text{C}\equiv\text{CH}$	$35.2 \pm 1.3$ Kcal
 CH <sub>3</sub>	11.4	$\text{CH}_2=\text{CHCH}=\text{CH}_2$	$44.6 \pm 25$ Kcal
		$\text{CH}_3\text{C}\equiv\text{CCH}_3$	$34.6 \pm 0.7$ Kcal
		$\text{CH}_2=\text{C}=\text{CHCH}_3$	$37.1 \pm 5.6$ Kcal

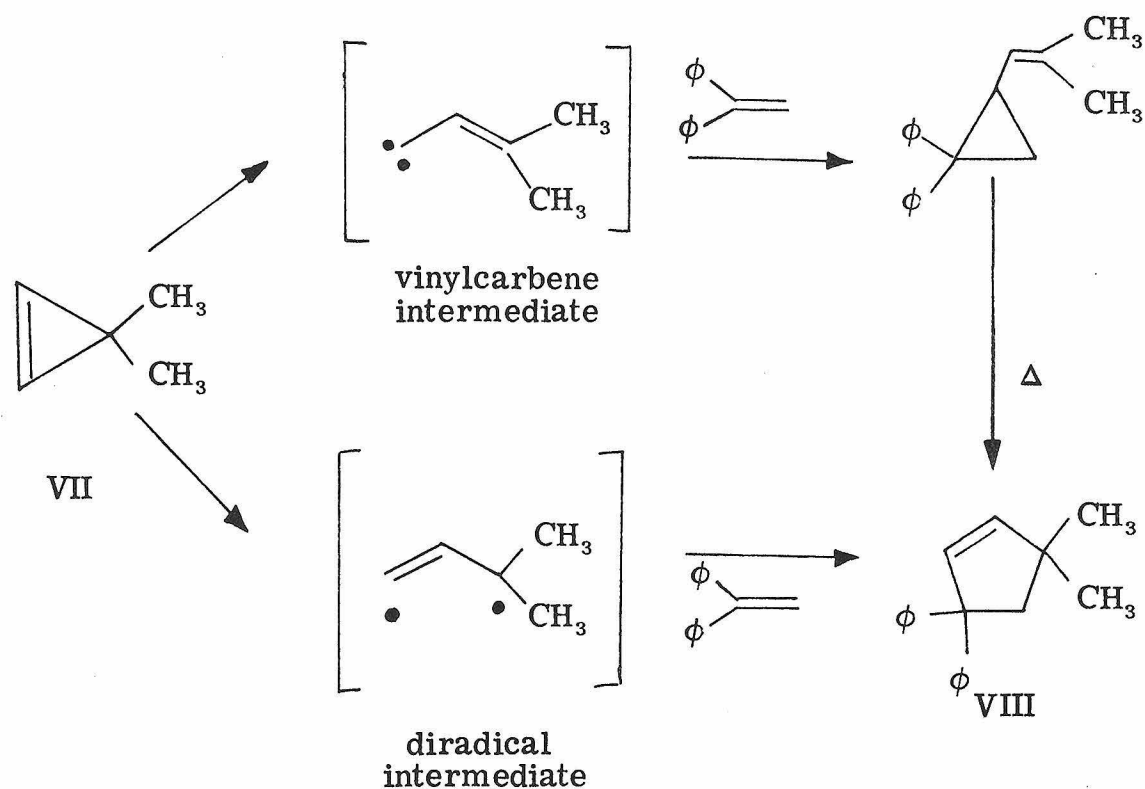
TABLE 2: KINETIC PARAMETERS FOR THERMAL REARRANGEMENT OF ALKYL CYCLOPROPENES<sup>15</sup>

	log A	Activation Energy	
	13.5 ± 0.5	37.60 ± 1.20	 10% CH <sub>3</sub> CH <sub>2</sub> C≡CH 90%
	13.0 ± 0.4	36.60 ± 0.85	 90% (CH <sub>3</sub> ) <sub>2</sub> CHC≡CH
	13.4 ± 0.6	39.00 ± 1.35	 71%  21% 5 Minor Products
	12.5 ± 0.8	39.97 ± 2.00	 5%  85%  10%

A final indictment of vinylcarbenes as intermediates in cyclopropene isomerizations comes about from the recent observation by York, *et. al.*, that optically active 1,3-diethylcyclopropene racemizes 8.4 to 9.2 times faster than it undergoes structural isomerization.<sup>16</sup>

In an attempt to intercept the putative vinylcarbene, Closs decomposed 3,3-dimethylcyclopropene, VII, in a sealed tube with 1,1-diphenylethylene as solvent at 250°. The product, the cyclo-

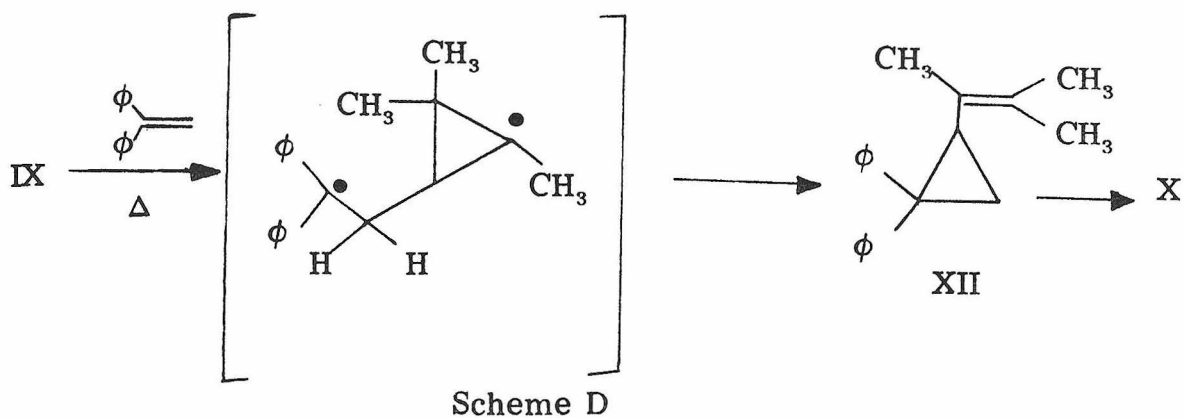
tene VIII, was that expected from the addition of the vinylcarbene intermediate to a double bond followed by a vinylcyclopropane rearrangement, or by the 1,3 addition of a diradical intermediate, both depicted in Scheme C.



Scheme C

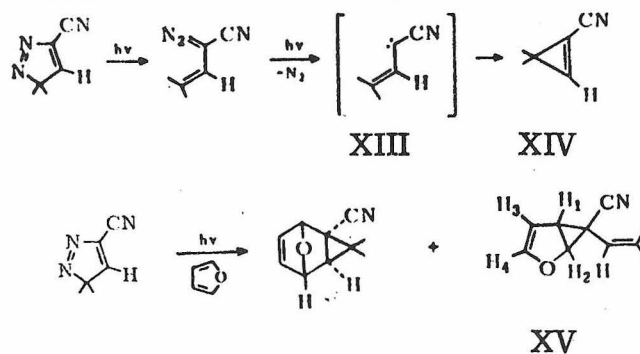
However, upon repeating the experiment with IX, the cyclopropene derived from the tosylhydrazone of mesityl oxide,<sup>10</sup> the product from decomposition at 250° in 1,1-diphenylethylene was found to be X. This was seemingly inconsistent with the fact that the decomposition of IX in inert solvent afforded products arising from cleavage of the more highly substituted single bond, and the expected





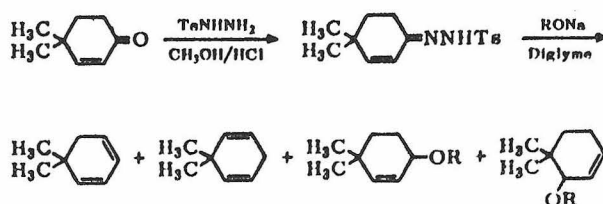
In Scheme D, the preference for a tertiary cyclopropyl radical over a secondary radical in the intermediate is supposed to lead to the exclusive formation of X. Closs is currently investigating the rate of unimolecular rearrangement of IX in solution in order to see if that rate is comparable to the rate of formation of X.

Other attempts to demonstrate the carbenoid nature of vinylcarbene appear no less equivocal. Franck-Neumann and Buchecker's report<sup>19</sup> of the addition of XIII to furan to give XV, Scheme E, suffers from the fact that their communication makes no mention of the stability of cyclopropene XIV under the reaction conditions. In fact, Franck-Neumann and Buchecker observe that the 1-cyano cyclopropenes are unstable, and a mechanism akin to the latter of Closs' can easily be envisioned.



Scheme E

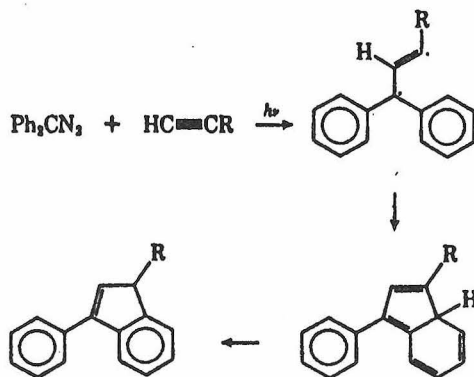
The  $\alpha$ ,  $\beta$  unsaturated diazo compounds that would be most likely to produce carbenoid vinylcarbenes would be those for which cyclopropane formation would be exceedingly unlikely. Kirmse and Ruetz decomposed a number of cyclic diazo compounds such as shown in Scheme F.<sup>20</sup>



Scheme F

Unfortunately, they report neither the isolation of the diazo compounds nor the decomposition of the tosylhydrazones in the presence of olefins.

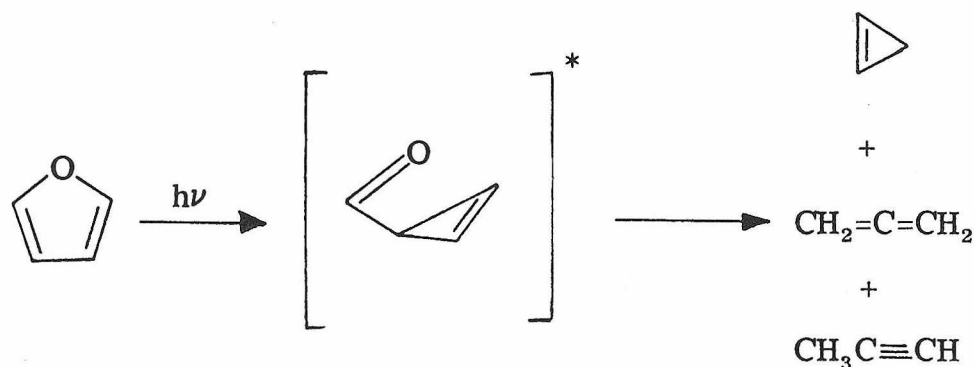
Hendrick, Baron, and Jones<sup>21</sup> have observed chemistry indicative of a triplet vinylcarbene upon the addition of diphenyl carbene to 2-butyne (Scheme G). However, neither direct nor sensitized



Scheme G

irradiation of the corresponding cyclopropenes produced any indene products. The role of triplet states in thermal isomerizations is, however, still unclear.

The photochemical production of cyclopropenes is a complex process which may involve the intermediacy of a vinylcarbene or diradical rotamer. Hiraoka and Srinivasan have examined the direct photolysis of furan, and they observe photoproducts arising from the decarbonylation of cyclopropene 3-carboxaldehyde that are the same as those arising from pyrolytic rearrangement of cyclopropene,<sup>22</sup> as shown in Scheme H.



Scheme H

The wavelength dependence of the reaction is summarized in Table 3.

It is difficult to assess the contribution of the possible intermediates in this reaction, particularly in light of the fact that many of them may be in vibrationally and electronically excited states.

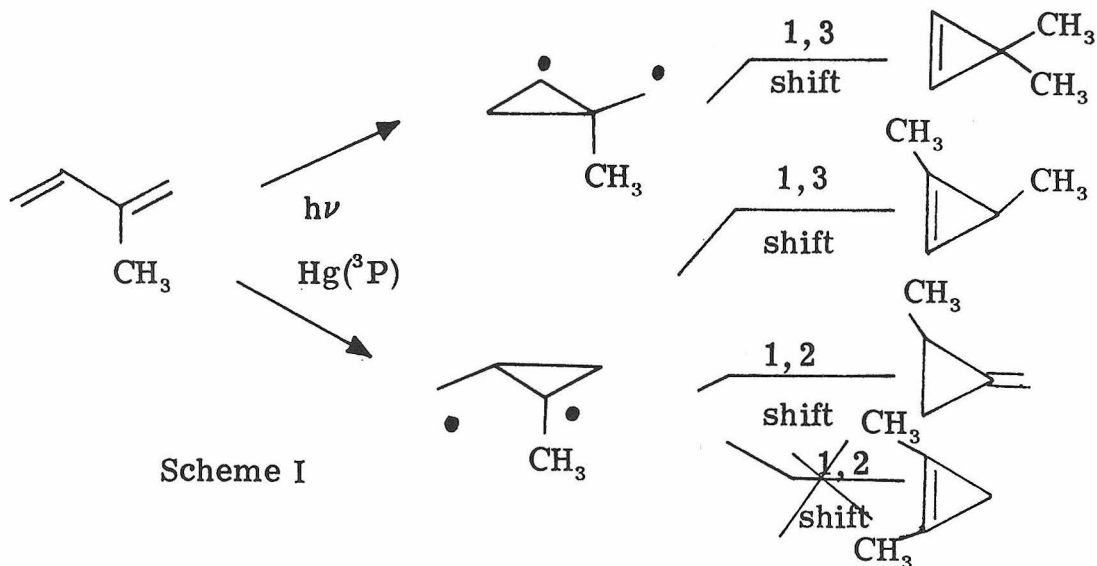
Similarly, the production of cyclopropene from mercury sensitized irradiation of furan<sup>23</sup> and of  $\alpha, \beta$ -unsaturated lactones<sup>24</sup> should also

TABLE 3: HYDROCARBON PRODUCTS FROM DIRECT IRRADIATION OF FURAN<sup>22</sup>

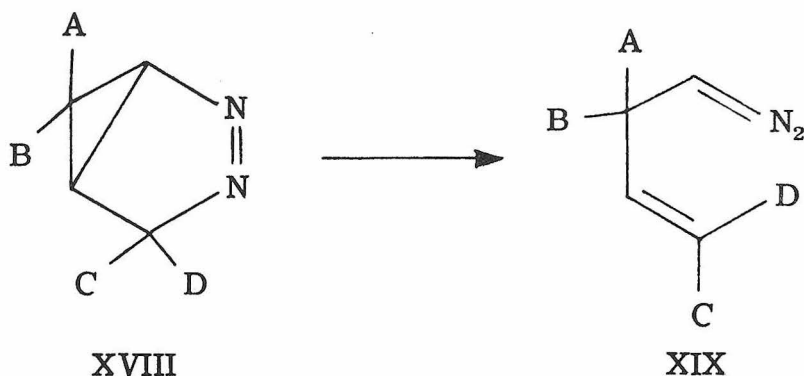
Wavelength	Proportion cyclopropene	Proportion $\text{CH}_2=\text{C}=\text{CH}_2$	Proportion $\text{CH}_3\text{C}\equiv\text{CH}$
2600-2800 Å	0.04	0.54	0.42
2100-2800 Å	0.00	0.78	0.22
2654 Å	trace	trace	ca. 1
2225 Å	0.01	0.26	0.73

involve excited state intermediates, including triplet states.

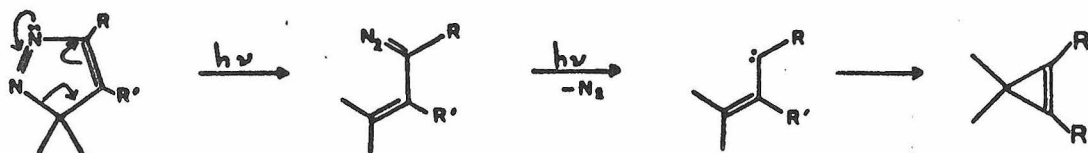
Srinivasan cites different sorts of intermediates in the production of cyclopropenes from mercury sensitized irradiation of conjugated dienes, as shown in Scheme I.<sup>25</sup> Although vinylcarbenes are not absolutely excluded from intermediacy in this reaction, the diradical intermediates XVI and XVII appear fully consistent with the formation of the cyclopropene products.<sup>26</sup>



Attempts to verify the mechanism of Scheme I by pyrolytic generation of the intermediates have, thus far, proved unsuccessful, as pyrazolines of the form XVIII apparently rearrange to diazo compounds of the form XIX prior to expulsion of nitrogen.<sup>27</sup>



At this point, the question arises as to whether the "diradical" rotamer of vinylcarbene plays a significant role as an intermediate in the thermal reactions of cyclopropenes. Efforts to prepare the 1,3-diradical directly from pyrazolenines have failed, primarily because pyrazolenines are, thermally, much more stable than the corresponding diazo compounds.<sup>10</sup> Indeed, diazo compound intermediates have been observed from the photolysis of pyrazolenines, as depicted in Scheme J;<sup>28-32</sup> likewise, the flash vacuum pyrolysis of pyrazoles<sup>33</sup> probably involves a diazo intermediate as well as a pyrazolenine.

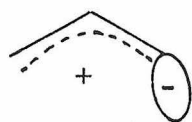


Scheme J

The question also arises as to the chemical nature of vinylcarbenes. Although many preparations of vinylcarbenes as cyclopropene precursors exist,<sup>9,10,28-37</sup> there is no unambiguous evidence for the intermolecular addition of a vinylcarbene to a double bond. In this respect, vinylcarbenes differ from carbenecyclopentadiene, where only intermolecular reactions are observed,<sup>38,39</sup> and tropylicarbenes, where additions to double bonds and dimerizations compete with intramolecular rearrangements.<sup>40-42</sup>

Intramolecular reactions of vinylcarbenes, on the other hand, are reported for vinylcarbenes generated in the presence of transition metal catalysts. Corey and Achiwa have reported several syntheses of natural products utilizing decomposition of  $\alpha, \beta$ -unsaturated diazo compounds in the presence of cupric fluoborate,<sup>43</sup> cuprous iodide,<sup>43,44</sup> and mercuric iodide,<sup>44</sup> followed by intramolecular addition of the carbene to a remote double bond. Wittig and Hutchison report the transannular C-H insertion of the vinylcarbene intermediate produced by Simmons-Smith addition to cyclooctyne; however, this reaction is not observed when carbenes generated from other reactions are added to cyclooctyne.<sup>45</sup> These reports and the results of Kirmse and Ruetz<sup>20</sup> constitute the only evidence for the formation of other products beside cyclopropenes from thermally generated vinylcarbenes.

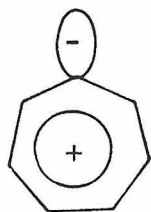
It is possible that the chemical properties of vinylcarbenes may be explained in terms of 1,3-dipolar structures such as XX, an allyl cation with a lone pair, or XXI, an allyl anion with a vacant lobe. A precedent for structure XX may be seen in the electronic distribution imputed for tropylic carbene,<sup>40</sup> structure XXII. The structure XXI is



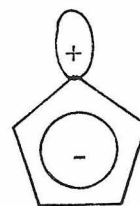
XX



XXI

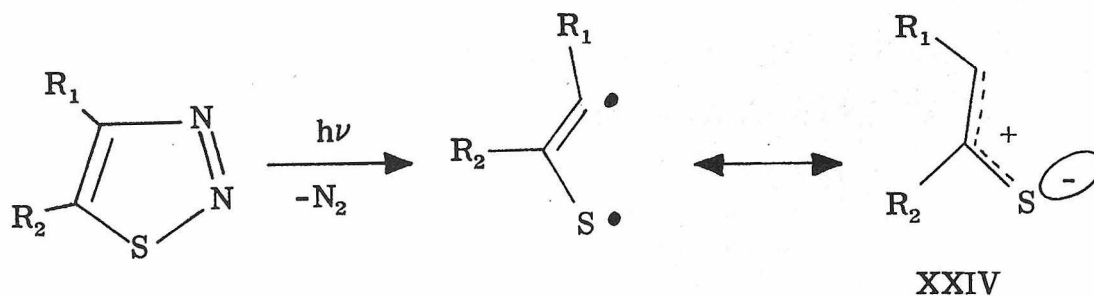


XXII



XXIII

analogous to carbenacyclopentadiene, XXIII, or to the structure drawn for the intermediate, XXIV, in the photolysis of 1,2,3-thiadiazoles, shown in Scheme K.<sup>46</sup>

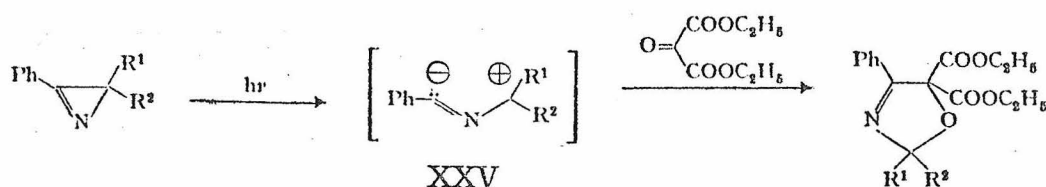


XXIV

Scheme K

Other heteroatom analogues of vinylcarbenes also appear to react as if they are 1,3-dipolar structures. The photolysis of 3-phenyl-2H-azirenes is inferred to give rise to an intermediate of structure XXV in Scheme L.<sup>47,48</sup> This dipolar form of the molecule appears to be preferable to a nitrile ylid structure such as XXVI (which is

analogous to the intermediates from irradiation of aziridines<sup>49</sup>), since addition of the intermediate to diethyl carbonate yields the product shown in Scheme L. A dipolar vinyl carbenoid-like structure XXVII may be an intermediate in the addition of isonitriles to strained alkynes.<sup>50</sup>



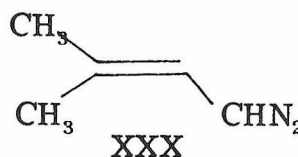
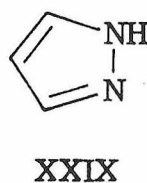
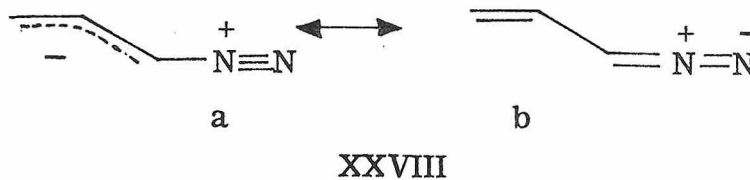
Scheme L



In order to examine the questions of the chemical nature of vinylcarbenes and of their diradical  $90^\circ$  rotamers, a program of research was commenced in September, 1969. One of the first efforts of this investigation was an attempt to isolate a triplet vinylcarbene in a low temperature matrix. The success of Closs and coworkers in the EPR identification of triplet 1,3-diradicals from photolysis of 3H-indazoles<sup>51</sup> and of the diradical intermediates from their addition to olefins<sup>52</sup> led us to investigate the photolysis of vinyl diazomethane at low temperature in an EPR cavity.

Vinyldiazomethane (resonance structures XXVIII a and b) was prepared by the method of Brewbaker and Hart,<sup>53</sup> dissolved in 2-methylpentane, and degassed in a quartz EPR tube. The tube was cooled slowly in liquid nitrogen until the solvent formed a clear glass.

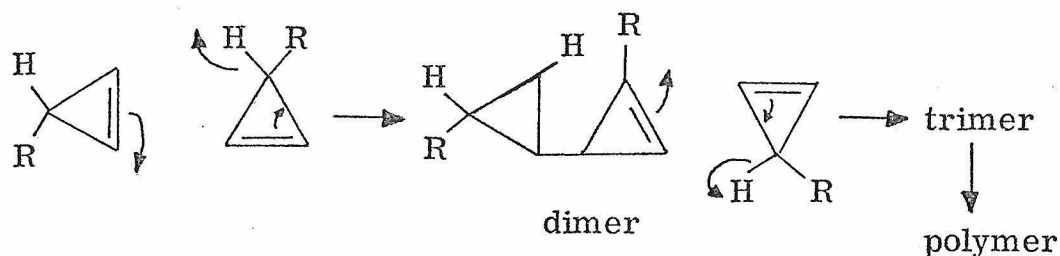
The tube was irradiated in an EPR cavity cooled below  $-100^{\circ}\text{C}$  with a 2500 watt Hanovia Xenon-Mercury DC lamp.<sup>54</sup> Only signals indicative of monoradical absorptions were detected.



An effort to observe an EPR spectrum with perfluoromethylcyclohexane<sup>55</sup> was not successful, as even the alkyl substituted diazo compound XXX is not sufficiently soluble in the perfluorinated solvent. Closs, too, has been unable to observe EPR spectra from the irradiation of allyl substituted  $\alpha, \beta$ -unsaturated diazo compounds; however, he has found that triplets can be detected from the irradiation of alkyl substituted,  $\alpha$ -phenyl vinyl diazomethanes at low temperatures.<sup>17</sup>

Part I of this thesis is a study of the thermal rearrangement of 3,3-dimethylcyclopropene (VII), in an effort to find out whether there is one intermediate or two along the reaction coordinate. Compound VII was chosen for study because it offered a chance to observe alkyne products as well as diene products from the thermal rearrangement.<sup>15</sup> Moreover, the geminal dimethyl substitution in VII prevents

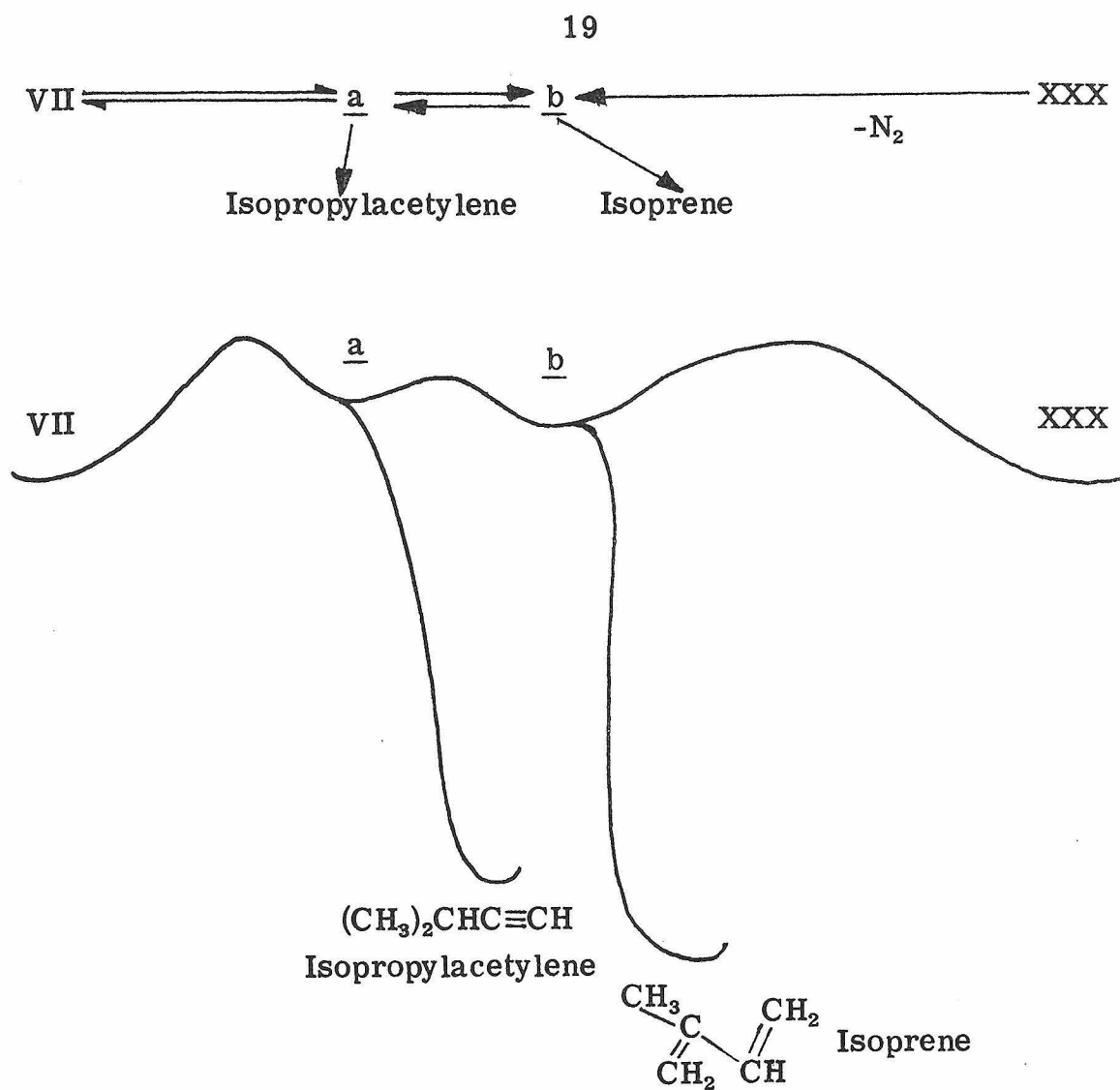
the polymerization of the cyclopropene via the Alder "ene" reaction shown in Scheme M.<sup>56</sup>



Scheme M

The plan of this investigation was to enter the energy surface for the isomerization of VII by two routes and compare product distributions. The decomposition of XXX is known as a synthetic route to VII.<sup>10</sup> If a vinylcarbene is a common intermediate for both reactions, i. e. the thermal rearrangement of VII and the pyrolysis of XXX, then acyclic isomers of VII may be expected to result from the latter. If the vinylcarbene is the only intermediate on both pathways, then the same acyclic products will be formed, and they will be in the same proportions.

If, as was found in our experiments, the same acyclic products arise from both reactions, but in different proportions, then two intermediates are implicated in the thermal rearrangement of VII, depicted in Scheme N on the next page.



Scheme N

The gem-dimethyl substituted system was found to be desirable for a product distribution study because the diazo compound XXX cannot undergo cyclization and intramolecular hydrogen transfer to yield a pyrazole, as the rearrangement of vinyl diazomethane, XXVIII, to pyrazole XXIX.<sup>53</sup> Although the aldehyde precursor to XXX presented some difficulties in preparation, acyclic product distributions were determined both for thermal rearrangement of cyclopropene VII and for pyrolysis of diazo compound XXX.

Part I is divided into four sections:

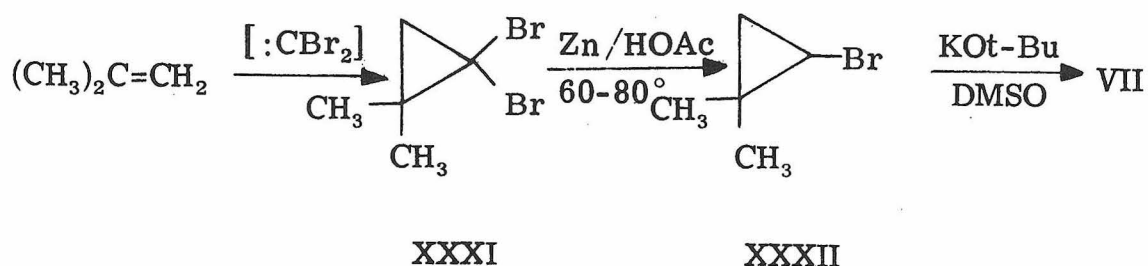
- A. The thermal isomerization of 3,3-dimethylcyclopropene;
- B. The thermal decomposition of 3-methyl-1-diazo-2-butene;
- C. Calculations on  $C_3H_4$  rotamers; and
- D. Discussion.

The experimental results are presented in Sections A and B of Part I of this thesis; data from calculations using Hückel and CNDO/2 methods are presented in Section C. Conclusions and a map of the free energy surface are drawn in Section D.

### A. The Thermal Rearrangement of 3,3-Dimethylcyclopropane

The measurement of the kinetics of the thermal rearrangement of 3,3-dimethylcyclopropane, compound VII, in an unpacked static system was performed in Crellin Laboratories and completed in August, 1970. First order rate constants were determined over a range of 53.8° C in a conventional static gas phase reactor<sup>7</sup> with surface-to-volume ratio = 1, and are tabulated in Table 4.

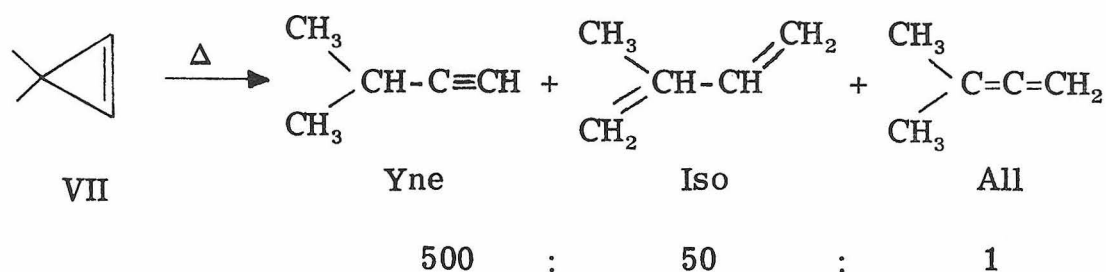
Compound VII was prepared in the straightforward manner depicted in Scheme O. This mode of preparation of cyclopropenes was developed by Dr. J. R. Stevenson in these laboratories, and details are presented in the experimental part of this section. Also described in the experimental section is the preparation of 1-deuterio-2,2-dimethylbromocyclopropane from zinc reduction of XXXI in acetic acid -d<sub>1</sub> and the deuteration of the vinylic sites of VII by base catalyzed exchange.



Scheme O

Three products of the thermal rearrangement of VII were identified in the pyrolysis: 3-methyl-1-butyne (isopropylacetylene, abbreviated

below simply as Yne), 2-methyl-1,3-butadiene (isoprene, abbreviated below as Iso), and 2-methyl-1,2-butadiene (gem-dimethylallene, abbreviated below as All), depicted below in Scheme P. These products, in the temperature range studied in the static reactor, were found, roughly, in the ratio 500:50:1. The ratio of isoprene to isopropylacetylene was found to change over the temperature range; this ratio, averaged over each run, is designated as  $\bar{C}$  and included in Table 4.



Scheme P

The products of pyrolysis of VII were analyzed exhaustively by VPC. Only the three acyclic products listed above were found; these were identified spectroscopically and by comparison with authentic samples. For each kinetic run, the value of the ratio of isoprene to isopropylacetylene at each point after the zero point (C) was plotted as a function of time; the slope of every plot was within experimental error of zero, indicating that C did not vary with time and permitting a straightforward calculation of  $\bar{C}$ , the value of C averaged over a run. The rates of product appearance were determined and found to be fully consistent with the measured rates of disappearance of VII.

TABLE 4: FIRST ORDER RATE CONSTANTS AND PRODUCT RATIOS FOR THERMAL  
REARRANGEMENT OF 3, 3-DIMETHYLCYCLOPROPENE

Run #	Measured Temperature	$k_{\text{Obs}}$ , Disappearance of VII	Standard Deviation of $k_{\text{Obs}}$ <sup>57</sup>	$\bar{C}$ <sup>a</sup>
6	503.6°K	$1.57 \times 10^{-3}$	$2.3 \times 10^{-5}$	0.108
8	503.7°K	$1.58 \times 10^{-3}$	$3.5 \times 10^{-5}$	0.113
11	487.4°K	$4.44 \times 10^{-4}$	$6.3 \times 10^{-6}$	0.103
12	474.9°K	$1.51 \times 10^{-4}$	$2.5 \times 10^{-6}$	0.101
13	461.4°K	$4.61 \times 10^{-5}$	$2.8 \times 10^{-6}$	0.096
14	449.9°K	$1.65 \times 10^{-5}$	$4.7 \times 10^{-7}$	0.085

<sup>a</sup>  $\bar{C} = \frac{[\text{Iso}]_0 - [\text{Iso}]_t}{[\text{Yne}]_0 - [\text{Yne}]_t}$ , averaged over a run. Values of  $[\text{Iso}]_0$  and  $[\text{Yne}]_0$  are taken from the first aliquot in the run.

Arrhenius plots were made for the temperature dependence of  $k_{\text{obs}}$ , the first order rate constant for disappearance of VII, and of  $\bar{C}$ , the average ratio of isoprene to isopropylacetylene. A plot of  $\log k_{\text{obs}}$  versus  $1/T$  reveals a pre-exponential factor of  $10^{13.9}$  and an activation energy of 38.5 Kcal/mole. A plot of  $\log \bar{C}$  versus  $1/T$  shows that the pre-exponential factors for formation of isoprene and formation of isopropylacetylene are the same within experimental error, and that the prevalence of the alkyne over the diene product represents a difference of 2 Kcal/mole in the activation energy. Uncertainty and error limits on these values are discussed extensively in the experimental part of this section.

The conventional method of demonstrating that a gas phase reaction is homogeneous is a comparison of the rates in two vessels having different surface-to-volume ratios. Although the fact that a reaction may proceed with the same rate in a packed reactor as in an unpacked reactor does not constitute proof that a reaction is surface independent,<sup>58</sup> it appears that it is routinely accepted in the literature as an adequate demonstration.

Srinivasan has reported that no alteration in the rates of rearrangement of cyclopropene and 1-methylcyclopropene is observed in a packed reactor with a 17-fold increase in surface-to-volume ratio.<sup>14</sup> This occurs despite the fact that his pre-exponential factor for these pyrolyses is unusually small, a result from which the suspicion of a surface effect often arises, and that his pyrolysis of more highly substituted cyclopropenes show much larger pre-exponential factors.<sup>15</sup> Srinivasan's kinetic parameters for rearrangement of VII

differ appreciably from those determined in this study; although he reports an activation energy 2 Kcal lower and a pre-exponential factor an order of magnitude smaller than this study has found, he asserts that a surface effect is not found in this pyrolysis.

Our efforts to discount surface effects through packed reactor kinetics, on the other hand, have shown an ineradicable surface effect on the pyrolysis of VII. We have investigated numerous static reactors, conditioning procedures, and flow systems in an effort to eliminate surface effects. These efforts are detailed in the experimental part of this section, and they have been, to date, unsuccessful. An effort is being made, with the assistance of Professor J. E. Taylor, to examine the behavior of VII in the rigorously homogeneous conditions of a "wall-less" reactor. <sup>59</sup>

EXPERIMENTALPreparation of 1,1-dibromo-2,2-dimethylcyclopropane<sup>60,61</sup> (XXXI)

Potassium metal (67 g., 1.7 moles) was dissolved under nitrogen in 1570 ml. t-butanol (freshly distilled from lithium aluminum hydride) in a 3 liter three-necked flask at reflux with mechanical stirring. When dissolution was complete, the heating mantle was removed and the solution permitted to cool to room temperature. 800 ml. pentane was added with continued stirring, and the solution was cooled in a Dry Ice-acetone slush. A reflux condenser filled with Dry Ice-acetone was fitted on the flask and 350 g. (6.2 moles) isobutylene was introduced from a lecture bottle via the reflux condenser. With continued stirring, 320 g. (1.28 moles) bromoform was added dropwise over 1½ hours. The mixture was left stirring overnight and allowed to reach room temperature. The next day, the entire mixture was quenched with 2 liters of water, the lower organic phase separated, and its volume reduced on a rotary evaporator until no more solvent would come over. The material was washed and once again evaporated; this procedure was repeated four more times to free the product from pentane, isobutylene, and t-butanol. The material was then dried over sodium sulfate. The resulting material was >95% pure by VPC on a 5 ft. x ¼ in. 3% SE 30 column, injector = 145°, column = 85° (retention time 3 minutes). NMR (CCl<sub>4</sub>): δ 1.4 (s, methyl groups), shoulder (s) 1½ cps downfield from this peak (ring protons). Yield, 239 g. (1.05

moles), 81% of theoretical, NMR and VPC retention time identical to that of a sample made by this procedure in a prior preparation with bp (746 mm.) 162-166°,  $n_D^{25} = 1.5115$  ( $n_D^{25}$  lit<sup>60</sup> = 1.5110,  $n_D^{25}$  lit<sup>61</sup> = 1.5114).

Reduction of 1,1-Dibromo-2,2-dimethylcyclopropane (XXXI) to 1-1-Bromo-2,2-dimethylcyclopropane (XXXII)

128 g. (0.56 moles) was added at once to a mixture of 1100 ml. glacial acetic acid in which 12 g. zinc dust had been suspended and magnetically stirred for 15 minutes at 80°C. Immediately the zinc dust aggregated into small clumps and settled to the bottom of the flask. Excess zinc dust (150 g.) was added in small portions over the the next three hours (VPC monitor of aliquots from the reaction following each addition of zinc dust). When no further change in product concentration was observed, the mixture was removed from the bath and washed repeatedly with water. The lower phase was found to be pure by VPC, save for a few percent of 1,1-dimethylcyclopropane (identified by NMR<sup>62</sup>). The retention time of XXXII on a 5 ft. x  $\frac{1}{4}$  in. 3% SE 30, 60/80 Chromosorb P column, injector = 140°, column = 80°, He flow = 1 cm<sup>3</sup>/sec, was 2 minutes. The 43.5 g. collected from the organic phase was dried over magnesium sulfate and distilled at aspirator pressure. The first portion, 13.8 g., showed the presence of a persistent dimethylcyclopropane impurity. The second cut (bp. 70-71° (170 mm) ) was 19.5 g. pure by VPC and gave an identical NMR spectrum to a previously prepared sample which had distilled at 105-110°C at atmospheric pressure (bp. lit. 63 107°-108°). NMR (CCl<sub>4</sub>): $\delta$  2.75 (quartet of peaks of equal height and spacing of 4-5 cps,

ring proton geminal to bromine),  $\delta$  1.23 (s, methyl cis to bromine),  $\delta$  1.11 (methyl trans to bromine),  $\delta$  1.1 - 0.5 (m, other ring protons). Yield of XXXII free from impurities, 0.13 moles, 23% of theoretical.

Subsequently, it was found that the XXXII could be freed from volatile impurities simply by rotary evaporation for several hours. In this manner, yields of up to 65% pure XXXII could be obtained.

#### Preparation of 1-deuterio-2,2-dimethylbromocyclopropane

Acetic acid- $d_1$  was prepared by the hydration of 281 g. (2.76 moles) acetic anhydride with 55 g (2.75) moles) deuterium oxide (Columbia Organic Chemicals, 99.7 atom % D). 275 ml. acetic acid- $d_1$  32 g. (0.14 moles) XXXI was added at once to a mixture of 275 ml. acetic acid -  $d_1$  in which 3 g. zinc dust had been suspended and magnetically stirred at 85°. 38 g. more zinc dust was added in small portions over the next 2 hours, and the reaction was monitored by VPC. The reaction was worked up in the same manner as the preparation of XXXII but was not distilled. VPC analysis showed a small impurity dimethylcyclopropane (presumably  $d_2$ ). NMR shows greater than 90 atom % of  $d_1$  product. Mass spectrum (ICR, 12 eV):  $m/e$  70 [M - Br]. Ratio of  $m/e$  69 (from XXXII impurity) to  $m/e$  70 shows the product to be 92 atom %  $d_1$ . This relatively large percentage (8%) of undeuterated product is taken to reflect the fact that acetic acid impurity in the acetic acid- $d_1$  probably reacts much faster than acetic acid- $d_1$ . Yield 10.8 g. (0.72 moles), 52% of theoretical.

Dehydrobromination of 1-Bromo-2,2-Dimethylcyclopropane (XXXII):  
Preparation of 3,3-Dimethylcyclopropane (VII)<sup>64</sup>

Dimethylsulfoxide used in this preparation was freshly distilled from calcium hydride. A stoppered 1 liter three-necked flask was charged with 30 g. (0.27 moles) potassium t-butoxide from a freshly opened bottle (Alpha Inorganics, free from t-butanol) and 250 ml. dimethylsulfoxide and stirred magnetically until the solid was dissolved. An addition funnel with a pressure equalizing arm was fitted on the flask, and the flask was connected through a cold trap, a stopcock, and a drying tube filled with Drierite to an aspirator. The cold trap consisted of a 100 ml. pear-shaped flask filled with glass helices and fitted with a distillation receiving adapter that reached to the bottom of the pear-shaped flask. The adapter was connected to the reaction vessel with an elbow connector. A VPC collector was connected to the adapter with Tygon tubing and, in turn, to the stopcock connected to the drying tube and aspirator assembly. The pear-shaped flask was immersed in a Dry Ice-acetone bath, while the VPC collector was immersed in liquid nitrogen to insure efficient trapping of the volatile cyclopropene (bp. <sup>lit.</sup><sub>lit.</sub> <sup>10</sup> 14°C). 16 g. (0.11 mole) XXXII, free from dimethylcyclopropane impurities, dissolved in 35 ml. dimethylsulfoxide was added at once from the addition funnel to the magnetically stirred potassium t-butoxide solution. After a few minutes magnetic stirring, the stopcock to the aspirator was cracked and reclosed. Immediate frothing resulted, and a clear liquid began to collect in the cold trap. When frothing had subsided, the stopcock was again cracked, and this procedure was continued for a half hour until continuous

suction on the reaction mixture yielded no more bubbles. The contents of the cold traps were vacuum transferred into a vacuum stopcock gas flask and vacuum transferred back and forth between gas flasks five times to free the product from t-butanol and other nonvolatile impurities. Yield was 3.8 g. (0.056 moles), 52% of theoretical, 99% pure by VPC on a 25 ft. x  $\frac{1}{8}$  in. 25%  $\beta, \beta'$ -ODPN, 100/120 Chromosorb P column. NMR ( $\text{CCl}_4$ ):  $\delta$  7.31 (septet,  $J = 0.8$  cps, ring vinyl protons),  $\delta$  1.13 (t,  $J = 0.8$  cps, methyl protons), nearly identical to published spectrum of VII.<sup>10</sup> IR (carbon tetrachloride, taken on a Perkin-Elmer 457): 2970, 2940, 2930  $\text{cm}^{-1}$  (s), 2880  $\text{cm}^{-1}$  (m), 2865  $\text{cm}^{-1}$  (s), 1625  $\text{cm}^{-1}$  (s, possible shoulder at 1615  $\text{cm}^{-1}$ ). Published value for  $A_1$  mode, 1632  $\text{cm}^{-1}$ ; vinyl C-H stretches visible only in Raman.<sup>34</sup> Mass Spectrum (70 volts, 10 microamps Isatron on CEC 21-103c mass spectrometer): m/e (% of base peak) 70 (0.07), 69 (0.64), 68 (14), 67 (96), 66 (8.4), 65 (1.5), 63 (3.0), 62 (2.8), 61 (2.1), 54 (4.5), 53 (100), 52 (2.3), 51 (1.5), 50 (16), 49 (3.7), 43 (0.93), 42 (17), 41 (49), 40 (32), 39 (63), 38(33), 37 (7.9), 36 (0.93).

An attempt to perform this dehydrohalogenation using 11 g. (0.07 moles) XXXII and 0.18 moles of t-butoxide (freshly prepared by dissolving 7 g. potassium metal in excess t-butanol and removal under vacuum of the excess solvent) dissolved in 100 ml. dimethylsulfoxide was unsuccessful. After 20 minutes stirring, no reaction was observed.

### Deuteration of VII

The vinyl positions of VII were deuterated using a modification of the method of Dorko and Mitchell.<sup>65</sup> T-butanol- $\text{d}_1$  was prepared

by the method of Young and Guthrie<sup>66</sup> from t-butyl borate<sup>67</sup> as follows: a mixture of 25 g. (0.4 moles) orthoboric acid, 135 g. t-butanol (1.8 moles), and 100 ml. benzene was refluxed for one week with a Vigreux column connected to a Barret trap to permit drainage of water removed from the refluxing mixture as the azeotrope. After 16½ ml. water had been drained from the trap, no more water was observed to come over. The reflux was ceased, and excess t-butanol and benzene were cautiously removed on a steam bath followed by rotary evaporation at aspirator pressure (attempts to remove all excess solvent on a steam bath resulted in the decomposition of the borate). The residue was a clear liquid standing over a white solid. NMR of the supernatant showed a singlet at 1.3 ppm. and a smaller singlet (not possible to separate the integrals; ratio of heights = 4:1) at 1.4 ppm. No signal indicative of a hydroxyl proton was detected, and the two singlets were attributed to t-butyl borate and t-butyl boroxin respectively.<sup>66</sup>

To the mixture of borate and boroxin was added 18 g. (0.9 moles) deuterium oxide (Columbia, 99.7%), and the mixture was refluxed for 8 hours on a steam bath. The supernatant was distilled at atmospheric pressure at 81°, and an NMR showed no indications of hydroxylic protons. Yield 32 g. (0.43 moles) t-butanol-d<sub>1</sub>, 36% of theoretical.

The following procedure was repeated three times starting with 0.8 g. (0.012 moles) VII: 0.4-0.5 g. (0.01 - 0.013 moles) potassium metal was dissolved in 5.2 - 5.5 g. t-butanol-d<sub>1</sub> (0.07 moles, vacuum transferred from the t-butanol-d<sub>1</sub> described above stored over sodium wire), and the solution was introduced into a gas flask equipped with a magnetic micro spinbar. The solution was frozen in liquid nitrogen and

the gas flask evacuated. The cyclopropene VII was vacuum transferred into the gas flask, and the mixture was allowed to reach room temperature. After stirring for 10 hours - 1 week, the mixture was chilled in ice and cyclopropene vacuum transferred out of the flask. The cyclopropene was then freed from t-butanol impurity by vacuum transfer back and forth several times between gas flasks.

The yield from the first deuteration was 0.4 g., from the second 0.2 g. About half of the yield from the third deuteration was lost through accidental opening of the gas flask; recovered was 0.05 g. (0.0007 moles), 6% yield. Mass spectrum (same conditions as above): m/e (% of base peak) 79 (32), 69 (100), 68 (45), 67 (9.1), 66 (5.4), 65 (1.8), 64 (2.5), 63 (3.0), 62 (2.2), 61 (1.5), 57 (7.9), 56 (12), 55 (93), 54(45), 53 (23), 52 (18), 51 (18), 50 (8.4), 49 (2.5), 43 (30), 42 (40), 41 (69), 40 (51), 39 (64), 38 (17), 37 (8.5), 36 (1.3). Estimated from this spectrum that this sample consisted of 70% VII-d<sub>2</sub> and 25% VII-d<sub>1</sub> (80% deuterium incorporation).

#### Pyrolysis of 3,3-dimethylcyclopropene, VII, and identification of products

A 200 microliter sample of VII was passed through a Pyrex tube at 290°C (volume of heated portion of tube = 10 cm<sup>3</sup>) in a 1 cm<sup>3</sup>/sec stream of nitrogen gas. The pyrolysate was collected in a spiral trap immersed in liquid nitrogen and analyzed on the VPC columns shown on Table 5.

Only columns H and J gave full separation of the pyrolysate into seven peaks. One peak corresponded to VII and another to gem-

TABLE 5: VPC COLUMNS USED IN ANALYSIS OF PYROLYSATE OF  
3,3-DIMETHYLCYCLOPROPENE

Dimensions	Liquid Phase	Solid Support	Inj.	Temperature Col.	VPC
A 15' x $\frac{1}{4}$ "	10% UCCW-982	60/80 Chromosorb P Non-Acid Washed	120°	RT	Aerograph
B 12' x $\frac{1}{4}$ "	20% DBTCP	"	120°	RT	"
C 12' x $\frac{1}{4}$ "	20% $\beta$ , $\beta'$ -ODPN	HMDS Treated 60/80 Chrom P Non-Acid Washed	120°	RT	"
D 10' x $\frac{1}{4}$ "	20% DEGS	"	120°	RT	"
E 6' x $\frac{1}{4}$ "	Porapak Q	"	120°	100°	" 33
F 10' x $\frac{1}{4}$ "	20% TCEP	60/80 Chrom P Non-Acid Washed	120°	RT	"
G & 6' x $\frac{1}{4}$ "	15% $\beta$ , $\beta'$ -ODPN (in tandem with C)	"	120°	RT	"
10' x $\frac{1}{4}$ "	20% SE-30	"	125°	50°	"
H 25' x $\frac{1}{8}$ "	25% Dimethyl- sulfolane	100/120 Chrom P Non-Acid Washed	120°	RT	H-P 5750
I 25' x $\frac{1}{8}$ "	15% TCEP	100/120 Chrom W Acid Washed; DMCS	120°	RT	"
J 25' x $\frac{1}{8}$ "	25% $\beta$ , $\beta'$ -ODPN	100/120 Chrom P Non-Acid Washed	130°	RT	"

All Aerograph VPC's were run with helium flow = 1 cm<sup>3</sup>/sec; H-P 5750 VPC's were run at 15 cm<sup>3</sup>/min helium flow.

dimethylcyclopropane, an impurity in VII. Two more peaks corresponded to impurities (less than  $\frac{1}{2}\%$  each) in VII, and three peaks, ratio 1:6:60, corresponded to products of the pyrolysis. The retention times on J are given below.

VII and its most volatile pyrolysis product were not separated on G; consequently, 250 microliters VII was completely converted to products by passage through the Pyrex tube at  $350^\circ$ , and the three products separated by preparative VPC on G with  $1 \text{ cm}^3/\text{sec}$  helium flow.

The first and largest peak (retention time 6 minutes on G) was identified as isopropylacetylene,  $(\text{CH}_3)_2\text{CHC}\equiv\text{CH}$ . NMR ( $\text{CCl}_4$ ):  $\delta$  2.5 (septet of doublets,  $J = 7 \text{ cps}$ ,  $J = 2\frac{1}{2} \text{ cps}$ ,  $(\text{CH}_3)_2\text{CH}$ ), 1.8 (d,  $J = 2\frac{1}{2} \text{ cps}$ ,  $\equiv\text{CCH}$ ), 1.2 (d,  $J = 7 \text{ cps}$ ,  $(\text{CH}_3)_2\text{C}$ ). IR (carbon tetrachloride):  $3310$ ,  $2970$ ,  $2930$ ,  $2890$ ,  $2875 \text{ cm}^{-1}$  (s),  $2120 \text{ cm}^{-1}$  (m).

The second peak (retention time 8 minutes on G) was identified as isoprene,  $\text{CH}_2=\text{CH}-\text{C}(\text{CH}_2)=\text{CH}_2$  (Iso). NMR ( $\text{CCl}_4$ ):  $\delta$  6.55-6.10 (complex quartet of peaks, ratio 8:11:13:17, 6.55, 6.38, 6.26, 6.10 ppm.  $=\text{CH}-$ ), 5.2 (d,  $J = 10 \text{ cps}$ ,  $\text{CH}_2=\text{CH}$ ), 4.88 (broad singlet,  $=\text{CH}_2$ ), 1.80 (broad singlet,  $\text{CH}_3$ ), identical to the NMR of a commercial sample of isoprene.

The third and smallest peak (retention time 6 minutes on G) was identified as gem-dimethylallene,  $(\text{CH}_3)_2\text{C}=\text{C}=\text{CH}_2$ . NMR ( $\text{CCl}_4$ ):  $\delta$  4.25 (septet,  $J = 3 \text{ cps}$ ), 1.65 (t,  $J = 3 \text{ cps}$ ), identical to published spectrum.<sup>68</sup> IR (carbon tetrachloride):  $2980$ ,  $2930$ ,  $2910$ ,  $2870$ ,  $2850 \text{ cm}^{-1}$  (s),  $1965 \text{ cm}^{-1}$  (s).

Preparation of 3-methyl-1-butyne, (isopropylacetylene, Yne)

A solution of isopropylacetylene in t-butanol was prepared by R. G. Bergman using the dehydrohalogenation with potassium t-butoxide of the adduct of bromine and 3-methyl-1-butene. This solution was purified by preparative VPC on G, and the collected first peak gave an NMR identical to that of the first peak collected from the pyrolysis of VII.

Preparation of 3-methyl-1,2-butadiene (gem-dimethylallene, All)

1,1-Dibromo-2,2-dimethylcyclopropane (XXXI) was dehalogenated to the allene by the method described by Fieser and Fieser.<sup>69</sup> A 25 g. portion of XXXI (0.11 moles) was dissolved in 75 ml. dry ether from a freshly opened can. 65 ml. 2.3M methylithium (Alpha Inorganics) was added to the solution of XXXI under nitrogen in a three necked flask in 15 minutes with magnetic stirring, the temperature being maintained between  $-50^{\circ}$  and  $-20^{\circ}$  in a bath of acetone cooled with Dry Ice. The mixture was allowed 1 hour to come to room temperature; then it was re-cooled and quenched with water. The ethereal solution of gem-dimethylallene was dried over magnesium sulfate, and pure gem-dimethylallene was collected by preparative VPC of the ethereal solution on a 10 ft. x  $\frac{3}{8}$  in. UCCW-982, 60/80 Chromosorb P column with helium flow =  $1 \text{ cm}^3/\text{second}$ , injector temperature =  $100^{\circ}$ , and the column at ambient temperature. 1 ml. of solution was purified, and the NMR of the collected pure gem-dimethylallene found to be identical to that of the last peak collected from the pyrolysis of VII.

Determination of Rate Constants and Kinetic Parameters for Thermal Rearrangement of VII

The kinetics of the rearrangement of VII were measured in a conventional static gas phase reactor of 200 ml. volume.<sup>7</sup> The reaction flask was enclosed in the air cavity of a hollow brass block heated by seven 200 watt CalRod heaters inserted into shafts drilled into the block. Temperature was controlled to within 0.1 °C with a Bayley model 253 proportional temperature controller connected to an eighth heater. The sensor of the controller was inserted into a well in the block and the block buried in diatomaceous earth for insulation.

Temperature was measured by inserting an iron-constantan thermocouple into a glass well built into the reactor; voltage was read on a Leeds and Northrup 8686 millivolt potentiometer. The procedure for removing aliquots was modified from that of Bergman and Carter.<sup>7</sup> Many variations and solvents were tried before the final technique was perfected.

Because of the volatility of VII, aliquots were condensed at 78°K in pyrex tubes, 50-100 microliters of acetone vacuum transferred into the tubes, and the tubes sealed under vacuum. For analysis, the ends of the sealed tubes were cooled in liquid nitrogen to condense the contents, the tube opened and placed in Dry Ice. The analyses were performed on a Hewlett-Packard 5750 VPC using a 25 ft. x  $\frac{1}{8}$  in. 25%  $\beta$ ,  $\beta'$ -oxydipropionitrile on 100/120 Chromosorb P column (Column J) at room temperature. A low temperature injection technique was employed, in which the 10 microliter syringe, quarter full of acetone, was cooled in liquid nitrogen prior to injection of 0.5-2.0 microliters

of the aliquot. Peaks for runs 6-14 were integrated with a Disc integrator on a Mosely recorder and, for successive runs, on a H-P 3370A automatic digital integrator. Analyses of each aliquot were performed a sufficient number of times so that the standard deviation of the mean of the ratio of VII to internal standard was less than 2%. No attempt was made to calibrate the response of the flame ionization detector of the Hewlett-Packard 5750.

The VII used in the kinetics experiments was shown by VPC on column J to contain less than 0.1% impurities of isoprene, gem-dimethylallene, and 1,1-dimethylcyclopropane, and no detectable impurity of isopropylacetylene. The pressure in the reaction flask was 50-100 torr, of which 40% was methylcyclopentane (Calbiochem, no impurities detected by VPC) as an internal standard.

The retention times of products and starting materials on J at 15 cm<sup>3</sup>/min Helium flow are

3,3-Dimethylcyclopropene (VII)	8 minutes
Methylcyclopentane (standard)	17 minutes
Gem-dimethylallene (All)	19 minutes
Isoprene (Iso)	21 minutes
Isopropylacetylene (Yne)	23 minutes

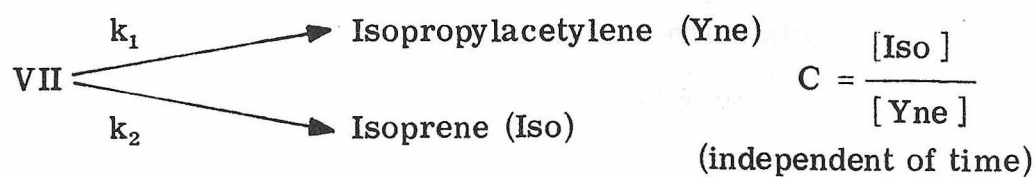
At room temperature, acetone remains unobtrusively on the column for at least four hours. During analyses, the column was periodically purged of acetone by flushing one hour at 100°C.

The contents of the reactor were allowed 10 to 30 minutes to equilibrate before a zero point was taken. In runs 6, 11, and 13, five points were taken beyond the zero point. In runs 8, 12, and 14, six points were taken beyond the zero point.

The rate of disappearance of VII was calculated as follows: the area of the peak corresponding to VII was divided by the area of the peak corresponding to the internal standard, methylcyclopentane, to give a quotient called [VII]. The natural logarithm of [VII]  $\times 10^3$  was determined, and the plot of the logarithm versus time was made. The slope of the plot and the concentration of VII extrapolated to zero time were calculated using a least squares program on an Olivetti Programma 101 desk calculator.<sup>70</sup> The least squares fits to the data points are shown in Figures 1-6. The value of the slope is  $k_{\text{obs}}$ , the first order rate constant for disappearance of VII.

Numbers called  $k_a$  and  $k_i$  were also calculated by the method of least squares. These numbers are the rates of appearance of isopropylacetylene and isoprene, respectively, and they represent independent calculations of the rate of disappearance of VII.

The numbers  $k_a$  and  $k_i$  do not represent the rates with which VII goes to the respective products. Those rates are represented by  $k_1$  and  $k_2$  in the kinetic scheme below (gem-dimethylallene, All, is neglected in the following expressions):



$$(1) \quad \frac{d[\text{VII}]}{dt} = -(k_1 + k_2) [\text{VII}] = k_{\text{obs}} [\text{VII}]$$

and

$$(2) \quad [\text{VII}] = [\text{VII}]_0 - [\text{Yne}] - [\text{Iso}]$$

Therefore

$$(3) \quad \frac{d[\text{Yne}]}{dt} = k_1 [\text{VII}] = k_1 \{ [\text{VII}]_0 - [\text{Yne}] - [\text{Iso}] \}$$

Substituting C,

$$(4) \quad \frac{d[\text{Yne}]}{dt} = k_1 \{ [\text{VII}]_0 - (1 + C)[\text{Yne}] \}$$

Integrating and applying initial conditions,

$$(5) \quad \ln [\text{VII}]_0 - \frac{1}{1 + C} \ln \{ [\text{VII}]_0 - (1 + C)[\text{Yne}] \} = k_1 t$$

Likewise

$$(6) \quad \ln [\text{VII}]_0 - \frac{1}{1 + C} \ln \left\{ [\text{VII}]_0 - \frac{1 + C}{C} [\text{Iso}] \right\} = k_2 t$$

However, it is also true that

$$(7) \quad k_1 = \frac{1}{1 + C} k_{\text{obs}}$$

and

$$(8) \quad k_2 = \frac{C}{1 + C} k_{\text{obs}}$$

Now, equations (5) and (6) represent calculations of  $k_1$  and  $k_2$  independent from the calculation of  $k_{\text{obs}}$ ; however, the value of C is needed in order to calculate  $k_1$  and  $k_2$  from the rates of product appearance. Since the application of equations (5) and (6) is quite involved, equations (7) and (8) are used to determine the values of  $k_1$  and  $k_2$ ; clearly, such a determination of  $k_1$  and of  $k_2$  is not independent from the determination of  $k_{\text{obs}}$ .

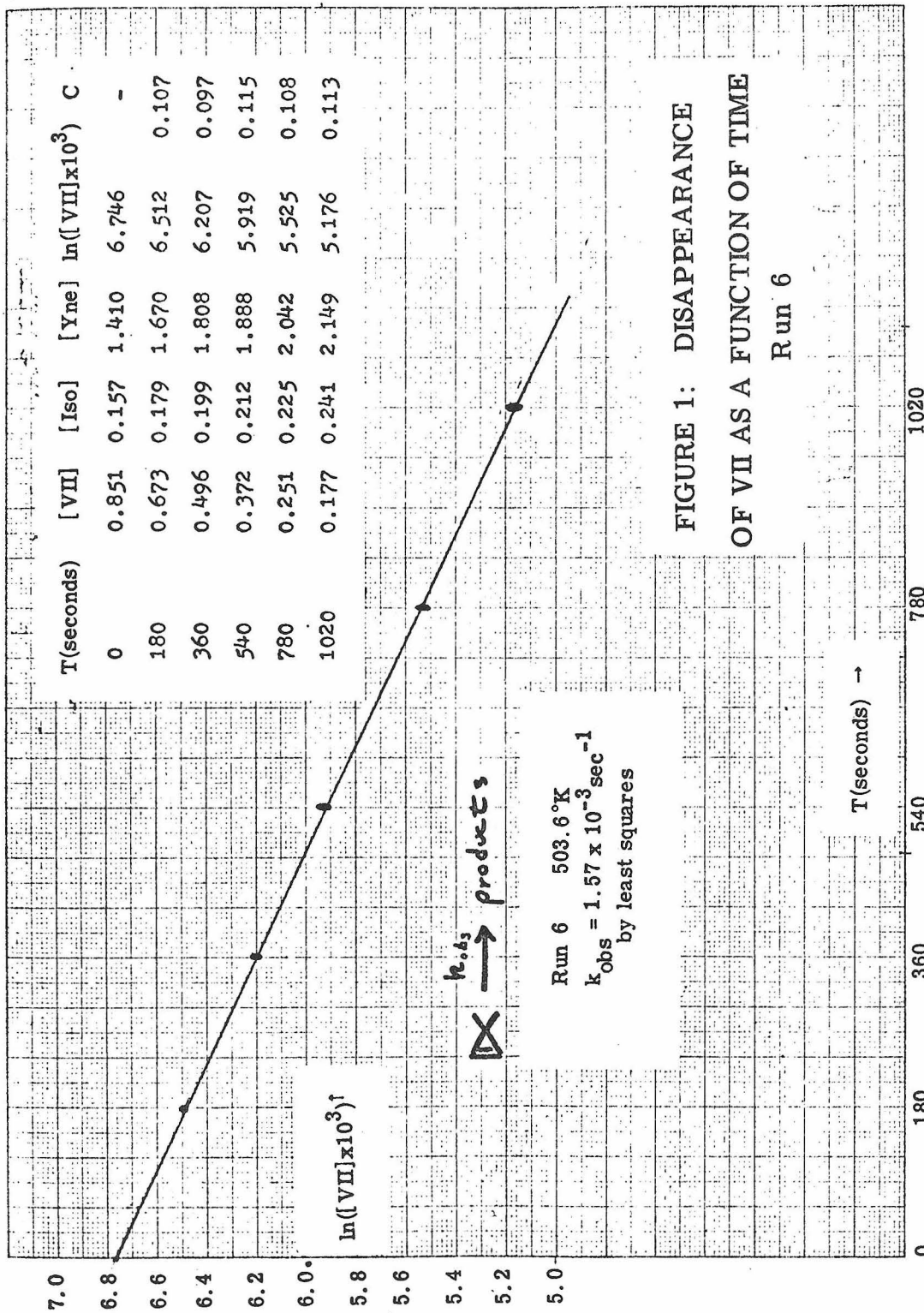


FIGURE 1: DISAPPEARANCE  
 OF VII AS A FUNCTION OF TIME  
 Run 6

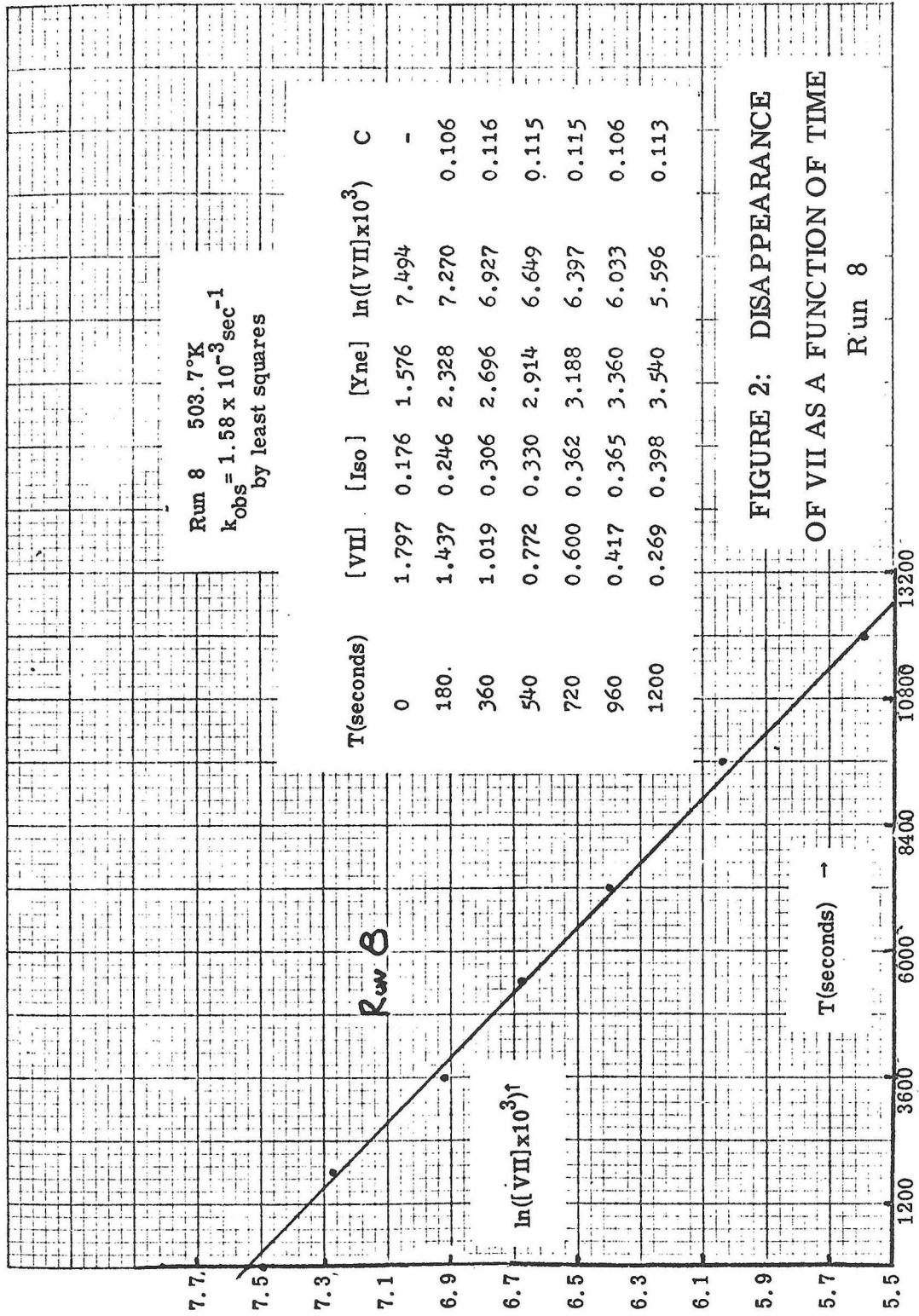


FIGURE 2: DISAPPEARANCE  
 OF VII AS A FUNCTION OF TIME  
 Run 8

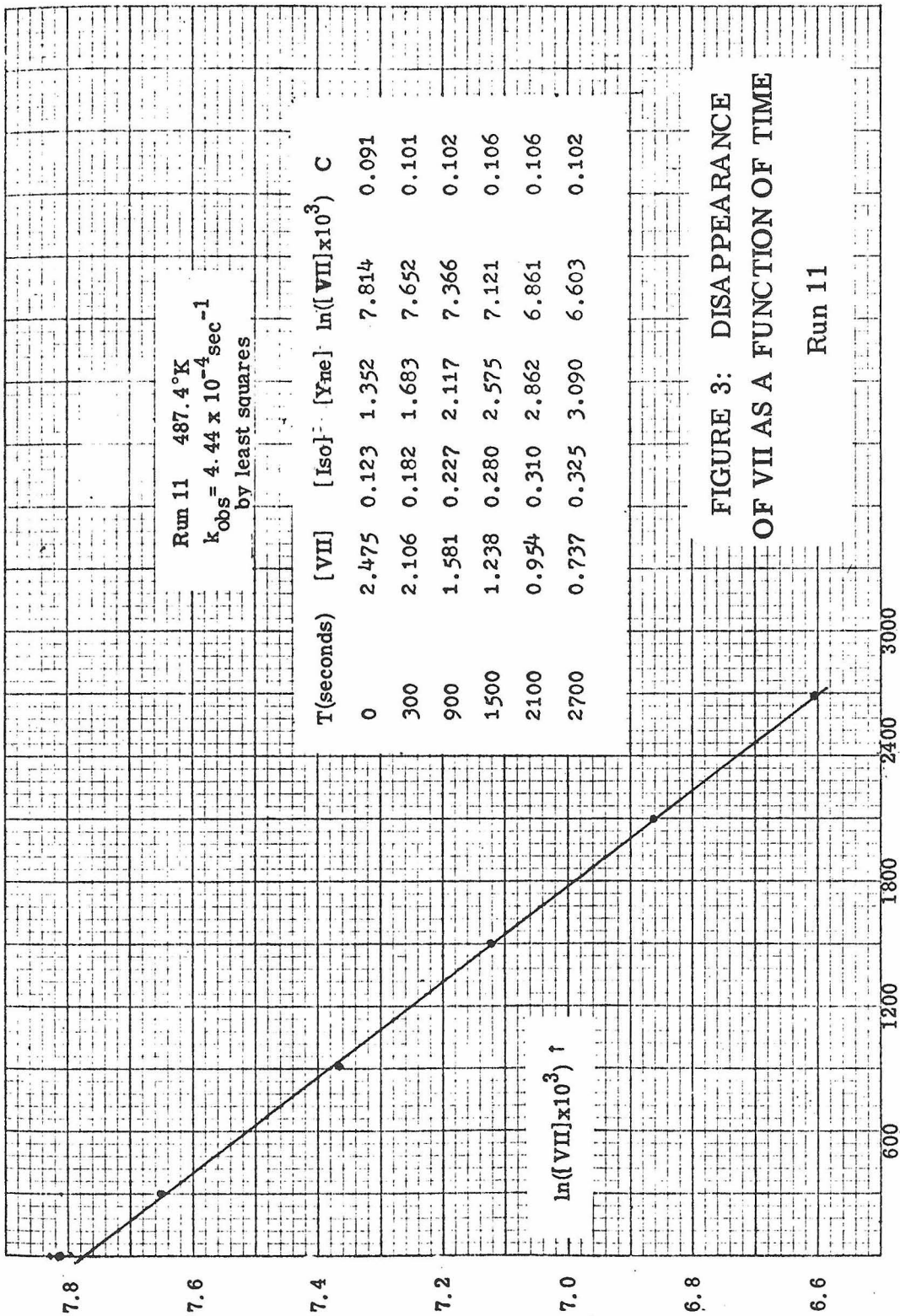


FIGURE 3: DISAPPEARANCE OF VII AS A FUNCTION OF TIME

Run 11

T(seconds) →

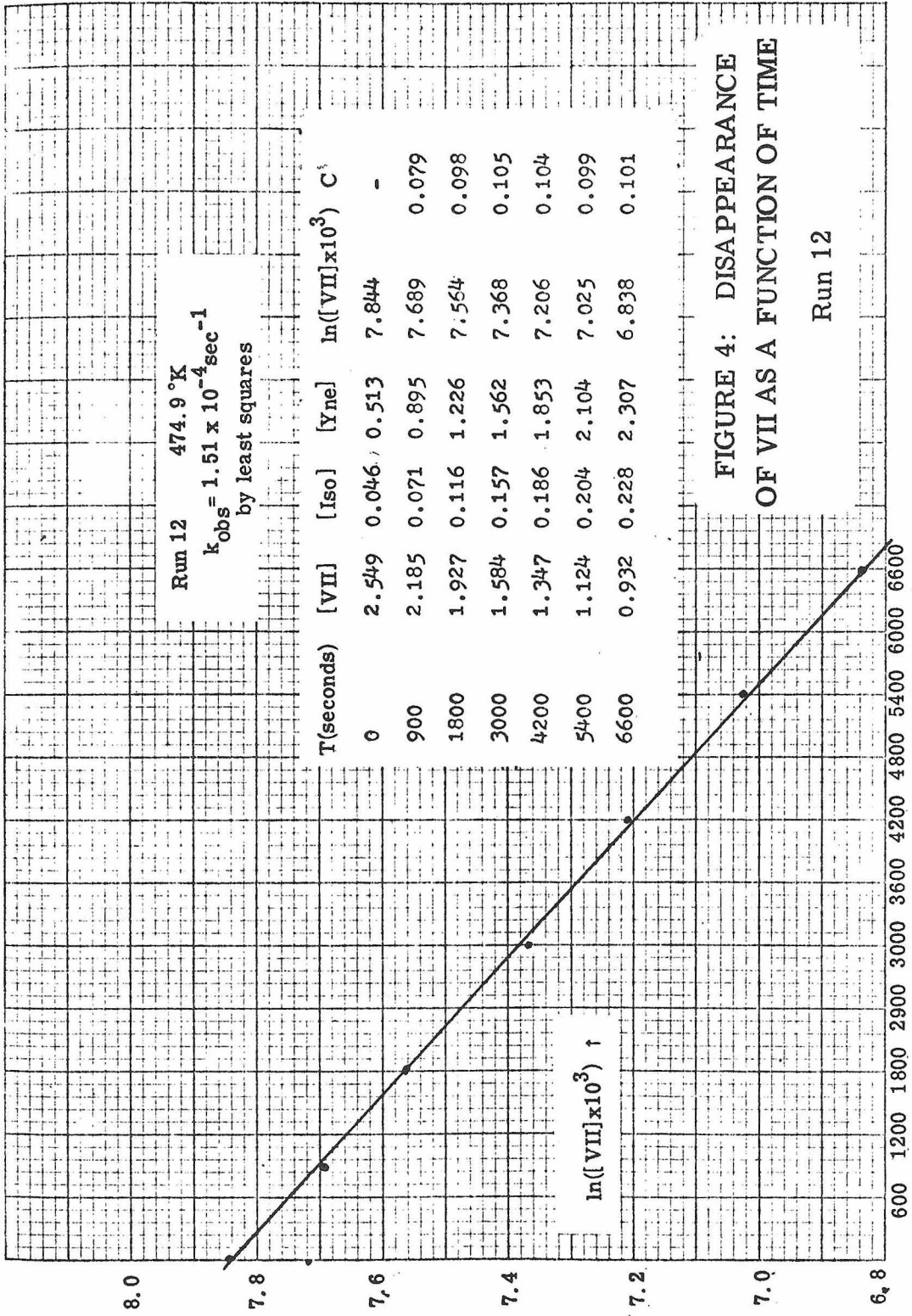


FIGURE 4: DISAPPEARANCE OF VII AS A FUNCTION OF TIME

Run 12

T(seconds) →

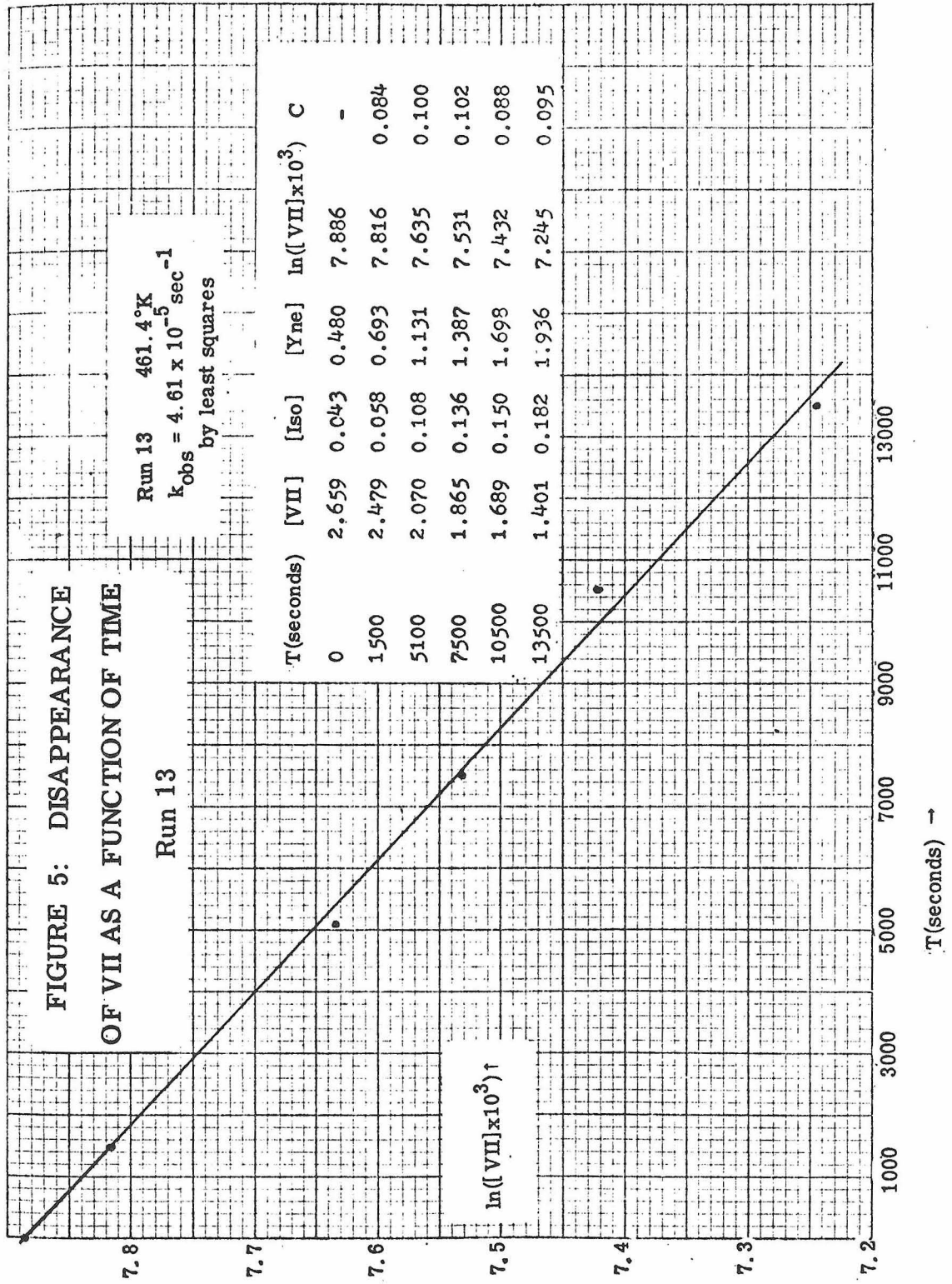
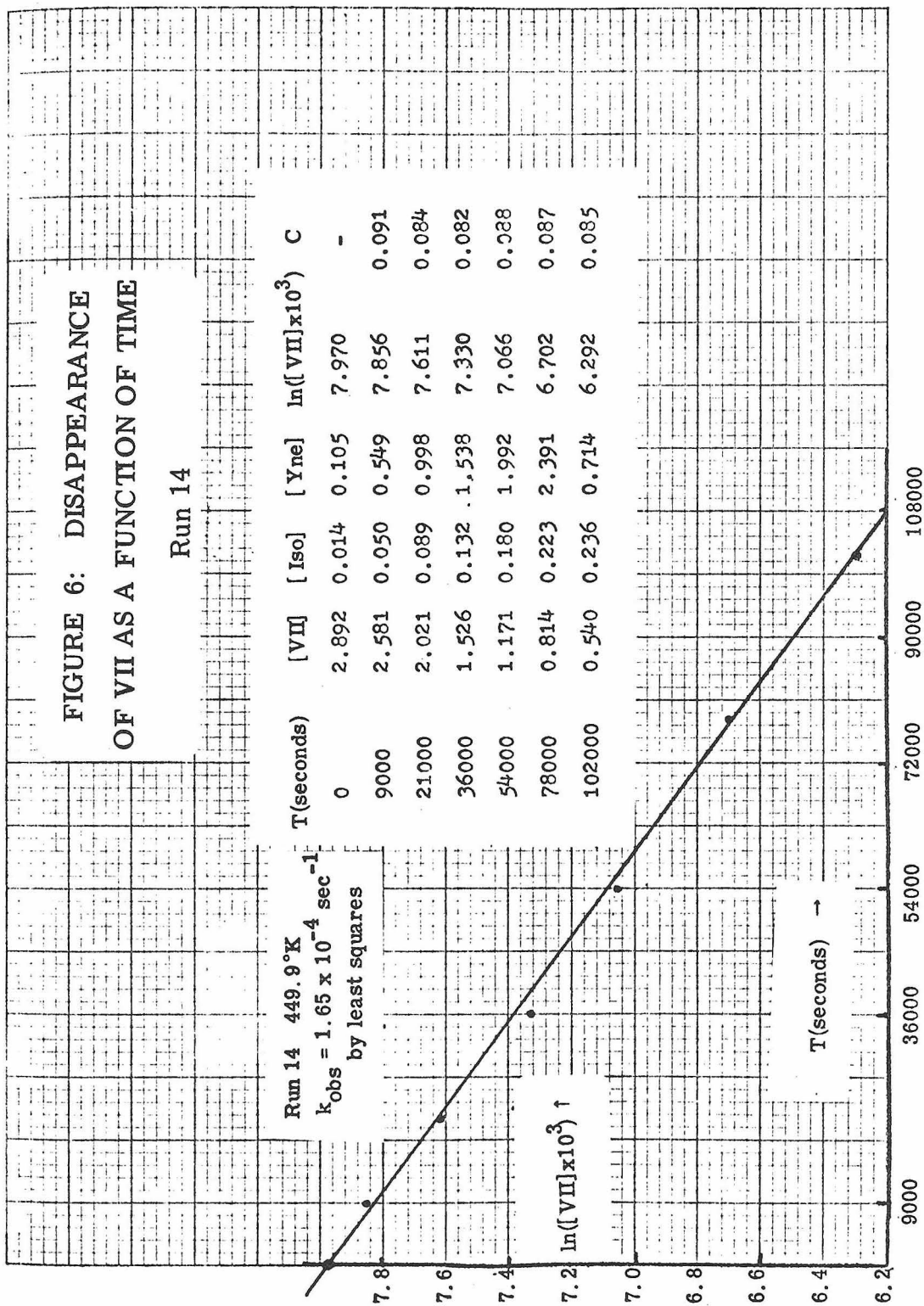


FIGURE 6: DISAPPEARANCE  
OF VII AS A FUNCTION OF TIME

Run 14



The rates of product appearance are used for the calculation of  $k_a$  and  $k_i$ . As remarked above, these numbers represent calculations of rate of disappearance of VII independent from the calculation of  $k_{obs}$ . Since the purpose of calculations from product appearance rates is merely to ascertain that products are not appearing at a rate inconsistent with the rate of disappearance of starting material, we feel that this application of the product appearance rates is justified. The derivation below demonstrates how  $k_a$  and  $k_i$  constitute independent calculations of the rate of disappearance of VII.

$$(9) \quad [VII] = \left( \frac{C}{1+C} \right) [VII] + \left( \frac{1}{1+C} \right) [VII]$$

Hence

$$(10) \quad \frac{d[VII]}{dt} = \frac{d}{dt} \left\{ \left( \frac{1}{1+C} \right) [VII] \right\} + \frac{d}{dt} \left\{ \left( \frac{C}{1+C} \right) [VII] \right\}$$

But,

$$(11) \quad \left( \frac{1}{1+C} \right) [VII] = [Yne]_{\infty} - [Yne]$$

And

$$(12) \quad \left( \frac{C}{1+C} \right) [VII] = [Iso]_{\infty} - [Iso]$$

Define

$$(13) \quad k_a \{ [Yne]_{\infty} - [Yne] \} = \frac{d}{dt} \{ [Yne]_{\infty} - [Yne] \}$$

and

$$(14) \quad k_i \{ [Iso]_{\infty} - [Iso] \} = \frac{d}{dt} \{ [Iso]_{\infty} - [Iso] \}$$

Therefore, by substituting and rearranging terms,

$$(15) \quad \frac{d[VII]}{dt} = k_a \{ [Yne]_{\infty} - [Yne] \} + k_i \{ [Iso]_{\infty} - [Iso] \}$$

But, also, from (1), (9), (11), and (12)

$$(16) \quad \frac{d[VII]}{dt} = k_{obs} \{ [Yne]_{\infty} - [Yne] + [Iso]_{\infty} - [Iso] \}$$

That is,

$$(17) \quad k_{obs} \{ [Yne]_{\infty} - [Yne] + [Iso]_{\infty} - [Iso] \} = k_a \{ [Yne]_{\infty} - [Yne] \} + k_i \{ [Iso]_{\infty} - [Iso] \}$$

Since this must be true for all concentrations of products, then

$$(18) \quad k_{obs} = k_a = k_i$$

Integrating (13) and applying boundary and initial condition,

$$(19) \quad \ln \{ [Yne]_{\infty} - [Yne] \} - \ln [Yne]_{\infty} = k_a t$$

Likewise, from (14), get

$$(20) \quad \ln \{ [Iso]_{\infty} - [Iso] \} - \ln [Iso]_{\infty} = k_i t$$

Tables 6 and 7 give an idea of the precision and accuracy of  $k_{obs}$ .

Table 6: Precision of  $k_{\text{obs}}$  \*

Run #	% Deviation of Calc'd Zero from Expt'l Zero	# of Half Lives Spanned	Empirical Correlation Coefficient
6	+2%	2.3	0.99954
8	+2%	2.7	0.99916
11	-2%	1.7	0.99938
12	-1%	1.4	0.99973
13	0-%	0.96	0.99730
14	0-%	2.4	0.99912

Table 7: Rate Constants Calculated from  
Product Appearance Rates

Run #	$k_a$	$k_i$	% Deviation from $k_{\text{obs}}$		Ratio $k_i / k_a$
			$k_a$	$k_i$	
6	$1.47 \times 10^{-3}$	$1.62 \times 10^{-3}$	-6%	-3%	1.10
8	$1.46 \times 10^{-3}$	$1.42 \times 10^{-3}$	-8%	-10%	0.97
11	$4.48 \times 10^{-4}$	$4.52 \times 10^{-4}$	+1%	+2%	1.01
12	$1.49 \times 10^{-4}$	$1.45 \times 10^{-4}$	-1%	-4%	0.97
13	$4.77 \times 10^{-5}$	$4.45 \times 10^{-5}$	+3%	-4%	0.93
14	$1.69 \times 10^{-5}$	$1.74 \times 10^{-5}$	+2%	+5%	1.03

\* Values of  $k_{\text{obs}}$  tabulated above in Table 4.

Table 8: Values of  $\bar{C}$

Run #	$\bar{C}$	Slope of $\bar{C}$ in minutes <sup>-1</sup>	# of points averaged	$\ln \bar{C}$	$1/T$
6	0.108	0.001	4	-2.226	$1.985 \times 10^{-3}$
8	0.113	-0.0004	5	-2.181	$1.985 \times 10^{-3}$
11	0.103	0.00006	5	-2.273	$2.052 \times 10^{-3}$
12	0.101	0.000000	5	-2.293	$2.106 \times 10^{-3}$
13	0.096	-0.00006	4	-2.344	$2.167 \times 10^{-3}$
14	0.085	0.000002	5	-2.465	$2.222 \times 10^{-3}$

The ratio,  $C$ , of the two principal products, isoprene and isopropylacetylene, was found to vary with temperature. The value for each run was determined using the least squares program as follows. The concentration of the products of the zero time aliquot (ie.  $[Yne]_0$ , the ratio of the area of the peak for isopropylacetylene to the area of the internal standard peak and  $[Iso]_0$ , ratio of the area of the peak for isoprene to the area of the internal standard peak) was subtracted from the product concentrations of succeeding aliquots. The ratio,  $C_i = ([Iso]_i - [Iso]_0) / [Yne]_i - [Yne]_0$  for each  $i^{th}$  aliquot, was fed into the least squares program as the values for the ordinate, with the corresponding abscissa being the time,  $t_i$ , at which the aliquot was taken. Thus, the program computed a weighted average of the ratios for each run, that is  $\bar{C} = \sum_i C_i t_i / \sum_i t_i$ . Ordinarily, the first value of  $C_i$  after the  $t_0$  aliquot was discarded, since not enough product had been formed for this value to be at all reliable.

Along with the calculation of  $\bar{C}$ , the least squares program also determined a slope for the graph of  $C$  as a function of time. This slope was always very close to zero, permitting the conclusion that the value  $\bar{C}$  was truly time independent, shown in Table 8.

The product mixture was found to be stable under the reactor conditions for indefinite periods of time. Isoprene is expected to be the most thermodynamically stable of the three products; indeed, a BASF process for preparing isoprene uses a 40-50 mm. vacuum flow system through an alumina catalyst at  $400^\circ$  to obtain a 50% yield of isoprene from isopropylacetylene.<sup>71</sup> Similarly, gem-dimethyl-

allene (XXI) is converted in nearly 100% yield to isoprene at 300° over alumina.<sup>72</sup>

Table 9 summarizes data acquired by Y. M. Slobodin in the USSR in 1934<sup>72</sup> using a flow system over activated "Floridin" as a catalyst.

The concentration of gem-dimethylallene in the products of pyrolysis of VII in the unpacked reactor was at a limit of our ability to integrate. As a consequence, only an order of magnitude for the ratio [All]/[Iso] was measured. The range of our reproducibility for this ratio on a given aliquot was from 1:30 to 1:70, and all measurements of the ratio over the temperature span fell within this range.

Because of the possibility that our product distribution arose from the rearrangement of gem-dimethylallene, an authentic sample of gem-dimethylallene was introduced into the reactor at 229°C. After 2 hours in the reactor (17 halflives for rearrangement of VII), the concentration of gem-dimethylallene was within 2% of the initial concentration, and the formation of no other products was detected.

The thermocouple used for temperature measurements was calibrated by the freezing curves of three pure metals, shown in Table 10. These voltage corrections correspond to a correction in the measured temperature of +0.2° to +0.6°C in the temperature range. Including these corrections has a negligible effect upon the slope and intercept of an Arrhenius plot; consequently, the values of  $1/T_{\text{measured}}$  are used for the abscissa rather than using values with interpolated corrections.

Table 9: Equilibration of C<sub>5</sub>H<sub>8</sub> Isomers Over Floridin<sup>72</sup>

Reactant	Flow Rate (g/min)	Temperature	Product Ratios	% Recovered Starting Material	% Polymer
Isopropylacetylene	0.48	270 °C	All/Yne = 0.08000	--	5%
			Iso/Yne = 0.001081		
gem-Dimethylallene	0.26	215 °C	Iso/All = 0.04451	61.8%	14%
			Yne/All = 0.3463		
"	0.23	232 °C	Iso/All = 0.2068	35.6%	19%
			Yne/All = 1.066		
"	0.23	280 °C	Iso/All = 0.6135	21.8%	33%
			Yne/All = 1.454		
"	0.3	300 °C	Iso/All = 0.9852	12.2%	40%
			Yne/All = 2.941		

Table 10: Calibration of Thermocouple

Metal	# of Trials	Stated Purity	Freezing Point	Correction (mV)
Indium	3	99.97+%	156.6 °C	+ 0.04 mV
Tin	4	99.98+%	231.9 °C	+ 0.02 mV
Lead	1	--	327.3 °C	+ 0.04 mV

The slope, intercept, error, and correlation coefficient of the Arrhenius plot were determined by the same least squares program and methods of computation as the rate constants. The fit of the least squares values to the data is shown in Figure 7.

Using the group additivity method of Benson,<sup>73</sup> the heat of formation of isopropylacetylene at 230 °C is estimated to be 39 kcal/mole. By the same method, the heat of formation of isoprene is estimated to be 24 kcal/mole. Since the value of  $S_0$  at 298 °K for isopropylacetylene is estimated by this method to be 102.5 e.u., and the value estimated for isoprene is 80.7 e.u., and since the estimated heat capacities are within 1 e.u. of one another, the estimated free energy difference between isopropylacetylene and isoprene at 500 °K is about 4 Kcal/mole.

From this estimation, and from the stability of the products to the reactor conditions, it is reasonable to assume that the product distribution observed is the reflection of the relative rates,  $k_1$  and  $k_2$ , by which VII goes to isopropylacetylene and isoprene. Thus, the value  $\bar{C}$  is indeed the ratio  $\frac{k_2}{k_1}$ , and a pseudo-Arrhenius plot of  $\ln \bar{C}$

Note on Figures 7 and 8:

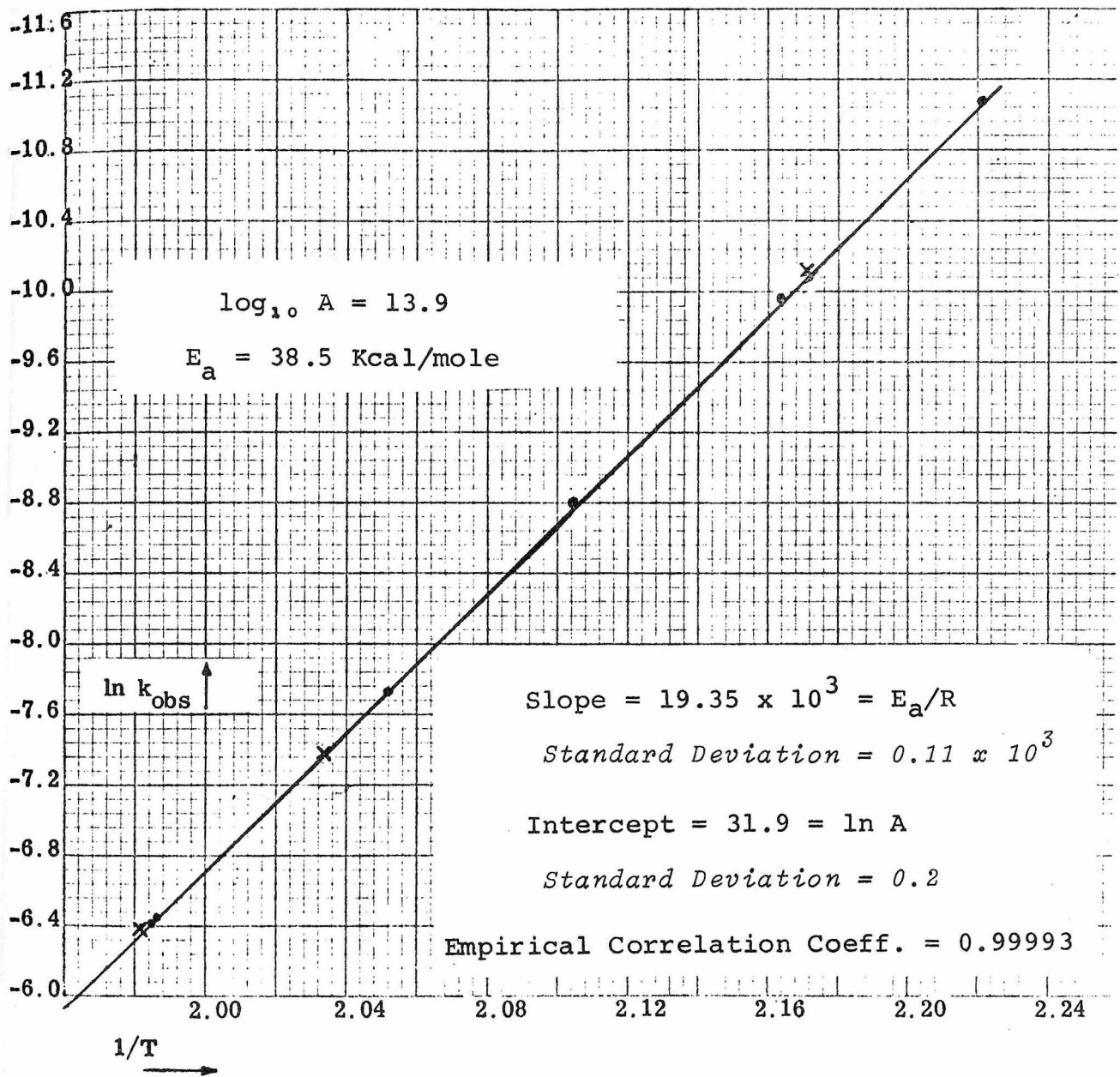
Points marked with • are from Runs 6, 8, 11-14 (unpacked Pyrex bulb).

Points marked with × are from Runs 19-21 (unpacked Quartz bulb).

Arrhenius Parameters: for disappearance of 3,3-dimethylcyclopropene:

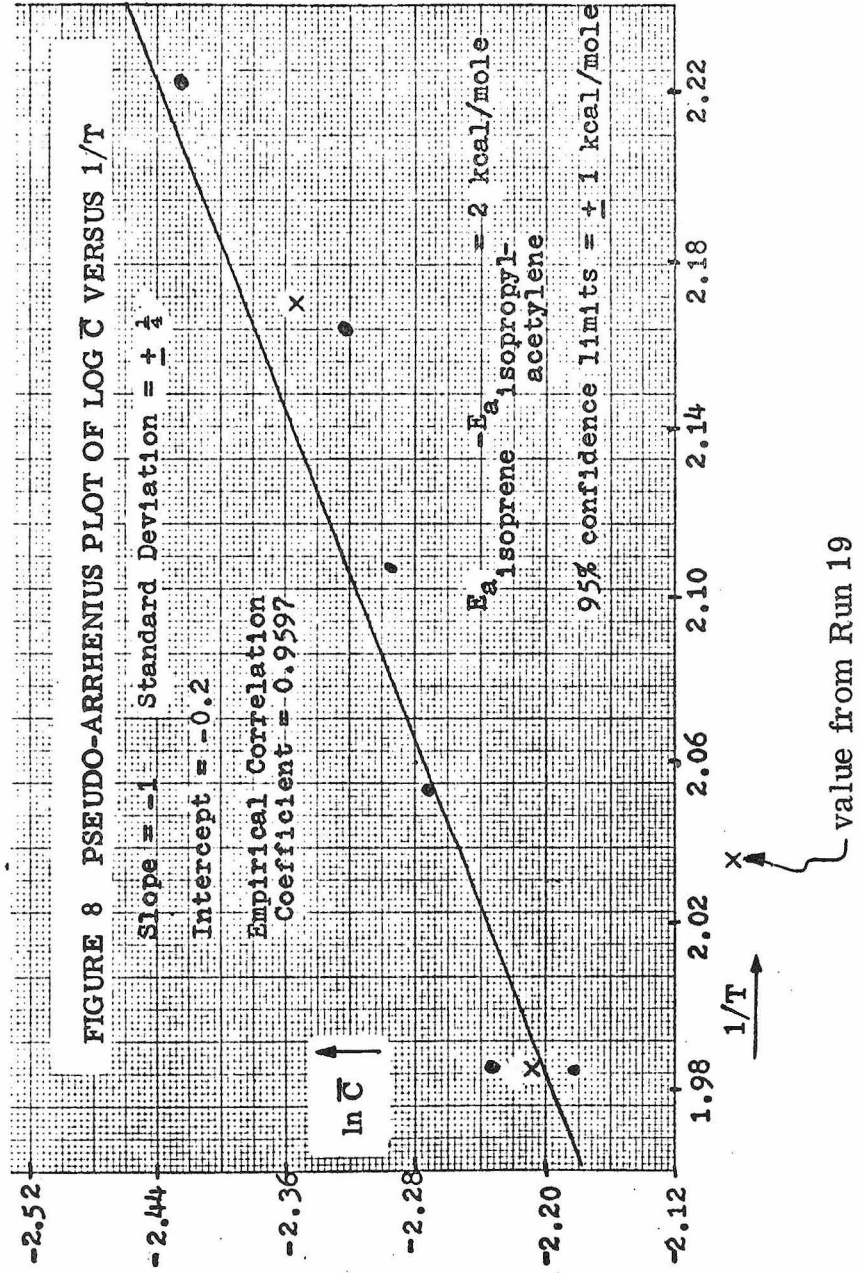
$E_a = 38.5$ Kcal/mole	95% confidence limits $\pm 0.5$ Kcal
$\log_{10} A = 13.9$	95% confidence limits $\pm 0.2$
$\Delta S^\ddagger = 2$ e.u.	95% confidence limits $\pm 1$ e.u.

FIGURE 7: ARRHENIUS PLOT OF THE RATE OF DISAPPEARANCE OF 3,3-DIMETHYLCYCLOPROPENE



Error in  $\ln A$  and in  $E_a$  due to uncertainty in individual values of  $k_{\text{obs}}$  is negligible. Error in  $\ln A$  due to uncertainty in temperature is 0.1 and in  $E_a$  is less than 0.4%.

FIGURE 8: PSEUDO-ARRHENIUS PLOT OF LOG  $\bar{C}$  VERSUS 1/T



versus  $1/T$  should yield as its intercept the logarithm of the ratio of the pre-exponential factors of  $k_2$  and  $k_1$ . The slope of the plot should have the value  $(E_{a_{\text{Iso}}} - E_{a_{\text{Yne}}})/R$ . The values of these parameters were determined by the least squares program, and the fit of the least squares curve to the data is shown in Figure 8. The pre-exponential factors for  $k_1$  and  $k_2$  are within experimental error of one another.

### Packed Reactor Pyrolyses and Surface Effect Studies

Our first packed reactor system was a 200 ml. Pyrex bulb identical to the unpacked reactor bulb described above, having a surface-to-volume ratio of 1:1, packed with  $\frac{1}{2}$  - 2 cm. lengths of 3-10 mm. Pyrex tubes. The resulting reactor had a surface-to-volume ratio of 10:1. M. B. D'Amore, working in these laboratories, found that the rate of the isomerization of trans-diethynylcyclopropane to [3.2.0]-bicyclohepta-1,4,6-triene ( $E_a = 42.6$  kcal/mole;  $\Delta S^\ddagger = 8.5$  e.u.) was unchanged in this packed reactor relative to the unpacked reactor, but that the rate of isomerization of cis-diethynylcyclopropane to the same product ( $E_a = 23$  kcal/mole;  $\Delta S^\ddagger = -18$  e.u.) was increased 80% in the packed reactor. In this latter case, D-Amore was unable to observe any product in the analysis of his aliquots; this occurred despite the facts that (1) rate of product formation corresponded to within 25% of the rate of starting material disappearance in both the cis and trans in the unpacked reactor and trans in the packed reactor, (2) although the product triene was unstable in the reactor (apparently polymerized), the halflife for its disappearance was more than twice that of the diethynylcyclopropanes. <sup>74</sup>

3, 3-Dimethylcyclopropene (VII) polymerized in this packed reactor. Despite attempts to condition the reactor with isoprene, isopropenyl acetylene, and 1, 5-hexadiyne, introduction of ca. 60 torr VII into the reactor at 230°C produced a smoky aerosol containing a yellow polymer. VPC analysis of this liquid dissolved in acetone showed the presence of the three products of pyrolysis of VII in the ratio 25:7:1 (Yne:Iso:AlI), and that this mixture was stable in the packed reactor.

At the suggestion of D. Golden,<sup>75</sup> an attempt was made to condition the reactor with Teflon. Teflon monomer was generated by the pyrolysis of Teflon tape in the vacuum system, and the monomer was then polymerized by introduction of benzoyl peroxide and AIBN into the system. Although Teflon polymer was observed to have formed in the reactor vessel, the polymerization of VII did not abate, nor did the product ratio come closer to that for the unpacked reactor.

At this juncture, it was suspected that a surface effect may have been operative in the Pyrex unpacked reactor, so the kinetics were repeated in a quartz reaction flask. The following Table 11 indicates the results from runs in an unpacked quartz reactor; and the fit of the least squares calculation to the data points is shown in Figures 9-11.

The quartz reaction flask was conditioned with isopropenyl acetylene before run 19, and the high value for  $\bar{C}$  in this run may be attributable to the fact that the reactor was not sufficiently conditioned. Run 20 was found to have its first point (zero point) to be far off the line (extrapolated zero 16% higher than the experimental zero). A

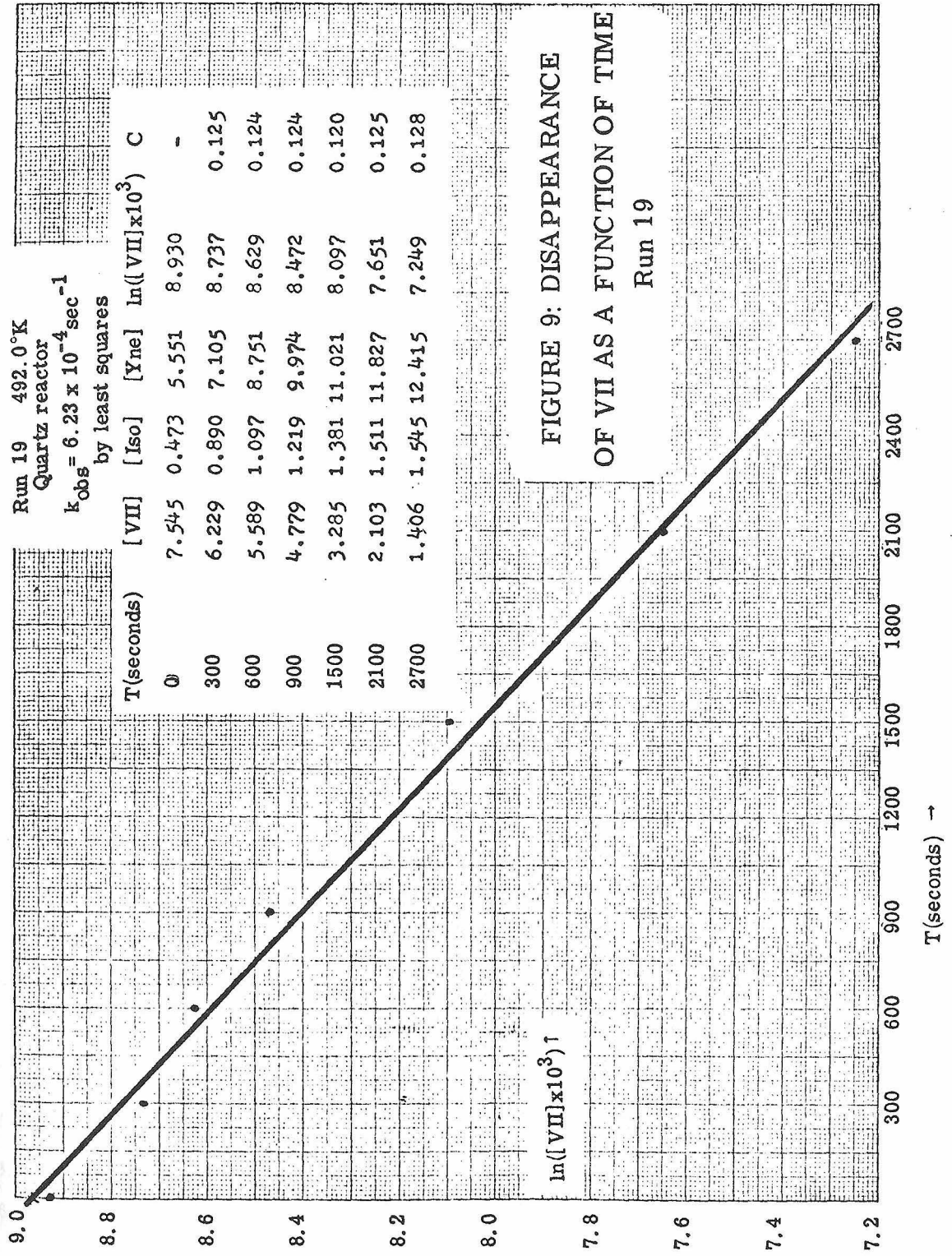


FIGURE 10: DISAPPEARANCE OF VII AS  
A FUNCTION OF TIME - Run 20

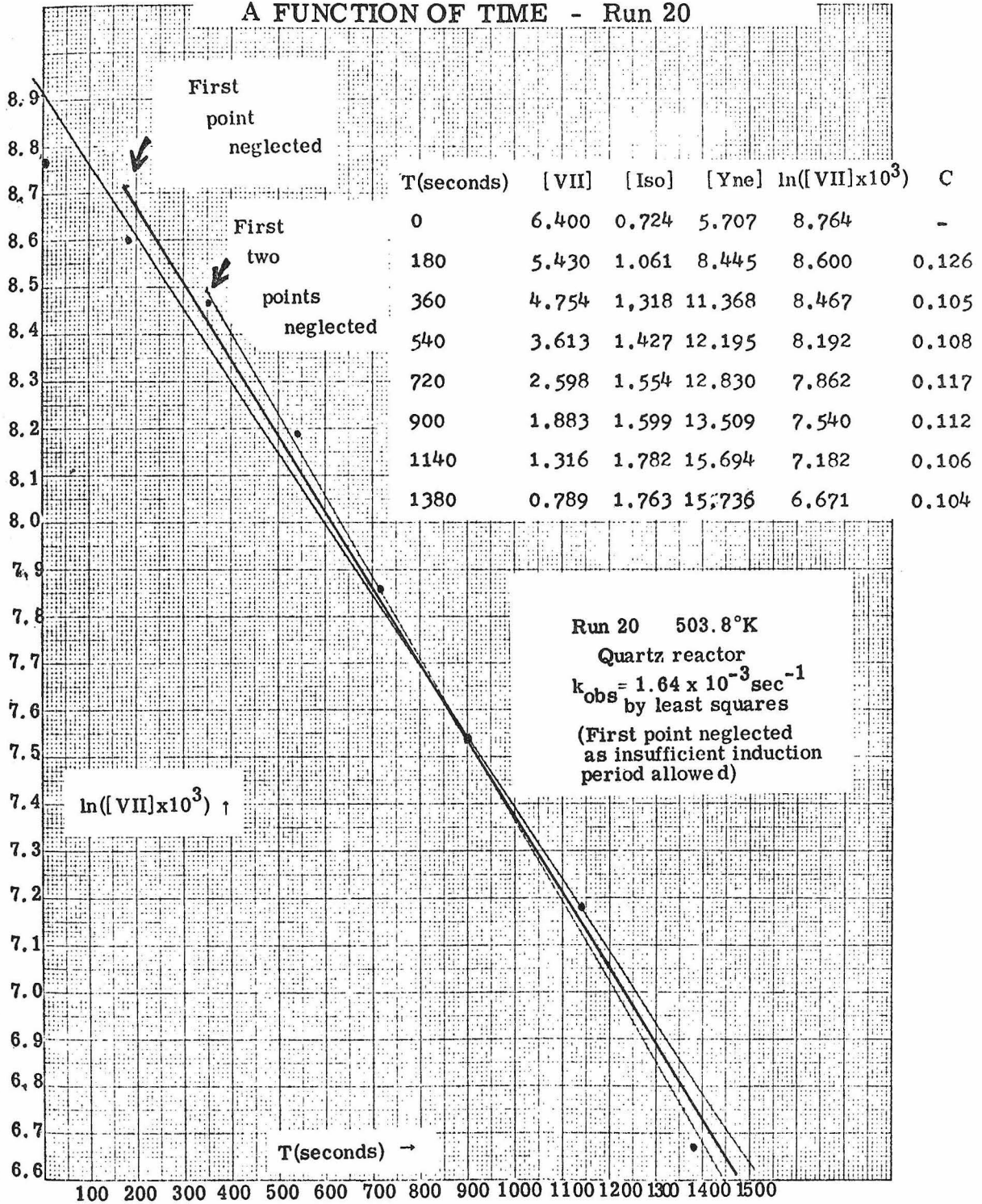


FIGURE 11: CONTROL RUN - - -  
DISAPPEARANCE OF VII AS A FUNCTION  
OF TIME - Runs 21 and 24

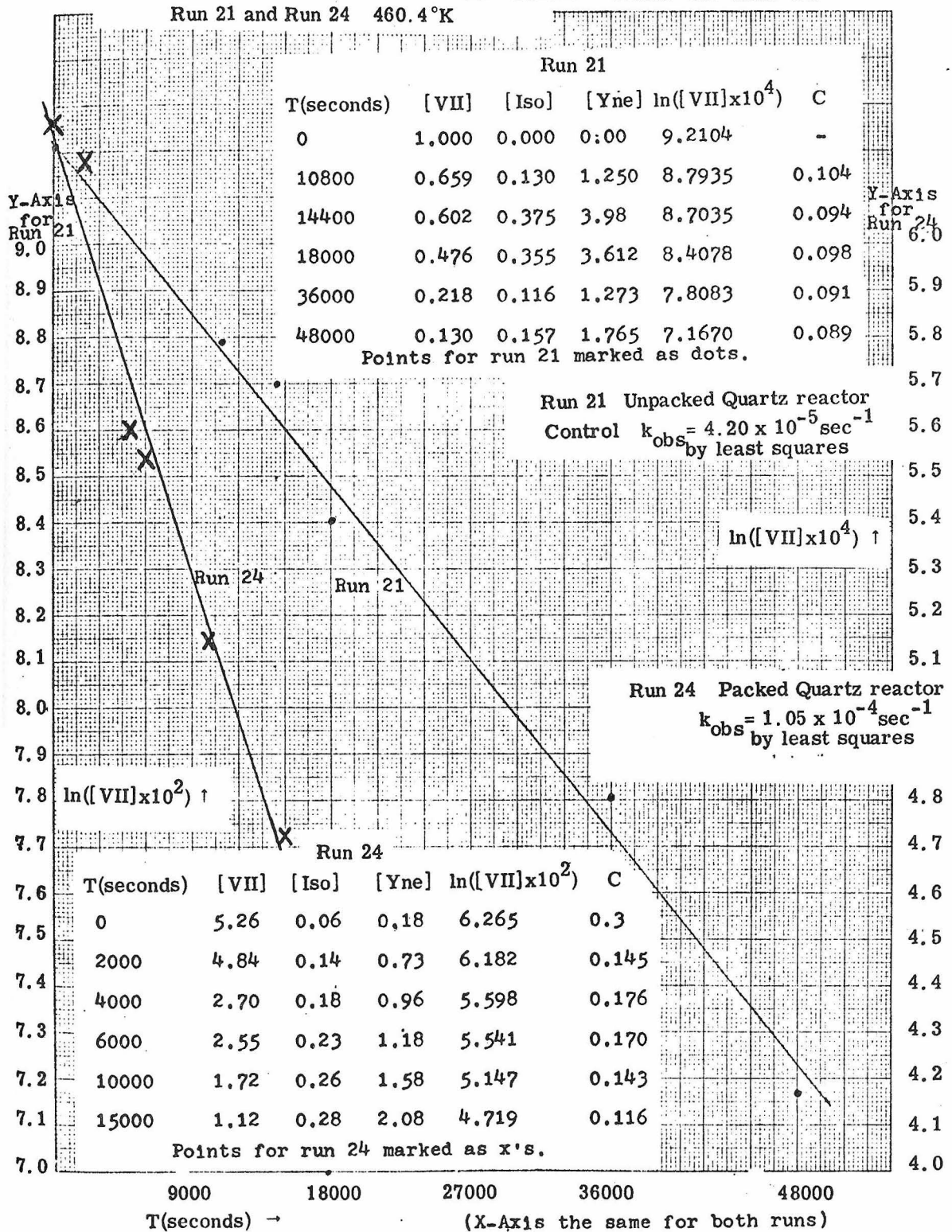


Table 11: Thermal Rearrangement of VII in a Quartz Reactor<sup>a</sup>

Run #	Measured Temperature	# of Half Lives Spanned	$k_{obs}$	$\bar{C}$	# of points for calc. of $\bar{C}$
19	492.0°K	2.4	$6.23 \times 10^{-4}$	0.124	6
20	503.8°K	2.9	$1.64 \times 10^{-3}$	0.109	6
21	460.4°K	2.9	$4.20 \times 10^{-5}$	0.095	5

<sup>a</sup> Runs 15 - 18 were performed in a quartz vessel connected to the vacuum line with a ground glass joint. It was found to give rise to anomalous values for the rate constant both for the rearrangement of VII and for M. B. D'Amore's trans-diethynylcyclopropane. Ultimately the cause for these anomalous values was assigned to a slow leak in the joint, and the runs 19 - 21 were performed in a quartz reactor of different design. Run 24 was performed in a packed quartz reactor with surface-to-volume ratio of  $> 4.5:1$  (vide infra).

similar sort of behavior was observed in run 6, and, in both runs, the first point was discarded as a zero point and the second point used. This was justified on the basis that the 6 minute induction period allowed in these runs was not sufficient.

Before run 21 was performed, the quartz reactor flask was conditioned with Dow-Corning 705 oil using the method of Benson and Egger.<sup>75</sup> Run 21 was a control run designed to verify the accuracy of our sampling technique. Instead of using 50 Torr VII and taking periodic aliquots, we performed run 21 by taking a series of one point rate constants. From 17 to 35 Torr of VII with internal standard was introduced into the entire system with the vacuum pump stopcock closed. After allowing 5 minutes for equilibration, the reactor flask was sealed off from the rest of the system, and the contents of the unheated portion of the system were condensed for a  $t_0$  sample. After from 180 to 800 minutes had elapsed from the closing of the heated vessel, the stopcock was opened and the entire contents of the flask allowed 5 minutes to condense for a  $t_1$  sample.

The points marked X on the Arrhenius plots in Figures 7 and 8 correspond to runs 19-21. In the plot of  $\ln(k_{obs})$ , these points fall very close to the line, whereas the plot of  $\ln(\bar{C})$  shows a profound deviation for run 19.

A quartz reactor was packed with 150 one centimeter lengths of 7 mm. O. D. quartz tubes. The ends of the tubes were fire polished, and their total surface area was greater than 600 cm.<sup>2</sup> The addition of these tubes to the 200 cc. bulb increased the surface-to-volume ratio from 1 to greater than 4.5.

The conditioning procedure using Dow-Corning 705 was followed;<sup>75</sup> however, polymer formation was still observed in this packed reactor upon the addition of 50 mm. VII at 500°K, as evidenced by the formation of a smoky aerosol. The rearrangement products were found to have the ratio 35:7:1 (Yne:Iso:All).

The conditioning procedure with Dow-Corning 705 was repeated until no further change in product distribution was observed; this required six conditionings, and the product ratio ultimately achieved was 108:12:1 (Yne:Iso:All). Aerosol was still being observed, so the reactor was further conditioned at 370°K with 3-hexene-1,5-diyne,<sup>76</sup> a hydrocarbon well-known to polymerize readily. After this conditioning, the aerosol still persisted, and the product ratio was found to have changed to 64:8:1 (Yne:Iso:All). The value for  $k_{\text{obs}}$  at 460.4° in this reactor with 50 Torr of VII was found to be 6 times greater than the value for  $k_{\text{obs}}$  in the unpacked reactor. Strangely, no matter what precautions were taken, a pressure of several Torr refused to condense in liquid nitrogen at the end of a run.

The reactor was then conditioned with an excess of VII. 0.7 g. was introduced into the reactor at 508°K and left overnight. An enormous amount of polymer was produced, and although the products of the rearrangement could be collected, there was again an appreciable partial pressure (greater than 50 Torr) of gas in the system that would not condense in liquid nitrogen.

The reactor was conditioned a second time with 0.7 g. VII, and again copious amounts of polymer were formed. An appreciable uncondensable pressure was again observed, and the product ratio

from the rearrangement of VII was 75:7:1 (Yne:Iso:All).

At this point, we decided to investigate how successful the conditioning procedure had been. 50 Torr of VII with internal standard was heated in the reactor for 50 minutes at 460°K. The concentration of VII was found to have diminished to 8% of its initial concentration, whereas the half-life at this temperature was 12 hours in an unpacked reactor.

The system was evacuated and closed off from the vacuum; the reactor was heated at 700°K for 3 days. Polymer was seen to reflux in the stem of the reactor, and, following this treatment, the reactor temperature was returned to 460°K. 60 Torr VII with internal standard was introduced into the system with the vacuum closed off. The pressure was monitored and was found to have fallen to 30 Torr in one hour. After another 80 minutes, the pressure was still the same; the contents of the reactor were condensed (with a few Torr of uncondensable pressure), and the product ratio from rearrangement of VII was found to be 0.7:1.7:1 (Yne:Iso:All).

At this juncture, we felt it useful to examine the behavior of VII in solution. Consequently, an 8% solution of VII in ethylbenzene with internal standard was heated for 25 minutes at 496°K in a quartz tube. The VII in the solution was found to have disappeared entirely, and only a tiny amount of product was detected. We concluded that the polymerization of VII was enhanced in condensed phases.

Since Srinivasan had been able to overcome polymerization problems by using low partial pressures of cyclopropene,<sup>14</sup> we decided to examine the rate using a few Torr of VII diluted with

neopentane. At 457°K and a 5 Torr partial pressure of VII with 45 Torr neopentane, the ratio of VII to internal standard was found to diminish to 10% of its initial value in 3 hours. Because of our experience with VII in ethylbenzene solution, we concluded that polymerization might be enhanced by the presence of liquid polymer, and that reasonable rates might be observed upon removal of polymer from the reaction bulb.

The bulb was washed out with carbon tetrachloride and dried. An attempt to gather kinetic data using one point rate constants (cf. run #21) was unsuccessful, owing to the irreproducibility of the results.

A run was then performed using our aliquot technique on 1.5 Torr VII plus internal standard with 20 Torr neopentane diluent (run 24). The results of run 24 are tabulated above in Table 11. Whereas all of our runs in unpacked reactors showed empirical correlation coefficients greater than 0.995, the empirical correlation coefficient for run 24 was 0.977. Moreover, the value for  $k_a$  was  $2.0 \times 10^{-5} \text{ sec}^{-1}$ , and our conclusions are twofold:

(1) Despite all our efforts at conditioning, even a 1.5 Torr partial pressure of VII polymerizes at a rapid rate in our packed reactor, and

(2) The product distribution may be surface dependent.

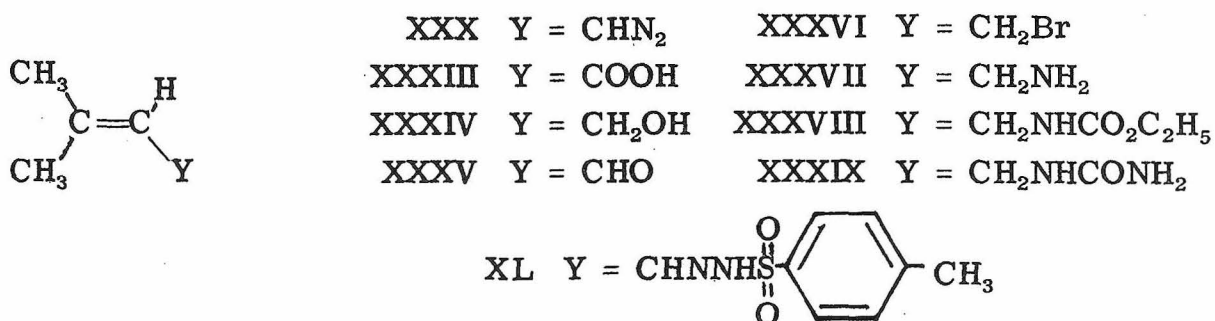
In order to investigate (2) more thoroughly, VII was decomposed in a quartz flow tube and in a Teflon tube. The product ratio, C, was found to vary between 0.3 and 0.1 in the quartz tube, depending upon the degree of conditioning. Decomposition of VII in the Teflon tube was even more discouraging; with the tube heated to 500°K, the

product ratio C was found to be 1.6. The mass balance for this pyrolysis was very poor, and extensive polymer formation (brown solid) was found on the surface of the Teflon. At this point, we draw a third conclusion:

(3) VII polymerizes, and its rearrangement may be profoundly surface catalyzed on Teflon.

## B. The Thermal Decomposition of 3-Methyl-1-diazo-2-butene

The flow pyrolysis of compound XXX, the diazo precursor to  $\gamma,\gamma$ -dimethyl vinylcarbene, was performed in Crellin Laboratory and completed in spring, 1971. The purpose of this investigation, as stated above, was to enter the  $C_5H_8$  energy surface via direct generation of a vinylcarbene and to compare the acyclic product distribution from this route with the distribution arising from the thermal rearrangement of 3,3-dimethylcyclopropene (VII). That the diazo compound does lead to the vinylcarbene (rather than to its diradical rotamer) is inferred from two prior observations: (1) that the pyrazolenine isomers of vinyl diazo compounds (vide supra, Scheme J) are thermally more stable than the corresponding diazo compounds<sup>10</sup>, and (2) that photolysis of pyrazolenines involves the intermediacy of the more labile diazo compounds<sup>30</sup>. These observations imply that expulsion of nitrogen from a vinyl diazo compound does not occur through a pyrazolenine intermediate.



In his preparations of cyclopropenes from pyrolysis of the sodium salts of  $\alpha,\beta$ -unsaturated tosylhydrazones (via vinyl diazo intermediates such as XXX), Closs observed the production of small amounts of diene impurities<sup>10</sup>. Although Closs reports no isoprene impurity in the preparation of VII from the sodium salt of XL, we believed that a closer

examination of the pyrolysis of XXX would reveal small amounts of acyclic products in addition to the cyclopropene VII. If the relative proportions of isoprene, isopropylacetylene, and gem-dimethylallene were the same from pyrolysis of XXX as from thermal rearrangement of VII, then it would be inferred that all three acyclic products arise from a common intermediate. A different distribution of acyclic products, on the other hand, would imply that two different intermediates -- i.e. the vinylcarbene and its diradical rotamer -- lie on the  $C_5H_6$  energy surface and that each is a precursor to different acyclic products.

The pyrolysis of XXX was performed in a quartz flow tube system<sup>77</sup> heated to 175°C, with nitrogen carrier gas at atmospheric pressure. The distribution of acyclic products was found to differ considerably from the thermal rearrangement of VII, as indicated in Table 13. Whereas the ratio Yne:Iso from thermal rearrangement of VII is ca. 10, the ratio Yne:Iso from pyrolysis of XXX is 0.4.

TABLE 12: PRODUCT DISTRIBUTION FROM PYROLYSIS OF  
3-METHYL-1-DIAZO-2-BUTENE

Run #	Temperature of flow tube	$\frac{\text{Iso}^a}{\text{Yne}}$	$\frac{\text{VII}^a}{\text{Iso} + \text{Yne}}$	$\frac{\text{Iso}^a}{\text{All}}$
XIV.D.6	447°K	2.6 <sup>b</sup>	56 <sup>b</sup>	--
XIV.D.7	449°K	2.3 ± 0.2	19 ± 1	100 <sup>c</sup>

a. Based on ratios of VPC peak areas (H.-P. 5750 with digital integrator connected to flame ionization detector).

b. Based on one analysis. c. Order of magnitude only

The determination of the product distribution from pyrolysis of XXX was complicated by the difficulties encountered in obtaining XXX free from a small isoprene impurity. Several methods of preparation of XXX were tried, among which are those listed on the next page:

A. Formation of the sodium salt of XL by reaction of XL with sodium hydride in tetraglyme, followed by thermal decomposition of the salt at 87 °C ('aprotic conditions');<sup>78</sup>

B. Preparation of the sodium salt by reaction of XL with sodium hydride in tetrahydrofuran, followed by removal of the solvent under reduced pressure and thermal decomposition of the dry salt at 90 °;<sup>78</sup>

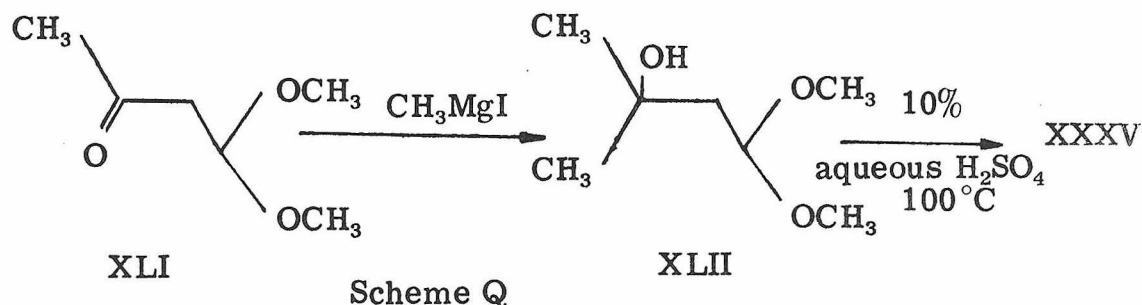
C. Preparation of amine XXXVII<sup>79, 80</sup> from the bromide XXXVI,<sup>81</sup> conversion to the urethane XXXVIII,<sup>82</sup> formation of the N-nitroso urethane<sup>82, 83</sup> and decomposition of the N-nitroso urethane with methanolic base;<sup>84</sup>

D. Preparation of urea XXXIX from XXXVII,<sup>85</sup> conversion to the N-nitroso urea,<sup>86</sup> and decomposition of the N-nitroso urea with methanolic base.

None of these methods afforded XXX free from the isoprene impurity. Thermal decomposition of the lithium salt formed by reaction of XL with n-butyllithium<sup>78</sup> yielded no diazo compound. Attempts to free XXX from isoprene by reaction of the impurity with the dienophiles tetracyanoethylene and N-phenylmaleimide resulted in reaction of the diazo compound, too.

The diazo compound was finally purified by vacuum transfer of volatiles out of a pristane solution of XXX. This resulted in the loss of a significant portion of XXX from the pristane solution, as well. Consequently, only small quantities of XXX were decomposed in our pyrolysis runs.

Diazo compound XXX was prepared by method A above. The aldehyde precursor XXXV presented unexpected difficulties in synthesis, and two different preparations were used. One consisted of reduction of the commercially available senecioic acid ( $\gamma, \gamma$ -dimethylacrylic acid, XXXIII) to alcohol XXXIV, followed by oxidation of the alcohol to senecialdehyde, XXXV. The other preparation used 4,4-dimethoxybutanone (acetylacetaldehyde dimethyl acetal, XLI) as starting material and is represented in Scheme Q.<sup>87</sup>



The mechanistic implications of the pyrolysis of XXX are discussed in detail in Section D. The difficulties encountered in surface effect studies with compound VII have led us to consider the possibility that the product distributions observed in the pyrolysis studies may reflect surface catalysis. Unfortunately, efforts to decompose XXX in solution were thwarted, as XXX has a tendency to rearrange to a pyrazolenine in solution upon heating.<sup>10</sup>

EXPERIMENTALReduction of senecioic acid (XXXIII) to 3-methyl-2-butene-1-ol (XXXIV)

A 2 liter three-necked flask fitted with mechanical stirrer was charged with 31 g. lithium aluminum hydride (0.82 mole) and 200 ml. ether from a freshly opened can. The suspension was cooled in an ice bath as 64 g. (0.75 mole) 3,3-dimethylacrylic acid (XXXIII, Aldrich) in 400 ml. ether was added dropwise. After addition was complete, the reduction was quenched with saturated aqueous sodium sulfate until the suspension was light gray. After a few hours stirring, the suspension had turned completely white, at which time the ethereal solution was filtered and the residue washed with more ether. Removal of solvent under reduced pressure left 48 g. of a pale yellow liquid. VPC on a 6 ft. x  $\frac{1}{8}$  in. UCCW 982, 60/80 Chromosorb P column at 70° with 1 cc/sec helium flow showed this to consist of a large peak (retention time = 11 min) and two small impurity peaks, one 5% of the large peak (retention time = 8 min), and the other 10% of the large peak (ether, retention time = 2 min). Assuming 85% purity, this yield corresponds to 41 g. (0.49 mole) of 3-methyl-2-butene-1-ol,  $(\text{CH}_3)_2\text{C}=\text{CHCH}_2\text{OH}$  (XXXIV), 69% of theoretical. IR (neat film): 3400-3350 (s), 2960 (s), 2910 (s), 2860 (s), 1670 (m). NMR ( $\text{CDCl}_3$ ):  $\delta$  5.3 (trio of quartets,  $J = 7$  cps,  $J = 1$  cps, 1H =  $\text{CHCH}_2\text{OH}$ ), 4.0 (d,  $J = 7$ , 2H,  $\text{CH}_2\text{OH}$ ), 3.2 (s, 1H,  $\text{CH}_2\text{OH}$ ), 2.6 (s,  $\text{CH}_3$  cis), 2.5 (s,  $\text{CH}_3$  trans).

Pyridinium Dichromate oxidation of 3-methyl-2-buten-1-ol (XXXIV)  
to senecialdehyde (XXXV)

Pyridinium dichromate was prepared by the method of Coates and Corrigan.<sup>88</sup> A solution of 1 pound (4.6 moles) of chromium trioxide in 300 ml. water was added slowly to a stirred solution of 400 g. (5.1 moles) pyridine and 40 ml. water. The suspension was chilled and filtered to yield 725 g. (1.9 moles) orange crystals of pyridinium dichromate (83% yield).

A 15 g. portion of XXXIV, (0.175 moles) was dissolved in 1 liter of methylene chloride. To this solution 150 g. pyridinium dichromate (0.4 mole) was swiftly added with vigorous mechanical stirring, and stirring was continued for one-half hour. The suspension was filtered through alumina and the filtrate vigorously stirred while another 150 g. pyridinium dichromate was added. After another half-hour stirring, the suspension was again filtered and the filtrate again stirred vigorously while a third 150 g. portion of pyridinium dichromate was added. The suspension was filtered a third time through alumina and the 975 ml. of filtrate washed with 100 ml. of 2N hydrochloric acid saturated with sodium chloride, and the volume of the solution reduced to 200 ml. by distillation of the methylene chloride at atmospheric pressure. The resulting solution of XXXV,  $(\text{CH}_3)_2\text{C}=\text{CHCHO}$ , was then dried over sodium sulfate. IR (methylene chloride): 2960 (s), 2890 (m), 2860 (m), 1675 (s), 1665 (s), 1585 (s). NMR (methylene chloride):  $\delta$  9.8 (d,  $J = 8$  cps,  $\text{CHO}$ ),  $\delta$  5.8 (doublet of quartets,  $J = 8$  cps,  $J = 1$  cps,  $\text{CHCHO}$ ),  $\delta$  2.15 (d,  $J = 1$  cps,  $\text{CH}_3$  cis),  $\delta$  1.95 (d,  $J = 1$  cps,  $\text{CH}_3$  trans) identical to reported spectrum.<sup>87</sup> NMR integration showed

the solution to be 5.5% XXXV by weight and free from pyridine. Yield of senecialdehyde (in solution), 14 g. (0.167 moles), 95% of theoretical.

3-Hydroxy-3-methylbutyraldehyde dimethyl acetal (XVIII) from 4,4-dimethoxy-2-butanone (XVII) and methyl Grignard

A saturated solution of methyl Grignard was prepared by dissolving 50 g. magnesium turnings (2.1 moles) in a solution of 280 g. methyl iodide (2.0 moles) in 500 ml. ether from a freshly opened can. The reaction was carried out with mechanical stirring under an atmosphere of nitrogen, and the syrupy solution of methyl Grignard was decanted from the undissolved magnesium turnings into a 1 liter addition funnel under a constant stream of nitrogen. The Grignard reagent was added dropwise under nitrogen to a mechanically stirred solution of 180 g. XVII (1.4 mole) in 300 ml. ether in a 1500 ml. three-necked flask cooled in an acetone-Dry Ice slush. The addition was complete after 5 hours, and the mixture was permitted to come to room temperature overnight. The mixture was then quenched with 400 ml. saturated aqueous ammonium chloride and extracted three times with 600 ml., 500 ml., and 400 ml. portions of ether. These ether washings were dried over sodium sulfate and the solvent removed under reduced pressure. The yields from the three extractions were 99 g., 33 g., and 10 g., respectively. The first of these portions was distilled on a 180° oil bath at atmospheric pressure until the clear distillate in the range 40-85° ceased coming over. The bath temperature was then reduced to 115-120°, and the pressure was reduced to 25 mm. with an aspirator. Under aspirator pressure, 46 g. clear distillate came over

in the range 84-85° and was collected as two equal fractions. The portions from the other two extractions were combined and distilled in this manner to yield 13 g. clear distillate in the range 82-84°. VPC of these fractions on the 10 ft. x  $\frac{1}{4}$  in. 20% SE 30, 60/80 Chromosorb P column at 100° (retention time of principal peak = 10 min. at 1 cc./sec. helium flow) showed the second fraction of the 84-85° distillation and the fraction from the 82-84° distillation to be largely free from impurities. The spectra were identical to those reported for  $(\text{CH}_3)_2\text{C}(\text{OH})\text{CH}_2(\text{OCH}_3)_2$ , NMR ( $\text{CCl}_4$ ):  $\delta$  1.14 (s,  $(\text{CH}_3)_2$ ), 1.66 (d,  $J = 5\frac{1}{2}$  cps,  $\text{CH}_2$ ), 3.01 (s,  $\text{OH}$ ), 3.3 (s,  $(\text{OCH}_3)$ ), 4.6 (t,  $J = 5\frac{1}{2}$  cps); IR: 3450  $\text{cm}^{-1}$  (broad, strong), 2940 (broad, strong), 2840 (sharp, strong).<sup>87</sup> Yield 59 g. (0.40 mole), 29% of theoretical.

Senecialdehyde (XXXV) from 3-hydroxy-3-methylbutyraldehyde dimethyl acetal (XLII)

A 20 g. portion of the first fraction of the 84-85° distillation of XLI was heated on a steam bath for one-half hour with 100 ml. 10% sulfuric acid in a flask equipped with a reflux condenser. The organic layer which separated at the top was dissolved in ether and separated. The aqueous layer was cooled in an ice slush and solid sodium bicarbonate added in small portions until bubbling ceased. The solution was extracted with 200 ml. ether, but examination of this solution showed nothing dissolved in it. The volume of ethereal solution of the organic layer gave 6 g. impure senecialdehyde. The 2 g. senecialdehyde from above was combined with this 6 g., dried over magnesium sulfate, and distilled at aspirator pressure to yield 7.7 g. (0.092 mole)

senecialdehyde (XXXV), 23% of theoretical from XLIII. VPC on 10 ft. x  $\frac{1}{4}$  in. in 20% SE 30, 60/80 Chromosorb P column at 100° showed this material indeed to be senecialdehyde with a small water impurity. In addition to the principal peak (helium flow = 1 cc./sec.) with retention time of  $4\frac{1}{2}$  minutes, there appeared a sizable peak (15% of the principal) at  $3\frac{3}{4}$  minutes. The NMR spectrum, however, gave no indication of any impurity of nearly this magnitude.

Senecialdehyde tosylhydrazone (XL) from senecialdehyde XXXV

(1) To 10 ml. of a 6% methylene chloride solution of senecialdehyde (XXXV) stirred in an ice bath was added 2.3 g. (0.012 moles) tosylhydrazine (Eastman). The yellow solution turned cloudy, and a VPC monitor of an aliquot showed a small amount of senecialdehyde still remaining in solution. The solution, which cleared upon the addition of sodium sulfate, was filtered, chilled in an ice bath, and 100 ml. pentane was added. A yellow oil separated which crystallized upon scratching. The solid was recovered to yield 1.4 g. (0.055 moles) white crystals of XL upon drying, mp. 96-98° (ml. lit.<sup>10</sup> 97-98°), 45% of theoretical, identified by NMR as  $(\text{CH}_3)_2\text{C}=\text{CHCH}=\text{NNHSO}_2\text{C}_6\text{H}_4\text{CH}_3$ . NMR ( $\text{CDCl}_3$ ):  $\delta$  8.4 (broad singlet,  $\text{CH}=\text{N}$ ) 7.5 (m,  $\text{C}_6\text{H}_4$ ), 5.8 (doublet of quartets,  $J = 10$  cps,  $j = 1$  cps,  $\text{C}=\text{CH}$ ), 2.35 (s,  $\text{C}_6\text{H}_4\text{CH}_3$ ), 1.8 - 1.7 (two overlapping doublets,  $J = 1$  cps,  $(\text{CH}_3)_2$ ).

(2) An Ehrlenmeyer flask charged with 250 g. of a methylene chloride solution of senecialdehyde (5.5% solution from the pyridinium dichromate oxidation described above, 0.16 moles of XXXV) was chilled in an ice bath, and 25.0 g. (0.135 moles) tosylhydrazine was added,

followed by sodium sulfate. The solution was filtered, reduced to a volume of 80 ml. on a rotary evaporator, and 600 ml. pentane was added. The suspension was chilled, and the separated oil crystallized by scratching. Collection of the solid afforded 29.2 g. (0.116 moles) of XL, 86% of theoretical.

(3) To a solution of 15 g. tosylhydrazine (0.08 moles) dissolved in 35 ml. hot methanol was added 7.7 g. neat senecialdehyde (XXXV prepared from XLII, as described above). The light yellowish solution was cooled in an ice bath and a seed crystal added. The precipitated crystals were collected by suction filtration, redissolved in 100 ml. hot methanol and set in a refrigerator overnight. The resulting crystals were collected by suction filtration to afford 15 g. (0.06 moles) XL. The mother liquor was cooled in a Dry Ice-acetone slush to afford 2 g. more of crystals (0.008 moles). The crystals were found to give a poor melting point, as there was residual methanol that could not be removed from the crystals (this was substantiated by the presence of a methanol peak in the NMR); however, discoloration and decomposition were not observed upon heating a sample of recrystallized XL to 140°.

3-Methyl-1-diazo-2-butene (XXX) from senecialdehyde tosylhydrazone (XL)

Tetraglyme was distilled at 1 torr pressure from lithium aluminum hydride and stored over molecular sieves. A solution of 0.95 g. (0.0040 mole) recrystallized XL in 10 ml. tetraglyme was added dropwise with magnetic stirring to a 25 ml. round bottom flask charged with 0.38 g. sodium hydride (56% dispersion in mineral oil, 0.0088 mole) suspended

in a few milliliters of tetraglyme, and the evolution of hydrogen gas was noted. When addition was complete, the addition funnel was removed and the flask connected through a cold trap to a vacuum pump. The flask containing the suspension of the sodium salt of XL was evacuated, and pumping continued until no more bubbling was observed. The leak valve on the vacuum system was connected to a nitrogen tank and gas leaked into the system so that the pressure read 7 torr on a MacLeod gauge. The flask was then immersed in an oil bath and heating commenced, while the cold trap receiver, a 5 ml. pear shaped flask, was immersed in a Dry Ice-acetone slush. The temperature of the oil bath was monitored and, at 87 °C, the suspension turned a deep crimson; 0.1 g. of a blood red liquid, XXX, was distilled over in a few minutes (0.001 mole, 25% of theoretical). A solution of XXX in acetone was quenched with benzaldehyde;<sup>89</sup> VPC analysis of the resulting yellowish solution on column J revealed the presence of an isoprene impurity. Repetition of the above preparation using XL made from preparative VPC purified XXV and recrystallized tosylhydrazine (and carefully recrystallized from ethanol) still showed the presence of the isoprene impurity.

#### Purification and identification of XXX

A red solution of 0.2 g. XXX in 5 ml. pristane (2,6,10,14-tetramethylpentadecane, Aldrich) was degassed on a vacuum line and purged of impurities by 2 hours vacuum transfer. Volatile materials, mostly XXX, were collected in another flask on the vacuum line cooled in liquid nitrogen. The contents of this flask examined by NMR showed a spectrum consistent with the structure for XXX,  $(\text{CH}_3)_2\text{C CHCHN}_2$ .

NMR ( $\text{CD}_3\text{COCD}_3$ ):  $\delta$  5.45 (doublet of quartets,  $J = 9$  cps and  $J = 1.5$  cps,  $\text{C}=\underline{\text{C}}\text{H}$ ), 4.82 (d,  $j = 9$  cps,  $\text{C}\underline{\text{H}}\text{N}_2$ ), 1.75 (d,  $J = 1.5$  cps  $\text{C}\underline{\text{H}}_3$  cis), 1.53 (d,  $J = 1.5$  cps,  $\text{C}\underline{\text{H}}_3$  trans). Also a multiplet,  $\delta$  3.1-3.7, from tetraglyme impurity. IR of a pristane solution of XXX showed a sharp diazo stretch at  $2070\text{ cm}^{-1}$ .

#### Pyrolysis of XXX: Run XIV. D. 7

The flow pyrolysis system consisted of a 12 mm. O.D. quartz tube in a 1000 Watt cylindrical furnace.<sup>77</sup> The length of the heated portion of the tube was 37 cm., and an iron-constantan thermocouple inside the tube showed the hottest portion to be at  $176^\circ\text{C}$ . The pink solution of XXX remaining after the vacuum transfer of volatiles was diluted by addition of 20 ml. more pristane. Methylcyclopentane was added as internal standard and the solution divided into two parts. The first part was blown through the heated flow system with a  $500\text{ cm}^3/\text{min}$ . stream of nitrogen for  $2\frac{3}{4}$  hours, and products were collected in two glass helices-filled traps cooled in liquid nitrogen. The colorless pyrolysis products were vacuum transferred to a Pyrex tube and sealed. The second portion of the pristane solution was blown through the quartz tube at room temperature with conditions otherwise identical (control run); VPC analysis was performed as for the kinetic runs in Section A. VPC analysis of the contents of the trap in the control run showed no volatile products.

Products from the flow pyrolysis of diazo compound XXX were characterized not only by their retention times on column J, but also by their mass spectra. The mass spectra were taken on a VPC-Mass Spectrometer system consisting of a Hewlett-Packard 7624A VPC connected to a QUAD 300 EAI Quadrupole Mass Spectrometer. Separation was performed on column J, and ionization was carried out at 70 volts. The resulting spectra were compared with those from the VPC-MS of a partially pyrolyzed, authentic sample of cyclopropene VII. The results are summarized in Table 13.

#### Pyrolysis of XXX in solution

A pink solution of XXX in acetone was degassed, sealed in a Pyrex tube, and heated in the vapors of refluxing diglyme (165°) for a few minutes. VPC analysis of the solution did not reveal volatile products. Removal of the acetone left a small amount of a yellowish oil, which, on IR analysis, appeared to be mostly tetraglyme. A small peak band was seen, however, at  $1680\text{ cm}^{-1}$ , indicating the presence of a pyrazolenine.<sup>10</sup>

TABLE 13: GC-MS ANALYSIS OF PRODUCTS OF PYROLYSIS OF XXX: % OF BASE  
PEAK AT m/e 27

m/e	VII*	9 minute peak from XXX	All	19 minute** peak from XXX	Iso	21 minute peak from XXX	Yne	23 minute peak from XXX
68	3	2	2	-	14	12	2	2
67	22	17	9	-	22	20	20	18
54	2	2	2	-	2	2	2	2
53	41	38	29	60	45	44	54	47
52	3	3	6	-	4	4	6	6
51	12	11	6	-	11	10	15	13
50	10	8	11	-	8	9	14	12
49	2	2	-	-	2	2	3	2
42	14	15	-	-	22	22	12	12
41	46	39	71	80	48	46	22	24
40	33	29	35	40	51	50	22	22
39	67	60	78	90	92	93	39	40
38	13	12	15	-	19	19	10	11
27	100	100	100	100	100	100	100	100

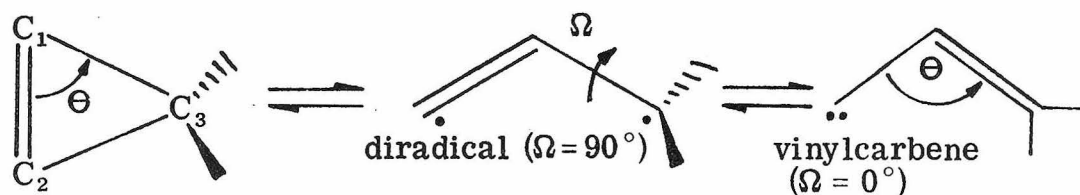
\* Note that this mass spectrum differs from that recorded on the CEC machine (vide supra).

\*\* This was a very small peak on the VPC.

### C. Calculations on $C_3H_4$ Rotamers

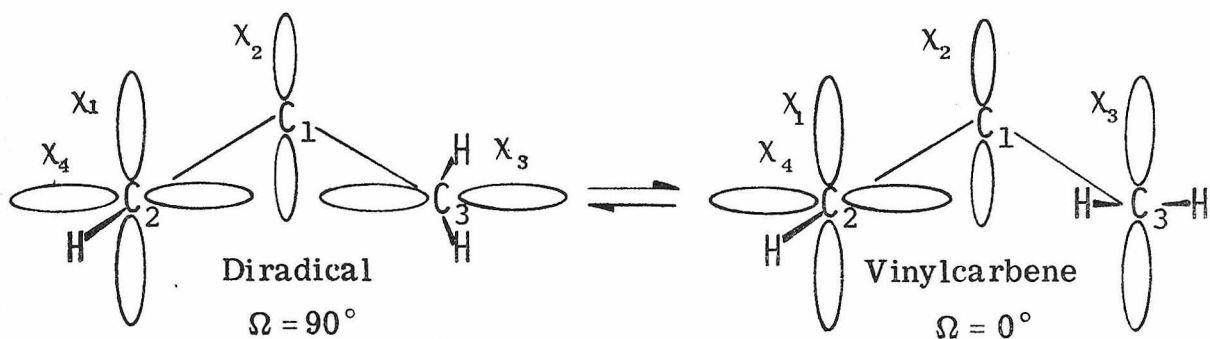
Molecular orbital calculations were performed on vinylcarbene (V) and its  $90^\circ$  rotamer (IV), which are proposed as intermediates in the rearrangement of cyclopropene. The purpose of these calculations was to acquire an idea of what happens as vinylcarbene travels along the reaction coordinate: specifically, to make estimates of the structure and electron distribution of vinylcarbene and of its behavior as it is converted to its diradical rotamer.

Two parameters of particular interest in the isomerization of cyclopropenes are the angles  $\Theta$  (the  $C_2-C_1-C_3$  angle) and  $\Omega$  (the angle of rotation about the  $C_1-C_3$  axis) depicted in Scheme R. The ring opening of cyclopropene to the diradical corresponds to an increase of angle  $\Theta$  from  $65^\circ$  ( $64^\circ 36'$  in cyclopropene itself<sup>91</sup>) to an obtuse angle in the intermediate structures. The rotation from diradical to vinylcarbene corresponds to the decrease of angle  $\Omega$  from  $90^\circ$  to  $0^\circ$ .



Scheme R

An idea of the  $\Theta$  and  $\Omega$  dependence of the intermediates may be gained by examining a Hückel molecular orbital treatment of the four p-orbitals involved, shown in Scheme S. The treatment and terminology used below are taken from J. D. Roberts, Notes on Molecular Orbital Calculations (Benjamin, 1961). A matrix is set up whose elements



Scheme S

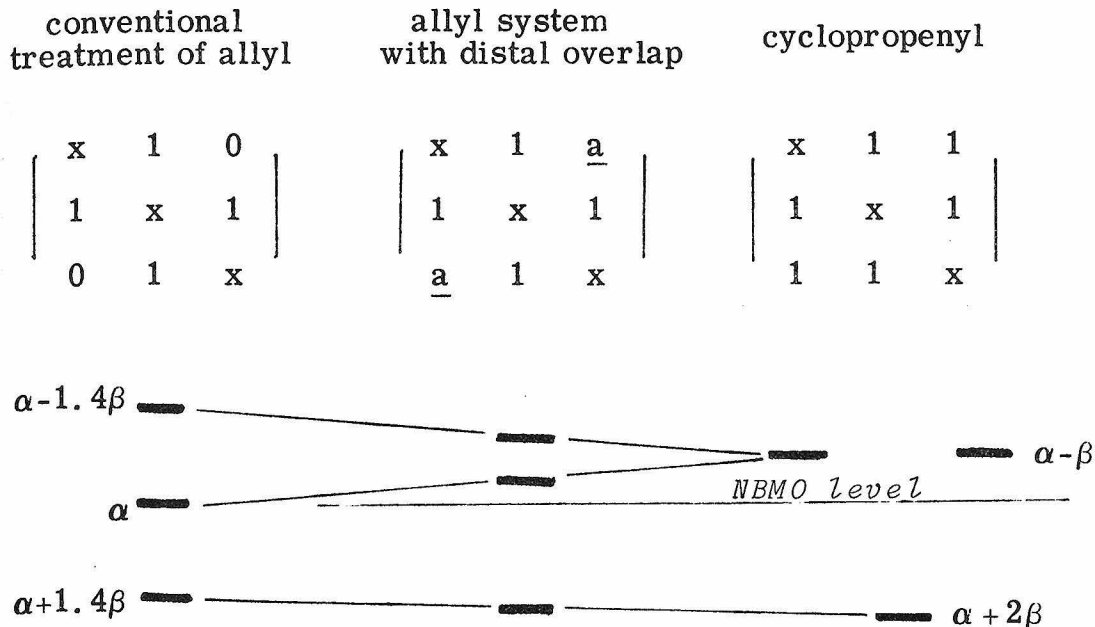
are the values of the integrals  $\int \chi_i \mathcal{H} \chi_j d\tau$ , where the  $\chi$ 's are wavefunctions for carbon atomic p-orbitals. All Coulomb integrals, the diagonal elements ( $i = j$  in the integral), are taken to have the same value, a negative number  $\alpha$ . The off-diagonal elements are expressed in terms of another negative number,  $\beta$ , which, although it is not well defined experimentally, is usually assigned the value of the Resonance integral ( $i \neq j$  in the integral above) for ethylene. Eigenvalues,  $E$ , are found by converting the matrix to a secular determinant (in which the diagonal elements are represented by the variable  $x = \frac{E - \alpha}{\beta}$ ) converting the determinant to a secular equation (a polynomial in  $x$ ) and finding the roots of the polynomial. The roots are converted to values of  $E$ , the molecular orbital energy levels.

In a conventional Hückel treatment, each off-diagonal element in the secular determinant is either 1 or 0, depending whether the atomic orbitals  $\chi_i$  and  $\chi_j$  are on adjacent atoms or not. In an unconventional treatment, which is necessary in order to examine vinylcarbene and its rotamer, off-diagonal elements are used that lie between 0 and 1, since important interactions are present between orbitals that are not adjacent and overlap to a much smaller extent than the  $\pi$ -orbitals in ethylene.

Values of the resonance integral  $\beta'$  for two non-adjacent orbitals (e. g. the parallel p-orbitals  $\chi_1$  and  $\chi_3$  on  $C_2$  and  $C_3$  in vinylcarbene) are determined using the expression  $\beta' = \frac{S'(1+S')}{S(1+S)} \beta$ .  $S$  is the value of the overlap integral,  $\int \chi_i \chi_j d\tau$  ( $i \neq j$ ), for ethylene ( $S = 0.28$ ;  $S(1+S) = 0.358$ ), and  $S'$  is the value of the overlap integral for the two orbitals in question. For orbitals  $\chi_1$  and  $\chi_3$  in vinylcarbene at a distance of  $1.88 \text{ \AA}$ ,  $S' = 0.121$  and  $\frac{S'(1+S')}{S(1+S)} = 0.348$ . Values of  $S'$  for different interatomic distances and orientations (hence, different values of  $\Theta$  and  $\Omega$ ) are calculated utilizing a table of overlaps reproduced from Kopineck and a method outlined by Roberts.<sup>90</sup>

From this sort of Hückel treatment, which is described below in greater detail, it is found that the  $\pi$ -electron energy ( $E_\pi$ ) of vinylcarbene decreases with decreasing  $\Theta$  in the same fashion as the lowest level of the allyl system becomes lower in energy when the distal lobes are brought together (i. e. to approach the cyclopropenyl system, as shown in Scheme T). In Scheme T, the off-diagonal element  $\underline{a}$  ( $0 \leq \underline{a} \leq 1$ ) represents a value of the resonance integral for the two non-adjacent  $\pi$ -orbitals, or distal lobes, in the allyl system. Values of  $\underline{a}$  are calculated for a given interatomic distance as described above. The conventional Hückel treatment of the allylic system corresponds to  $\underline{a} = 0$ , of the cyclopropenyl system to  $\underline{a} = 1$ .

In vinylcarbene (V), for  $\Theta > 90^\circ$ , rotation by angle  $\Omega$  from  $0^\circ$  to  $90^\circ$  raises  $E_\pi$  of the system, since allylic resonance is lost, and this loss is not balanced by the increasing overlap of  $\chi_3$  and  $\chi_4$ . Interestingly, for  $\Theta < 90^\circ$ , the reverse is true: rotation by angle  $\Omega$  about the  $C_1$ - $C_3$  bond lowers  $E_\pi$  of the intermediate.



Scheme T

Because of the dependence upon  $\Theta$  and  $\Omega$  inferred from Hückel calculations, computer calculations using the CNDO/2 method were performed in order to find an optimum geometry for vinylcarbene, so as to be able to approximate the behavior of the experimental system as  $\Theta$  and  $\Omega$  change. The variations of energy as angles  $\Theta$  and  $\Omega$  are varied independently from their values at the CNDO/2 energy minimum are summarized in Figure 12. A more detailed description of the calculations follows.

### Hückel Calculations

Vinylcarbene is treated as an allyl system with a single orthogonal lobe,  $\chi_4$ , on  $C_2$ . In this Hückel treatment, the  $\pi$ -overlap

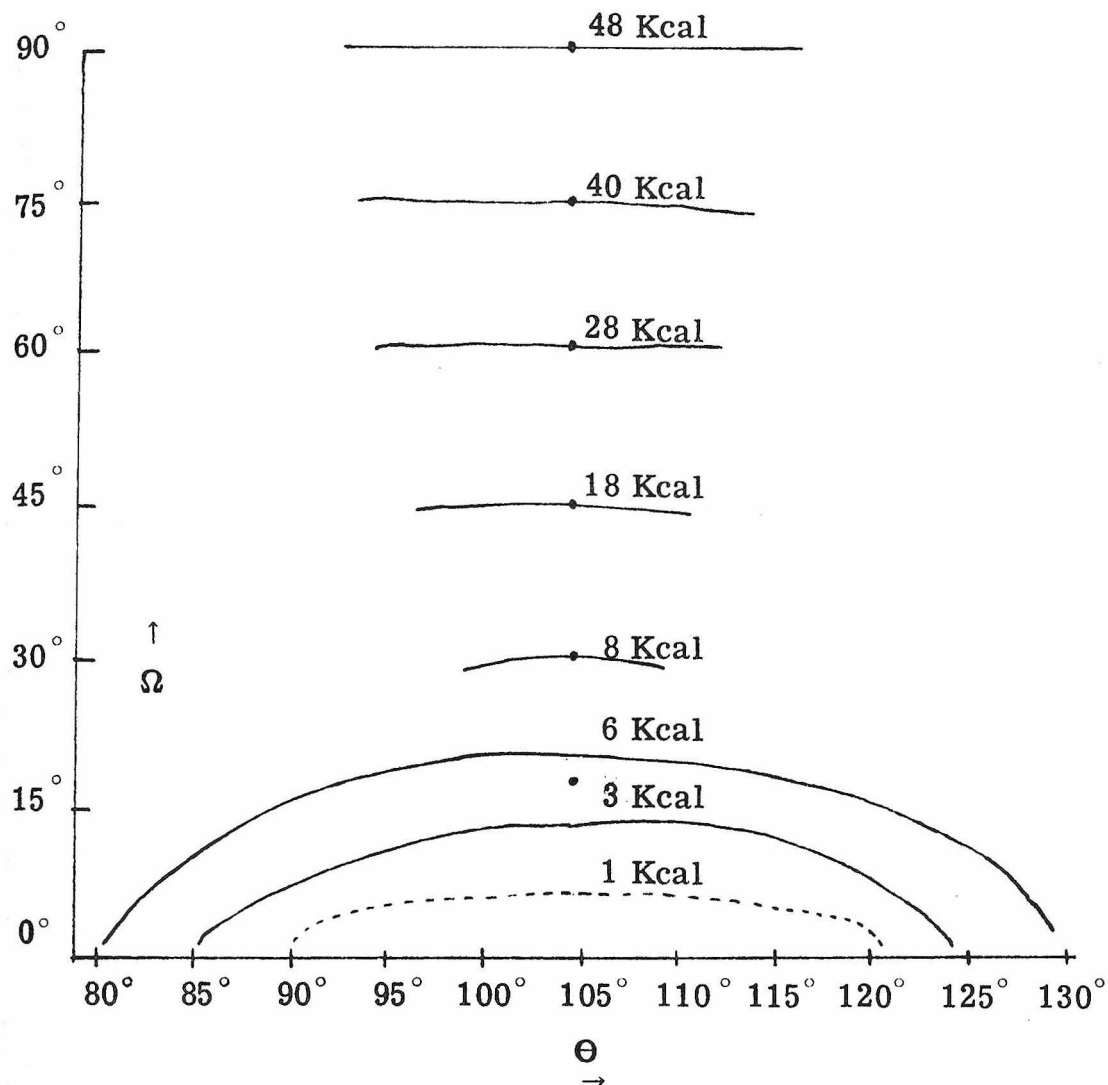


FIGURE 12: CNDO/2 POTENTIAL FOR VARIATION OF VINYL CARBENE FROM MINIMUM

Values of the binding energy are calculated in atomic units and have been converted to Kcal/mole by the factor 627.5 Kcal/mole. Use of this conversion factor, however, for CNDO/2 energies, leads to heats of atomization for simple hydrocarbons that are 2 to 3 times larger than experimental values, and the use of a conversion factor of 218 Kcal/a.u. has been suggested for energy differences.<sup>92</sup>

of the distal lobes  $\chi_1$  and  $\chi_3$  must be considered if a variation of  $\Theta$  is to have any effect, for which reason, the off-diagonal element  $\underline{a}$  is introduced into the secular determinant below. The value of  $\underline{a}$  is determined by the method described above, in which  $S'$  is the  $\pi$ -overlap of  $\chi_1$  and  $\chi_3$ . Similarly, an off-diagonal element  $\underline{b}$ ,  $0 \leq \underline{b} \leq 1$ , is introduced into the secular determinant for the diradical (IV), which is treated as two independent  $2 \pi$ -systems:  $\chi_1$  and  $\chi_2$ , which overlap to the same extent as the  $\pi$ -orbitals in ethylene, and  $\chi_3$  and  $\chi_4$ , which overlap to a smaller extent,  $S'$ , from which the value of  $\underline{b}$  is determined.<sup>90</sup>

$$\begin{vmatrix} x & 1 & \underline{a} & 0 \\ 1 & x & 1 & 0 \\ \underline{a} & 1 & x & 0 \\ 0 & 0 & 0 & x \end{vmatrix}$$

Secular Determinant  
for vinylcarbene (V)

$$\begin{vmatrix} x & 1 & 0 & 0 \\ 1 & x & 0 & 0 \\ 0 & 0 & x & \underline{b} \\ 0 & 0 & \underline{b} & x \end{vmatrix}$$

Secular Determinant  
for diradical (IV)

In vinylcarbene, the orbital orthogonal to the allyl system,  $\chi_4$ , is considered to be completely localized and to lie at the nonbonding (NBMO) level. As a consequence, the  $\Theta$  dependence of the bonding and antibonding levels in vinylcarbene is equivalent to the  $\Theta$  dependence of the allyl system, as the progression of allyl to cyclopropenyl raises the NBMO level of allyl to an antibonding level, as depicted above in Scheme T. Hückel theory thus predicts vinylcarbene to be an allyl cation with an orthogonal negative lobe (XX above), much like tropylicarbene.

Hence,  $E_{\pi}$  for vinylcarbene, V, is equal to  $4\alpha - 2z\beta$ , where  $z$ , a function of  $\underline{a}$ , is the negative root of the secular equation,

$$z = \left[ (-\underline{a} + \sqrt{\underline{a}^2 - \frac{(2+\underline{a}^2)^3}{27}})^{\frac{1}{3}} + (-\underline{a} - \sqrt{\underline{a}^2 - \frac{(2+\underline{a}^2)^3}{27}})^{\frac{1}{3}} \right].$$

The  $C_1-C_2-H$  bond angle is taken to be  $180^\circ$ , and the C-C bond distances in our Hückel calculation are both taken to be  $1.34 \text{ \AA}$ ; values of  $\underline{a}$  and  $\underline{b}$  are determined from Kopineck's table of orbital overlaps.<sup>90</sup> Values of  $E_{\pi}$  for vinylcarbene calculated in this manner are listed in Table 14.

TABLE 14:  $\pi$ -ELECTRON ENERGIES OF IV AND V AS A FUNCTION OF ANGLE  $\Theta$

$C_2-C_3$ Distance	$\Theta$	Diradical (IV)	Vinylcarbene (V)
1.88 $\text{\AA}$	$90^\circ$	$4\alpha + 3.38\beta$	$4\alpha + 3.24\beta$
2.05 $\text{\AA}$	$100^\circ$	$4\alpha + 3.00\beta$	$4\alpha + 3.10\beta$
2.22 $\text{\AA}$	$112^\circ$	$4\alpha + 2.68\beta$	$4\alpha + 3.02\beta$
2.39 $\text{\AA}$	$126^\circ$	$4\alpha + 2.43\beta$	$4\alpha + 2.96\beta$

Because the lowest orbital of allyl decreases in energy as the allyl system approaches cyclopropenyl, shown above in Scheme T, it is seen that  $E_{\pi}$  for vinylcarbene increases with decreasing  $\Theta$ . In other words, the greater delocalization of the cyclopropenyl system may contribute to a driving force for the diminution of  $\Theta$ .

The dependence of  $E_{\pi}$  of diradical IV upon  $\Theta$  is also shown in Table 14. With the structural parameters that have been assumed, it appears that a graph of the resonance energy of vinylcarbene versus  $\Theta$  will cross a graph of the resonance energy of the diradical at a value of  $\Theta$  roughly halfway between  $90^{\circ}$  and  $100^{\circ}$ .

The variation in  $E_{\pi}$  as  $\Omega$  changes from  $0^{\circ}$  to  $90^{\circ}$  was examined for several different structures with the aid of a computer program for Hückel calculations, HK6.<sup>93</sup> The results show that the transition from vinylcarbene to diradical is smooth and monotonic. Since this indicates that there is no barrier to rotation from the higher to the lower lying rotamer, it seems worthwhile to investigate which geometry for vinylcarbene is an energy minimum. If there is no maximum in the surface connecting vinylcarbene and cyclopropene, this is tantamount to the assertion that vinylcarbene does not lie in a potential energy well.

#### CNDO/2 Calculations

The Hückel treatment shows nothing opposing the change in vinylcarbene from  $\Theta > 120^{\circ}$  to  $\Theta = 90^{\circ}$ . The creation of angle strain, however, cannot be taken into account by the Hückel method. On the basis of calorimetric experiments, a strain energy of 52 Kcal/mole is reported for cyclopropene;<sup>94</sup> hence, it seems reasonable to infer that strain will oppose the diminution of  $\Theta$  in vinylcarbene.

Calculations of the relative energies of several geometries were made using a semiempirical molecular orbital approximation, CNDO/2. This method has been described in detail elsewhere; it employs an LCAO-SCF computation comprising all valence electrons,

utilizing empirically derived values of  $\alpha$  and  $\beta$  and making a simple approximation for electron repulsion terms.<sup>95</sup> The computer program for this method is published,<sup>96</sup> and the results of calculations for several geometries of  $C_3H_4$  are summarized in Figure 12 and Tables 15 through 20.

In the application of the CNDO/2 approximation for examination of molecular geometries, there are several points to be borne in mind. First, a calculation of molecular geometry requires that all molecular parameters be optimized.<sup>97</sup> The molecule  $C_3H_4$  has 15 internal degrees of freedom; a precise use of CNDO/2 calculations requires that every structural parameter be optimized in order for any single parameter to be optimized.

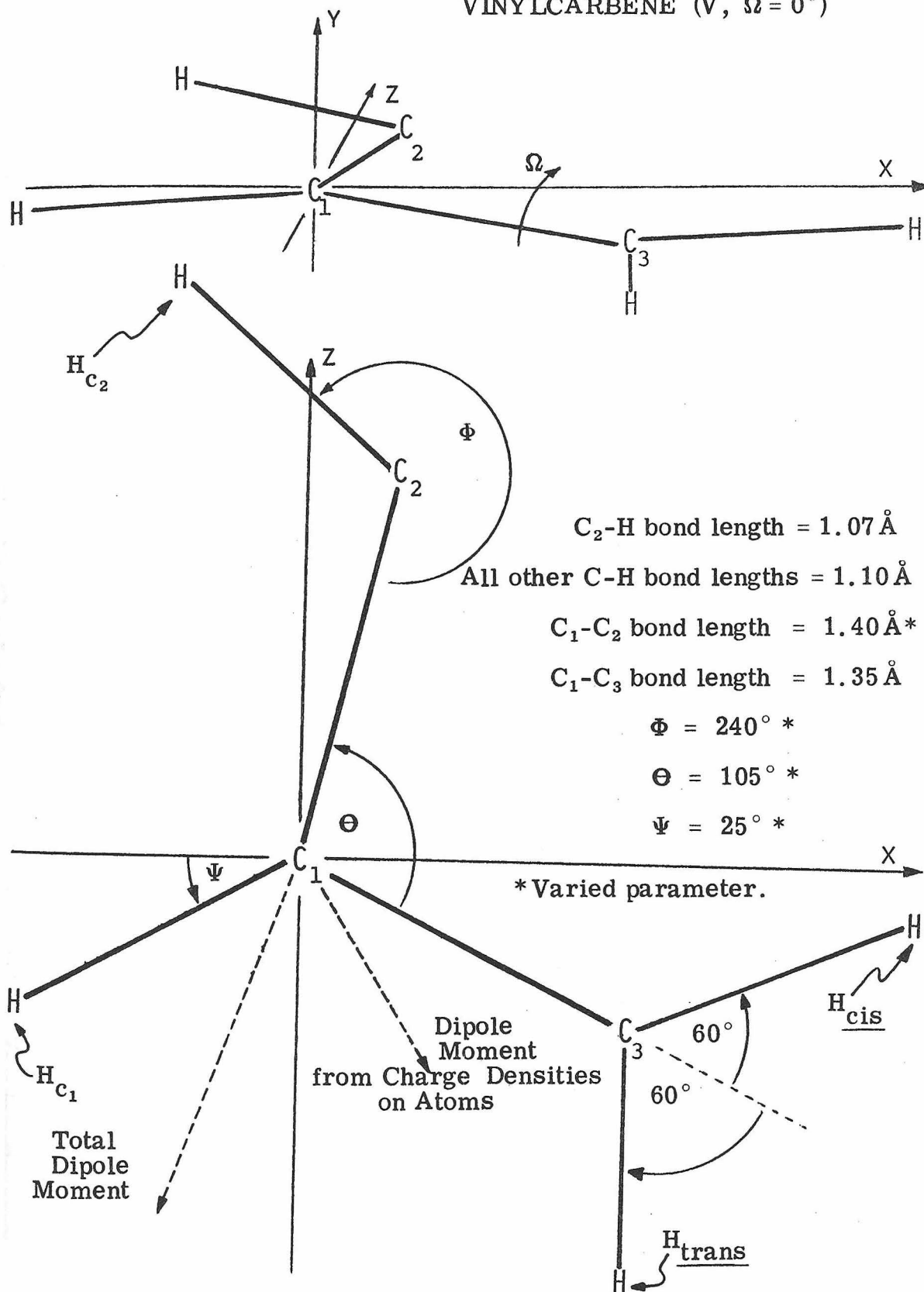
In our CNDO/2 calculations on the vinylcarbene-diradical system, only the five parameters considered most crucial were varied: the angles  $\Theta$  and  $\Omega$ , the C-C-H bond angles for the two methine carbons  $C_1$  and  $C_2$  ( $\Psi$  and  $\Phi$ ), and the length of the bond connecting  $C_1$  and  $C_2$ . Extended Hückel calculations have previously been performed on vinylcarbene to determine a potential energy surface for in-plane and out-of-plane bending of the  $C_2$ -H bond.<sup>98</sup>

A second consideration is that an artifact of the CNDO/2 method is a preference for small ring structures. The extent to which this may reflect a poor choice of geometric parameters is unknown, yet it has been reported that cyclopropyl cation has a lower binding energy calculated by CNDO/2 than allyl cation, a result that is contradicted by many experimental studies.<sup>99</sup> A further discussion of this artifact is presented below.

A third caveat applies not only to the CNDO/2 method, but to all LCAO methods derived from the Hartree-Fock treatment. A molecular orbital picture of a molecule is probably inadequate for systems where two orbital levels are close in energy, with one level filled (highest occupied molecular orbital or HOMO) and the other empty (lowest unoccupied molecular orbital, or LUMO). The molecular orbital wavefunction for such a molecule may be written as  $\Psi = (\psi_{\text{everything else}})^2 \phi^2_{\text{HOMO}}$ . In instances where the HOMO and LUMO are close in energy, a more appropriate description of the molecule is a state function derived from valence bond theory,  $\Psi = (\psi_{\text{everything else}})^2 (\phi^2_{\text{HOMO}} - \lambda \phi^2_{\text{LUMO}})/N$ , where  $\lambda$  is an optimized coefficient and  $N$  is a normalization factor.<sup>100</sup> In the CNDO/2 calculation, when a HOMO and a LUMO change places as a consequence of varying a structural parameter, a discontinuity is seen in the energy. The energies of the two levels may approach one another in a smooth manner as a bond angle is varied in small increments, but the energies of the levels change abruptly when the levels cross.

Our initial CNDO/2 calculations were made using the program CNDO/2<sup>101</sup> on an IBM 360/75 computer in winter, 1970. Further calculations on the best of these structures (Table 15) and for other geometries (Tables 16-20) were performed in summer, 1971, on an IBM 370/155 computer using the expanded, double precision program CNINDO.<sup>102</sup> Vinylcarbene was assumed planar, and the optimum geometry calculated for vinylcarbene ( $V, \Omega = 0^\circ$ ) is depicted in Figure 13:  $\Theta = 105^\circ$ . Closure to  $\Theta = 80^\circ$  causes a smooth rise of 0.01 a.u. (6 Kcal/mole) in the calculated energy. For the optimum geometry,

FIGURE 13: CNDO/2 OPTIMUM GEOMETRY OF VINYL CARBENE ( $V, \Omega = 0^\circ$ )



a rotation of  $\Omega$  through  $90^\circ$  to the diradical (IV) results in a monotonic rise of 0.075 a.u. (47 Kcal/mole) in the calculated energy. A potential surface derived from these calculations as a function of  $\Theta$  and  $\Omega$  is sketched above in Figure 12.

For the optimum geometry of vinylcarbene, the HOMO is a linear combination of all the atomic orbitals in the plane of the molecule: 
$$\text{HOMO} = (0.024 S + 0.185 P_x + 0.024 P_z)_{C_1} - (0.414 S + 0.726 P_x - 0.045 P_z)_{C_2} + (0.152 S - 0.115 P_x + 0.170 P_z)_{C_3} - (0.255 S)_{H_{C_1}} + (0.335 S)_{H_{C_2}} + (0.056 S)_{H_{\text{cis}}} - (0.139 S)_{H_{\text{trans}}}$$
 The major contribution is seen from the orbitals on  $C_2$ , and the HOMO may be crudely pictured as an  $sp^2$  lobe on  $C_2$ . The LUMO, on the other hand, is a linear combination of the three atomic orbitals perpendicular to the plane of the molecule: 
$$\text{LUMO} = (0.270 P_y)_{C_1} + (0.664 P_y)_{C_2} - (0.698 P_y)_{C_3}$$
 This is the second molecular orbital of the allyl system, having a nodal plane passing between  $C_1$  and  $C_3$  near  $C_1$ .

The dipole moment of the optimum structure of vinylcarbene is calculated to be quite large, 2.61 Debye. This value is greater and lies in a different direction from the dipole moment calculated simply on the basis of charge densities on the atoms. From the standpoint of charge densities alone, the molecule resembles a dipolar species with charges  $+\frac{1}{8}$  on  $C_3$  and  $-\frac{1}{8}$  on  $C_2$ . The negative charge on  $C_2$ , however, juts out in an  $sp^2$  lobe, and the total dipole moment of the molecule is changed accordingly, as depicted in Figure 13.

A bizarre effect of the CNDO/2 program is that, when  $\Theta$  is reduced to below  $80^\circ$ , the calculated energy plummets. This is accompanied by the interchange of the HOMO and LUMO levels described

above. An energy minimum for vinylcarbene is calculated for  $\Theta = 75^\circ$  that lies 0.042 a.u. (26 Kcal/mole) below the optimum structure described above. At this absolute minimum,  $\Psi$  is equal to  $15^\circ$ , a  $C_2-C_1-H$  equilibrium bond angle of  $150^\circ$ . This structure resembles an allyl anion with a positive lobe (see above, structure XXI); however, the extraordinarily strained geometry indicates that it is an artifact.

A similar sort of effect has been seen in calculations on ozone, which has a similar  $\pi$ -system to vinylcarbene, using the INDO modification of this program. The ground state of ozone ( ${}^1A^1$ ) may be described as an allyl system with 5 orthogonal lone pairs in the plane of the molecule. The excited  ${}^1A^1$  state (the 6  $\pi$  state) has two lone pair electrons excited into the allyl system; this state has a minimum calculated O-O-O bond angle of  $60^\circ$  and this minimum lies about 30 Kcal/mole above the ground state minimum.<sup>103</sup> An INDO calculation<sup>102</sup> on this excited state shows the energy of the 6  $\pi$  state to about 90 Kcal/mole below the ground state.<sup>104</sup> This is apparently an artifact of the program, and it closely resembles the behavior of vinylcarbene for  $\Theta < 80^\circ$ . The origin of this artifact is currently under investigation.

Note on Tables 15-20.

All binding energies in a. u.

Dipole moments in Debye.

The calculated binding energies have been rounded off to five decimal places.  $\text{Binding energy} = \text{Total energy} + 21.04990 \text{ a. u.}$

TABLE 15: CNDO/2 CALCULATIONS ON  $C_3H_5$  USING QCPE #141;  
 VARIATION OF ANGLE  $\Theta$  WITH A LINEAR CARBENE

All C-H Bond Lengths = 1.10 Å;  $C_1-C_2 = 1.33$  Å;  $C_1-C_3 = 1.34$  Å;  
 $\Phi = 180^\circ$ ;  $\Psi = 30^\circ$

Job Name	$\Theta$	Binding Energy for $\Omega = 0^\circ$	Binding Energy for $\Omega = 90^\circ$
CNINDO #171	120°	-2.70867	-2.65005
RUTABAGA	110°	-2.71119	-2.7004
"	100°	-2.72292	-2.76221
"	90°	-2.74422	-2.83284
"	88°	-2.74895	-2.84727
"	86°	-2.75347	-2.86150
"	84°	-2.75750	-2.87525
"	82°	-2.76078	-2.88844
"	80°	-2.76289	-2.90070
"	78°	-2.76334	-2.91160
"	76°	-2.76160	-2.92085
"	74°	-2.75698	-2.92794
"	72°	-2.74873	-2.93227
"	70°	-2.73593	-2.93326
"	68°	-2.71750	-2.93014
"	66°	-2.69229	-2.92207
"	64°	-2.65881	-2.90809
"	62°	--	-2.88706
"	60°	--	-2.85770

TABLE 16: CNDO/2 CALCULATIONS ON  $C_3H_5$  USING QCPE #141;  
 VARIATION OF ANGLE  $\Phi$

$C_2$ -H Bond Length = 1.07 Å; All other C-H bond lengths = 1.10 Å;  
 $C_1$ - $C_2$  = 1.42 Å;  $C_1$ - $C_3$  = 1.35 Å;  $\Theta$  = 120°;  $\Psi$  = 30°;  $\Omega$  = 0°

JOB NAME: EGGPLANTS

$\Phi$	Binding Energy	$\Phi$	Binding Energy <sup>a</sup>
180°	-2.69386	180°	-2.69386
175°	-2.69425	185°	-2.69219
170°	-2.69332	190°	-2.68897
165°	-2.69140	195°	-2.68497
160°	-2.68855	200°	-2.68013
155°	-2.68432	205°	-2.67392
150°	-2.67874	210°	-2.68351
145°	-2.78418	215°	-2.78998
140°	-2.79041	220°	-2.79622
135°	-2.79612	225°	-2.80181
130°	-2.80100	230°	-2.80649
125°	-2.80476	235°	-2.81000
120°	-2.80746	240°	-2.81244
115°	-2.80849	245°	-2.81327
110°	-2.80806	250°	-2.81273
105°	-2.80560	255°	-2.81030
100°	-2.80145	260°	-2.80639
95°	-2.79485	265°	-2.80037
90°	-2.78658	270°	-2.79300

TABLE 17: CNDO/2 CALCULATIONS ON  $C_3H_4$  USING QCPE #141:  
 VARIATION OF  $C_1-C_2$  BOND LENGTH

$C_2-H$  Bondlength = 1.07 Å; All other C-H bondlengths = 1.10 Å;  
 $C_1-C_3$  Bondlength = 1.35 Å;  $\Phi = 240^\circ$ ;  $\Theta = 120^\circ$ ;  $\Psi = 30^\circ$ ;  $\Omega = 0^\circ$

JOB NAME: SOYBEANS

$C_1-C_2$ Bondlength	Binding Energy	$C_1-C_2$ Bondlength	Binding Energy
1.30 Å	-2.79321	1.43 Å	-2.81136
1.31 Å	-2.79747	1.44 Å	-2.80993
1.32 Å	-2.80119	1.45 Å	-2.80817
1.33 Å	-2.80438	1.46 Å	-2.80610
1.34 Å	-2.80706	1.47 Å	-2.80374
1.35 Å	-2.80925	1.48 Å	-2.80108
1.36 Å	-2.81098	1.49 Å	-2.79815
1.37 Å	-2.81225	1.50 Å	-2.79496
1.38 Å	-2.81310	1.51 Å	-2.79151
1.39 Å	-2.81352	1.52 Å	-2.78783
1.40 Å	-2.81354	1.53 Å	-2.78392
1.41 Å	-2.81318	1.54 Å	-2.77979
1.42 Å	-2.81244		

TABLE 18: CNDO/2 CALCULATIONS ON  $C_3H_4$  USING QCPE #141:  
 VARIATION OF ANGLE  $\Theta$  WITH A BENT CARBENE

$C_2$ -H Bondlength = 1.07 Å; All other C-H bondlengths = 1.10 Å;  
 $C_1$ - $C_2$  Bondlength = 1.40 Å;  $C_1$ - $C_3$  Bondlength = 1.35 Å;  
 $\Phi = 240^\circ$ ;  $\Psi = 30^\circ$ ;  $\Omega = 0^\circ$

## JOB NAME: CABBAGES

$\Theta$	Binding Energy	Dipole Moment		
		X	Z	Absolute Value
130°	-2.80482	-0.09580	-3.15431	3.15576
125°	-2.80996	-0.27444	-3.02185	3.03429
120°	-2.81354	-0.44622	-2.88602	2.92031
115°	-2.81571	-0.61158	-2.74563	2.81292
110°	-2.81677	-0.76952	-2.60322	2.71457
105°	-2.81692	-0.92056	-2.46009	2.62668
100°	-2.81640	-1.07130	-2.31534	2.55117
95°	-2.81543	-1.21848	-2.17553	2.49352
90°	-2.81404	-1.37158	-2.04191	2.45980
85°	-2.81170	-1.53519	-1.91792	2.45667
80°	-2.80667	-1.71737	-1.79660	2.48539
75°	-2.84180	+0.30256	-0.98518	1.03059
70°	-2.82839	+0.33099	-1.21499	1.25927
65°	-2.82233	+0.34962	-1.01362	1.07222
60°	-2.76180	+0.68448	-1.80151	1.92716

TABLE 19: CNDO/2 CALCULATIONS ON  $C_3H_4$  USING QCPE #141:  
 VARIATION OF ANGLE  $\Psi$

$C_1$ -H Bondlength = 1.07 Å; All other C-H bondlengths = 1.10 Å;  
 $C_1$ - $C_2$  = 1.40 Å;  $C_1$ - $C_3$  = 1.35 Å;  $\Phi$  = 240°;  $\Omega$  = 0°

JOB NAME: PARSNIPS ( $\Theta$  = 105°)

JOB NAME: RADISHES ( $\Theta$  = 75°)

$\Psi$	Binding Energy	$\Psi$	Binding Energy
+15°	-2.81426	-45°	-2.78731
+20°	-2.81716	-40°	-2.79456
+25°	-2.81805	-35°	-2.80226
+30°	-2.81692	-30°	-2.81007
+35°	-2.81376	-25°	-2.81771
+40°	-2.80855	-20°	-2.82491
+45°	-2.80132	-15°	-2.83145
		-10°	-2.83716
		- 5°	-2.84190
		0°	-2.84556
		+ 5°	-2.84807
		+10°	-2.84936
		+15°	-2.84939
		+20°	-2.84815
		+25°	-2.84562
		+30°	-2.84180
		+35°	-2.83673
		+40°	-2.83042
		+45°	-2.82295

TABLE 20: CNDO CALCULATIONS ON  $C_3H_4$  USING QCPE #141:  
 ROTATION BY ANGLE  $\Omega$  ABOUT THE  $C_1-C_3$  BOND

$C_2-H$  Bondlength = 1.07Å; All other C-H Bondlengths = 1.10Å;  
 $C_1-C_3$  Bondlength = 1.35Å;  $\Phi = 240^\circ$ ;  $\Theta = 105^\circ$ ;  $\Psi = 25^\circ$

JOB NAME: PUMPKINS

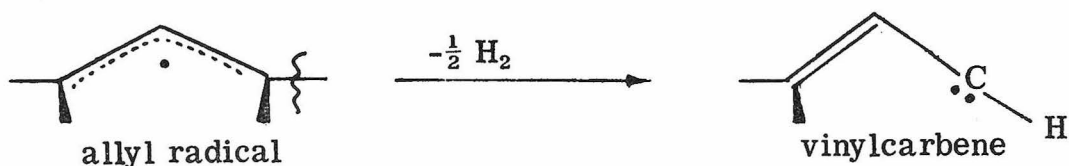
Dipole Moment

$\Omega$	Binding Energy	X	Y	Z	Absolute Value
0°	-2.81805	-0.94555	0.00000	-2.43446	2.61164
15°	-2.80908	-1.00629	0.32563	-2.37675	2.60146
30°	-2.80523	-0.71821	-0.81765	-2.48944	2.71693
45°	-2.79018	-0.46802	-1.01668	-2.59492	2.82601
60°	-2.77126	-0.15727	-1.01448	-2.78508	2.96826
75°	-2.75240	0.17842	-0.71713	-3.07736	3.16485
80°	-2.74755	0.27691	-0.52479	-3.10251	3.23736
85°	-2.74426	0.34903	-0.28047	-3.26520	3.29576
90°	-2.74309	0.37622	0.00000	-3.29763	3.31902

#### D. Discussion

The experimental results of the first two sections and the results of the calculations in the previous section will now be combined to draw a free energy surface for the rearrangement of 3,3-dimethylcyclopropene. First, two estimates will be made of energy differences not directly derivable from the experimental data: (1) the difference in  $\Delta H_f^0$  between cyclopropene and vinylcarbene, and (2) the difference in  $E_\pi$  between vinylcarbene and its diradical rotamer. No pretence will be made that these estimates represent quantitative predictions; rather, they are guesses of the orders of magnitude of these differences made using the prosthetic devices of thermochemical calculations and molecular orbital theory.

To make estimate (1), methods described by Benson are employed.<sup>105</sup> Vinylcarbene (V) would result from the removal of a vinylic hydrogen atom from a terminal position of allyl radical, as shown in Scheme U.



Scheme U

The heat of formation of an allyl radical is  $41.5 \pm 2$  Kcal/mole.<sup>106</sup> It will be assumed that the dissociation energy of a vinyl C-H bond is the same as the dissociation energy of a C-H bond in ethylene,  $108 \pm 2$  Kcal/mole.<sup>73</sup> The enthalpy recovered when a hydrogen atom is returned

to its standard state ( $\Delta H_f^0 = 0$ ) is -52 Kcal/mole. Summing these values,  $41.5 + 108 - 52 = 97.5$  Kcal/mole which, with an uncertainty of  $\pm 4$  Kcal/mole, is the estimated heat of formation of vinylcarbene. Note that it is indeed vinylcarbene (V) for which this heat of formation has been calculated, rather than the diradical (IV). This is due to the fact that the allylic stabilization of the new radical center on  $C_3$  exists only in vinylcarbene, and not in the diradical. Note also that the heat of formation of cyclopropene is 66.6 Kcal/mole;<sup>94</sup> hence, vinylcarbene lies about 30 Kcal/mole higher in energy than cyclopropene.

Estimate (2) will be made on the basis of the molecular orbital calculations in the previous section. The CNDO/2 energy barrier calculated for rotation of vinylcarbene to the diradical is very large, particularly if the values in Figure 12 are used; however, this barrier is on the order of magnitude of the barrier to rotation calculated for the allyl cation.<sup>107</sup> The variation of  $\Omega$  in Figure 12, though, was made without any attempt to optimize the geometry of the diradical--in particular, the  $C_1$ - $C_2$  bondlength of 1.40 Å is probably too long. In order to make a better guess of the energy difference between vinylcarbene and diradical isomers of  $C_3H_4$ , an estimate will be made in the difference in  $E_\pi$  from the Hückel calculations using the  $C_2$ - $C_3$  distance predicted by CNDO/2 for the optimum geometry of vinylcarbene. For  $\Theta = 105^\circ$ , this difference is about  $0.2 \beta$ .

The point of this discussion is that the energy difference between vinylcarbene and its diradical rotamer, IV, is predicted to be smaller than the energy difference between allyl and a  $90^\circ$  rotamer of allyl in which one of the  $\pi$ -orbitals is no longer in conjugation with the other

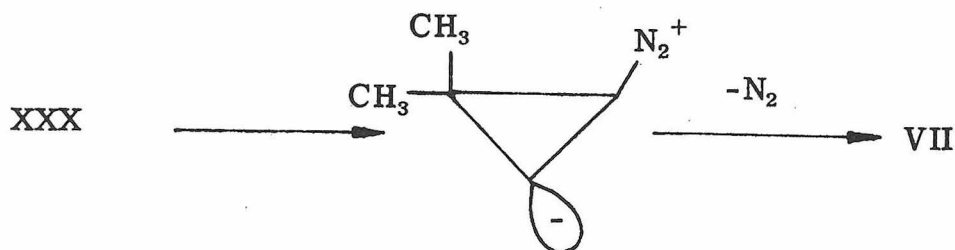
two. Since simple Hückel theory predicts this latter energy difference to be  $0.8\beta$ , the energy difference between vinylcarbene and its diradical rotamer should be about  $\frac{1}{4}$  the energy difference between rotamers of the allyl system.

The problem is, then, to find an experimental value for the energy difference between allyl rotamers. Likely values for this energy difference include the thermochemically determined "allylic resonance energy,"<sup>106</sup> the barrier to rotation in the allyl radical,<sup>108</sup> and the barrier to rotation in allyl cations.<sup>107,109,110</sup> These experimental determinations vary considerably. The "allylic resonance energy" has been measured as  $\Delta H = 9.3$  Kcal/mole, the difference between dissociation energy of a terminal C-H bond in propane and an allylic C-H bond in propene.<sup>106</sup> The barrier to rotation in an allyl radical, on the other hand, is estimated as  $\Delta G^\ddagger = 21 \pm 3$  Kcal/mole, based on the rate of trans-cis isomerization in 1-methylallyl radical.<sup>108</sup> Values for rotational barriers in allyl cations depend greatly upon the extent of alkyl substitution: the barrier in 1,1,2 trimethylallyl cation is  $\Delta G^\ddagger = 11.7 \pm 1$  Kcal/mole.<sup>109</sup> In 1,1-dimethylallyl cation  $\Delta G^\ddagger = 12.5 - 13.5$  Kcal/mole, in 1-methylallyl cation  $\Delta G^\ddagger$  is estimated to be 25-27 Kcal/mole, and, in allyl cation,  $\Delta G^\ddagger$  is estimated as 38-43 Kcal/mole.<sup>110</sup>

With this welter of different values, it is possible that these machinations will result in a value no less inaccurate than one based upon a random guess. Nonetheless, we forge on. The energy barrier for rotation of the allyl radical is chosen as the favored experimental value, as this experiment seems to bear the closest relation to our own.

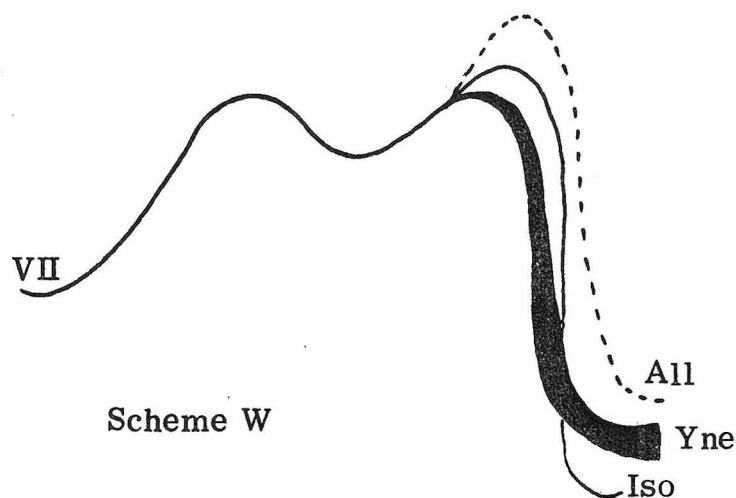
This choice is made despite the fact that the determination of  $\Delta G^\ddagger$  is rough, based upon rates of azo-compound decomposition and of radical recombination and upon comparisons of product distributions. The consequent estimate of the energy difference between vinylcarbene and its rotamer is 5 Kcal/mole. Combining estimates (1) and (2), the energy difference between cyclopropene and the diradical IV is guessed to be 35 Kcal/mole.

The rest of this discussion will be a treatment of the experimental data. Since this work was performed in gases, at pressures sufficiently high for thermal equilibrium to be assumed, it seems justifiable to construct a free energy surface based on the calculated rate constants. A kinetic scheme will be drawn consistent with the data and values of rate constants extracted. Before proceeding further, it should be noted that the experimental results do not exclude every alternative mechanism. In particular, the fortuitous circumstance is not excluded in which rearrangement of VII and pyrolysis of XXX proceed by paths that do not cross. Such a possibility, as depicted in Scheme V for pyrolysis of XXX, appears unlikely, since both reactions do give rise to the same acyclic products.

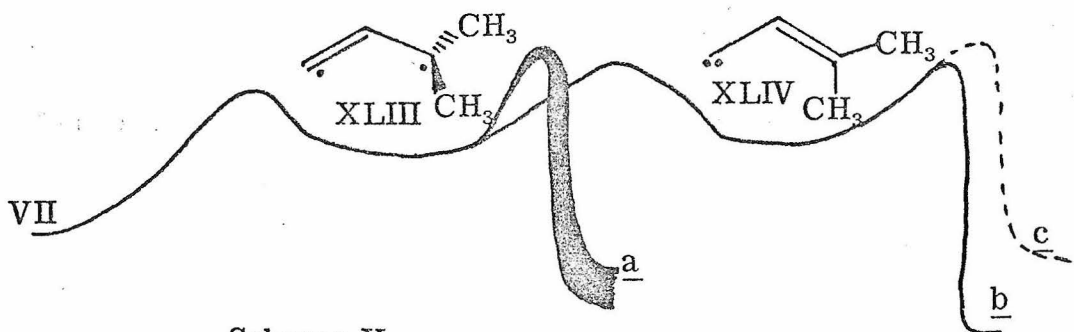


Scheme V

Among the reaction schemes eliminated is one in which a single intermediate lies between VII and its acyclic isomers, Scheme W. Were this the case, a common intermediate for the two reactions, represented by the dip in the curve, would give rise to the same distribution of acyclic products.



The double intermediate pathway shown in Scheme X will give the same result as the single intermediate pathway if the intermediate common to thermal rearrangement of VII and pyrolysis of XXX is XLIII. In other words, if the paths from the two reactions cross in this dip, the result should be the same as if only one intermediate existed. The experimental results (different acyclic product distributions from the two reactions) require that the common intermediate be XLIV, i. e. the dip to the right. For reasons outlined above in section B, XLIV is identified as  $\gamma, \gamma$ -dimethyl vinylcarbene. The experimental results further necessitate that Product a be isopropylacetylene, Product b be isoprene, and Product c be gem-dimethylallene.



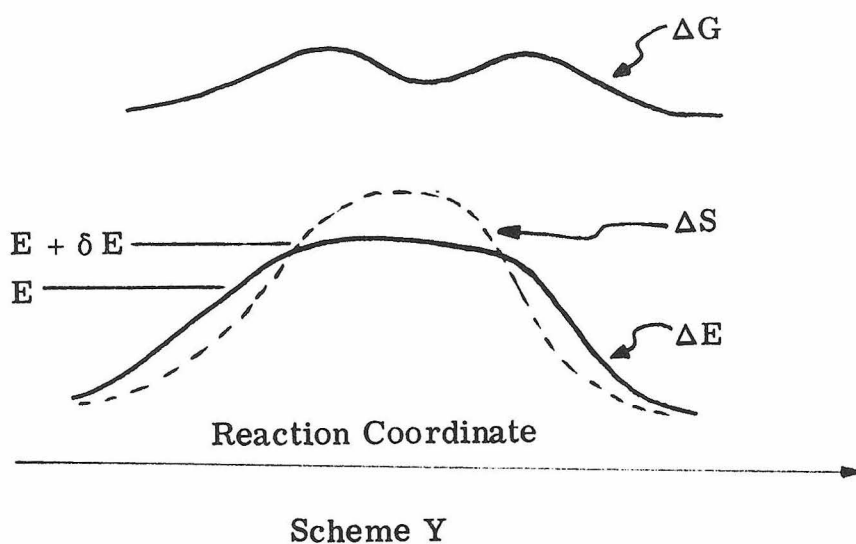
Scheme X

The intermediate lying in the dip to the left in Scheme X is identified with the diradical rotamer, XLIII, because of the paucity of other candidates and by analogy with the trimethylene diradical.<sup>6, 111</sup> Calculations ab initio have suggested that trimethylene does not lie in a potential energy well.<sup>111, 112</sup> There are other examples of intermediate diradicals which do not lie in potential wells: such species have been called "twixtyls" and are imagined to correspond to a nearly flat portion of a potential energy surface.<sup>113</sup>

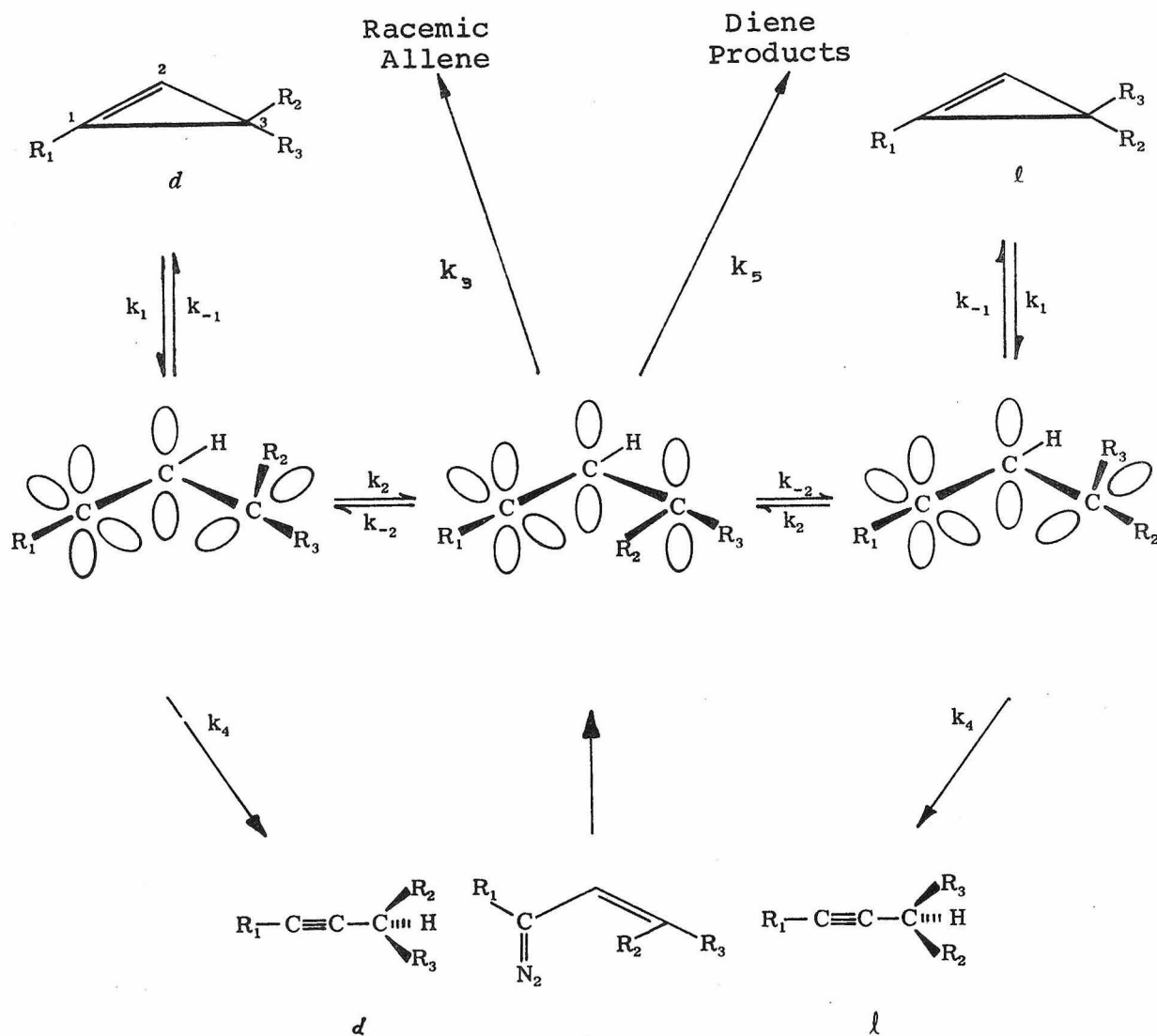
The point must be made, however, that the fact that a local minimum may not exist on a potential energy surface is not the equivalent of a claim that a local minimum does not occur on the corresponding free energy surface.

Consider the analogy of a ball rolling on a potential energy surface. The ball will have many more places to roll on a flat portion than on a curved portion. This notion may be clarified in terms of degrees of freedom along a reaction coordinate. Consider the 1-dimensional case shown in Scheme Y. In the band of energies between  $E$  and  $E + \delta E$ , there are more structures included (i. e. more degrees of freedom) near the top of the curve (where it is flat) than to either side. The consequence is that, although the potential energy is a maximum at the top of the curve, the entropy (that is, the entropy of mixing energetically equivalent geometries) is also at a maximum, and the sum

of these effects will result in the free energy curve drawn in Scheme Y, in which there is a local minimum at the same point where there is a maximum in the potential energy. As a consequence, it may be inferred that it is not necessary for the diradical XLIII to lie in a potential energy minimum in order for it to lie in a free energy well.



A general kinetic scheme for cyclopropene thermal rearrangements is shown in Scheme Z. There is a plane of symmetry in cyclopropene VII ( $R_1 = H$ ,  $R_2 = R_3 = CH_3$ ); hence, a chirality study is not possible for this compound. Nevertheless, it is possible to predict from our results relative rates of isomerization versus racemization of optically active cyclopropenes.



Scheme Z

The following kinetic expressions may be written, based upon a steady state approximation for each of the intermediates:

$$(1) \frac{d[\text{XLIII}]}{dt} = k_1 [\text{VII}] + k_{-2} [\text{XLIV}] - (k_{-1} + k_2 + k_4)[\text{XLIII}] = 0$$

and

$$(2) \frac{d[\text{XLIV}]}{dt} = k_2[\text{XLIII}] - (k_3 + k_5 + k_{-2})[\text{XLIV}] = 0$$

Therefore,

$$(3) [\text{XLIII}] = \frac{k_1[\text{VII}]}{k_{-1} + k_2 + k_4 - \frac{k_{-2}k_2}{k_3 + k_5 + k_{-2}}}$$

and

$$(4) [\text{XLIV}] = \frac{k_2}{k_3 + k_5 + k_{-2}} [\text{XLIII}]$$

Because  $k_3 \ll k_5$ ,  $k_3$  will be neglected.

$$(5) \frac{d[\text{Iso}]}{dt} = k_5[\text{XLIV}]$$

and

$$(6) \frac{d[\text{Yne}]}{dt} = k_4[\text{XLIII}]$$

whence, in the thermal rearrangement of VII,

$$(7) \frac{[\text{Iso}]}{[\text{Yne}]} = \bar{C} = \frac{k_5}{k_4} \frac{[\text{XLIV}]}{[\text{XLIII}]} = \frac{k_5 k_2}{k_4(k_5 + k_{-2})} = \frac{k_2}{k_4} \left( \frac{1}{1 + \frac{k_{-2}}{k_5}} \right).$$

In the pyrolysis of XXX,  $k_1$  may be neglected,

$$(8) \frac{d[\text{XLIII}]}{dt} = k_{-2}[\text{XLIV}] - (k_{-1} + k_2 + k_4)[\text{XLIII}].$$

Making the steady state assumption,  $\frac{d[\text{XLIII}]}{dt} = 0$ , and neglecting  $k_4 \ll k_{-1}$ , get

$$(9) \quad [\text{XLIII}] = \frac{k_{-2}[\text{XLIV}]}{k_{-1} + k_2}$$

whence, in pyrolysis of XXX,

$$(10) \quad \frac{[\text{XLIV}]}{[\text{XLIII}]} = \frac{k_{-1} + k_2}{k_{-2}}$$

Therefore,

$$(11) \quad \left\{ \frac{[\text{Iso}]}{[\text{Yne}]} \right\}_{\text{Pyrolysis of XXX}} = D = \frac{k_5(k_1 + k_2)}{k_4 k_{-2}} = \frac{k_5}{k_{-2}} \left( \frac{k_{-1}}{k_4} + \frac{k_2}{k_4} \right)$$

Designate the following ratios with symbols:

$$k_4/k_2 = X, \quad k_5/k_{-2} = Y, \quad k_{-1}/k_4 = Z.$$

Therefore,

$$(12) \quad \bar{C} = Y/X(Y+1)$$

and

$$(13) \quad D = Y(Z + 1/X).$$

Substituting experimentally determined values,

$$\bar{C} = 0.1, \quad D = 2.5, \quad Z = 10^2,$$

it is found that

$$X = 0.4 \quad \text{and} \quad Y = 0.04.$$

The implication of these results is that the hydrogen shifts which give rise to the acyclic products occur much more slowly than interconversion of the intermediates. The vinylcarbene XLIV reverts to the diradical 25 times faster than it rearranges to isoprene. Diradical XLIII closes to cyclopropene VII  $10^2$  times faster and rotates to the vinylcarbene XLIV  $2\frac{1}{2}$  times faster than it is converted to isopropylacetylene. An optically active cyclopropene following the same trend should initially open to a diradical, in which chirality is preserved. The diradical has a greater chance to proceed to a vinylcarbene than to rearrange to acetylene. The diradical has only a small chance to go to diene; the bulk of it will revert to diradical, of which nearly all will revert to cyclopropene. Since anything which passes through a vinylcarbene, which has a plane of symmetry, will become racemized, the prediction is that an optically active cyclopropene will racemize faster than it rearranges.

A further prediction is made for the thermal rearrangement of optically active cyclopropenes in the event that an acetylene is the major product. If there is an asymmetric propargyl carbon in this acetylene, then, at low conversion, this product should exhibit optical activity. The ratio of optically active to racemic acetylene extrapolated to zero conversion will equal the value of the ratio X above.

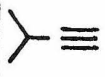
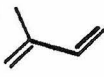
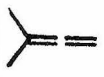
The ratios X, Y, and Z derived above are used to construct a free energy diagram along the reaction coordinate for thermal rearrangement of VII at  $500^\circ\text{K}$ , Figure 14. Since the pre-exponential factors are the same for formation of the two major products, the

difference in activation energies is also the difference in barrier heights,  $\Delta E_a = \Delta\Delta G^\ddagger = 2$  Kcal/mole.

The absolute barrier heights,  $\Delta G^\ddagger$ , are calculated from the kinetic parameters,  $\Delta G^\ddagger = \Delta H^\ddagger - T\Delta S^\ddagger$ . As  $E_a = 39$  Kcal/mole for the unimolecular rearrangement of VII to isopropylacetylene,  $\Delta H^\ddagger = 39$  Kcal/mole +  $RT = 38$  Kcal/mole, whence  $\Delta G^\ddagger = 37$  Kcal/mole at  $500^\circ\text{C}$ . From the value of Z, it is concluded that the barrier height for ring opening of VII to the diradical XLIII at  $500^\circ\text{K}$  is  $\Delta G = 33 \pm 1$  Kcal/mole. This value is consistent with the crude estimates, (1) and (2) above, of a potential energy difference of ca. 35 Kcal/mole between VII and diradical XLIII.

Other values of  $\Delta\Delta G^\ddagger$  in Figure 14 are derived from product ratios and the values of X and Y.  $\Delta H_f$  values for the hydrocarbons are listed in Table 21.

TABLE 21: HEATS OF FORMATION OF  $\text{C}_5\text{H}_8$  HYDROCARBONS  
AT  $298^\circ\text{K}$

	 (VII)	 (Yne)	 (Iso)	 (All)
$\Delta H_f^\circ(\text{g})$	$66.6^{94}$	$33^{73}$	$18^{114}$	$30^{73}$

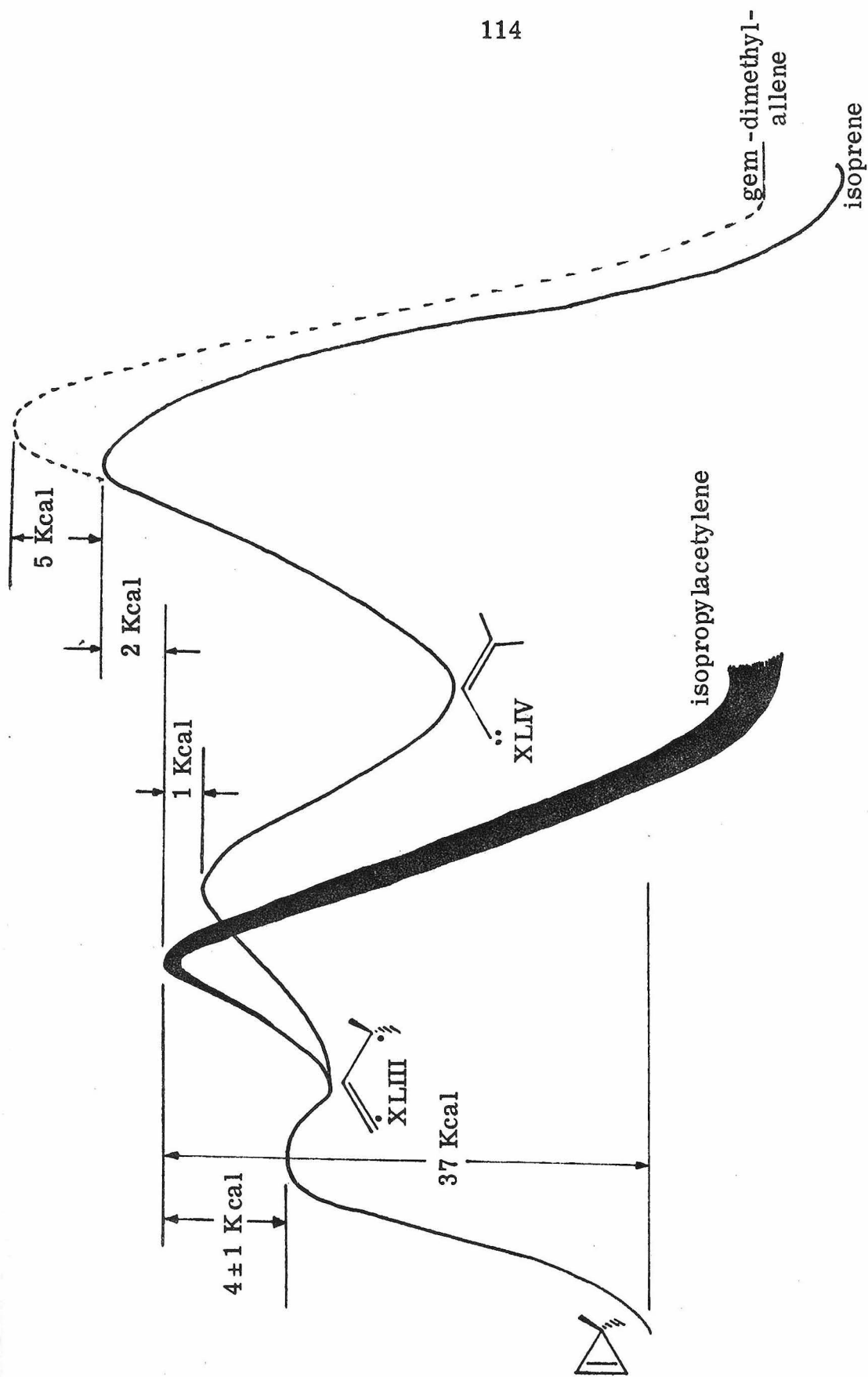


FIGURE 14: FREE ENERGY DIAGRAM FOR THERMAL REARRANGEMENT OF  
3,3-DIMETHYLCYCLOPROPENE AT 500°K

REFERENCES

1. A. Freund, *Mh. Chem.*, 3, 625 (1882).
2. T. S. Chambers and G. B. Kistiakowsky, *J. Amer. Chem. Soc.*, 56, 399 (1934).
3. B. S. Rabinovitch, E. W. Schlag, and K. B. Wiberg, *J. Chem. Phys.*, 28, 504 (1958).
4. E. W. Schlag and B. S. Rabinovitch, *J. Amer. Chem. Soc.*, 82, 5996 (1960).
5. R. Hoffmann, *Accts. Chem. Res.*, 4, 1 (1971).
6. R. J. Crawford and A. Mishra, *J. Amer. Chem. Soc.*, 88, 3963 (1966); R. Hoffmann, *J. Amer. Chem. Soc.*, 90, 1475 (1968).
7. R. G. Bergman and W. L. Carter, *J. Amer. Chem. Soc.*, 91, 7411 (1969).
8. Reviewed by R. G. Bergman in "Trimethylene: Case History of a Diradical," in J. Kochi, ed., Free Radicals, Wiley-Interscience, New York, 1972.
9. G. L. Closs and L. E. Closs, *J. Amer. Chem. Soc.*, 85, 99 (1963).
10. G. L. Closs, L. E. Closs, and W. A. Böll, *J. Amer. Chem. Soc.*, 85, 3796 (1963).
11. G. Büchi and J. D. White, *J. Amer. Chem. Soc.*, 86, 2884 (1964).
12. H.-H. Stechl, *Ch. Ber.*, 97, 2681 (1964).
13. M. A. Battiste, B. Halton, and R. H. Grubbs, *Chem. Comm.* 907 (1967).
14. R. Srinivasan, *J. Amer. Chem. Soc.*, 91, 6250 (1969).

15. R. Srinivasan, Chem. Comm., 1041 (1971).
16. E. J. York, W. Dittmar, J. R. Stevenson, and R. G. Bergman, J. Amer. Chem. Soc., 94, 2881 (1972).
17. G. L. Closs, personal communication.
18. S. W. Benson and H. E. O'Neal, Kinetic Data on Gas Phase Unimolecular Reactions, NBS-NSRDS 21, U.S. Gov't. Printing Office, Washington, 1970.
19. M. Franck-Neumann and C. Buchecker, Angew. Chem. Int. Eng. Ed., 9, 526 (1970).
20. W. Kirmse and L. Ruetz, Ann., 726, 30 (1969).
21. M. E. Hendrick, W. J. Baron, and M. Jones, Jr., J. Amer. Chem. Soc., 93, 1554 (1971).
22. H. Hiraoka and R. Srinivasan, J. Chem. Phys., 48, 2185 (1968).
23. H. Hiraoka and R. Srinivasan, J. Amer. Chem. Soc., 90, 2720 (1968); S. Boué and R. Srinivasan, J. Amer. Chem. Soc., 92, 1824 (1970).
24. I. S. Krull and D. R. Arnold, Tet. Letters, 1247 (1969).
25. R. Srinivasan, Tet. Letters, 203 (1970).
26. S. Boué and R. Srinivasan, J. Amer. Chem. Soc., 92, 3226 (1970); J. Saltiel, L. Metts, M. Wrighton, J. Amer. Chem. Soc., 92, 3227 (1970).
27. D. F. Eaton, R. G. Bergman, and G. S. Hammond, J. Amer. Chem. Soc., 94, 1352 (1972).
28. M. Franck-Neumann and C. Buchecker, Tet. Letters, 15 (1969).
29. A. C. Day and M. C. Whiting, J. Chem. Soc. C, 1719 (1966).

30. G. L. Closs, W. A. Böll, H. Heyn, and V. Dev, *J. Amer. Chem. Soc.*, 90, 173 (1968).
31. A. C. Day and R. N. Inwood, *J. Chem. Soc. C*, 1065 (1969).
32. L. Schrader, *Chem. Ber.* 104, 941 (1971).
33. C. Wentrup and W. D. Crow, *Tetrahedron*, 27, 361 (1971).
34. G. L. Closs, *Adv. Alicyclic Chem.*, 1, 53 (1966).
35. H. Werner and J. H. Richards, *J. Amer. Chem. Soc.*, 90, 4976 (1968).
36. R. Köster, S. Arora, and P. Binger, *Angew. Chem. Int. Eng. Ed.*, 9, 810 (1970).
37. H. Dürr, *Ch. Ber.*, 103, 369 (1970).
38. H. Dürr, L. Schrader, and H. Seidl, *Ch. Ber.*, 104, 391 (1971).
39. H. Dürr and H. Kober, *Angew. Chem. Int. Eng. Ed.*, 10, 342 (1971).
40. W. M. Jones and C. Lawrence Ennie, *J. Amer. Chem. Soc.*, 91, 6391 (1969); L. W. Christenson, E. E. Waali, W. M. Jones, *J. Amer. Chem. Soc.*, 94, 2118 (1972).
41. C. Wentrup and K. Wilczek, *Helv. Chim. Act.*, 53, 1459 (1970).
42. G. G. Vander Stouw, A. R. Kraska, and H. Shechter, *J. Amer. Chem. Soc.*, 94, 1655 (1972).
43. E. J. Corey and K. Achiwa, *Tet. Letters*, 3257 (1969).
44. E. J. Corey and K. Achiwa, *Tet. Letters*, 2245 (1970).
45. G. Wittig and J. J. Hutchison, *Ann.*, 741, 79 (1970).
46. K.-P. Zeller, H. Meier, and E. Müller, *Tet. Letters*, 537 (1971).

47. N. Gakis, M. Märky, H. -J. Hansen, and H. Schmid, *Helv. Chim. Acta*, 55, 748 (1972).
48. B. Jackson, N. Gakis, M. Märky, H. -J. Hansen, W. von Philipsborn and H. Schmid, *Helv. Chim. Acta*, 55, 916 (1972); B. Jackson, M. Märky, H. -J. Hansen, and H. Schmid, *Helv. Chim. Acta*, 55, 919 (1972).
49. T. DoMinh and A. M. Trozzolo, *J. Amer. Chem. Soc.*, 92, 6997 (1970).
50. A. Krebs and H. Kimling, *Angew. Chem. Int. Eng. Ed.*, 10, 409 (1971).
51. G. L. Closs, L. R. Kaplan, and V. I. Bendall, *J. Amer. Chem. Soc.*, 89, 3376 (1967).
52. G. L. Closs and L. R. Kaplan, *J. Amer. Chem. Soc.*, 91, 2168 (1969).
53. J. L. Brewbaker and H. Hart, *J. Amer. Chem. Soc.*, 91, 711 (1969).
54. E. J. Hamilton, D. E. Wood, and G. S. Hammond, *Rev. Sci. Instr.*, 41, 452 (1970). I am grateful to Dr. T. L. Penner for assistance in performing these experiments.
55. P. Dowd and K. Sachdev, *J. Amer. Chem. Soc.*, 89, 715 (1967).
56. F. J. Weigert, R. L. Baird, and J. R. Shapley, *J. Amer. Chem. Soc.*, 92, 6630 (1970).
57. Least squares value calculated using formulae in H. Margenau and G. M. Murphy, *The Mathematics of Physics and Chemistry*, Second Edition, Van Nostrand, Princeton, 1956, 9. 519.

58. F. O. Rice and K. F. Herzfeld, *J. Phys. Coll. Chem.*, 55, 975 (1951).
59. J. E. Taylor, D. A. Hutchings, and K. J. Frech, *J. Amer. Chem. Soc.*, 91, 2215 (1969); see also *Chem. and Eng. News*, 50 (16), 36 (17 April 1972).
60. P. S. Skell and A. Y. Garner, *J. Amer. Chem. Soc.*, 78, 5430 (1956).
61. W. von E. Doering and W. A. Henderson, Jr., *J. Amer. Chem. Soc.*, 80, 5274 (1958).
62. B. C. Anderson, *J. Org. Chem.*, 27, 2722 (1962).
63. D. Seyferth, H. Yamazaki, and D. L. Alleston, *J. Org. Chem.*, 28, 703 (1963).
64. C. L. Osborne, T. C. Shields, B. A. Shoulders, G. F. Krause, H. V. Cortez, and P. D. Gardner, *J. Amer. Chem. Soc.* 87, 3158 (1965).
65. E. A. Dorko and R. W. Mitchell, *Tet. Letters* 341 (1968).
66. A. T. Young and R. D. Guthrie, *J. Org. Chem.*, 35, 853 (1970).
67. S. Lippincott, U. S. Patent #2, 642, 453, reported in *Chem. Abstracts*, 48, 458lh (1954).
68. H. A. Szymanski and R. E. Yelin, *NMR Band Handbook*, Plenum, New York, 1968, p. 67.
69. L. Fieser and M. Fieser, *Reagents for Organic Synthesis*, Wiley, New York, 1967, p. 687.
70. Least squares program written and lent by Dr. J. W. Meyer.
71. G. Egloff, *The Reactions of Pure Hydrocarbons*, ACS Monograph #73, Reinhold, New York, 1937, p. 462.

72. G. Egloff, G. Hulla, and V. I. Komarewsky, Isomerization of Pure Hydrocarbons, ACS Monograph #88, Reinhold, New York, 1942, pp. 270-272.
73. S. W. Benson, Thermochemical Kinetics, Wiley, New York, 1968.
74. M. B. D'Amore, Ph.D. Thesis, California Institute of Technology, 1972, pages 109 - 126.
75. K. W. Egger and S. W. Benson, J. Amer. Chem. Soc., 87, 3314 (1965); D. Golden, private communication.
76. R. R. Jones and R. G. Bergman, J. Amer. Chem. Soc., 94, 660 (1972).
77. M. B. D'Amore, Ph.D. Thesis, California Institute of Technology, 1972, pages 178-180.
78. G. M. Kaufman, J. A. Smith, G. G. Vander Stouw, and H. Shechter, J. Amer. Chem. Soc., 87, 935 (1965).
79. M. Olomucki and P. Hebrard, Tet. Letters, 13 (1969).
80. P. Hebrard and M. Olomucki, Bull. Soc. Chim. France, 1938 (1970).
81. H. Staudinger, W. Kries, and M. Schill, Helv. Chim. Acta, 5, 743 (1922).
82. T. J. Lobl, Ph.D. Thesis, John Hopkins University, 1970, pages 95-99.
83. C. A. Aufdermarsh, Jr., Ph.D. Thesis, Yale University, 1958, pages 71-72.
84. C. D. Hurd and S. C. Lui, J. Amer. Chem. Soc., 57, 2656 (1935).

85. K. E. Schulte, J. Reisch, and M. Sommer, *Arch. Pharm.*, 299, 107 (1966).
86. E. A. Werner, *J. Chem. Soc.*, 115 (2), 1093 (1919).
87. J. G. Welch, Ph.D. Thesis, Rice University, 1968, pages 84-90.
88. W. M. Coates and J. R. Corrigan, *Chem. and Ind.*, 1594 (1969).
89. C. D. Gutsche, *Organic Reactions* VIII, 364 (1954).
90. J. D. Roberts, Notes on Molecular Orbital Calculations, Benjamin, New York, 1961, pages 82-90.
91. P. H. Kasai, R. J. Myers, D. F. Eggers, and K. B. Wiberg, *J. Chem. Phys.*, 30, 512 (1959).
92. K. D. Wiberg, *J. Amer. Chem. Soc.*, 90, 59 (1968).
93. Courtesy of Professor J. D. Roberts.
94. K. B. Wiberg and R. A. Fenoglio, *J. Amer. Chem. Soc.*, 90, 3395 (1968).
95. J. A. Pople and D. L. Beveridge, Approximate Molecular Orbital Theory, McGraw-Hill, New York, 1970, pages 57-84.
96. *Ibid.*, pp. 163-193.
97. *Ibid.*, pp. 85-127.
98. R. Gleiter and R. Hoffmann, *J. Amer. Chem. Soc.*, 90, 5457 (1968).
99. R. G. Weiss, *Tetrahedron* 27, 271 (1971).
100. G. Salem and G. Rowland, *Angew. Chem. Int. Eng. Ed.*, 11, 92, (1972).
101. QCPE 91, Program CNDO/2 written by G. A. Segal.
102. QCPE 141, Program CNINDO written by P. A. Dobosh. Modified for multiple computations by Dr. R. E. Carhart.

103. P. J. Hay and W. A. Goddard, III, *Chem. Phys. Letters*, 14, 46 (1972).
104. W. R. Wadt and W. A. Goddard, III, unpublished results.
105. H. E. O'Neal and S. W. Benson, *J. Phys. Chem.*, 72, 1866 (1968).
106. R. J. Field and P. J. Abell, *J. Amer. Chem. Soc.*, 91, 7226 (1969).
107. S. D. Peyerimhoff and R. J. Buenker, *J. Chem. Phys.*, 51, 2528 (1969).
108. R. J. Crawford, J. Hamelin, and B. Strehlke, *J. Amer. Chem. Soc.*, 93, 3881 (1971).
109. J. M. Bollinger, J. M. Brinich, and G. A. Olah, *J. Amer. Chem. Soc.*, 92, 4025 (1970).
110. V. Buss, R. Gleiter, and P. v. R. Schleyer, *J. Amer. Chem. Soc.*, 93, 3927 (1971).
111. P. J. Hay, W. J. Hunt, and W. A. Goddard, *J. Amer. Chem. Soc.*, 94, 638 (1972).
112. J. A. Horseley, Y. Jean, C. Moser, L. Salem, R. M. Stevens, J. S. Wright, *J. Amer. Chem. Soc.*, 94, 279 (1972).
113. R. Hoffmann, S. Swaminathan, B. G. Odell, R. Gleiter, *J. Amer. Chem. Soc.*, 92, 7091 (1970).
114. J. D. Cox and G. Pilcher, Thermochemistry of Organic and Organometallic Compounds, Academic Press, London, 1970, pp. 144-5.

PART II: Interaction of Remote Functional Groups in the  
Ion Chemistry of Bifunctional Ethers

*If the stars that move together as one, disband,  
Flying like insects of fire in a cavern of night,  
Pipperoo, pippera, pipperum ... the rest is rot.*

Wallace Stevens, *On an Old Horn*

BACKGROUND

The scientific study of the chemical interactions of electrons with matter commences with the observations by Priestley<sup>1</sup> and by Cavendish<sup>2</sup> in 1785 that air is converted to oxides of nitrogen by an electric spark. The understanding of the mechanisms of electron-induced chemical reactions was advanced by Goldstein's observations a century later of "canal rays,"<sup>3</sup> luminous streams of positive ions produced by electrical discharge in rarefied gases. The knowledge of the connections between ionization phenomena and chemical reactions at the close of the 19th century was summarized by Stark in the last few pages of his compendious Electricity in Gases.<sup>4</sup>

The discovery by Wien<sup>5</sup> that canal rays could be deflected by parallel electric and magnetic fields led to the development of the mass spectrometer by J. J. Thomson in 1906.<sup>6</sup> Thomson recognized two of the fundamental processes arising from the production of ions by electron impact: dissociation of molecular ions and chemical reaction between ions and neutral species.<sup>7</sup>

Until recently, the principal technique of investigating reactions between molecules and electrons has been conventional mass spectrometry.<sup>8</sup> This technique, of course, has been used largely to examine the ionization and subsequent dissociation of molecules, a process most frequently considered as the initial step in chemical reactions induced by electrons. The stages of chemical reaction posterior to ionization, however, have been best examined by newer methods:

high pressure mass spectrometry,<sup>9</sup> flowing afterglow,<sup>10</sup> and Ion Cyclotron Resonance (ICR).

Of these newer techniques, ICR appears to be the most versatile. In the past seven years, the ICR method has been used in a large variety of experiments. These include the study of inaccessible excited states of organic molecules,<sup>11</sup> characterization of structures of ions in the gas phase,<sup>12-15</sup> determination of the effect of dipole moment on the efficiency of momentum transfer from an ion to a neutral,<sup>16</sup> examination of the molecular orbital levels of nitrogen,<sup>17</sup> determination of the gas phase acidities and basicities of large numbers of compounds,<sup>18-20</sup> measurement of the rate constants for bi- and termolecular ion-molecule reactions,<sup>21,22</sup> and investigations of the mechanisms of ionic reactions of organic compounds.<sup>20,23</sup>

An ICR is a mass spectrometer which utilizes a magnetic resonance phenomenon for detection. An ion orbiting in a magnetic field will absorb electromagnetic radiation at the cyclotron frequency; this frequency is a function of the magnetic field strength and the  $m/e$  value of the ion. The theory and implementation of ICR are discussed extensively in the literature<sup>20</sup>.

The examination of ion-molecule reactions has enhanced the understanding of electron-induced chemical reactions, for when a substance is irradiated, many of the important secondary processes are ion-molecule reactions. Equally important, however, is the fact that the study of ion-molecule reactions provides insight into the primary processes which occur in ionized molecules. This arises because an ion-molecule reaction is the reverse of a fragmentation, as

depicted in Scheme I. The association of an ion and a neutral molecule ( usually exothermic), such as observed in the ICR, is the reverse of the fragmentation of an ionized molecule into charged and uncharged moieties ( usually endothermic ), such as observed in the mass spectrometer. In this manner, ions may be generated in the ICR whose structure and thermochemistry may be defined, and subsequent rearrangements of the complex may be investigated.



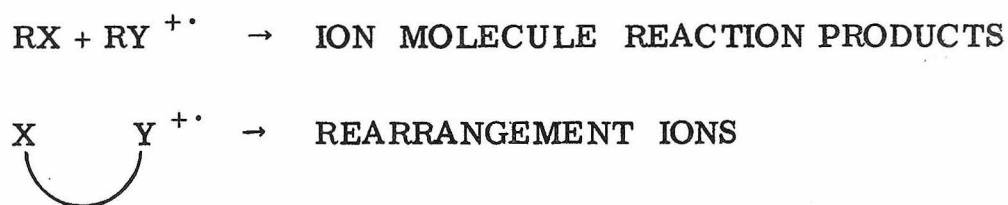
#### SCHEME I

The field of mass spectrometry of organic compounds has been developed to a point where many fragmentation and rearrangement processes may be explained as analogues of more familiar organic reactions.<sup>24</sup> Such an analysis presumes that charge be localized in the parent ion. This is based upon the assumption that the bulk of molecular ions are formed by removal of an electron from the highest occupied energy levels of the neutral; in a functionalized molecule, this is taken to mean that the molecular ion is formed by removal of an electron from a non-bonding lone pair on the functional group.<sup>25</sup>

The successes of mass spectral analysis of monofunctional molecules have prompted the following query: do two functional groups on the same ion react independently from one another or do they act in concert?<sup>26</sup> The observation by Bowie, *et. al.*, in 1965 that the mass

spectra of bifunctional esters manifest rearrangements in which remote functional groups interact<sup>27</sup> has led to extensive research into the mass spectrometry of polyfunctional compounds.<sup>26-35</sup>

The inference that many functional group interactions resemble "internal ion-molecule reactions,"<sup>29</sup> depicted in Scheme II, suggested that an ICR study of the mass spectra and ion-molecule reactions of bifunctional compounds would lead to further insights regarding these processes. Reports of chainlength effects on remote oxidation in solution,<sup>36,37</sup> on "internal solvation" in the loss of water from long chain alcohols,<sup>38</sup> and of a stereoselective mass spectral rearrangement analogous to the Barton reaction<sup>39</sup> indicated that an investigation of the effects of chainlength might lead to detailed information regarding the mechanisms by which remote functional groups interact.



SCHEME II

The work described below consists of ICR investigations of bifunctional ethers carried out in Noyes Laboratory from September, 1971, through June, 1972. The ethers were chosen for investigation because of the simplicity of their ion chemistry, their volatility, and the ease with which deuterium labels can be placed at specific positions in the molecule. Portions of this work were presented before the organic section of the 163rd national meeting of the American Chemical Society in Boston, 12 April 1972.<sup>40</sup>

NOTE ON TERMINOLOGY

The intensity of an ICR peak,  $I_i$ , is directly proportional to the abundance of the ion. For comparison of ions of different masses, however, peak intensities must be normalized by dividing the intensity by the mass of the ion,  $I_i/m_i$ . Ion abundances are tabulated as the fraction of total ionization,

$\frac{I_i/m_i}{\Sigma I_i/m_i}$ . In this thesis, the fraction is frequently converted to a percent total ionization or  $\% \Sigma$ . The terms  $\frac{I_i/m_i}{\Sigma I_i/m_i}$ , percent total ionization, and  $\% \Sigma$  are used interchangeably.

A. Electron impact and chemical ionization mass spectra of bifunctional ethers studied by ICR

Most mass spectral studies of ethers are concerned with structural elucidation and analysis.<sup>41-43</sup> Consequently, high energy electron impact ionization is routinely employed, and the bulk of the ions arise from fragmentations of carbon-carbon bonds of the molecular ion. Examples are to be found in the 70 eV mass spectra of monofunctional aliphatic ethers: where R is an n-alkyl group longer than ethyl, the base peak from ROCH<sub>3</sub> is the m/e 45 ion, CH<sub>3</sub>OCH<sub>2</sub><sup>+</sup>, resulting from α-cleavage (fission of an α,β carbon-carbon bond<sup>24</sup>), while the base peaks from R<sub>2</sub>O are hydrocarbon fragments (eg. C<sub>4</sub>H<sub>9</sub><sup>+</sup> from di-n-octyl ether).<sup>41</sup>

Rearrangements, processes not explicable as simple bond fissions, are also seen. Prominent among these are "hydrogen rearrangements," which may be described as internal hydrogen shifts followed by fragmentation.<sup>44,45</sup> Other rearrangements occur that are quite extraordinary, for instance the rearrangement by which C<sub>2</sub>H<sub>3</sub>D<sub>2</sub> (and no C<sub>2</sub>H<sub>5</sub>) is lost from C<sub>2</sub>H<sub>5</sub>OCD<sub>2</sub>CH<sub>2</sub>C<sub>2</sub>H<sub>5</sub>.<sup>46</sup>

Effects of variation of ionization energy

As the energy of the ionizing electrons is reduced to within a few eV of the ionization potential, varieties of rearrangement become pronounced that are minor at 70 eV. As an example, two

ions in the ICR mass spectra of 1-methoxyoctane,  $[M-C_5H_9]^+$  (m/e 75) and  $[M-CH_3OH-C_2H_6]^+$  (m/e 82), are insignificant at 70 eV (0.5% and 3%  $\Sigma$ , respectively), but become prominent below 20 eV. This is illustrated in Table I.

Table I: ICR MASS SPECTRA OF 1-METHOXYOCTANE: % $\Sigma^a$   
(Ten most prominent ions)

Electron Energy	m/e	45	29	69	84	41	83	70	112	56	43
70 eV		17	7	7	6	6	6	6	5	4	4
	m/e	75	84	83	70	112	45	69	57	82	68
16 eV		17	10	10	9	9	8	7	6	6	4
	m/e	112	75	83	84	82	70	(Only ions observed)			
12 eV		27	19	15	15	14	10				
	m/e	112	$[M-CH_3OH]^+$				m/e	69	$C_5H_9^+$		
	m/e	84	$[M-CH_3OH-C_2H_4]^+$				m/e	56	$C_4H_8^+$ ; $C_3H_4O^+$		
	m/e	83	$[M-C_2H_5-CH_3OH]^+$				m/e	45	$CH_3OCH_2^+$		
	m/e	82	$[M-CH_3OH-C_2H_6]^+$				m/e	43	$C_3H_7^+$		
	m/e	75	$[M-C_5H_9]^+$				m/e	41	$C_3H_5^+$		
	m/e	70	$C_5H_{10}^+$				m/e	29	$C_2H_5^+$		

$a \frac{I_i/m_i}{\Sigma I_i/m_i}$ ; to nearest %

Another example is the breakdown of methoxycyclopentane, shown in Table II.

Table II: ICR MASS SPECTRA OF METHOXYCYCLOPENTANE:  
 $\% \Sigma^a$   
 (Ten most prominent ions<sup>b</sup>)

Electron  
Energy

	m/e	71	41	100	43	58	39	67	29	57	45
70 eV		42	10	8	4	4	3	3	3	3	2

	m/e	100	71	69	85	
12 eV		54	35	6	4	(Only ions observed)

m/e 100	Molecular Ion, [M] <sup>•+</sup>	m/e 57	C <sub>4</sub> H <sub>9</sub> <sup>+</sup>
m/e 85	[M-CH <sub>3</sub> ] <sup>+</sup>	m/e 45	C <sub>2</sub> H <sub>5</sub> O <sup>+</sup>
m/e 71	[M-C <sub>2</sub> H <sub>5</sub> ] <sup>+</sup>	m/e 43	C <sub>3</sub> H <sub>7</sub> <sup>+</sup>
m/e 69	[M-CH <sub>2</sub> O•] <sup>+</sup>	m/e 41	C <sub>3</sub> H <sub>5</sub> <sup>+</sup>
m/e 67	[M-H•-CH <sub>3</sub> OH] <sup>+</sup>	m/e 39	C <sub>3</sub> H <sub>3</sub> <sup>+</sup>
m/e 58	[M-C <sub>3</sub> H <sub>6</sub> ] <sup>•+</sup>	m/e 29	C <sub>2</sub> H <sub>5</sub> <sup>+</sup> ; CHO <sup>+</sup>

a  $\frac{I_i/m_i}{\Sigma I_i/m_i}$ ; to nearest %.

b m/e 28 omitted as N<sub>2</sub> impurity

Rearrangements in which a neutral molecule is expelled from the molecular ion to leave behind an odd electron ion are subject to the same constraints usually inferred for both mass spectral fragmentations and for ion-molecule reactions. First, the process occurs without an activation energy barrier. Second, the rate is a function of a frequency factor for the process and of the endothermicity of the reaction.

A general expression for the unimolecular rate constant for mass spectral rearrangements is  $k = \nu \left( \frac{E^* - E}{E^*} \right)^{s-1}$ , where  $\nu$  is a frequency factor,  $E^*$  the energy content of the reactant, and  $s$  a number related to the number of vibrational modes which participate in the reaction.  $E$  is the endothermicity of the reaction, and  $E^*$  must be greater than  $E$  for the reaction to occur. Note that the separation of an ion and a molecule is always an endothermic process, as an ion will polarize a neutral and attract it, even in the absence of chemical bonding.<sup>47</sup>

At high electron energies, fragmentations, in which a neutral radical is expelled from the molecular ion to leave behind an even electron ion, predominate because the energy content of the parent ion is quite large. As a consequence, relative rates of daughter ion formation are controlled more by the frequency factor than by the endothermicity of the reaction.

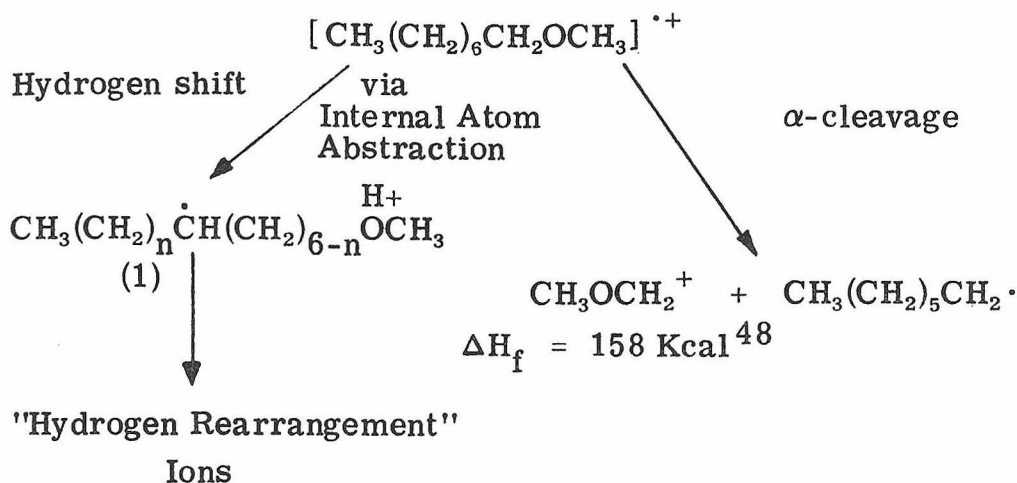
At electron energies approaching threshold, however, rearrangement processes, for which the frequency factor is less favorable than for simple fragmentations, begin to dominate and often become exclusive processes. This can be rationalized on the

basis that simple fragmentations are too endothermic to occur in a molecular ion with small energy content.

Most of the rearrangement ions from 1-methoxyoctane and methoxycyclopentane arise via complex processes, for which many different mechanisms can be drawn. The elucidation of these mechanisms should be an interesting study, but not within the scope of this thesis. Instead, the ICR mass spectra of bifunctional ethers of the structure  $\text{CH}_3\text{O}(\text{CH}_2)_n\text{OR}$ , where  $\text{R} = \text{H}$  ( $n = 2-4$ ),  $\text{CH}_3$  ( $n = 1-6$ ), or  $\text{C}_2\text{H}_5$  ( $n = 2-6$ ) have been examined. Only a few processes are common to both  $n$ -alkyl monofunctional ethers and the bifunctional ethers studied. Surprisingly, it is the bifunctional ethers that manifest the simpler spectra.

#### Hydrogen shifts and $\alpha$ -cleavage

Two ions of particular interest are the  $\alpha$ -cleavage ion,  $\text{CH}_3\text{OCH}_2^+$  ( $m/e$  45, base peak at high electron energy), and the hydrogen rearrangement ion  $[\text{M}-\text{CH}_3\text{OH}]^{+\cdot}$  (base peak at low electron energy). These ions are prominent in the bifunctional ethers studied as well as in 1-methoxyoctane. The  $\alpha$ -cleavage ion usually disappears at low electron energy. An estimation of the thermochemistry of the  $\alpha$ -cleavage process provides a rationalization of this result.



Scheme III

From Scheme III, it is seen that the  $\alpha$ -cleavage of 1-methoxyoctane is in competition with hydrogen rearrangements. Thermodynamic estimates based upon bond dissociation energies<sup>49</sup> and upon ionization potentials<sup>48, 50</sup> indicate that  $\alpha$ -cleavage is endothermic by about 10 Kcal. The hydrogen rearrangement may be depicted as proceeding from an intermediate, ion (1), which results from internal hydrogen atom abstraction. This hydrogen shift is estimated to be 10 Kcal exothermic, based upon the hydrogen atom affinity of the ionized functional group<sup>20, 51</sup> and the hydrocarbon bond dissociation energy.<sup>49</sup>

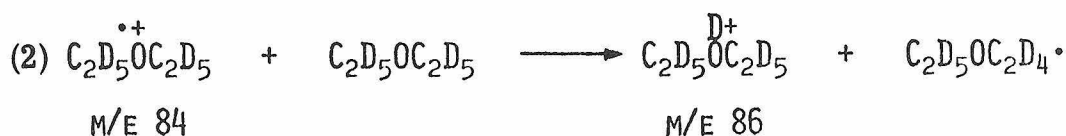
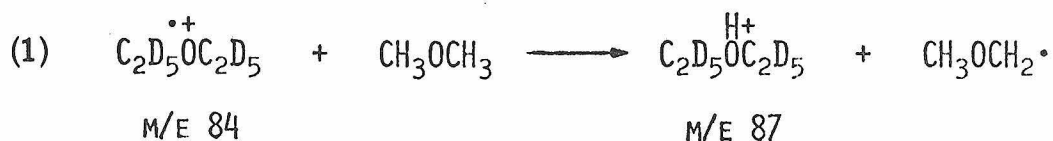
The hydrogen shift to form ion (1) is considered to be rate limiting for three reasons. First, the loss of a neutral fragment may be considered as irreversible at low pressures. Second, no molecular ion is observed, even at low electron energies. Therefore, the exothermicity of the hydrogen shift is sufficient to separate the

ion and the neutral fragment (an endothermic step), giving rise to the observed rearrangement ions. Third, the frequency factor for the hydrogen shift (and for the reverse reaction, reversion of ion (1) to the molecular ion) is undoubtedly smaller than the frequency factor for fragmentation. At high electron energy, the energy content of the molecular ion is sufficiently great for the  $\alpha$ -cleavage process, an endothermic reaction with a large frequency factor, to compete favorably with the hydrogen shift, an exothermic reaction with a small frequency factor. As the energy content of the molecular ion is diminished, the hydrogen shift becomes the favored competitor, and, ultimately,  $\alpha$ -cleavage is no longer observed.

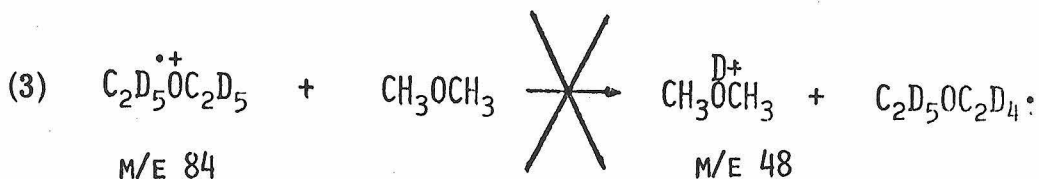
Thermodynamic considerations are equally important in ion-molecule reactions, as exemplified by the following observations. At a pressure of  $3 \times 10^{-5}$  Torr, a mixture of dimethyl ether and diethyl ether- $d_{10}$  was bombarded with 9.5 eV electrons. The only primary ion observed under these conditions is the molecular ion of diethyl ether, as the ionization potentials of dimethyl and diethyl ether are 10.00 and 9.53 eV respectively.<sup>50</sup> Two secondary ions are observed: the protonated parent and the deuterated parent of diethyl ether- $d_{10}$ . ICR double resonance<sup>20</sup> confirms that Reactions (1) and (2) in Scheme IV, both hydrogen atom abstractions, are occurring.

All three reactions in Scheme IV are exothermic. The values of  $\Delta H$  for reactions (1) and (2), estimated as the difference between the hydrogen atom affinity of  $(C_2H_5)_2O^+$ <sup>20,51</sup> and the C-H bond dissociation energy of dimethyl ether,<sup>32</sup> lie between -10 and -15 Kcal/mole.

ION-MOLECULE REACTIONS OBSERVED AT 9.5 E.V. ELECTRON ENERGY  
IN A MIXTURE OF DIETHYL ETHER- $d_{10}$  AND DIMETHYL ETHER



NO IONS OBSERVED AT 46, 47, OR 48 AMU.



Scheme IV

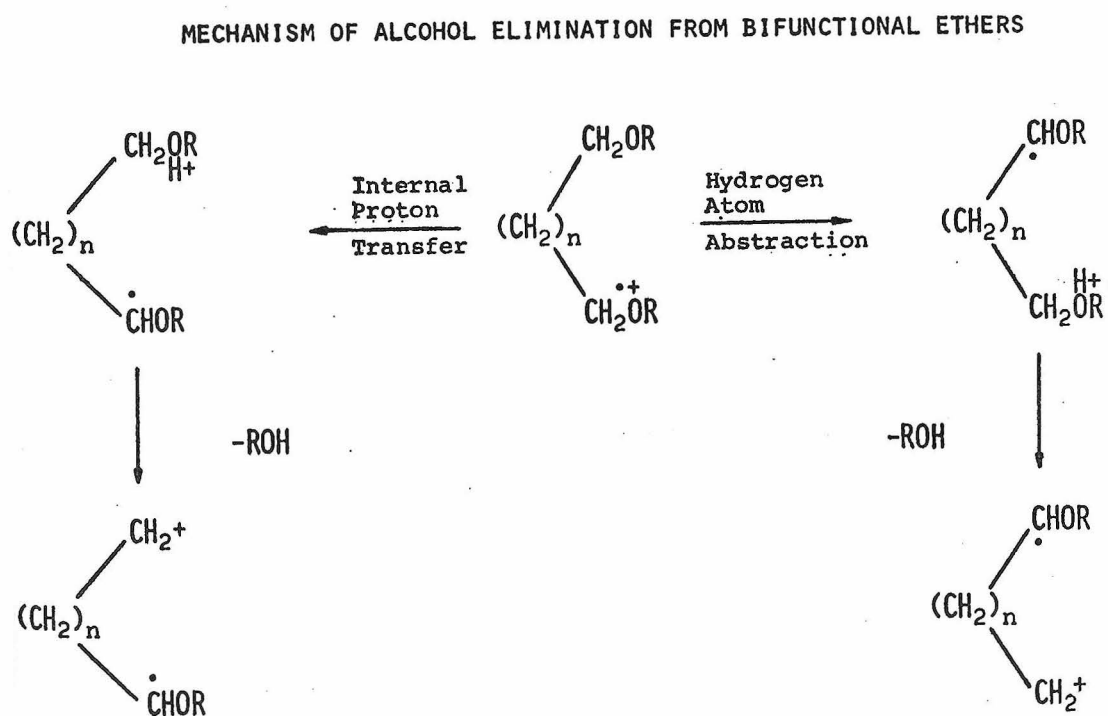
Reaction (3) is a deuteron transfer from the molecular ion of  $(\text{C}_2\text{H}_5)_2\text{O}$  to dimethyl ether. Although this reaction is estimated to be exothermic by 3 Kcal/mole, it is not observed.

Interestingly, when methyl ethyl ether is used in place of dimethyl ether, the deuteron transfer from  $(\text{C}_2\text{D}_5)_2\text{O}^{\cdot+}$  to  $\text{CH}_3\text{OC}_2\text{H}_5$  is observed by ICR double resonance. The value of  $\Delta H$  for this reaction is estimated to be about -9 Kcal/mole.

The intramolecular analogue of these ion-molecule reactions is the hydrogen rearrangement in bifunctional ethers, represented in Scheme V. Here, unlike the monofunctional ethers, the hydrogen shift, initial step in the hydrogen rearrangement, may be either an atom abstraction or an internal proton transfer; these reactions are indistinguishable, as indicated in Scheme V.

### The Type E<sub>1</sub> hydrogen rearrangement

The hydrogen rearrangement by which a molecule of alcohol is lost from the molecular ion (Scheme V) falls into the category designated as Type E<sub>1</sub> rearrangement by Biemann.<sup>8</sup> Type E<sub>1</sub>



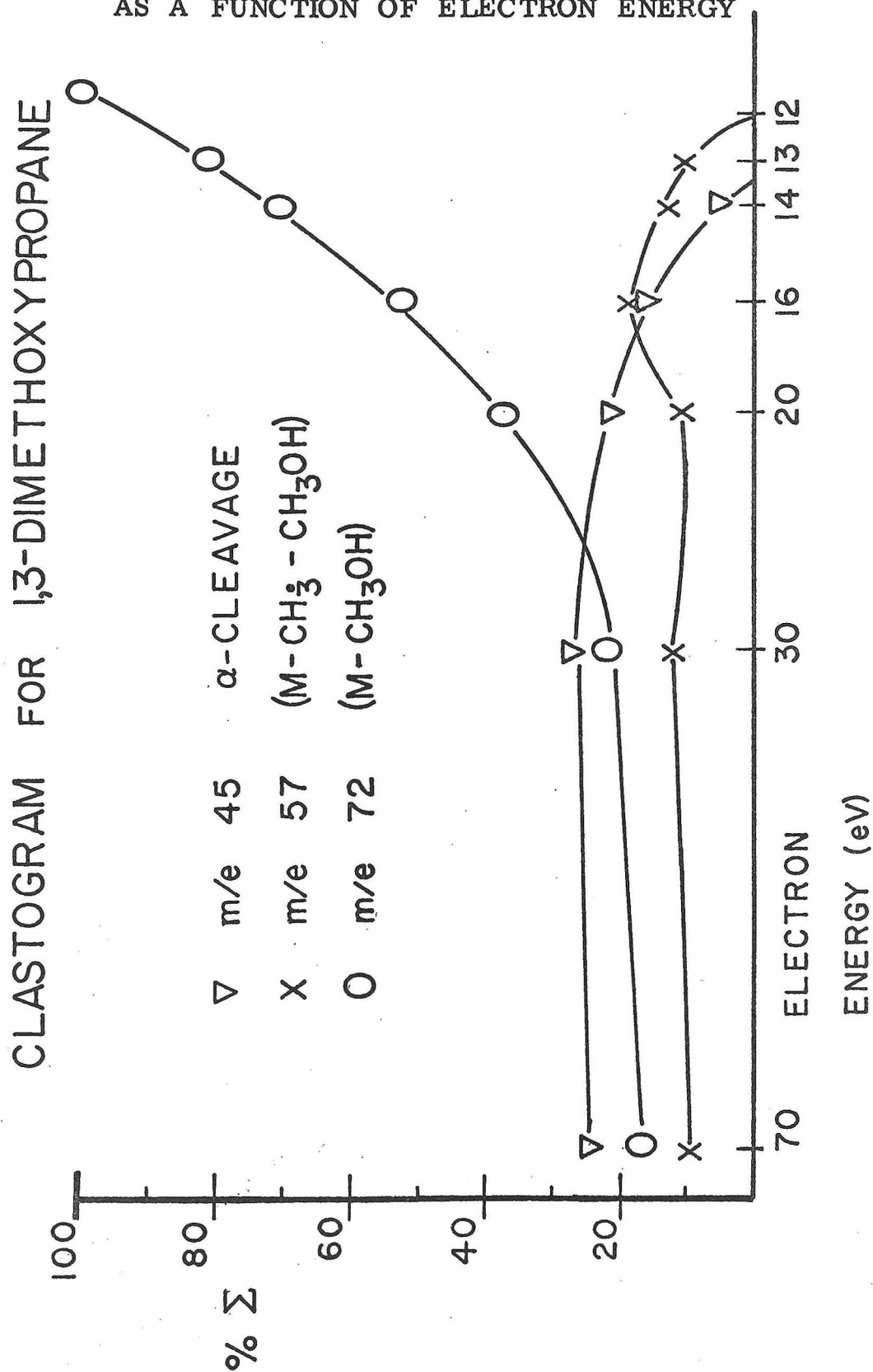
Scheme V

rearrangements predominate in the low energy mass spectra of many bifunctional ethers. The clastogram in Figure 1 depicts the fates of the three most abundant ions from 1,3-dimethoxypropane as the electron energy is diminished. The  $\alpha$ -cleavage ion,  $m/e$  45, is seen to disappear below 14 eV ionizing energy. The most prevalent even-electron rearrangement ion,  $[M-CH_3 \cdot -CH_3OH]^+$  ( $m/e$  57), is not seen below 13 eV. The odd-electron Type  $E_1$  ion,  $[M-CH_3OH]^{\cdot+}$  ( $m/e$  72), comprises all of the ionization at 12 eV and below. Similar trends, although none so dramatic, are seen in the other dimethoxyalkanes, as listed in Table III. Where the  $[M-CH_3OH]^{\cdot+}$  ion does not prevail, other interesting rearrangements are taking place. These competitive rearrangements are often specific for a given chainlength, and it is the investigation of these chainlength effects with which this thesis is concerned.

An examination of the threshold behavior of 1-methoxy, 3-ethoxypropane in a photoionization mass spectrometer<sup>53</sup> indicates that the Type  $E_1$  rearrangement occurs even at onset of ionization: irradiation at 1303 Å (9.51 eV) shows the two ions,  $[M-CH_3OH]^{\cdot+}$  and  $[M-C_2H_5OH]^{\cdot+}$  in the ratio of ca. 4:3. No molecular ion is seen, and no ionization is seen from irradiation at longer wavelengths.<sup>54</sup>

The ICR mass spectra of the bifunctional ethers and of selected deuterated analogues are tabulated at the end of this section. One examination of particular interest is the site specificity of the hydrogen shift in the Type  $E_1$  rearrangement. Such a specificity has been observed in bifunctional alicyclic ethers; for instance, from

FIGURE 1: THREE MOST PROMINENT IONS FROM  $\text{CH}_3\text{O}(\text{CH}_2)_3\text{OCH}_3$  AS A FUNCTION OF ELECTRON ENERGY



# TYPE E<sub>1</sub> REARRANGEMENT OF DIMETHOXYALKANES

(M-CH<sub>3</sub>OH) IONS FROM CH<sub>3</sub>O(CH<sub>2</sub>)<sub>2n</sub>OCH<sub>3</sub>

n	70 eV	20 eV	16 eV	12 eV
2	4%Σ	8%Σ	11%Σ	23.5%Σ
3	16%Σ	35.5%Σ	51%Σ	>99.5%Σ
4	3%Σ	5.5%Σ	10%Σ	20.5%Σ
5	6.5%Σ	11.5%Σ	17.5%Σ	41.5%Σ
6	2%Σ	3%Σ	4%Σ	19%Σ

TABLE III

$\alpha, \alpha'$ -dideuterio-trans-1, 4-dimethoxycyclohexane only  $\text{CH}_3\text{OD}$  is lost in the Type  $\text{E}_1$  rearrangement.<sup>28</sup>

The hydrogen rearrangement in bifunctional aliphatic ethers appears to be site selective. Our results from a study of the  $[\text{M}-\text{CH}_3\text{OH}]^{\cdot+}$  and  $[\text{M}-\text{CH}_3\text{OD}]^{\cdot+}$  ions from specifically deuterated analogues are summarized in Table IV. These results indicate that  $\alpha$ -hydrogens are overwhelmingly preferred in the hydrogen shift of the Type  $\text{E}_1$  rearrangement to lose a molecule of alcohol. This selectivity is not found in monofunctional ethers<sup>45</sup> and is due to the presence of the second functional group.

#### Structure of $[\text{M}-\text{ROH}]^{\cdot+}$ ions

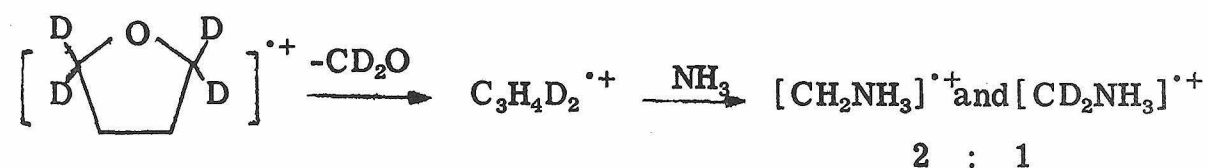
This selectivity implies that the  $[\text{M}-\text{CH}_3\text{OH}]^{\cdot+}$  ions from bifunctional ethers have the formula  $[(\text{CH}_2)_{n-1}\text{CHOR}]^{\cdot+}$ . It is possible that these ions may assume a cyclic structure that renders them identical to the molecular ions of the corresponding cycloalkyl ether,  $[(\text{CH}_2)_{n-1}\text{CHOR}]^{\cdot+}$ . A hint of this is seen in the low energy mass spectrum of methoxycyclopentane (Table II, above), all of whose ions are featured in the low energy mass spectrum of 1,5-dimethoxypentane ( $m/e$  100, 85, 71), albeit not in the same proportions.

Two methods were used to investigate whether cyclic structures are formed by  $[\text{M}-\text{CH}_3\text{OH}]^{\cdot+}$  ions. The first is an investigation of the further fragmentation of unstable  $[\text{M}-\text{CH}_3\text{OH}]^{\cdot+}$  ions: if cyclization is very rapid and competes with a fragmentation (e.g. loss of ethylene), then scrambling of a suitably labelled

Table IV: Proportions of ROH and of ROD Loss from Deuterium Labelled Bifunctional Ethers at 12 eV Ionizing Energy

Parent Neutral	R	$\frac{[M-ROH]^{\cdot+}}{[M-ROH]^{\cdot+} + [M-ROD]^{\cdot+}}$	$\frac{[M-ROD]^{\cdot+}}{[M-ROH]^{\cdot+} + [M-ROD]^{\cdot+}}$
$CH_3OCD_2CD_2OCH_3$	$CH_3$	0.06	0.94
$CD_3OCH_2CH_2CH_2OCD_3$	$CH_3$	0.97	0.03
$CH_3OCH_2CD_2CH_2OCH_3$	$CH_3$	0.95	0.05
$CH_3OCD_2CH_2CD_2OCH_3$	$CH_3$	0.04	0.96
$CH_3OCD_2(CH_2)_2CD_2OCH_3$	$CH_3$	0.07	0.93
$CH_3OCD_2(CH_2)_3CD_2OCH_3$	$CH_3$	0.13	0.87

methylene should occur. The second method involves examination of the scrambling process by an ion-molecule reaction. This method, designed for study of stable ions, is exemplified by Gross' examination of the  $C_3H_6^{\cdot+}$  ion produced by loss of formaldehyde from the molecular ion of tetrahydrofuran. Upon labelling one of the methylenes with two deuteria, Gross found that the reaction depicted in Scheme VI proceeds in a manner which indicates that the  $C_3H_4D_2^{\cdot+}$  ion has passed through a cyclic structure in which all three methylenes are equivalent.<sup>55</sup> This type of experiment is suitable for the study of long-lived ions.



Scheme VI

The first method, a search for scrambling in a unimolecular mass spectral process, revealed no evidence for formation of a cyclic structure. The rearrangements of 1-methoxy, 4-ethoxybutane were examined in order to discover if a 4-member cyclic structure might be intermediate in the fragmentation of the  $[M-CH_3OH]^{\cdot+}$  ion. Although no  $[M-CH_3OH]^{\cdot+}$  ions are observed from this compound, there is a prominent  $[M-CH_3OH-C_2H_4]^{\cdot+}$  ion,  $m/e$  72. It happens, also, that the same ion is a prominent fragmentation ion from cyclobutyl ethers ( $[M-C_2H_4]^{\cdot+}$ ).<sup>42</sup> If a 4-member cyclic structure were formed by a metastable  $[M-CH_3OH]^{\cdot+}$  from the bifunctional ether, then the 1- and 3-positions would be scrambled.

The ICR mass spectra of 1-methoxy, 4-ethoxybutane and of two gem-dideuterio analogues, 1,1-d<sub>2</sub> and 2,2-d<sub>2</sub>, are tabulated on page 182 . All three compounds show prominent m/e 72 peaks; neither of the dideuterio compounds show a peak at m/e 74. This indicates that the methylene of the C<sub>1</sub> and C<sub>2</sub> positions are lost in this rearrangement, and it appears that no 4-member cyclic structure is formed within the time scale of this rearrangement.

The second method, a search for scrambling of the deuterium label in an ion-molecule reaction of a long-lived ion, reveals evidence for formation of a cyclic structure in [M-CH<sub>3</sub>OH]<sup>+</sup> ions. At pressures between 10<sup>-6</sup> Torr and 10<sup>-5</sup> Torr, the Type E<sub>1</sub> rearrangement ions from dialkoxyalkanes are observed to react with the parent neutral to yield protonated parent ([M+1]<sup>+</sup>) ions. This permits a study of the structure of the ions arising from 1,3-dialkoxypropanes, since the only ions observed from these compounds at low ionizing energies result from the Type E<sub>1</sub> rearrangement.

In the cases of deuterium labelled 1,3-dialkoxyalkanes, transfer of either a proton or a deuteron to the parent neutral may occur, and the ratio of deuteron to proton transfer is equal to the ratio of [M+2]<sup>+</sup> ion to [M+1]<sup>+</sup> ion. Ratios from a series of deuterium labelled dialkoxypropanes are shown in Table V.

The ions 1 and 2 in Table V do not give appreciable amounts of deuteron transfer. Ions 3 and 4, however, are seen to transfer both protons and deuterons to a significant extent, as can be seen from the ICR spectra in Figure 2. The ratio of deuteron transfer to proton transfer from 3 is found to be the same, within experimental

error, as from 4. The common origin of the  $[M+2]^+$  and  $[M+1]^+$  ions from the reaction of neutral with the Type  $E_1$  fragments is verified by ICR double resonance,<sup>20</sup> and trapped-ion experiments<sup>56</sup> show that the appearance curves for  $[M+2]^+$  and  $[M+1]^+$  ion are similar in shape. Single resonance spectra of ions 3 and 4 are shown in Figure 2.

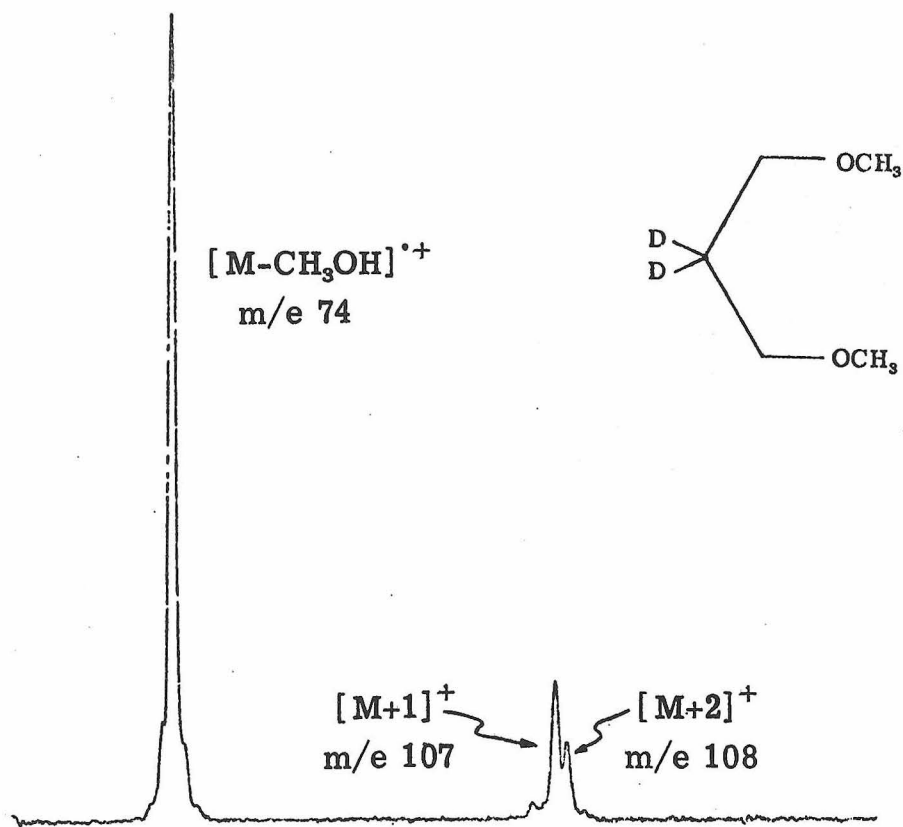
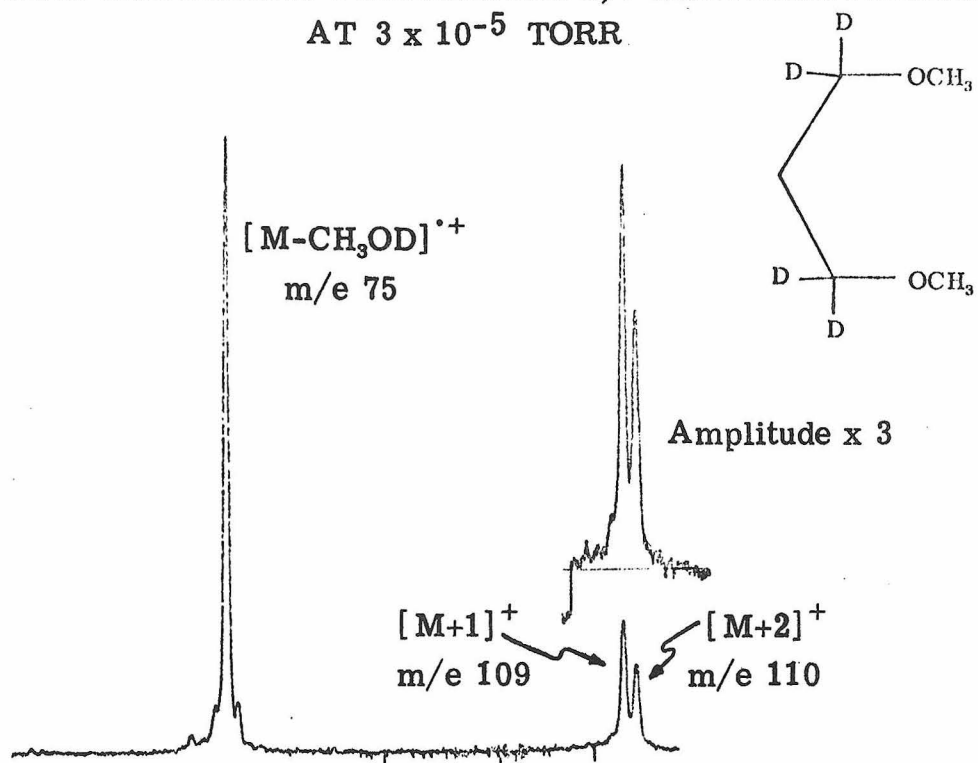
Table V: Ratios of Deuteron to Proton Transfer from Type  $E_1$  Ions from Deuterium Labelled Dialkoxypropanes at 12 eV Ionizing Energy

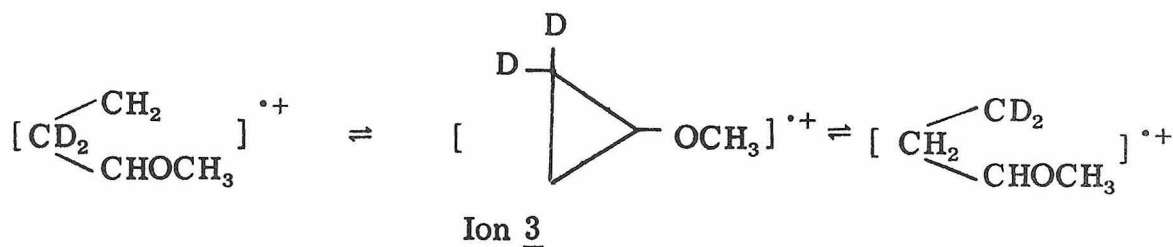
Ion	Parent Neutral	Acidic Primary Ion	$\frac{[M+2]^+}{[M+1]^+}$
1	$CD_3OCH_2CH_2CH_2OCD_3$	m/e 75 $[M-CD_3OH]^{\bullet+}$	$0.06 \pm 0.01$
2	$CH_3OCD_2CH_2CH_2OC_2H_5$	m/e 73 $[M-C_2H_5OH]^{\bullet+}$	$< 0.15^a$
3	$CH_3OCH_2CD_2CH_2OCH_3$	m/e 74 $[M-CH_3OH]^{\bullet+}$	$0.61 \pm 0.02$
4	$CH_3OCD_2CH_2CD_2OCH_3$	m/e 75 $[M-CH_3OD]^{\bullet+}$	$0.64 \pm 0.02$

<sup>a</sup> The presence of other ions prevented further resolution of the contribution of this species to the  $[M+2]^+$  ion.

We infer from these data that the isotopic label is efficiently scrambled between the  $\beta$  and  $\gamma$  positions of the rearrangement ion antecedent to the ion-molecule reaction. A plausible mechanism for this scrambling is the formation of the cyclic structure represented in Scheme VII.

FIGURE 2: ICR SPECTRA OF PRIMARY AND SECONDARY IONS  
FROM DEUTERIUM SUBSTITUTED 1,3-DIMETHOXYPROPANES  
AT  $3 \times 10^{-5}$  TORR

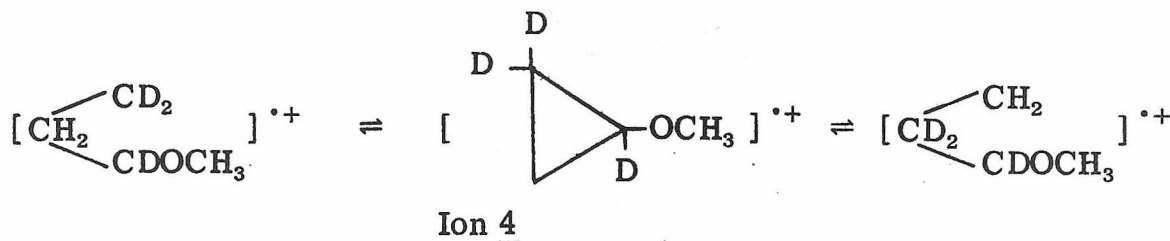




Scheme VII

This cyclic structure accounts for the scrambling of the  $\beta$  and  $\gamma$  positions, as these positions would not be expected to be chemically identical in a linear structure. The ion 4 can go to a similar intermediate structure, as shown in Scheme VIII. Since ion 2 is observed to transfer largely protons to a neutral, we infer that the  $\beta$  and  $\gamma$  positions are the acidic positions of the cation, and that the identical behavior of ions 3 and 4 results from the formation of a cyclic structure.

Since the isotope label is scrambled completely in ions 3 and 4, the ratio of proton transfer to deuteron transfer equals the value of the primary isotope effects,  $\frac{k_H}{k_D} = 1.6$ , for the protonation reaction. This isotope effect is, apparently, not greatly affected by the energy content of the ion, for the ratio  $\frac{[M+2]^+}{[M+1]^+}$  remains unchanged under conditions of electron bombardment as low as 10 eV.



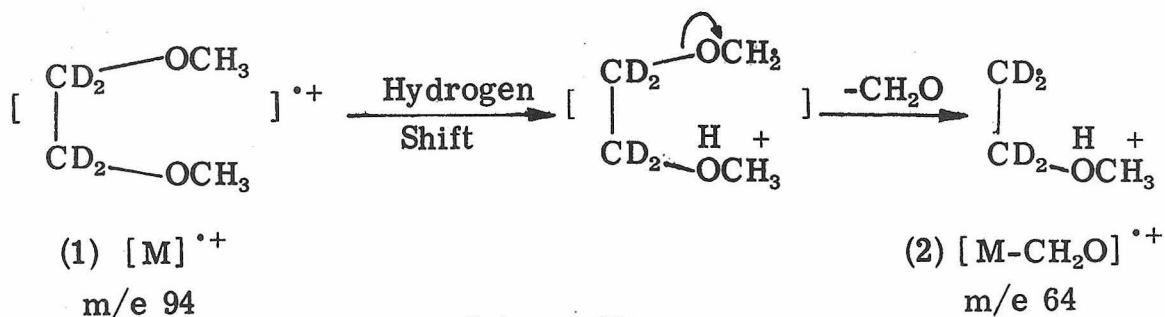
Scheme VIII

Chainlength effects

The rearrangements observed in bifunctional ethers appear to be characteristic more of the length of the methylene chain separating the functional groups than of the identity of the functional groups themselves. The  $\alpha$ ,  $\omega$ -dimethoxyalkanes exhibit the simplest mass spectra among the compounds studied. These spectra, however, are representative of the types of rearrangements observed in the  $\omega$ -methoxyalkanols and  $\alpha$ -methoxy,  $\omega$ -ethoxyalkanes of the same chain-lengths. The salient trends among the dimethoxyalkanes will be discussed.

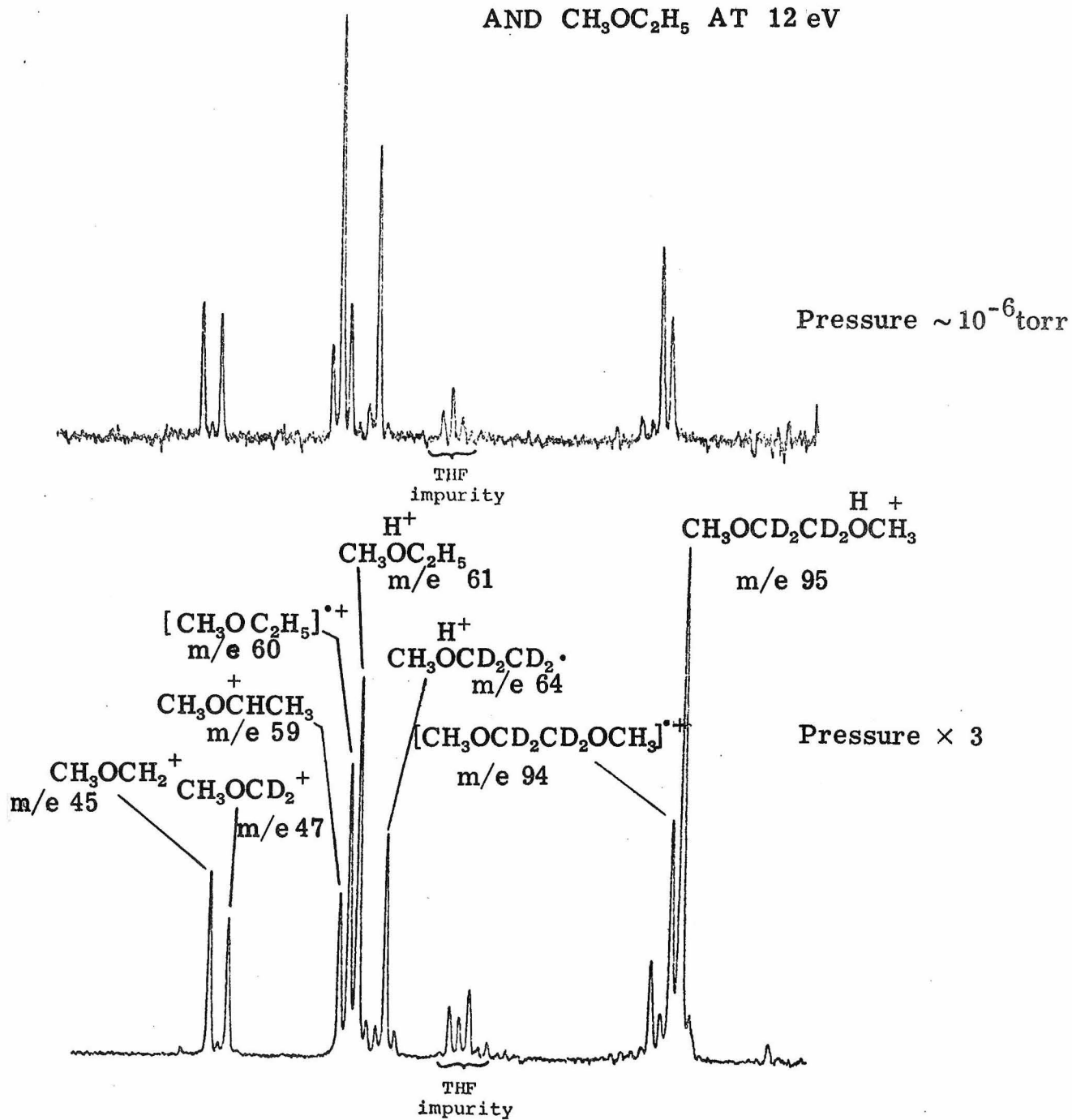
1,2-Dimethoxyethane (Glyme)

The base peak in the 12 eV mass spectrum of glyme is the  $[M-CH_2O]^{\cdot+}$  ion ( $m/e$  60, 40%  $\Sigma$ ), resulting from a Type  $E_1$  rearrangement whereby formaldehyde is lost following a hydrogen shift. Loss of formaldehyde is characteristic of cis-1,4-dimethoxycyclohexane,<sup>28</sup> and it appears that this rearrangement occurs in systems where the most favored site for the hydrogen shift is a methoxy methyl. The deuterium labelling experiment shown in Scheme IX confirms this mechanism.

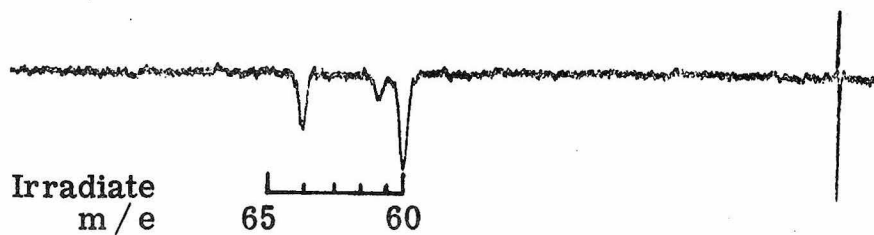


Scheme IX

FIGURE 3: ICR SPECTRA OF A MIXTURE OF  $\text{CH}_3\text{OCD}_2\text{CD}_2\text{OCH}_3$   
AND  $\text{CH}_3\text{OC}_2\text{H}_5$  AT 12 eV



DOUBLE RESONANCE SPECTRUM: OBSERVE  $[\text{M}+1]^+$  (m/e 95).

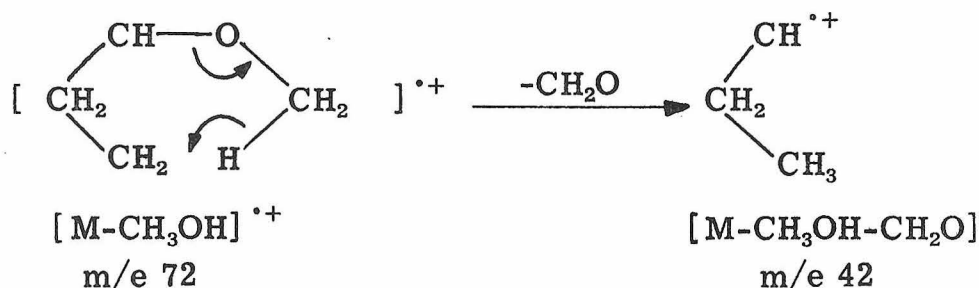


Ion (2) in Scheme IX,  $[M-CH_2O]^{\cdot+}$ , is an excellent gas phase acid. Consistent with its structure, it reacts with parent neutral to yield  $[M+1]^+$  ions ( $\frac{[M+1]^+}{[M+2]^+} > 10$ ). The  $[M-CH_2O]^{\cdot+}$  ion from glyme is an isomer of the molecular ion of methyl, ethyl ether, and the two isomers are distinguishable by their ion-molecule reactions, as indicated in the single and double resonance spectra in Figure 3. The  $[M-CH_2O]^{\cdot+}$  ion reacts with neutral glyme to yield  $[M+1]^+$  ions, while the molecular ion of methyl ethyl ether both transfers protons to glyme (producing  $[M+1]^+$  ions of glyme) and abstracts hydrogen from glyme (producing  $[M+1]^+$  ions of methyl ethyl ether, m/e 61); ICR spectra of  $CH_3OCD_2CD_2OCH_3$  plus  $CH_3OC_2H_5$  are shown in Figure 3.

### 1,3-Dimethoxypropane

At the lowest electron energies, only the  $[M-CH_3OH]^{\cdot+}$  ion is formed from 1,3-dimethoxypropane. At higher electron energies, other rearrangements occur; however, at 16 eV there is only one other odd electron ion besides  $[M-CH_3OH]^{\cdot+}$ . This ion is  $[M-CH_3OH-CH_2O]^{\cdot+}$  (m/e 42, 7%  $\Sigma$  at 16 eV), and isotope labelling confirms the fact that both carbons that are lost in this rearrangement come from the methoxy groups. Although this rearrangement is prominent in the dideuterio and tetradeuterio analogues (m/e 44 from  $CH_3OCH_2CD_2CH_2OCH_3$ , 9%  $\Sigma$  at 16 eV; m/e 45 from  $CH_3OCD_2CH_2CD_2OCH_3$ , 6%  $\Sigma$  at 16 eV), the rearrangement is suppressed in the hexdeuterio analogue (m/e 43 from  $CD_3OCH_2CH_2CH_2OCD_3$ , 2%  $\Sigma$  at 20 eV, not observed at 16 eV). The fact that this rearrangement occurs specifically in 1,3-dimethoxypropane to this extent ( $[M-CH_3OH-CH_3O]^{\cdot+} \leq 2\% \Sigma$  for the other dimethoxyalkanes) suggests the plausibility of a

6-member cyclic transition state, shown in Scheme X. An estimate of heats of formation of the ions involved<sup>47,50</sup> indicates that this rearrangement is endothermic by at least 20 Kcal, explaining why the rearrangement is not observed at lower electron energies.



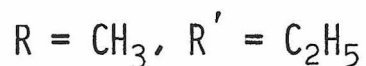
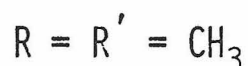
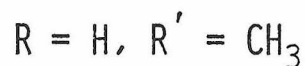
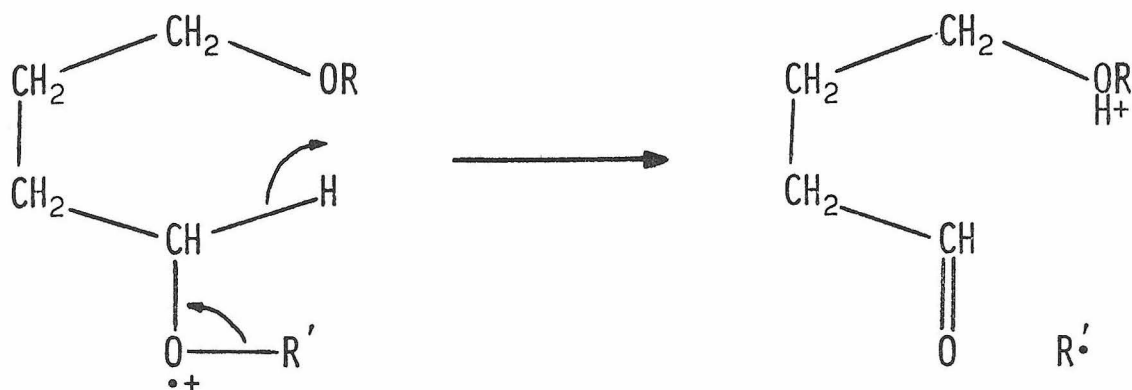
Scheme X

### 1,4-Dimethoxybutane

In 1,4-dimethoxybutane, the base peak at 12 eV corresponds to a different sort of rearrangement, which yields an even electron ion  $[ \text{M-CH}_3 ]^+$  (m/e 103, 49%  $\Sigma$ ). The loss of a methyl radical from the molecular ion is a process not observed among the other dimethoxyalkanes at low electron energy. The simple fission of a C-O bond is at least 10 Kcal more endothermic than the fission of a C-C bond to yield  $\text{CH}_3\text{OCH}_2^+$ , yet the  $[ \text{M-CH}_3 ]^+$  ion remains the base peak from 1,4-dimethoxybutane at electron energies where  $\text{CH}_3\text{OCH}_2^+$  is no longer observed.

The inference from this anomalous fragmentation and its dependence upon chainlength is that a rearrangement is occurring which facilitates the loss of a methyl radical. Such a rearrangement is depicted in Scheme XI.

## FRAGMENTATION OF 1,4-BIFUNCTIONAL BUTANES



Scheme XI

This rearrangement has been represented as an intramolecular proton transfer concomitant with a C-O bond fission. This internal hydrogen shift is sufficiently exothermic to render the loss of methyl radical roughly a thermoneutral process.<sup>49,50</sup> The strong chain-length dependence of this rearrangement, however, suggests a process which has stringent geometrical requirements. Since hydrogen rearrangements are prevalent in other members of the bifunctional series, a highly specific concerted process appears to be operative. The 6-member transition state depicted in Scheme XI fulfills the requirements for this rearrangement.

The substitution of deuterium into 1,4-dimethoxybutane has a curious effect. The amount of alcohol loss is unchanged ( $[M-CH_3OH]^{\cdot+} = 21\% \Sigma$  from  $CH_3O(CH_2)_4OCH_3$  at 12 eV;  $[M-CH_3OD]^{\cdot+} = 20\% \Sigma$  from  $CH_3OCD_2(CH_2)_2CD_2OCH_3$  at 12 eV), but loss of methyl radical is strongly affected ( $[M-CH_3] = 19\% \Sigma$  in  $CH_3O(CH_2)_4OCH_3$  versus  $10\% \Sigma$  from  $CH_3OCD_2(CH_2)_2CD_2OCH_3$  at 16 eV;  $49\% \Sigma$  versus  $26\% \Sigma$  at 12 eV). Expressing these data in a different way, the ratio  $\frac{[M-CH_3]^+}{[M-CH_3OH]^{\cdot+}}$  for 1,4-dimethoxybutane is 1.9 at 16eV and 2.4 at 12 eV. The ratio  $\frac{[M-CH_3]^+}{[M-CH_3OH]^{\cdot+} + [M-CH_3OD]^{\cdot+}}$  for 1,1,4,4-tetradeuterio-1,4-dimethoxybutane is 1.0 at 16 eV and 1.3 at 12 eV.

The  $[M-CH_3]^+$  ion from the tetradeuterio compound is found to react with the parent neutral almost exclusively by deutron transfer,  $\frac{[M+2]^+}{[M+1]^+} \geq 20$ . On the other hand, the  $[M-C_2H_5]^+$  ions from the gem-dideuterio 1-methoxy, 4-ethoxybutanes (m/e 107 in the 1,1-d<sub>2</sub> and 2,2-d<sub>2</sub> compounds on page 182 ) are found to transfer only protons to the neutral parent.

Finally, the published 70 eV mass spectra of cis and trans-dimethoxycyclohexanes<sup>28</sup> show no preference for the loss of CH<sub>3</sub>. A re-examination of the bifunctional cyclohexanes in the ICR confirms this, even at low electron energies. From these facts two conclusions are drawn. First, the loss of the neutral radical is not unassisted. Second, from the isotope effect, the assistance of the fragmentation differs measurably from a Type E<sub>1</sub> process. Hence, a concerted process with a stringent geometrical requirement is inferred for which a 6-member transition state is implicated.

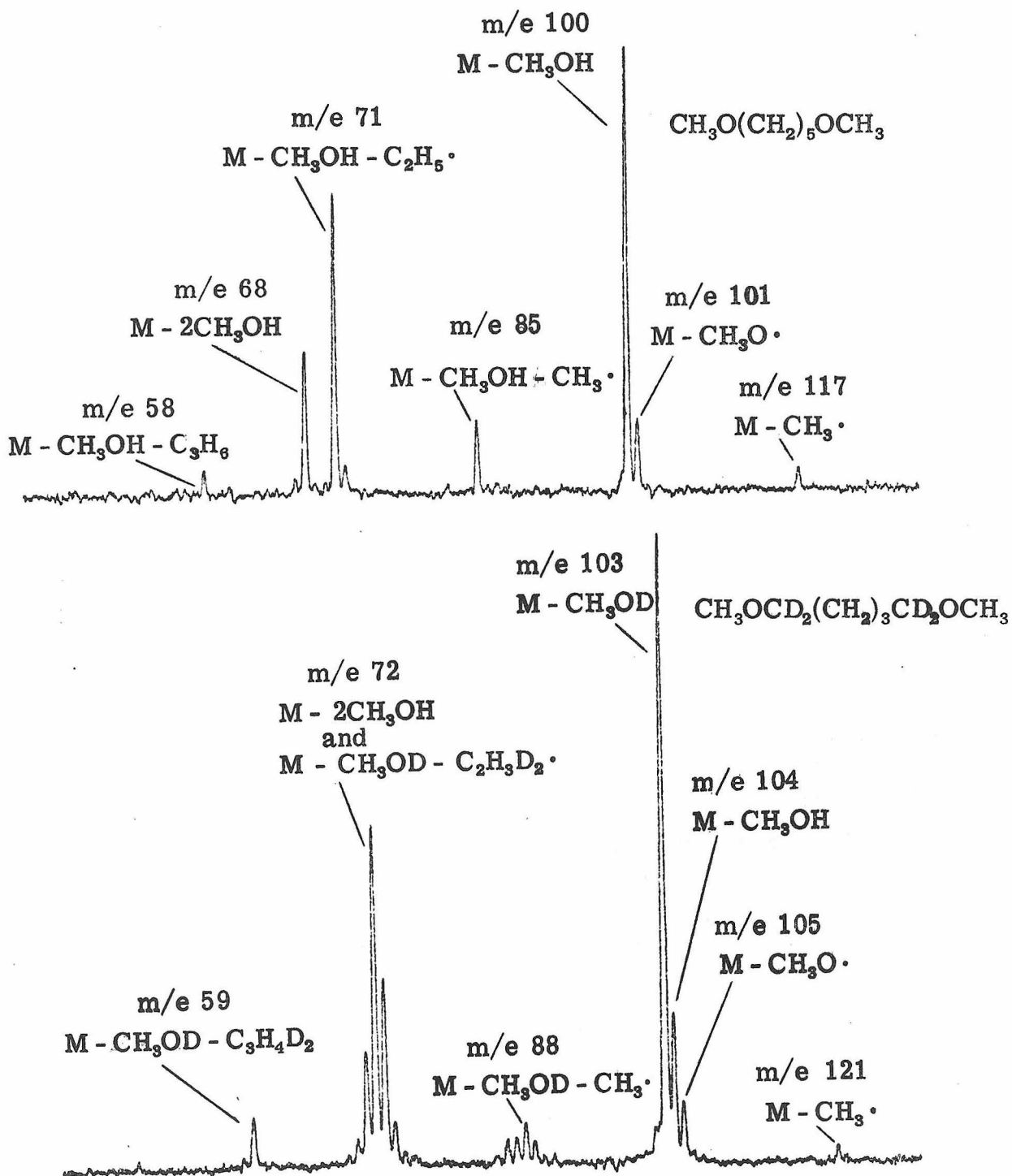
1,5-Dimethoxypentane

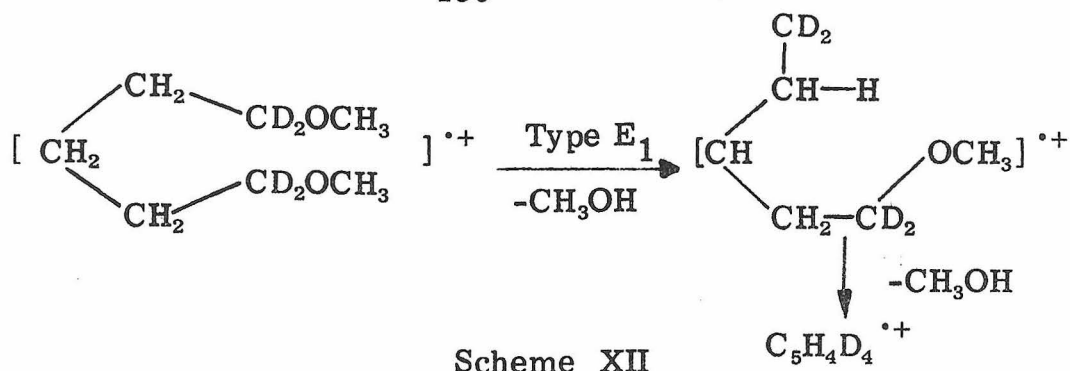
In the longer chain alkanes, the ions derived from Type  $E_1$  rearrangements may rearrange further as a consequence of interactions with the long alkyl chain. The mass spectra in Figure 4 depict the several ions observed at low electron energy. As stated above, three of these ions,  $m/e$  100,  $m/e$  85, and  $m/e$  71, compose the low energy mass spectrum of methoxycyclopentane (Table II). Conspicuously absent from this latter spectrum is the  $m/e$  68 ion, which is the prominent  $[M-2CH_3OH]^{\circ+}$  ion in the mass spectrum of 1,5-dimethoxy pentane. This ion,  $C_5H_8^+$ , is a very good proton donor, which is consistent with its hydrocarbon structure. The only ion of comparable acidity in the mass spectrum of 1,1,5,5-tetradeuterio-1,5-dimethoxypentane is the ion  $m/e$  72 ( $C_5H_4D_4^+$ ), observed by ICR double resonance.<sup>20</sup>

From the facts that (1)  $C_5H_8^+$  does not occur in the mass spectrum of methoxycyclopentane, and (2) four deuteria remain in the  $[M-2CH_3OH]^{\circ+}$  ion from the tetradeuterio compound, it is concluded that the mechanism for production of  $[M-2CH_3OH]^{\circ+}$  is a Type  $E_1$  rearrangement with the hydrogen shift from the  $\beta$  or  $\gamma$  positions in the methylene chain, eg. Scheme XII. The two Type  $E_1$  rearrangement ions,  $[M-CH_3OH]^{\circ+}$  (via hydrogen shift from an  $\alpha$ -position) and  $[M-2CH_3OH]^{\circ+}$  (via shift from a  $\beta$  or  $\gamma$  position) compose 60% of the total ionization from 1,5-dimethoxypentane at 12 eV.

FIGURE 4

ICR MASS SPECTRA OF 1,5-DIMETHOXPENTANE AT 13 eV





The third prominent rearrangement in 1,5-dimethoxypentane gives rise to the  $m/e$  71 ion,  $C_4H_7O^+$ . This formula, rather than  $C_5H_{11}^+$ , is indicated by the fact that this ion appears in the low electron energy mass spectrum of methoxycyclopentane, and, in both cases, the ion is slow to react with the parent neutral. A hydrocarbon ion would surely be an excellent gas phase proton donor. However, as described in the next section, the major reaction of  $m/e$  71 ion with 1,5-dimethoxypentane is simply attachment to form an  $[M+71]^+$  ion.

The corresponding ions in the tetradeuterio dimethoxypentane, however, range from  $m/e$  71 to  $m/e$  74. With such scrambling, it is difficult to draw a secure mechanism. Likewise, the  $m/e$  85 ion, also common to methoxycyclopentane and 1,5-dimethoxypentane, has analogues from  $m/e$  85 to  $m/e$  89 in the mass spectrum of the tetradeuterio dimethoxypentane, as shown in Figure 4.

### 1,6-Dimethoxyhexane

In the 1,6-dialkoxyalkanes, the loss of two molecules of alcohol affords the base peak at low electron energies:  $[M-2CH_3OH]^+$

( $m/e$  82, 70%  $\Sigma$  from 1,6-dimethoxyhexane at 11 eV). This rearrangement illustrates the effect of the second functional group in a long chain bifunctional compound. The methylene chain presents many sites from which hydrogen shift can occur in a Type  $E_1$  process, and subsequent loss of another molecule of alcohol takes place in much the same manner as in Scheme XII above.

The rest of the total ionization from 1,6-dimethoxyhexane at 11 eV is simply the  $[M-CH_3OH]^+$  ion. This is in contrast to the monofunctional ether in Table 1 above, in which many rearrangements are still taking place even at low ionizing energies. Apparently, the effect of a second functional group is to offer a small number of favorable pathways by which the molecular ion may rearrange. The result is a simpler spectrum for the dimethoxyalkanes compared to monofunctional ethers of the same length.

#### $\alpha$ -Methoxy, $\omega$ -ethoxyalkanes

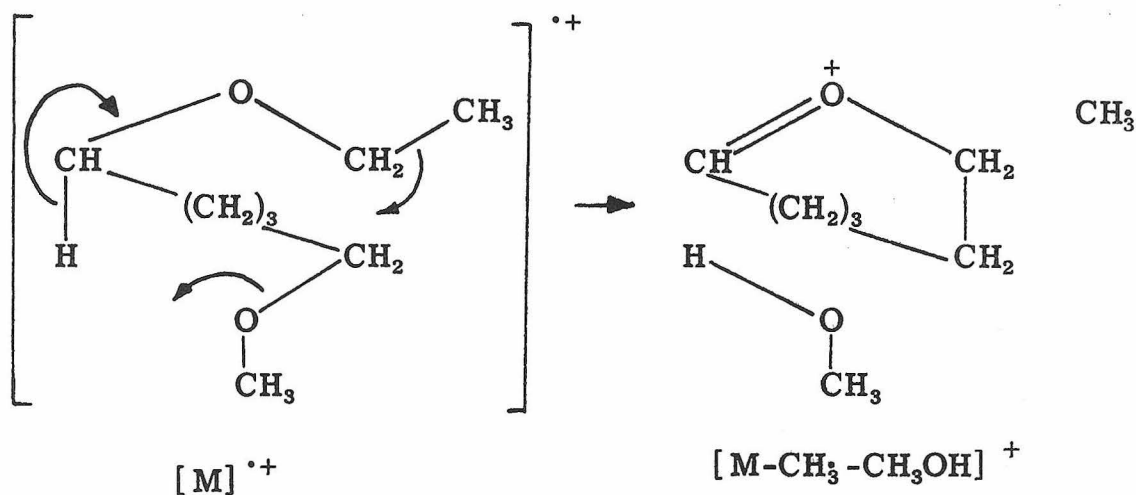
For longer chainlengths, the behavior of the  $\alpha$ -methoxy,  $\omega$ -ethoxyalkanes differs from that of the dimethoxyalkanes, not in the nature of the mass spectral processes observed, but in the profusion of ions at low electron energies. Although the same sorts of rearrangements are taking place, there seem to be many more pathways available. As a consequence, a large variety of ions is seen, even at the lowest electron energies; for example, the ICR mass spectrum of 1-methoxy, 5-ethoxypentane shown in Table VI.

With the exception of the minor ion  $m/e$  75 (for which no

Table VI: ICR Mass Spectrum of  $\text{CH}_3\text{O}(\text{CH}_2)_5\text{OC}_2\text{H}_5$  at 11 eV

m/e	Species	% $\Sigma$
117	$[\text{M}-\text{C}_2\text{H}_5]^+$	17
114	$[\text{M}-\text{CH}_3\text{OH}]^{\cdot+}$	14
102	$[\text{M}-\text{CH}_3\text{CHO}]^{\cdot+}$	6
101	$[\text{M}-\text{C}_2\text{H}_5\text{O}^{\cdot}]^+$	4
100	$[\text{M}-\text{C}_2\text{H}_5\text{OH}]^{\cdot+}$	12
99	$[\text{M}-\text{CH}_3-\text{CH}_3\text{OH}]^+$	8
85	$[\text{M}-\text{C}_2\text{H}_5-\text{CH}_3\text{OH}]^+$	14
75	$[\text{M}-\text{C}_4\text{H}_7\text{O}]^+$	4
73	$[\text{M}-\text{C}_2\text{H}_5\text{O}^{\cdot}-\text{C}_2\text{H}_4]^+$	4
72	$[\text{M}-\text{C}_2\text{H}_5\text{OH}-\text{C}_2\text{H}_4]^{\cdot+}$	6
71	$[\text{M}-\text{C}_4\text{H}_{11}\text{O}]^+$	4
70	$[\text{M}-\text{CH}_3\text{CHO}-\text{CH}_3\text{OH}]^{\cdot+}$	4
68	$[\text{M}-\text{C}_2\text{H}_5\text{OH}-\text{CH}_3\text{OH}]^{\cdot+}$	4

mechanism will be offered), all of the ions in Table VI are either familiar from the dimethoxyalkanes or arise from similar processes. A speculative mechanism for formation of the  $m/e$  99 ion is drawn in Scheme XIII to dramatize the prevalence of 6-member cyclic transition states which we have observed in the rearrangements of bifunctional ethers.

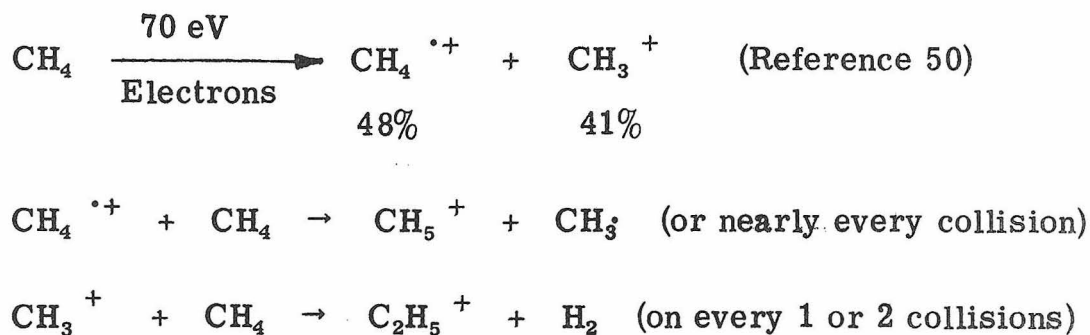


Scheme XIII

### Chemical ionization

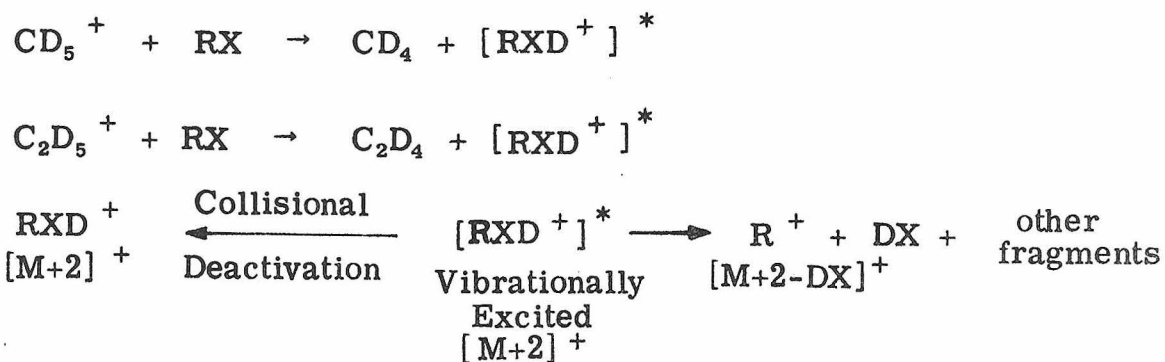
Chainlength effects in the bifunctional ethers are pronounced in the chemical ionization mass spectra, as well. Chemical ionization is the name applied to the formation of fragment ions by an ion-molecule reaction. The reagent conventionally used for chemical ionization studies is methane, in which secondary ions are rapidly formed by the reaction of methane molecular ion and the the methyl

cation with neutral methane.<sup>57</sup> These secondary ions, primarily  $\text{CH}_5^+$  and  $\text{C}_2\text{H}_5^+$ , are formed very rapidly in methane at pressures greater than  $10^{-5}$  Torr, as shown in Scheme XIV.<sup>58</sup>



#### Scheme XIV

The appeal of chemical ionization to organic chemists lies in the fact that the fragmentation process is induced by the exothermic protonation of a substrate. Since the proton affinity of  $\text{CH}_4$  is 126 Kcal and of  $\text{C}_2\text{H}_4$  is 160 Kcal, exothermic protonation of an ether admixed with ionized methane will take place, as the proton affinities of ethers are, ordinarily, greater than 180 Kcal.<sup>20</sup> As a result, chemical ionization may be likened to an acid induced decomposition, and analogies with solution phase reactions may be drawn. At total pressures below  $10^{-3}$  Torr, the protonated substrate is produced in a vibrationally excited state and remains in that state long enough to fragment, yielding a pattern which is termed the chemical ionization mass spectrum,<sup>59</sup> shown in Scheme XV.



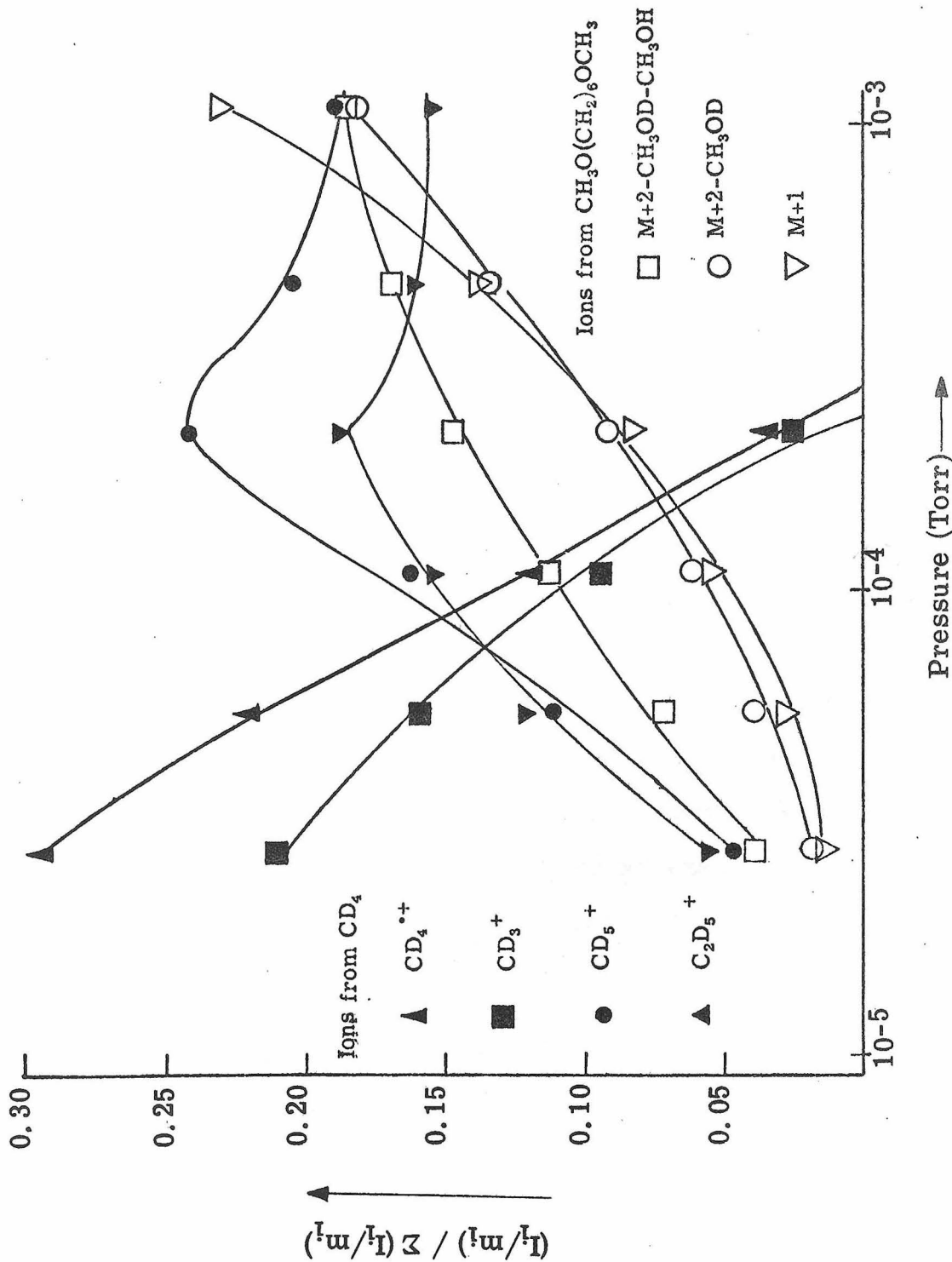
Scheme XV

### Chemical ionization of $\text{CH}_3\text{O}(\text{CH}_2)_n\text{OCH}_3$

ICR chemical ionization spectra were performed using  $\text{CD}_5^+$  and  $\text{C}_2\text{D}_5^+$  ions, which are produced in nearly equal amounts from the ion-molecule reactions of  $\text{CD}_4$  bombarded with 70 eV electrons at pressures between  $5 \times 10^{-5}$  and  $1 \times 10^{-3}$  Torr. Under these conditions, the vibrationally excited  $[\text{M}+2]^+$  ion, initially formed, fragments. A plot of ion abundance versus pressure in the chemical ionization of 1,6-dimethoxyhexane is shown in Figure 5. The primary ions,  $\text{CH}_4^+$  and  $\text{CH}_3^+$  diminish in abundance monotonically, while the secondary ions are seen to increase to a maximum at about  $10^{-4}$  Torr. At higher pressures, the rate of reaction of the secondary ions with the bifunctional ether becomes sufficiently great that the abundance of  $\text{CD}_5^+$  and  $\text{C}_2\text{D}_5^+$  begins to diminish. Tertiary ions,  $[\text{M}+2-\text{CH}_3\text{OD}]^+$  and  $[\text{M}+2-\text{CH}_3\text{OD}-\text{CH}_3\text{OH}]^+$ , increase in abundance as pressure is increased. The  $[\text{M}+1]^+$  ion, m/e 147, is probably formed by secondary processes from the electron impact ionized

FIGURE 5: CHEMICAL IONIZATION OF 1,6-DIMETHOXY HEXANE AT 70 eV

$$[CD_4] / [CH_3O(CH_2)_6OCH_3] = 30^a$$



<sup>a</sup> From ratio of ion currents ( $I_{CD_4} / I_{CH_3O(CH_2)_6OCH_3} = 4$ ) divided by ratio of ionization cross sections <sup>61</sup>

bifunctional ether as well as by reaction of the tertiary ions from chemical ionization.

The proportion of loss of 2 molecules of alcohol from the  $[M+2]^+$  ion is seen to be roughly constant in the pressure range  $5 \times 10^{-5}$  to  $5 \times 10^{-4}$  Torr:  $\frac{[m/e\ 83]}{[m/e\ 83] + [m/e\ 115]} = 2/3$ . At  $1 \times 10^{-3}$

Torr, this proportion diminishes to  $\frac{1}{2}$ . This occurs because, at higher pressures, collisional deactivation of vibrationally excited  $[M+2-CH_3OD-CH_3OH]^+$  ions competes effectively with loss of a second molecule of methanol from the ions which are still hot.

The proportion of  $[M+2-CH_3OD-CH_3OH]^+$  ions also diminishes with decreasing length of the methylene chain, as indicated in Table VII, and is not observed for chainlengths less than  $n = 4$ . This parallels the trend of  $[M-2CH_3OH]^+$  loss in the electron impact mass spectra, and may be explained by considering Scheme XVI. For longer chainlengths, the intramolecular proton transfer competes more effectively with collisional deactivation because the necessary cyclic transition state is more readily formed. Interestingly, the 7-member cyclic transition state of 1,6-dimethoxyhexane appears to be more favorable than the 6-member transition state of 1,5-dimethoxy-pentane.

#### Chemical ionization of $CH_3O(CH_2)_nOH$

The chemical ionization of the methoxyalkanols reveals a different sort of chainlength effect. The vibrationally excited  $[M+2]^+$  ion may decompose immediately or it may equilibrate the deuteron

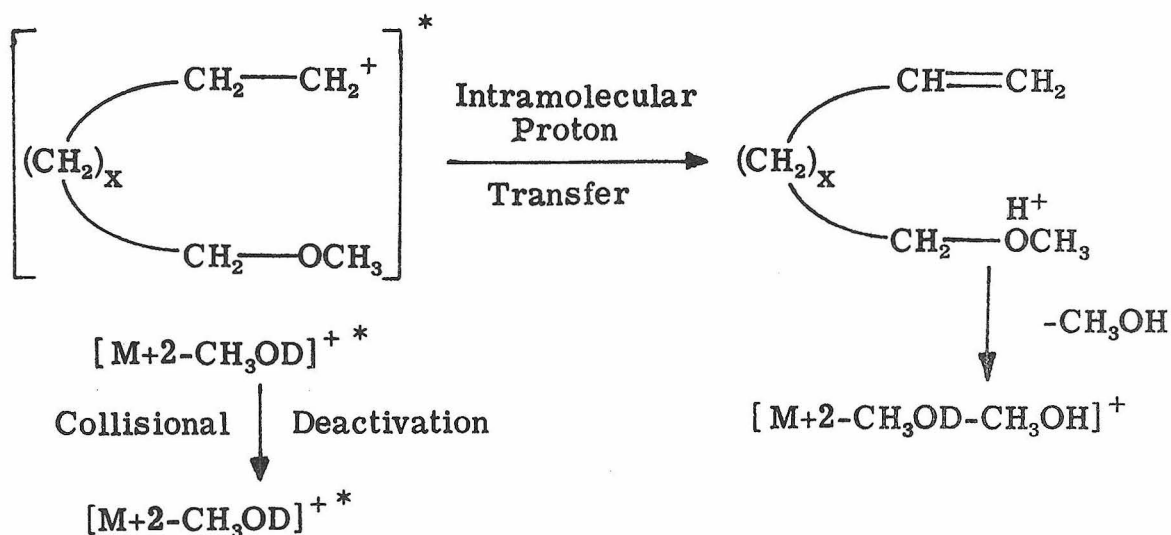
TABLE VII: CHEMICAL IONIZATION OF DIMETHOXYALKANES WITH CD<sub>4</sub> REAGENT GAS,  
 TOTAL PRESSURE ~ 5 x 10<sup>-5</sup> - 1 x 10<sup>-4</sup> TORR:

LOSS OF 1 VERSUS 2 MOLECULES OF METHANOL, COMPARISON WITH  
 ELECTRON IMPACT

Compound	Proportion of [M+2 - CH <sub>3</sub> OD - CH <sub>3</sub> OH] <sup>a</sup> from Chemical Ionization	Proportion of [M-2CH <sub>3</sub> OH] <sup>b</sup> from Electron Impact**	70 eV	16eV	12eV
CH <sub>3</sub> OCH <sub>2</sub> (CH <sub>2</sub> ) <sub>2</sub> CH <sub>2</sub> OCH <sub>3</sub>	0.08*	<0.03			
CH <sub>3</sub> OCH <sub>2</sub> (CH <sub>2</sub> ) <sub>3</sub> CH <sub>2</sub> OCH <sub>3</sub>	0.30*	0.44	0.46	0.31	
CH <sub>3</sub> OCH <sub>2</sub> (CH <sub>2</sub> ) <sub>4</sub> CH <sub>2</sub> OCH <sub>3</sub>	0.66**	0.83	0.86	0.81	
a	$\frac{[M+2 - CH_3OD - CH_3OH]}{[M+2 - CH_3OD] + [M+2 - CH_3OD - CH_3OH]}$	b	$\frac{[M - 2CH_3OH]}{[M - CH_3OH] + [M - 2CH_3OH]}$		

\* Ratios ± 10%

\*\*Ratios ± 5%



Scheme XVI

with the hydroxylic proton. This equilibration is indicated by the fact that both  $\text{CH}_3\text{OD}$  and  $\text{CH}_3\text{OH}$  are lost from the  $[\text{M}+2]^+$  ion. As indicated in Table VIII, the ratio of  $\text{CH}_3\text{OH}$  loss to  $\text{CH}_3\text{OD}$  loss diminishes as chainlength is increased. This parallels the trend toward a decreased proportion of hydrogen bonded structures in the neutral<sup>60</sup> and may be rationalized in terms of the structure of the neutral molecules, as depicted in Scheme XVII.

The relative proportions of loss of water versus loss of methanol from the  $[\text{M}+2]^+ *$  ions of  $\omega$ -methoxyalkanols are not easily explained; these values and the comparison to electron impact data are summarized in Table VIII. It is plausible, though, that the observed effects in chemical ionization and electron impact ionization may be linked to the proportion of hydrogen bonded structures in the neutral. A rationalization of observed effects for  $\beta$ -methoxyethanol may be based on the "football mechanism," in which the incoming deuteron kicks off a molecule of  $\text{CH}_3\text{OH}$  from the hydrogen bonded

TABLE VIII: CHEMICAL IONIZATION OF  $\omega$ -METHOXYALKANOLS WITH  $CD_4$  REAGENT GAS,  
TOTAL PRESSURE  $\sim 5 \times 10^{-5} - 1 \times 10^{-4}$  TORR:

LOSS OF METHANOL VERSUS WATER, COMPARISON WITH ELECTRON IMPACT

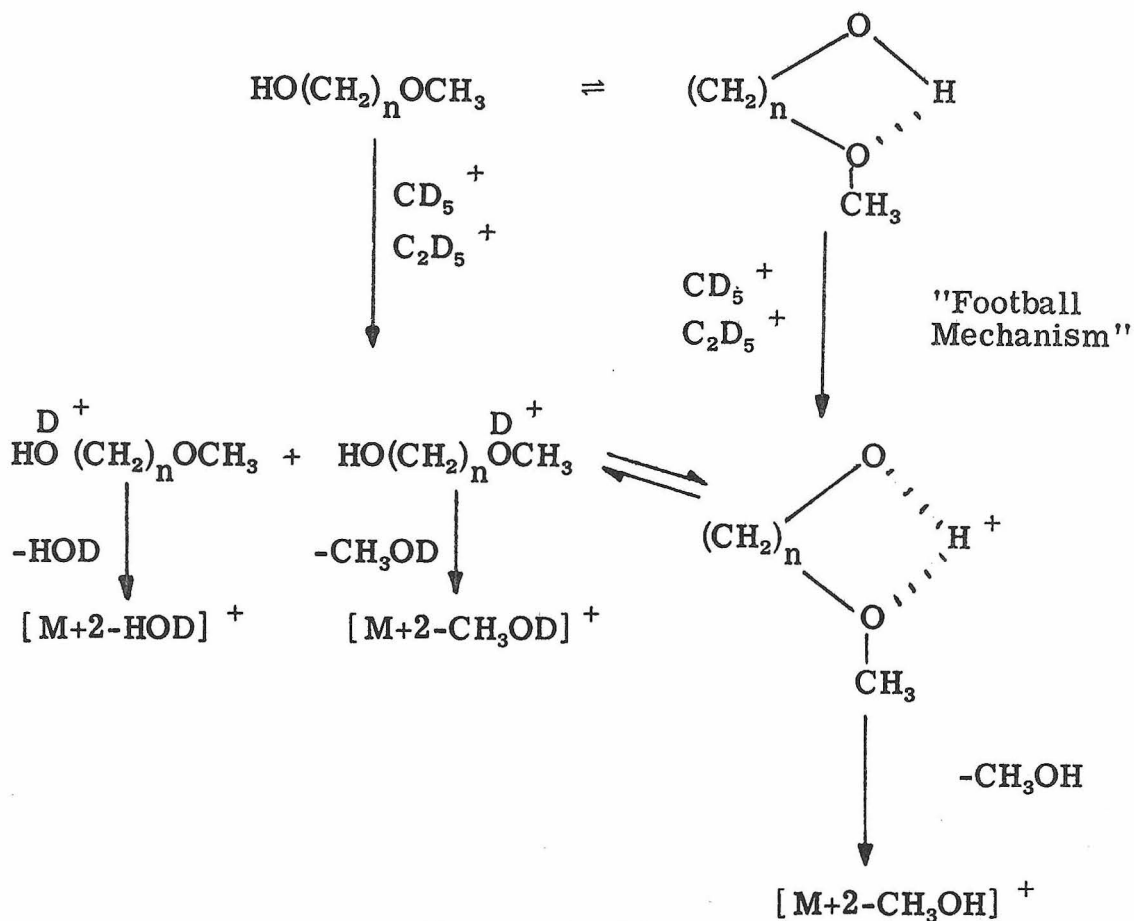
Compound	$\frac{[M + 2 - CH_3QH]}{[M + 2 - CH_3OD]}$	Proportion of $[M - H_2O]^b$	
		$[M + 2 - HOD]^a$ from Chemical Ionization*	from Electron Impact**
$CH_3OCH_2CH_2OH$	$> 5$	0.52	$> 0.95$
$CH_3OCH_2CH_2CH_2OH$	$1.4 \pm 0.1$	0.75	0.81 0.83 0.84
$CH_3OCH_2(CH_2)_2CH_2OH$	$0.5 \pm 0.1$	0.49	0.59 0.60 0.68
a	$[M + 2 - HOD]$		
	$\frac{[M + 2 - HOD] + [M + 2 - CH_3OH] + [M + 2 - CH_3OD]}{[M + 2 - HOD] + [M + 2 - CH_3OH] + [M + 2 - CH_3OD]}$		

b

$$\frac{[M - H_2O]}{[M - H_2O] + [M - CH_3OH]}$$

\* Ratios  $\pm 10\%$

\*\* Ratios  $\pm 5\%$



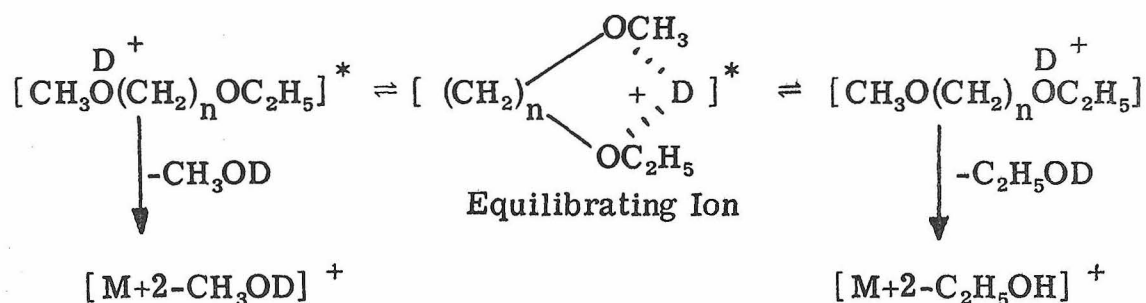
Scheme XVII

structure. Whereas  $\beta$ -functionalized ethanols exist almost entirely as hydrogen bonded structures in the gas phase,<sup>62</sup> longer chain  $\omega$ -methoxyalkanols are probably only 50:50 mixtures of hydrogen bonded and non-hydrogen bonded structures at best. Further rationalizations of observed behavior can be developed on this basis, but, in the absence of more data, more detailed elaboration will be omitted.

#### Chemical Ionization of $\text{CH}_3\text{O}(\text{CH}_2)_n\text{OC}_2\text{H}_5$

The chainlength effects in the chemical ionization of  $\alpha$ -methoxy,

$\omega$  - ethoxyalkanes appear to show a consistent trend: competition between loss of  $\text{CH}_3\text{OD}$  and  $\text{C}_2\text{H}_5\text{OD}$  from the  $[\text{M}+2]^+$  ion is summarized in Table IX. As the chainlength is increased, the reaction shows greater selectivity for loss of the ethoxy function. This may be explained by the increased interaction of the remote functional groups of the  $[\text{M}+2]^+$  ions as chainlength is increased, as shown in Scheme XVIII.



Scheme XVIII

As represented in Scheme XVIII, the equilibration of the deuteron is in competition with the loss of alcohol from the vibrationally excited  $[\text{M}+2]^+$  ion. The ICR study of the protonated dimethoxyalkanes, described in the next section, has shown that formation of an internal proton bridge is favored for longer chainlengths.<sup>15</sup> The initial deuteration of the neutral molecule is not expected to show much selectivity: if no equilibration could occur, equal proportions of  $\text{CH}_3\text{OD}$  and  $\text{C}_2\text{H}_5\text{OD}$  would be lost. The proton affinity of an ethoxy group is, however, greater than that of a methoxy group, and, as equilibration becomes competitive with alcohol loss, the ethoxy group will have a greater proportion of the deuterons than the methoxy group.

TABLE IX: CHEMICAL IONIZATION OF  $\alpha$ -METHOXY,  $\omega$ -ETHOXYALKANES WITH  $CD_4$  REAGENT GAS, TOTAL PRESSURE  $\sim 5 \times 10^{-5} - 1 \times 10^{-4}$  TORR:

LOSS OF METHANOL VERSUS LOSS OF ETHANOL, COMPARISON WITH E. I.

Compound	Proportion of $[M+2-C_2H_5OD]^a$ from		Proportion of $[M-C_2H_5OH]^b$ from Electron Impact**		
	Chemical Ionization*	70eV	16eV	12eV	
$CH_3OCH_2CH_2OC_2H_5$	0.55	0.20	0.09	0.08	
$CH_3OCH_2CH_2CH_2OC_2H_5$	0.57	0.58	0.53	0.48	
$CH_3OCH_2(CH_2)_2CH_2OC_2H_5$	0.60	>0.95			
$CH_3OCH_2(CH_2)_3CH_2OC_2H_5$	0.73	0.50	0.48	0.49	
$CH_3OCH_2(CH_2)_4CH_2OC_2H_5$	0.80	0.71	0.80	0.83	

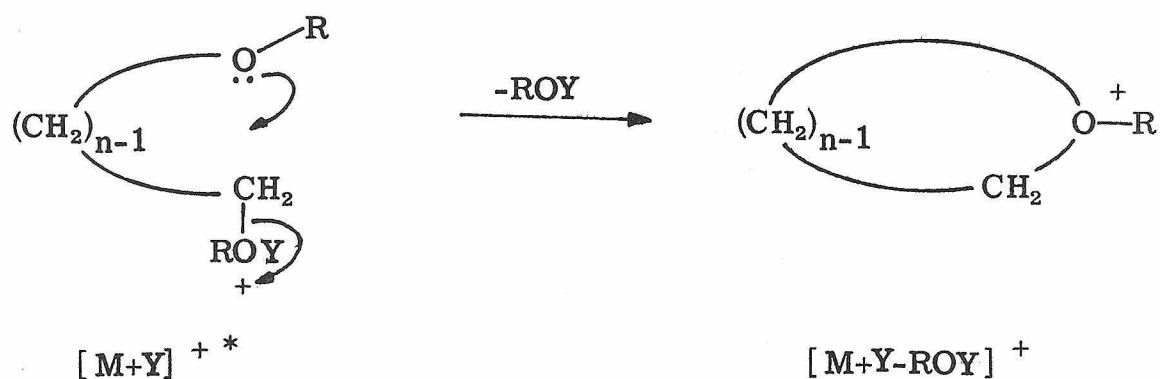
\* Ratios  $\pm 5\%$       \*\* Ratios  $\pm 2\%$

$$a \quad \frac{[M+2-C_2H_5OD]}{[M+2-CH_3OD] + [M+2-C_2H_5OD]}$$

$$b \quad \frac{[M-C_2H_5OH]}{[M-CH_3OH] + [M-C_2H_5OH]}$$

As chainlength is increased, equilibration becomes more favored because the equilibrating ion is more readily formed for longer cyclic structures. Hence, a greater proportion of  $C_2H_5OD$  is lost.

The results of chemical ionization of bifunctional molecules do not appear to support an internal backside displacement mechanism for loss of ROD from an  $[M+2]^+$  ion, analogous to anchimeric assistance in solution phase solvolyses.<sup>63</sup> A backside displacement mechanism for chemical ionization is drawn in Scheme XIX. It is difficult to reconcile such a scheme with the experimental results that (1) water is lost from the  $\omega$ -methoxyalkanols, and (2) ethanol is preferentially lost from  $\alpha$ -methoxy,  $\omega$ -ethoxyalkanols. Further work, described in the next section, will present other results which support the conclusion that the principal interaction of remote functional groups in chemical ionization is via internal solvation of the charge.



Scheme XIX

Comparison of electron impact and chemical ionization

The behavior of the  $\alpha$ -methoxy,  $\omega$ -ethoxyalkanes upon low energy electron impact provides an intriguing contrast to chemical ionization. No consistent trend is observed in loss of ethanol versus loss of methanol. Instead, alternating behavior is observed, whereby ethanol is preferentially lost from the compounds with an even number of methylenes in the intervening chain, but roughly equal proportions of ethanol and methanol are lost from the compounds with an odd number of methylenes. The interaction of oxygen lone pairs by through bond interaction has been estimated by photoelectron spectroscopy to create a splitting of about 0.25 eV between symmetric and antisymmetric combinations of the orbitals in 1,3-dioxane and a splitting of 1.2 eV in 1,4 dioxane.<sup>63</sup> This suggests the possibility that the assumption of remotely ionized functional groups is an inadequate description for bifunctional molecules.

The concept of localized charge seems more applicable to even electron species, such as those produced by chemical ionization, than to the odd electron species formed by rearrangement of molecular ions. In even electron species, eg.  $[M+1]^+$  ions, delocalization of charge appears to occur via through space interactions; for example, the bidentate coordination of the deuteron in the equilibrating ion in Scheme XVIII. Odd electron species, on the other hand, are imagined to be electron deficient molecules. It is suggested that, in such system, delocalization of charge may occur through the  $\sigma$ -bond framework.

What characteristics may typify a charge delocalized, electron

deficient system? The prevalence of 6-member cyclic transition states, for one. The trends seen in the loss of two molecules of alcohol from the  $[M+2]^+$  ion in chemical ionization studies reveal no preference for a 6-member cyclic transition state. In light of this fact, it may be speculated that the 6-member cycle is a reflection not simply of steric preference, but of a low energy pathway that is electronically determined.

The McLafferty rearrangement<sup>65</sup> is, perhaps, the most celebrated example of a 6-member transition state in the rearrangement of an odd electron mass spectral species. Our investigations have revealed other examples: the loss of formaldehyde from the molecular ion of glyme and from the  $[M-CH_3OH]^+$  ion of 1,3-dimethoxypropane, expulsion of a methyl radical from the molecular ion of 1,4-dimethoxybutane. If the transition states for these processes be not sterically determined, then it is surmised that they represent electronic preferences.

## BREAKDOWN OF DIMETHOXYMETHANE AS A FUNCTION OF ELECTRON ENERGY

		% $\Sigma$							
M/E		75	74	47	45	44	31	29	15
E.E.									
70	EV	22	1	2	42	2	3	16	11
20	EV	41	2	3	47	2	1	3	--
16	EV	57	3	3	38	--	--	--	--
12	EV	77	--	--	23	--	--	--	--

BREAKDOWN OF 1,2-DIMETHOXYETHANE AS A FUNCTION OF  
ELECTRON ENERGY: %  $\Sigma$ 

M/E		90	75	60	59	58	45	43	31	29	15
E.E.											
70	EV	5	0.5	9	2	4	53	3	3	12	7
20	EV	7	2	11	2	8	61	1	2	5	--
16	EV	10	3	23	2	11	50	--	--	--	--
12	EV	21	--	40	--	24	15	--	--	--	--





BREAKDOWN OF 1,5-DIMETHOXPENTANE AS A FUNCTION OF ELECTRON ENERGY

%Σ

M/E	101	100	87	85	72	71	70	69	68	67	58	57	55	45	43	42	41	39	29
E.E.																			
70 EV	2	7	0.5	2	1	20	0.5	2	5	4	5	1	2	31	2	2	5	2	4
20 EV	2	12	0.5	3	2	30	1	2	9	5	6	2	1	19	1	1	1	1	---
16 EV	3	17	---	5	3	35	2	1	13	5	6	---	---	10	---	---	---	---	---
12 EV	5	42	---	7	---	27	---	---	19	---	---	---	---	---	---	---	---	---	---

BREAKDOWN OF 1,6-DIMETHOXYHEXANE AS A FUNCTION OF ELECTRON ENERGY

%  $\Sigma$

M/E 131 115 114 99 86 85 83 82 81 73 72 71 69 68 67 58 56 55 54 45 43 42 41 39 29

E.E.

70 EV 0.5 0.5 2 0.5 0.5 2 2 10 2 2 1 1 12 1 1 9 3 1 3 4 29 2 1 4 2 3

20 EV 0.5 1 3 1 1 4 2 17 2 2 1 16 1 2 13 4 2 2 5 16 1 0.5 1 --- ---

16 EV 1 1 4 1 2 6 3 25 3 3 1 17 2 2 15 5 --- 5 6 --- --- --- ---

12 EV --- 19 --- --- --- 81 --- --- --- --- --- --- --- --- --- ---



BREAKDOWN OF 1,1,4,4-TETRADEUTERIO-1,4-DIMETHOXYBUTANE AS A FUNCTION OF ELECTRON ENERGY

M/E 107 92 91 90 89 88 85 74 73 72 71 61 60 59 58 47 46 45 44 43 42 41 32 31 30 29 15

E.E.

70 EV 4 0.5 1 0.5 3 1 0.5 2 0.5 1 1 2 3 23 3 23 3 3 3 4 1 2 1 3 2 4 2  
 20 EV 7 1 1 0.5 6 1 1 4 1 1 1 3 4 32 4 16 2 2 2 3 1 1 1 -- 2 0.5 2 2  
 16 EV 10 2 1 1 9 1 1 5 2 1 2 4 5 35 5 10 1 2 2 2 -- -- -- -- -- -- --  
 12 EV 26 3 -- -- 20 -- -- 8 -- -- -- 5 4 24 5 5 -- -- -- -- -- -- -- -- --

BREAKDOWN OF 1,1,5,5-TETRADEUTERIO-1,5-DIMETHOXPENTANE AS A FUNCTION OF ELECTRON ENERGY

M/E 105 104 103 90 89 88 87 86 73 72 71 70 60 59 58 57 47 46 45 44 43 41 31 30 29 15

E.E.

70 EV 1 1 5 0.2 0.5 1 0.5 0.5 7 12 4 2 0.5 5 1 1 21 3 3 3 2 2 2 2 1  
 20 EV 3 4 13 1 2 2 2 1 15 26 8 4 -- 8 -- -- 12 -- -- -- -- -- -- -- --  
 16 EV 4 6 20 1 2 2 2 2 15 25 8 3 -- 6 -- -- 3 -- -- -- -- -- -- -- --  
 12 EV 3 9 39 -- 1 2 2 2 10 17 7 -- -- 3 -- -- -- -- -- -- -- -- --

BREAKDOWN OF 1-METHOXY,2-ETHOXYETHANE AS A FUNCTION OF ELECTRON ENERGY

% Σ

M/E	M/E	104	89	86	73	72	60	59	45	43	41	31	29	27	26	15
70 EV	E.E.	1	0.2	0.2	1	4	10	16	18	4	0.5	23	12	7	4	3
20 EV		1	--	--	1	8	18	25	14	2	7	18	4	--	--	--
16 EV		2	--	--	--	13	27	28	9	3	6	12	--	--	--	--
12 EV		6	--	4	--	30	51	11	--	--	--	--	--	--	--	--



BREAKDOWN OF 1-METHOXY, 4-ETHOXYBUTANE AS A FUNCTION OF ELECTRON ENERGY: % $\Sigma$

m/e 117 103 101 88 87 86 85 72 71 59 58 57 56 55 45 44 43 42 41 40 31 29 27 15

E.E.

70 EV 0.5 5 1 1 3 0.5 1 5 8 6 11 1 2 2 14 3 7 2 5 1 8 6 3 1

20 EV 1 9 1 1 3 1 1 9 14 8 16 1 3 2 9 3 6 1 3 1 5 1 0.5 --

16 EV 1 15 1 3 4 1 1 10 17 8 16 1 5 -- 6 2 5 -- 2 -- 2 1 -- --

182

12 EV 3 33 -- 6 4 -- -- 8 18 9 11 -- 5 -- -- -- -- -- -- -- --

16 EV MASS SPECTRA OF GEM-DIDEUTERIO-1-METHOXY, 4-ETHOXYBUTANES: % $\Sigma$

m/e 105 104 103 90 89 88 87 73 72 60 59 58 57 56 47 45 44 43 42 41

1,1-D<sub>2</sub> 20 -- 4 2 2 3 16 13 -- 23 9 -- -- 3 -- -- 3 -- --

2,2-D<sub>2</sub><sup>a</sup> 10 4 2 2 4 2 2 11 13 9 11 5 5 2 -- 5 2 5 3 2

<sup>a</sup> Only 80 atom % deuterium, as indicated by presence of m/e 104 (d<sub>1</sub>) and m/e 103 (d<sub>0</sub>).





B. Ion-molecule reactions of mass spectral fragments of bifunctional ethers studied by Ion Cyclotron Resonance Spectroscopy

As the pressure of a gas in the ICR is increased to above  $10^{-6}$  Torr., ions are observed that are the products of reactions between other ions and neutral molecules. Since an ion must reside in the ICR cell for about one millisecond in order to be observed, an ion-molecule reaction "product" is defined, in the ICR, as a product with a lifetime greater than a millisecond. The ionic products of reaction between a mass spectral fragment (primary ion) and a neutral are termed "secondary ions"; the products of reaction of a secondary with neutral are termed "tertiary ions." With the exception of the chemical ionization processes discussed in the previous section, further ion-molecule reactions of tertiary ions are not observed in the ICR under the conditions of our examinations, *ie.* in the pressure range from  $5 \times 10^{-7}$  to  $1 \times 10^{-3}$  Torr.

Bimolecular reactions are usually imagined to result from collisions between two particles ( a collision is defined as an interaction wherein two particles change the directions of their momenta). This is not always true for bimolecular ion-molecule reactions. Some processes, notably electron or proton transfer, appear to take place at long range and not to result in deflection of the participants from their paths of flight.<sup>66</sup> In any event, the collision or reaction process takes place on a much shorter time scale than the ICR can detect: collision cross sections do not exceed  $10^3 \text{ \AA}^2$ , and, at thermal velocities, a particle requires a mean time less than  $10^{-10}$  seconds to travel a distance of  $100 \text{ \AA}$ .

## ICR DOUBLE RESONANCE

One of the advantages of the ICR method of studying ion-molecule reactions is the double resonance technique. A double resonance experiment is performed as follows. At a fixed magnetic field, a given ion is monitored by its absorption of radio frequency power at the cyclotron frequency. While the intensity of this absorption is being monitored, the ions in the cell are irradiated with a second radio frequency, which is varied. As this frequency is swept, the ions in the cell come into and go out of resonance, ie. absorb RF power (this absorption of power from the second frequency is not monitored directly). Each time an ion absorbs power, it increases its translational energy from thermal energies to up to several electron volts, an increase of one or two orders of magnitude, depending on the amplitude and duration of the RF power absorption.

The experiment monitors a given product ion and selectively heats the possible precursors. If a precursor is heated, then the intensity of the monitored ion will be altered. This experiment has two immediately apparent purposes: (1) to identify the precursors of a given ion, and (2) to examine the behavior of an ion-molecule reaction as the ion is heated. Often, the heating of a precursor results in the diminution of the intensity of the product.

## EFFECTS OF ION ENERGY ON REACTIVITY

Stated another way, an increase of an ion's kinetic energy usually results in a decrease of its reactivity with neutrals. This is tantamount

to heating a chemical reaction and finding that it proceeds more slowly, and it is thus inferred that most ion-molecule reactions occur without an activation energy barrier.

This phenomenon is rationalized by considering that the ion and neutral experience an electrostatic attraction, the force between an ion and an induced dipole. The rate of reaction is related to the length of time the ion feels the presence of the neutral. The faster the ion moves, the shorter the duration of its contact with a neutral, and, hence, the smaller its probability of reaction.

Most ion-molecule reactions observed among the bifunctional ethers show negative peaks in double resonance spectra, as shown in the bottom of Figure 2 in the previous section. In this double resonance spectrum, the intensity of the  $[M+1]^+$  ion from  $\text{CH}_3\text{OCD}_2\text{CD}_2\text{OCH}_3$  ( $m/e$  95) was observed while possible precursors were irradiated with RF. Heating the ions at  $m/e$  60, 61, and 64 results in the diminution of the intensity of  $m/e$  95, and that is how those ions are identified as proton donors to  $\text{CH}_3\text{OCD}_2\text{CD}_2\text{OCH}_3$ .

Negative double resonance peaks are a general rule for exothermic ion-molecule reactions. Heating an ion, however, may stimulate endothermic processes, such as the collisionally induced decomposition of the ion if, through collision with a neutral molecule, translational energy is converted into vibrational energy. Such a reaction is observed upon heating the molecular ion of glyme: the decomposition to  $[\text{M}-\text{CH}_2\text{O}]^+$  may be collisionally induced and gives rise to a positive ICR double resonance peak when the  $[\text{M}-\text{CH}_2\text{O}]^+$  ion is observed.

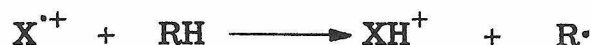
An exception to the general rule is seen when an exothermic reaction has two competing pathways. Heating a precursor will diminish the overall reaction, but may stimulate the less favored pathway at the expense of the more favored pathway. An example is found in the chemical ionization of  $\omega$ -methoxyethanol. The reaction to form  $[M+2-\text{CH}_3\text{OH}]^+$  ( $m/e$  46) shows normal, negative double resonance peaks upon heating the  $\text{CD}_5^+$  and  $\text{C}_2\text{D}_5^+$  ions. The reaction to form  $[M+2-\text{CH}_3\text{OD}]^+$  ( $m/e$  45) is not observed by ICR single resonance, but a double resonance examination of this ion shows positive peaks upon heating the  $\text{CD}_5^+$  and  $\text{C}_2\text{D}_5^+$  ions.

The favored pathway for chemical ionization of  $\omega$ -methoxyethanol is via the "football mechanism", described in the previous section, which yields exclusively loss of  $\text{CH}_3\text{OH}$  from the  $[M+2]^+$  ion. Other mechanisms, by which  $\text{CH}_3\text{OD}$  might be lost, have activation barriers. Whereas one mechanism is vastly favored over the others at thermal velocities of the precursor ions, heating the ions renders the other mechanisms more closely competitive.

### REACTION TYPES OBSERVED IN BIFUNCTIONAL ETHERS

The ion-molecule reaction processes observed to occur between bifunctional ethers and their mass spectral fragments fall into five general categories:

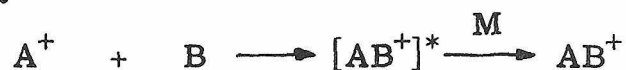
- (1) Atom abstraction



- (2) Proton transfer



## (3) Attachment



## (4) Attachment and rearrangement



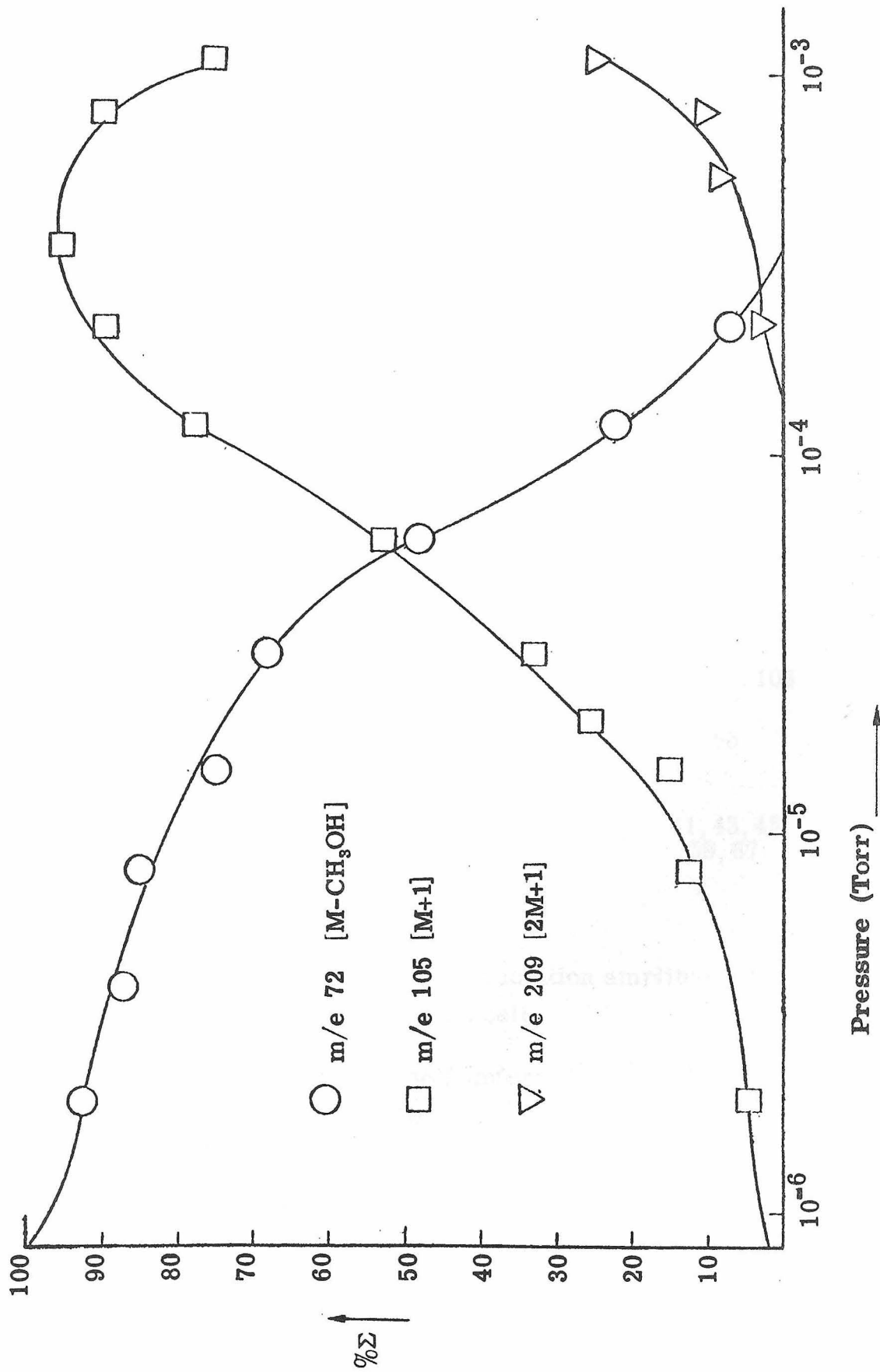
## (5) Hydride abstraction



A sixth category of reaction, charge transfer ( $A^+ + B \longrightarrow A + B^+$ ), was not observed.

Examples of the first category, atom abstraction, have been presented in the previous section in the reactions of molecular ions of ethers with parent neutrals. The only bifunctional ether studied in which molecular ion is observed is glyme (1,2-dimethoxyethane). This ion reacts with parent neutral to form an  $[M+1]^+$  ion. Such a reaction is usually depicted as an atom abstraction<sup>8</sup>, but, in light of our observations regarding the reaction of diethyl ether-d<sub>10</sub> with methyl ethyl ether, further experiments are needed to confirm this mechanism.

The second category of ion-molecule reactions, proton transfer, has also been exemplified in the previous section. With the exception of  $[CH_2=CHOCH_3]^{\cdot+}$  (m/e 58, the  $[M-CH_3OH]^{\cdot+}$  ion from glyme,  $[M-CH_3OH-C_2H_4]^{\cdot+}$  ion from 1,4-dimethoxybutane, etc.), all odd-electron species are observed to protonate the parent neutral. Proton transfer was investigated in the dimethoxyalkanes by examining the variation of ion abundances with increasing pressure of the neutral species at a constant electron energy. An ion abundance versus pressure curve for 1,3-dimethoxypropane at 12 eV is drawn in Figure 6.

FIGURE 6: ION ABUNDANCE VERSUS PRESSURE FOR  $\text{CH}_3\text{O}(\text{CH}_2)_8\text{OCH}_3$  AT 12 EV

Protonating species from the dimethoxyalkanes that were identified by ICR double resonance are listed in Table X.

TABLE X: ION-MOLECULE REACTIONS OF MASS SPECTRAL FRAGMENTS OF  $\text{CH}_3\text{O}(\text{CH}_2)_n\text{OCH}_3$  WITH PARENT NEUTRAL <sup>a</sup>

n	Electron Energy	Mass Spectral Ion Precursors to		
		$[\text{M}+1]^+$	$[\text{M}-1]^+$	$[\text{M}-\text{CH}_3\text{O}]^+$
1	70 eV	m/e --	29, 45	15, 29, 45 <sup>b</sup>
2	16 eV	m/e 60, 90	45, 58	45, 60
3	16 eV	m/e 42, 57, 72	45	45, 57
4	16 eV	m/e 58, 59, 71, 86, 88, 103	58, 86	45, 55, 56, 58, 103
5	20 eV	m/e 67, 68, 69, 71, 85, 100	45, 58, 68, 71	45, 68
6	70 eV	m/e 55, 67, 82, 114	45, 54, 58	41, 43, 45, 59, 67

<sup>a</sup> Determined by double resonance with irradiation amplitude of 12.5 mV into source region of the ICR cell.

<sup>b</sup> Role of m/e 45 as precursor to itself inferred from the isotope labelling experiment outlined below

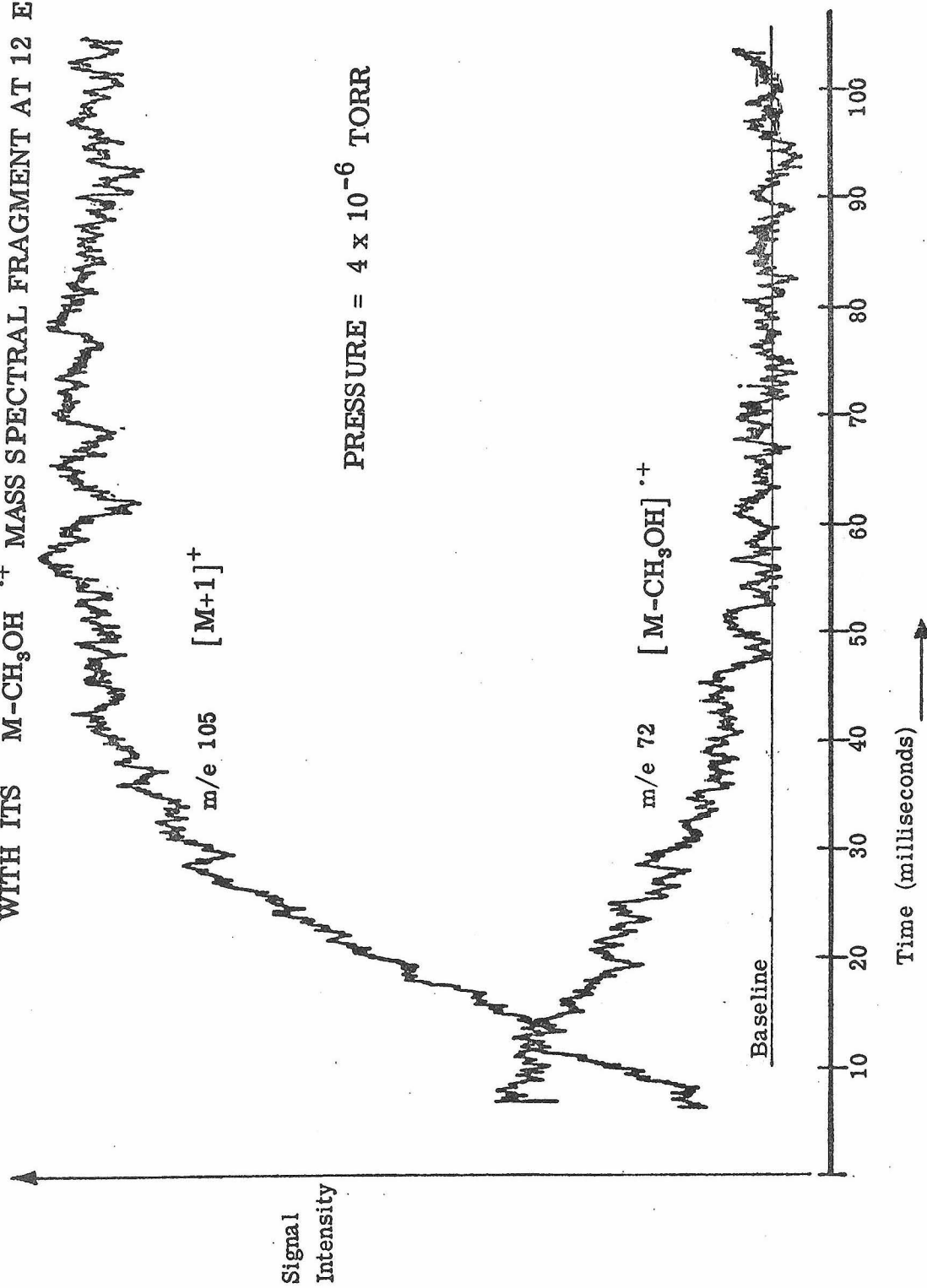
It is of interest to note that the  $[M-CH_3OD]^+$  ions from the tetradeuterio substituted dimethoxyalkanes are observed to transfer both protons and deuterons to the parent neutral. From the  $[M-CH_3OD]^+$  ion of  $CH_3OCD_2(CH_2)_2CD_2OCH_3$  at 12 eV, the ratio of proton transfer to deuteron transfer is about 3:2. From the  $[M-CH_3OD]^+$  ion of  $CH_3OCD_2(CH_2)_3CD_2OCH_3$  at 11 eV, the ratio of proton transfer to deuteron transfer is about 4:1.

#### RATE CONSTANTS FOR PROTON TRANSFER

The rate constant for protonation of 1,3-dimethoxypropane by its  $[M-CH_3OH]^+$  fragment was determined from the data in Figure 6 by an iterative method which calculates residence times of ions in the ICR cell and computes rate constants therefrom<sup>67</sup>. Based on absolute pressure measurements made with a capacitance manometer at pressures above  $10^{-5}$  Torr, the second order rate constant is calculated to be  $3.5 \pm 0.5 \times 10^{-10}$  cm<sup>3</sup>/molecule-second (the diffusion control limit in gas phase reactions of neutrals is on the order of  $1 \times 10^{-10}$  cm<sup>3</sup>/molecule-second<sup>68</sup>).

A determination of this rate constant by trapped-ion ICR<sup>22, 54</sup> methods at  $4 \times 10^{-6}$  Torr gives a value of  $3 \times 10^{-10}$  cm<sup>3</sup>/molecule-second. The trapped-ion method entails containment of the ions for a known length of time by placing appropriate electrical potentials on the plates of the ICR cell. After trapping for a known length of time, the ion abundances are measured. The rate constant was calculated from the disappearance of  $[M-CH_3OH]^+$  as a function of time. The abundance versus time curves plotted by the spectrometer for the  $[M-CH_3OH]^+$  and  $[M+1]^+$  ions are shown in Figure 7.

FIGURE 7: ICR TRAPPED ION SPECTRUM OF THE REACTION OF  $\text{CH}_3\text{O}(\text{CH}_2)_3\text{OCH}_3$   
WITH ITS  $\text{M}-\text{CH}_3\text{OH}^{+\cdot}$  MASS SPECTRAL FRAGMENT AT 12 EV



The rate constant for collision of  $\text{CH}_3\text{O}(\text{CH}_2)_n\text{OCH}_3$  with its  $[\text{M}-\text{CH}_2\text{OH}]^+$  fragment is calculated from the polarizability of the neutral (estimated as  $12 \text{ \AA}^3$  from the polarizability of dimethyl ether<sup>69</sup> and the polarizability of the C-C bond<sup>70</sup>) using the Langevin equation,  $k_L = 2\pi e (\alpha/\mu)^{\frac{1}{2}}$ , where  $e$  is the charge on the electron,  $\alpha$  the polarizability of the neutral, and  $\mu$  the reduced mass of the ion and neutral<sup>71</sup>. The calculated collision rate constant is  $1.2 \times 10^{-9} \text{ cm}^3/\text{molecule-second}$ . As no competitive reactions of any sort are observed at 12 eV, this indicates that only one collision in every 3 or 4 will result in proton transfer. By comparison, the calculated rate<sup>67</sup> of proton transfer from the  $[\text{M}-\text{CH}_2\text{O}]^+$  ion from glyme to the parent neutral is greater than  $10^{-9}$ , indicating that this proton transfer takes place on nearly every collision.

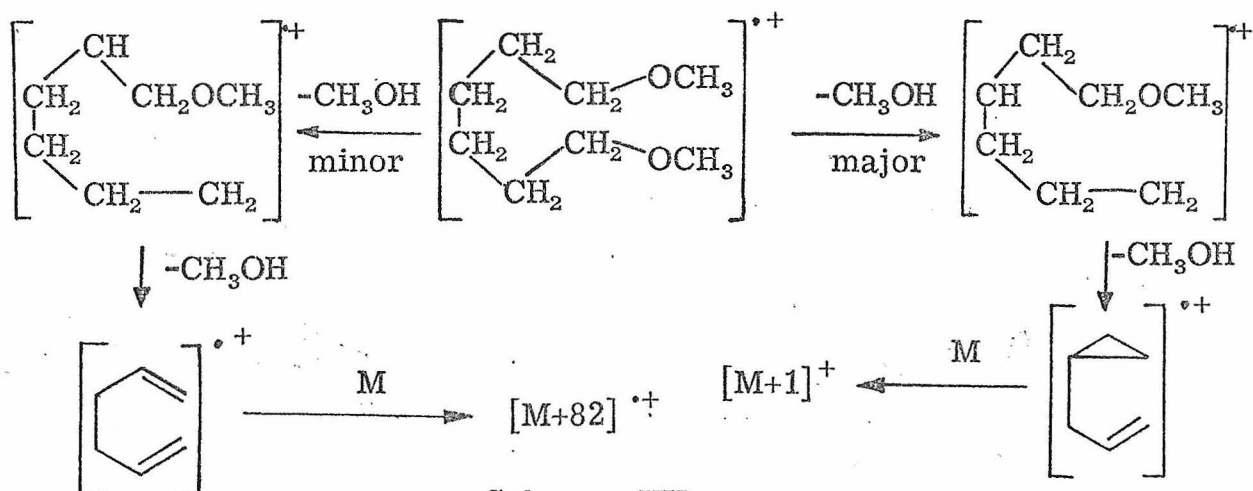
Tables of ion abundances versus pressure for  $\text{CH}_3\text{O}(\text{CH}_2)_n\text{OCH}_3$  ( $n = 3 - 6$ ) are listed at the end of this section. Ion abundance versus pressure curves for the cases  $n = 1$  and  $n = 2$  (methylal and glyme) are plotted in Figures 8 and 9.

### ATTACHMENT REACTIONS

The third reaction type, attachment of an ion to a neutral, will not be observed unless the vibrationally excited complex initially formed (lifetime less than  $10^{-3}$  seconds) is stabilized by collision with a third body (represented above as M). This reaction is observed extensively between  $[\text{M}+1]^+$  ions and their parent neutrals at higher pressures and will be discussed below. Only a few primary ions are sufficiently unreactive that attachment is a major

process. One such ion is  $C_4H_7O^+$  (  $m/e$  71 ) from 1,5-dimethoxy-pentane. Although this ion is seen to react with parent neutral to a small extent to yield  $[M+1]^+$  and  $[M-1]^+$  ions, the principal product of its reaction with neutral above  $1 \times 10^{-4}$  Torr is formation of an  $[M+71]^+$  ion (  $m/e$  203 ). On the basis of its reluctance to undergo other reactions, this ion is tentatively assigned the structure  $CH_3O^+=CHCH=CH_2$ , which is suggested as the most stable and least reactive isomer of  $C_4H_7O^+$ .

Attachment to parent neutral is seen as a minor reaction pathway for several mass spectral fragments of bifunctional ethers. The  $[M-2CH_3OH]^{\bullet+}$  ion of 1,6-dimethoxyhexane (  $m/e$  82 ) reacts primarily by proton transfer, but, at pressures greater than  $2 \times 10^{-4}$  Torr, the  $[M+82]^+$  attachment ion is seen. This behavior suggests the possibility of two  $C_6H_{10}$  isomers, one of which is a more vigorous proton donor than the other, depicted in Scheme XX. The  $CH_3OCH_2^+$  ion reacts by attachment with methylal and glyme; this will be discussed further below.



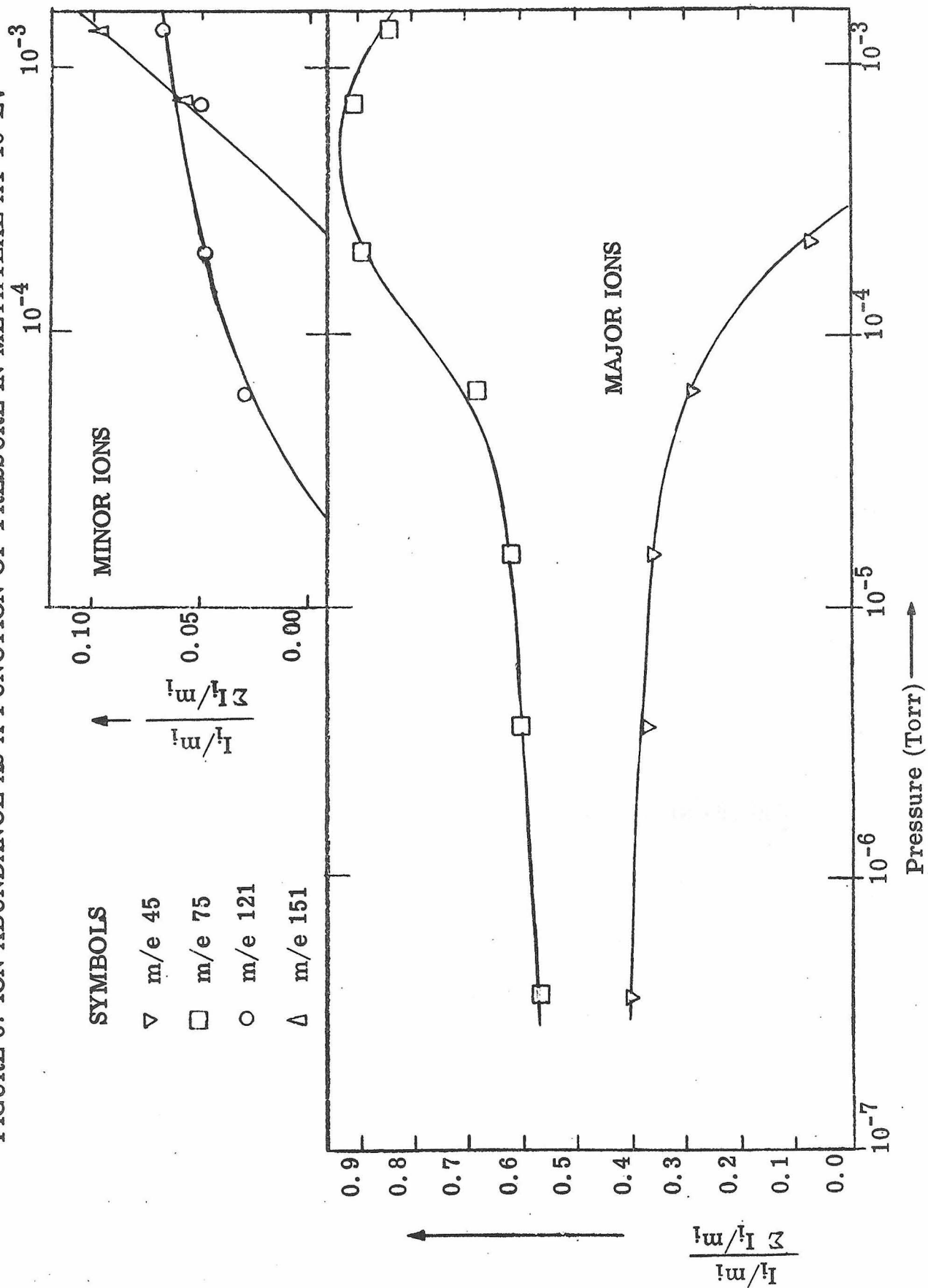
ATTACHMENT AND REARRANGEMENT REACTIONS;  
HYDRIDE ABSTRACTION

The most interesting ion-molecule reactions in bifunctional ethers turn out to be attachment and rearrangement processes. As the work below will show, this category subsumes the hydride abstractions. The intrinsic interest of these reactions is that the attachment process represents the reverse of a mass spectral fragmentation, while the rearrangement is the same as a mass spectral rearrangement. From the principles of rates of mass spectral processes (quasi-equilibrium theory) described in the previous section, it is seen that attachment and rearrangement offers a mechanism by which thermodynamic control may be exerted upon ion-molecule reactions. In order to characterize attachment and rearrangement reactions in bifunctional ethers, it is useful to examine the simplest cases, dimethoxymethane (methylal) and 1,2-dimethoxyethane (glyme).

ION-MOLECULE REACTIONS IN METHYLAL

A plot of ion abundance versus pressure for methylal is contained in Figure 8. At 16 eV, the two major primary ions are  ${}^+\text{CH}(\text{OCH}_3)_2$  ( $[\text{M}-1]^+$ ,  $m/e$  75) and  $\text{CH}_3\text{OCH}_2^+$  ( $[\text{M}-\text{CH}_3\text{O}]^+$ ,  $m/e$  45). The former ion undergoes two reactions: attachment, and attachment and rearrangement. The former process is manifested at pressures near  $10^{-3}$  Torr by the appearance of the  $[\text{M}+75]^+$  ion ( $m/e$  151). The latter reaction, which is seen in the pressure range  $10^{-4}$  to  $10^{-3}$  Torr, is attachment and loss of formaldehyde to yield  $\text{CH}_3\text{O}^+(\text{CH}_2\text{OCH}_3)_2$  ( $[\text{M}+\text{CH}_3\text{OCH}_2]^+$ ,  $m/e$  121), detected by

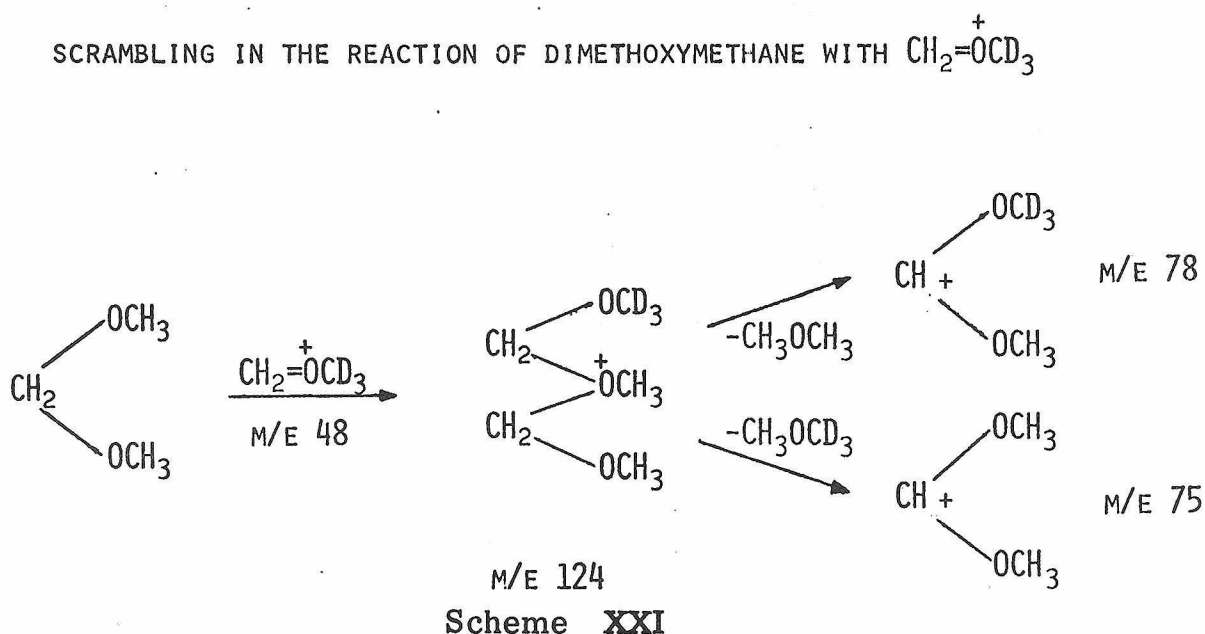
FIGURE 8: ION ABUNDANCE AS A FUNCTION OF PRESSURE IN METHYLAL AT 16 EV



double resonance. This ion is also produced by attachment of  $\text{CH}_3\text{OCH}_2^+$  to the parent neutral.

The reactions of  $\text{CH}_3\text{OCH}_2^+$  are more complex than Figure 8 would suggest. From the disappearance of  $\text{CH}_3\text{OCH}_2^+$  and the corresponding increase of  $[\text{M}-1]^+$  with increasing pressure, it appears that  $\text{CH}_3\text{OCH}_2^+$  reacts with neutral to form  $[\text{M}-1]^+$ . This is confirmed by double resonance, and the reaction is termed a hydride abstraction<sup>13</sup>.

The reaction of  $\text{CD}_3\text{OCH}_2^+$  (from 70 eV electron impact on  $\text{CD}_3\text{O}(\text{CH}_2)_3\text{OCD}_3$ ) with methylal yields an interesting result. The labelled methyl group shows up in about 50% of the product ion. This scrambling, depicted in Scheme XXI, implicates an attachment and rearrangement mechanism for the hydride abstraction which proceeds via loss of dimethyl ether from a symmetrical intermediate,  $\text{CH}_3\text{O}^+(\text{CH}_2\text{OCH}_3)_2$ .



We believe that this attachment and rearrangement mechanism is general not only for the reactions of  $\text{CH}_3\text{OCH}_2^+$  with ethers, but also for all hydride abstractions. In this manner, hydride abstractions may select the most stable carbonium ion as product: for example, the specific abstraction from the methylene of methyl ethyl ether by  $\text{CH}_3\text{OCH}_2^+$  is explained<sup>13</sup>. Loss of dimethyl ether from the attachment intermediate is identical to a mass spectral rearrangement, wherein thermodynamic considerations are important. Hydride abstractions by the  $[\text{CH}_2=\text{CHOCH}_3]^+$  ion also manifest selectivity. Deuteride abstraction from  $\text{CH}_3\text{OCD}_2(\text{CH}_2)_2\text{CD}_2\text{OCH}_3$  occurs 10 times more frequently than hydride abstraction.

The  $\text{CH}_3\text{OCH}_2^+$  ion exhibits a minor reaction pathway in methylal, transfer of a methyl cation. This reaction, which is presumed to result from attachment followed by loss of formaldehyde, is not directly observed at 16 eV. At  $8 \times 10^{-6}$  Torr with 70 eV electron impact, the  $[\text{M}+\text{CH}_3]^+$  ion (m/e 91) is found to occur. An ion ejection experiment indicates that the ratio of methyl cation transfer to hydride abstraction from  $\text{CH}_3\text{OCH}_2^+$  is 1:10.

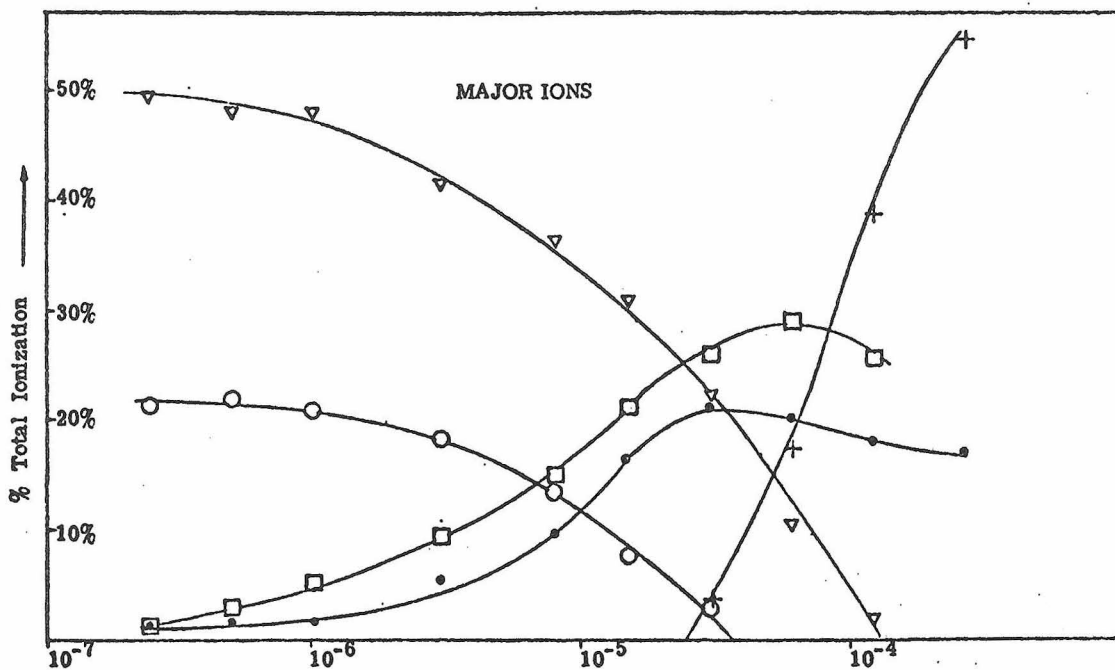
#### ION-MOLECULE REACTIONS IN GLYME AND OTHER DIMETHOXY-ALKANES

The  $\text{CH}_3\text{OCH}_2^+$  ion in glyme undergoes the same reactions with parent ion as described for methylal. Methyl cation transfer to form  $[\text{M}+\text{CH}_3]^+$  (m/e 105) is observed at 16 eV, and, at  $8 \times 10^{-6}$  Torr, the ratio of methyl cation transfer to hydride abstraction is 1:17. At pressures above  $10^{-5}$  Torr the ion resulting from attachment of  $\text{CH}_3\text{OCH}_2^+$  to neutral parent (m/e 135) is observed. This  $[\text{M}+45]^+$

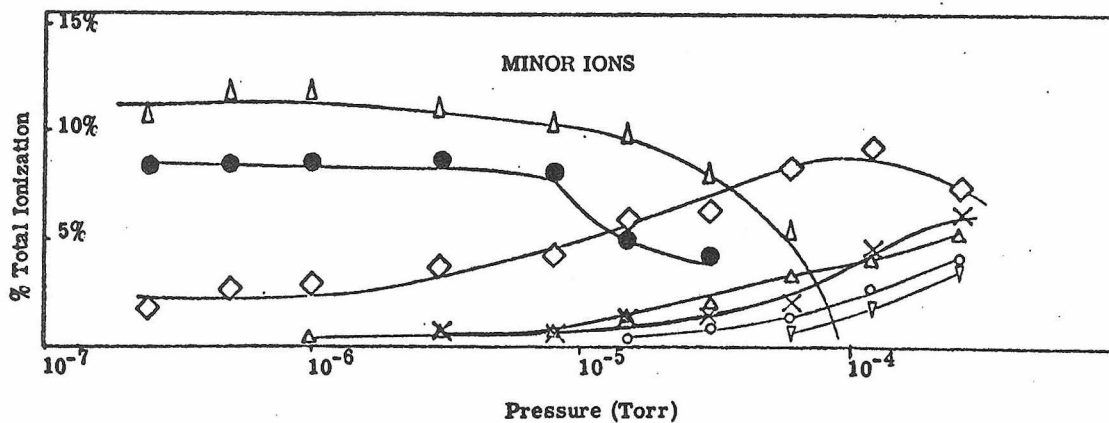
FIGURE 9

ION ABUNDANCE AS A FUNCTION OF PRESSURE FOR 1,2-DIMETHOXYETHANE  
AT 16 eV ELECTRON ENERGY

Symbols:  $\nabla$  m/e 45     $\circ$  m/e 60     $\bullet$  m/e 89     $\square$  m/e 91     $+$  m/e 181



$\Delta$  m/e 58     $\diamond$  m/e 59     $\times$  m/e 72     $\bullet$  m/e 90     $\triangle$  m/e 105     $\circ$  m/e 135     $\nabla$  m/e 149



ion is also formed by reaction of the molecular ion with parent neutral. Neither  $[M+CH_3]^+$  nor  $[M+CH_3OCH_2]^+$  ions are seen in the longer dimethoxyalkanes.

Another reaction of  $CH_3OCH_2^+$  with glyme (inferred to occur, as well, in methylal) is attachment followed by loss of methylal. This reaction gives rise to the  $[M-CH_3O]^+$  ion,  $m/e$  59. This reaction, seen to be minor in Figure 9, becomes very prominent in the longer chain dimethoxyalkanes. It is the major reaction of  $CH_3OCH_2^+$  with 1,5-dimethoxypentane and the only reaction of  $CH_3OCH_2^+$  with 1,4-dimethoxybutane. This behavior suggests an internal  $S_N2$  type mechanism for backside displacement of methylal from the attachment intermediate and implicates a favored 5 or 6-member cyclic transition state for the process depicted above in Scheme XIX, where the group Y is  $CH_3OCH_2^+$  rather than a deuteron. This explains why attachment ions are observed from methylal and glyme, for the backside displacement transition state is difficult to accomplish in these molecules. Note that a frontside interaction of the functional groups, as seen in the equilibrating ion in Scheme XVIII, cannot occur for the attachment complex of  $CH_3OCH_2^+$ .

Another ion,  $[CH_2=CHOCH_3]^+$ , makes its debut as a hydride abstractor; however, its contribution to the  $[M-1]^+$  ion of glyme is barely detectable by double resonance. This ion is the principal precursor (greater than 95%) to the  $[M-1]^+$  ion from 1,4-dimethoxybutane at 16 eV.

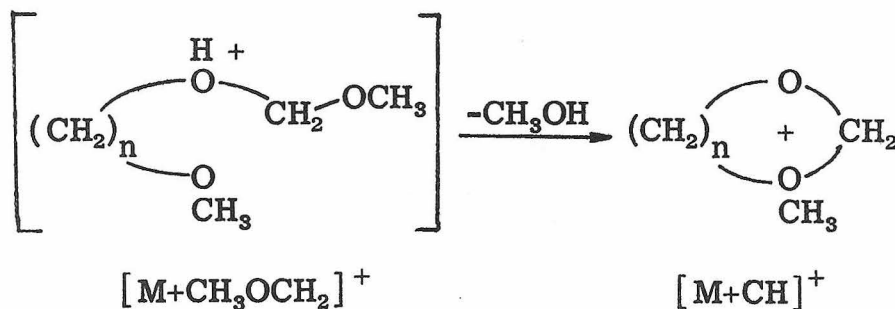
The protonation of glyme by its  $[M-CH_2O]^+$  ion ( $m/e$  60) has been described above. Interestingly, the  $[M+1]^+$  ion may lose methanol to form  $[M-CH_3O]^+$  ion, just as in a chemical ionization

experiment. Chemical ionization of a molecule by its mass spectral fragments is prominent in the longer chain dimethoxyalkanes.

$[M-CH_3O]^+$  ions arise from  $CH_3O(CH_2)_3OCH_3$  via exothermic protonation by its  $[M-CH_3-CH_3OH]^+$  ion,  $CH_3O(CH_2)_4OCH_3$  via its  $[M-CH_3]^+$  ion, and from  $CH_3O(CH_2)_5OCH_3$  via its  $[M-2CH_3OH]^+$  ion. In no case is loss of two molecules of methanol seen from the  $[M+1]^+$  ion produced when the parent neutral is chemically ionized by a mass spectral fragment.

### ION-MOLECULE REACTIONS IN OTHER BIFUNCTIONAL ETHERS

Ion-molecule reaction processes become quite complex in the  $\alpha$ -methoxy,  $\omega$ -ethoxyalkanes and  $\omega$ -methoxyalkanols. Only one reaction was studied in any detail, the reaction of  $CH_3OCH_2^+$  with the  $\omega$ -methoxyalkanols. This reaction consists of attachment followed by loss of methanol to leave an  $[M+CH]^+$  ion. When the reaction is run between any of the  $\omega$ -methoxyalkanols and  $CD_3OCH_2^+$ ,  $CD_3OH$  is lost from the attachment intermediate to leave the  $[M+CH]^+$  ion. This is consistent with several possible mechanisms, of which the most likely is depicted in Scheme XXII.

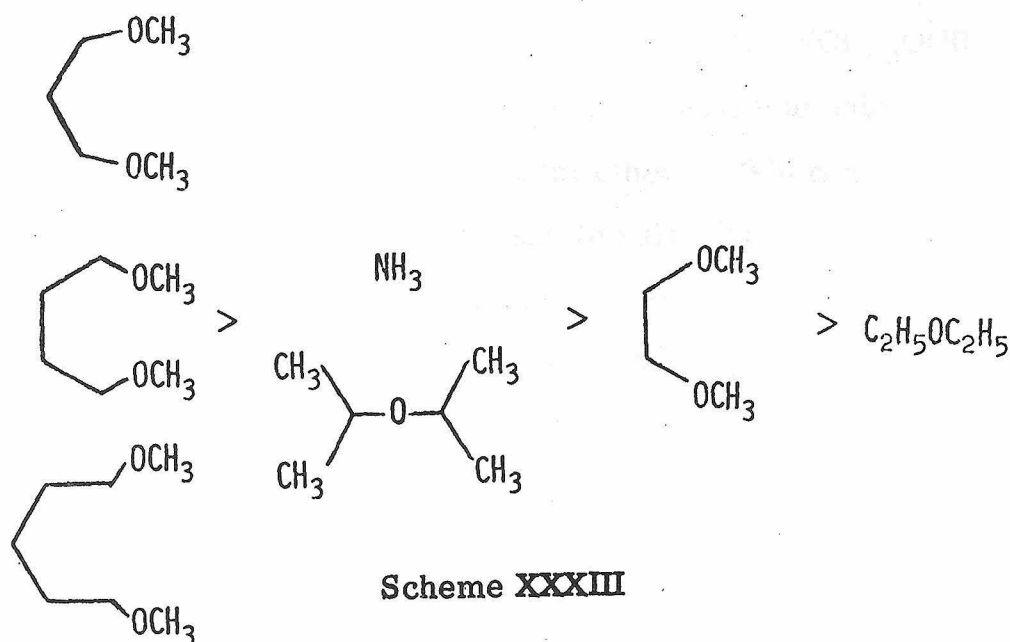


Scheme XXII

PROTON AFFINITIES OF BIFUNCTIONAL ETHERS

One consequence of the interaction of remote functional groups is the bidentate coordination of a proton, exemplified by the equilibrating ion in Scheme XVIII. It was anticipated that this interaction would lead to an increased proton affinity of the bifunctional ethers relative to monofunctional ethers. Proton affinities were determined in the ICR by trapped-ion equilibration of  $[M+1]^+$  ions with neutrals in mixtures of two ethers. This method of determination of proton affinities requires trapping of the ions for a sufficiently long time that equilibrium will be reached in a mixture of known proportions. A trapped-ion spectrum of a non-equilibrating system is pictured above in Figure 7.

RELATIVE GAS PHASE PROTON AFFINITIES OF BIFUNCTIONAL ETHERS



Unfortunately, it was found difficult to trap the  $[M+1]^+$  ions of the bifunctional ethers for the lengths of time required. Losses of ions from the trapping region of the ICR cell became very pronounced as trapping times exceeded 150 milliseconds. As a consequence, only the relative ordering indicated in Scheme XXXIII can be assigned with any certainty. The actual equilibrium constants determined are listed in Table XI. These results, albeit crude and uncertain, indicate that 1,4-dimethoxybutane has the greatest proton affinity among the bifunctional ethers studied. Since diisopropyl ether and ammonia have the same proton affinities, 207 Kcal<sup>20, 51</sup>, ammonia has been placed in Scheme XXXIII as a reference.

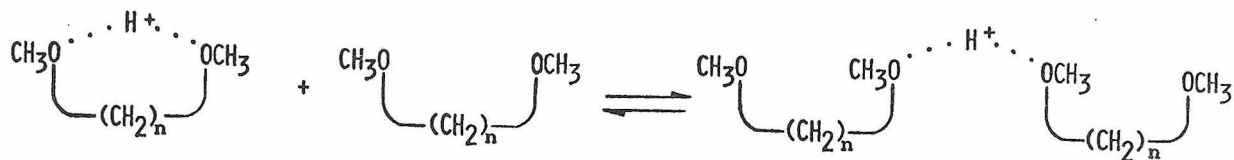
The basicity of 1,4-dimethoxybutane reflects the same preference for a 7-member cyclic system as inferred above for the chemical ionization of dimethoxyalkanes (Scheme XVI). This preference for a 7-member cycle has been noted in gas phase proton affinity studies of bifunctional amines, where the case  $n = 4$  for  $\text{NH}_2(\text{CH}_2)_n\text{NH}_2$  is inferred to be more basic than the cases  $n = 2, 3, 5, \text{ or } 6$ <sup>73</sup>.

The bidentate coordination of the proton by  $\text{CH}_3\text{O}(\text{CH}_2)_4\text{OCH}_3$  has been concluded from the NMR spectrum of a methylene chloride solution of the  $\text{HSbCl}_6$  salt of the bifunctional ether. Whereas the chemical shift of the acid proton in the monodentate salt  $[(\text{C}_2\text{H}_5)_2\text{OH}]^+\text{SbCl}_6^-$  is  $9.34\delta$ , the chemical shift of the acid proton in the bidentate salt  $[(\text{C}_2\text{H}_5)_2\text{OHO}(\text{C}_2\text{H}_5)_2]^+\text{SbCl}_6^-$  is  $16.42\delta$ . The chemical shift of the proton in  $[\text{CH}_3\text{O}(\text{CH}_2)_4\text{OCH}_3 \cdots \text{H}^+]\text{SbCl}_6^-$  is  $14.46\delta$ . The two methyl groups of the bis-diethyl ether salt are reported to have different chemical shifts. In the 1,4-dimethoxybutane salt, the  $\alpha$ -methylene

TABLE XI: EQUILIBRIUM CONSTANTS FOR PROTONATED PARENT IONS OF ETHERS

Ethers		Ratio	<sup>a</sup> K <sub>eq</sub> for		Trapping Time
A	B	A:B	AH <sup>+</sup> + B	BH <sup>+</sup> + A	(milliseconds)
(C <sub>2</sub> H <sub>5</sub> ) <sub>2</sub> O	CH <sub>3</sub> O(CH <sub>2</sub> ) <sub>2</sub> OCH <sub>3</sub>	4:1	12 ± 5		140
(C <sub>2</sub> H <sub>5</sub> ) <sub>2</sub> O	CH <sub>3</sub> O(CH <sub>2</sub> ) <sub>2</sub> OCH <sub>3</sub>	10:1	8 ± 2		150
CH <sub>3</sub> O(CH <sub>2</sub> ) <sub>2</sub> OCH <sub>3</sub>	((CH <sub>3</sub> ) <sub>2</sub> CH) <sub>2</sub> O	10:1	9 ± 2		190
CH <sub>3</sub> O(CH <sub>2</sub> ) <sub>2</sub> OCH <sub>3</sub>	((CH <sub>3</sub> ) <sub>2</sub> CH) <sub>2</sub> O	10:1	5 ± 3		325
CH <sub>3</sub> O(CH <sub>2</sub> ) <sub>2</sub> OCH <sub>3</sub>	CH <sub>3</sub> O(CH <sub>2</sub> ) <sub>3</sub> OCH <sub>2</sub>	11:1	14 ± 5		140
((CH <sub>3</sub> ) <sub>2</sub> CH) <sub>2</sub> O	CH <sub>3</sub> O(CH <sub>2</sub> ) <sub>3</sub> OCH <sub>3</sub>	10:1	1.5 ± 0.5		150
((CH <sub>3</sub> ) <sub>2</sub> CH) <sub>2</sub> O	CH <sub>3</sub> O(CH <sub>2</sub> ) <sub>3</sub> OCH <sub>3</sub> - d <sub>2</sub>	3:2	3 ± 1		100
((CH <sub>3</sub> ) <sub>2</sub> CH) <sub>2</sub> O	CH <sub>3</sub> O(CH <sub>2</sub> ) <sub>4</sub> OCH <sub>3</sub>	4:1	7 ± 3		170
CH <sub>3</sub> O(CH <sub>2</sub> ) <sub>3</sub> OCH <sub>3</sub>	CH <sub>3</sub> O(CH <sub>2</sub> ) <sub>4</sub> OCH <sub>3</sub>	3:1	3 ± 0.5		200
CH <sub>3</sub> O(CH <sub>2</sub> ) <sub>4</sub> OCH <sub>3</sub>	CH <sub>3</sub> O(CH <sub>2</sub> ) <sub>5</sub> OCH <sub>3</sub>	4:1	0.6 ± 0.5		200
CH <sub>3</sub> O(CH <sub>2</sub> ) <sub>4</sub> OCH <sub>3</sub>	CH <sub>3</sub> O(CH <sub>2</sub> ) <sub>5</sub> OCH <sub>3</sub>	4:3	0.3 ± 0.2		140
((CH <sub>3</sub> ) <sub>2</sub> CH) <sub>2</sub> O	CH <sub>3</sub> O(CH <sub>2</sub> ) <sub>5</sub> OCH <sub>3</sub>	1:1	4 ± 2		300

<sup>a</sup> Uncertainties are reported for the individual experiments; actual error is not known.



Scheme XXIV

protons and the methoxy methyl protons are superimposed in an un-resolvable multiplet, preventing determination of whether the proton is shared equally by the functional groups.<sup>74</sup>

### PROTON-BOUND DIMER FORMATION

A major reason for our diffidence of the data in Table XI is that equilibrium may not have been reached in the time spans used. It is plausible that, if an internal proton bridge is formed, the forward rate constant for equilibration between two bifunctional ethers may be less than  $10^{-11}$  cm<sup>3</sup>/molecule-second, too slow for equilibrium to be attainable in the present apparatus.

A different sort of experiment was performed to probe for intramolecular bidentate coordination of a proton. The competition between intramolecular and intermolecular proton bridge formation is illustrated in Figure XXIV. Internal bridging should shift the reaction to the left and, if it is strong enough, may inhibit it altogether. Proton-bound dimer formation is observed in monofunctional ethers, the  $\omega$ -methoxyalkanols ( $\text{CH}_3\text{O}(\text{CH}_2)_n\text{OH}$ ,  $n = 2-4$ ), and 1,4-dimethoxycyclohexanes. Decreasing amounts of proton-bound dimer formation are seen in the dimethoxyalkanes ( $\text{CH}_3\text{O}(\text{CH}_2)_n\text{OCH}_3$ ,  $n = 2-6$ ) as chain-length is increased, and none is seen in the cases  $n=5$  or 6. These results are described in Reference 15, reproduced on the next page.



The graph from Reference 15 is reproduced in Figure 10 with points added for cis and trans -1,4-dimethoxycyclohexane (identified by their mass spectra<sup>28</sup>). The trans compound is not readily protonated by its mass spectral fragments; consequently, the abundance of proton-bound dimer never becomes so great as in the other dimethoxyalkanes. Proton-bound dimer is observed at rather low pressures ( $8 \times 10^{-5}$  Torr,) but its abundance is not observed to increase greatly with increasing pressure, probably owing to the paucity of protonated parent ions.

The cis compound forms proton-bound dimer readily, but not so readily as glyme or a monofunctional ether. Although it is conceivable that a transannular proton bridge may occur in a boat conformation of this compound, it appears that such an interaction is minimal.

Inhibition of proton-bound dimer formation cannot be clearly ascribed to thermodynamic considerations alone. The attachment process is termolecular, as a third body collision is necessary to stabilize the attachment complex by carrying off excess energy. It is difficult to calculate the termolecular rate constant for such a process. It may be guessed, though, that, at sufficiently high pressures, the time between collisions is brief enough that the process may be treated as if it were bimolecular.

Having made such an assumption, we calculate a bimolecular rate constant of  $2.4 \times 10^{-12}$  cm<sup>3</sup>/molecule-second, with an uncertainty of  $\pm 10\%$ , in the pressure range  $2.2 \times 10^{-4}$  to  $8.0 \times 10^{-4}$  Torr. If the assumptions upon which this calculation is based hold true, then

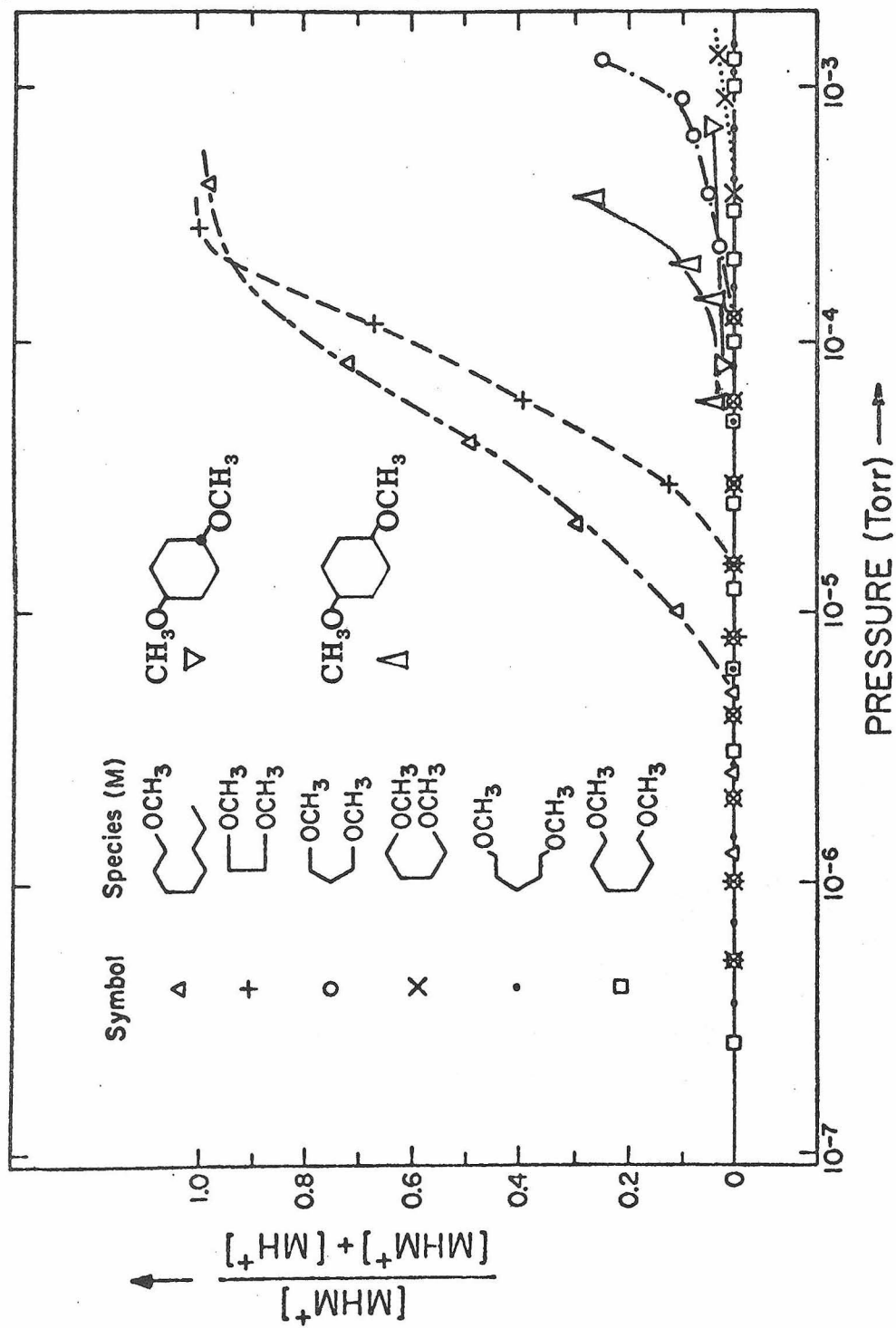


FIGURE 10: FRACTIONAL ABUNDANCE OF PROTON-BOUND DIMER AS A FUNCTION OF PRESSURE

it is possible that the creation of an internal proton bridge inhibits proton-bound dimer formation by slowing the rate.

ION ABUNDANCES IN 1,3-DIMETHOXYPROPANE AT 16 EV AS A  
FUNCTION OF PRESSURE: %  $\Sigma$

P (TORR)	42	45	57	71	72	73	103	105	175	177
$3 \times 10^{-7}$	7	14	16	7	51	3	--	1	--	--
$6 \times 10^{-7}$	7	11	15	8	53	3	0.5	2	--	--
$1.2 \times 10^{-6}$	6	11	14	8	54	3	1	3	--	--
$2.5 \times 10^{-6}$	6	10	13	8	52	5	2	6	--	--
$5 \times 10^{-6}$	4	8	10	8	48	6	3	12	--	--
$1 \times 10^{-5}$	3	7	7	8	45	7	4	19	--	--
$2 \times 10^{-5}$	1	4	4	8	36	7	6	29	--	--
$4 \times 10^{-5}$	--	3	2	9	28	7	5	41	3	3
$7 \times 10^{-5}$	--	--	--	11	14	5	6	55	5	5

ION ABUNDANCES IN 1,4-DIMETHOXYBUTANE AT 16 EV AS A  
FUNCTION OF PRESSURE: %  $\Sigma$

M/E	45	56	58	59	71	85	86	87	88	103	117	119	205	237
P (TO RR)														
$2.5 \times 10^{-7}$	13	3	50	4	6	--	10	--	--	15	--	--	--	--
$5 \times 10^{-7}$	11	2	44	3	7	2	10	1	1	17	1	--	--	--
$1 \times 10^{-6}$	11	2	41	3	7	2	10	2	1	16	2	2	--	--
$2 \times 10^{-6}$	10	3	40	3	6	2	9	3	2	13	5	4	--	--
$4 \times 10^{-6}$	8	2	34	3	6	3	7	6	1	13	9	6	--	--
$8 \times 10^{-6}$	7	1	29	3	6	3	6	9	1	9	14	11	--	--
$1.5 \times 10^{-5}$	6	2	22	2	5	4	5	12	2	6	19	16	--	--
$3 \times 10^{-5}$	4	--	14	3	5	4	4	15	2	3	24	23	--	--
$6 \times 10^{-5}$	1	--	5	2	4	6	--	20	--	1	29	31	--	--
$1.2 \times 10^{-4}$	--	--	2	--	--	7	--	18	--	--	36	35	--	--
$3.5 \times 10^{-4}$	--	--	--	--	--	--	--	18	--	--	41	41	--	--
$8 \times 10^{-4}$	--	--	--	--	--	--	--	12	--	--	42	43	2	1
$1.2 \times 10^{-3}$	--	--	--	--	--	--	--	13	--	--	42	41	3	1



ION ABUNDANCES IN 1,6-DIMETHOXYHEXANE AT 11 EV AS A  
FUNCTION OF PRESSURE: %  $\Sigma$

M/E	82	85	114	115	147	228
P (TORR)						
$2 \times 10^{-6}$	80	--	20	--	--	--
$4 \times 10^{-6}$	71	--	29	--	--	--
$8 \times 10^{-6}$	55	--	30	--	14	--
$1.5 \times 10^{-5}$	54	--	20	5	21	--
$3 \times 10^{-5}$	38	6	20	5	32	--
$6 \times 10^{-5}$	23	5	24	--	47	--
$1 \times 10^{-4}$	15	5	27	--	58	--
$2 \times 10^{-4}$	8	5	29	--	58	--
$3 \times 10^{-4}$	--	--	35	--	60	6
$8.5 \times 10^{-4}$	--	--	27	--	62	11

EXPERIMENTAL

A standard Varian V-5900 series ion cyclotron resonance mass spectrometer equipped with a dual inlet system was utilized in the studies reported herein. The instrumentation and experimental techniques associated with ion cyclotron resonance spectrometry have been described in detail.<sup>20</sup> All ICR experiments were performed at ambient temperature. Mass spectral intensities and product distributions were determined from single resonance peak intensities and double resonance techniques using previously described methods of analysis. Pressures in the ICR cell greater than  $10^{-5}$  Torr were measured using an MKS Baratron capacitance manometer. Reported lower pressures refer to calibrated ion gauge measurements.

Commercial dimethyl ether (Matheson), diethyl ether- $d_{10}$  (98 atom % D, Merck, Sharp, and Dohme), 1,2-dimethoxyethane (MCB), and methyl cellosolve (Pierce Chemical Co.) were used without further purification. All other ethers were prepared from the corresponding alcohols by conventional Williamson ether synthesis. The deuterium-labelled compounds utilized in the synthesis of the variously labelled bifunctional ethers included methyl- $d_3$  iodide (99 atom %D, Stohler Isotope Co.), lithium aluminum deuteride- $d_4$  (98 atom %D, Stohler Isotope Co.), methanol- $d_1$  (99 atom %D, Stohler Isotope Co.), and deuterium oxide (99.7 atom %D, Columbia Organic Chemical Corp.).

Deuterium substituted compounds. The  $\alpha, \alpha, \omega, \omega$ -tetradeuterio- $\alpha, \omega$ -alkanediols were prepared by reduction of the corresponding esters with lithium aluminum deuteride. 1,1-Dideuterio-3-ethoxypropanol was prepared from the methyl ester of 3-ethoxypropanoic acid. The acid was prepared by hydrochloric acid catalyzed hydrolysis of 3-ethoxypropionitrile (MCB) and esterified by reflux with methanol and a catalytic amount of sulfuric acid. The ester, purified by preparative vpc on a 7 ft. x  $\frac{1}{4}$  in. 8% FFAP (carbowax 20M-TPA), 60-80 mesh Chromosorb P column, was reduced with lithium aluminum deuteride suspended in dry tetrahydrofuran. The alcohol was characterized by conversion to the ether, 1,1-dideuterio-1-methoxy-3-ethoxypropane, by the procedure outlined below. The ether was purified by preparative vpc on the FFAP column and characterized by NMR ( $\text{CCl}_4$ ):  $\delta$  1.14 (3H, t, J = 7 Hz), 1.72 (2H, broadened triplet, J = 6.5 Hz), 3.25 (3H, s), 3.40 (2H, t, J = 6.5 Hz), 3.41 (2H, q, J = 7 Hz). The NMR and ICR mass spectra showed the ether to be greater than 98 atom %D in the 1 position.

2,2-dideuterio-1,3-propanediol. Diethyl-2,2-dideuterio-malonate was prepared from diethyl malonate by repetitive exchange with deuterium oxide in the presence of sodium acetate.<sup>75</sup> Initially, a 43 g. sample (0.25 mole) of diethyl malonate was refluxed overnight with 25 g. of 0.1 M sodium acetate in deuterium oxide. The upper organic layer was separated and dried over sodium sulfate. Two further treatments of the recovered diethyl malonate afforded 22 g. (0.12 mole) diethyl-2,2-dideuteriomalonate, 98 atom %D by NMR

(50% yield). The yield from this exchange was dissolved in 200 ml. ether (freshly distilled from lithium aluminum hydride) and added dropwise to a suspension of 12 g. lithium aluminum hydride in refluxing ether. After addition was complete, reflux was continued for 1 hour; the stirred solution was then cooled in an ice bath and quenched with a saturated solution of sodium sulfate in deuterium oxide. The suspension was filtered, dried over sodium sulfate, and the ether was removed under reduced pressure on a rotary evaporator to yield 4.0 g (0.05 mole, 40% yield) of 2,2-dideuterio-1,3-propanediol, which was characterized (greater than 98 atom %D) by the ICR mass spectrum of the corresponding dimethyl ether at 12 eV, one peak  $m/e$  74. No attempt was made to recover additional yield of diol from the residual aluminum salts.

Gem-dideuterio-1-methoxy,4-ethoxybutanes were prepared from 4-ethoxybutyric acid. The sodium salt of the acid was prepared from butyrolactone by the method of Fittig<sup>76</sup> and converted to the methyl ester.

The 1,1-dideuterio compound was prepared by reduction of the ester with lithium aluminum deuteride and conversion of the resulting alcohol to the methyl ether, 1,1-dideuterio-1-methoxy, 4-ethoxybutane. The ICR mass spectrum showed this compound to be  $> 98$  atom %D.

The 2,2-dideuterio compound was prepared by repetitive exchange of the ester in methanol- $d_1$  ca 1 M in sodium methoxide (prepared by dissolution of sodium metal in the methanol- $d_1$ ). The

exchange was monitored by NMR, but recovery was poor, and, after two exchanges, the material remaining was reduced to the alcohol with lithium aluminum hydride and converted to the methyl ether, 2,2-dideuterio-1-methoxy-4-ethoxybutane, 80atom %D by ICR.

Preparation of ethers. Ethers were prepared from the corresponding diols by reaction of the alcohol with sodium hydride in dry tetrahydrofuran followed by reflux with an alkyl halide. Sodium hydride was prepared from a 56% dispersion in mineral oil (Metal Hydrides, Inc.) by repeated washing with pentane under a stream of dry nitrogen followed by overnight drying in a vacuum desiccator at aspirator pressure.

In preparation of  $\omega$ -methoxyalkanols, 2 equivalents of diol was added to a stirred suspension of 1 equivalent of sodium hydride in dry tetrahydrofuran. The resulting suspension was refluxed for 1-2 hours, and cooled to ambient temperature. A two-fold excess of iodomethane was added and the suspension heated. Reaction was noted by the sudden refluxing of iodomethane. Following 1 hour further reflux, sodium iodide was precipitated from tetrahydrofuran solution by addition of two volumes of ether, the suspension filtered, and solvent removed under reduced pressure on a rotary evaporator. In preparation of  $\alpha$ -methoxy,  $\omega$ -ethoxyalkanes and of  $\alpha,\omega$ -dimethoxyalkanes, a similar procedure was followed using two equivalents of sodium hydride for each equivalent of alcohol. For preparation of the  $\alpha$ -methoxy,  $\omega$ -ethoxyalkanes, excess ethyl iodide was reacted with the sodium salt of the  $\omega$ -methoxyalkanol.

All synthesized compounds were purified by preparative vpc on a 10 ft. x  $\frac{1}{4}$  in. DEGS, 60-80 Chromosorb P column or on the FFAP column. The ICR mass spectra of deuterium labelled ethers prepared in the above manner showed isotopic purities to be greater than 98 atom %D, except where otherwise noted.

## REFERENCES

1. J. Priestley, *Phil. Trans. Roy. Soc.*, 75, 21 (1785); 78, 313 (1788).
2. H. Cavendish, *Phil. Trans. Roy. Soc.*, 75, 372 (1785); 78, 261 (1788).
3. E. Goldstein, *Akad. Berl. Sitzber.*, XXXIX, 691 (1886).
4. J. Stark, *Die Electricität in Gasen*, J. A. Barth, Leipzig, 1902, pp. 505-509.
5. W. Wien, *Wied. Ann.*, lxv, 445 (1898).
6. J. J. Thomson, *Phil. Mag.*, 13, 561 (1907).
7. J. J. Thomson, *Rays of Positive Electricity and their Application to Chemical Analyses*, Longmans Green, London, Second Edition, 1921.
8. K. Biemann, *Mass Spectrometry: Organic Chemical Applications*, McGraw-Hill, New York, 1962.
9. P. J. Ausloos, ed., *Ion-Molecule Reactions in the Gas Phase*, *Advances in Chemistry* No. 58, American Chemical Society, Washington, 1966.
10. E. E. Ferguson, F. C. Fehsenfeld, and A. L. Schmeltekopf, *Adv. Atom. Mol. Phys.*, 5, 1 (1969).
11. M. S. Foster and J. L. Beauchamp, unpublished results.
12. J. Diekman, J. K. MacLeod, C. Djerassi, and J. D. Baldeschwieler, *J. Amer. Chem. Soc.*, 91, 2069 (1969); G. Eadon, J. Diekman, C. Djerassi, *J. Amer. Chem. Soc.*, 91, 3987 (1969).

13. J. L. Beauchamp and R. C. Dunbar, *J. Amer. Chem. Soc.*, 92, 1477 (1970).
14. H. H. Jaffe and S. Billets, *J. Amer. Chem. Soc.*, 94, 674 (1972).
15. T. H. Morton and J. L. Beauchamp, *J. Amer. Chem. Soc.*, 94, 3671 (1972).
16. D. P. Ridge and J. L. Beauchamp, manuscript in preparation.
17. D. P. Ridge and J. L. Beauchamp, *J. Chem. Phys.*, 51, 470 (1969).
18. J. I. Brauman and L. K. Blair, *J. Amer. Chem. Soc.*, 90, 5636 (1968); 90, 6561 (1968); 91, 2126 (1969).
19. E. M. Arnett, et al., *J. Amer. Chem. Soc.*, 94, 4726 (1972); D. H. Aue, H. M. Webb, and M. T. Bowers, *J. Amer. Chem. Soc.*, 94, 4728 (1972).
20. J. L. Beauchamp, *Ann. Rev. Phys. Chem.*, 22, 527 (1971).
21. S. E. Buttrill, Jr., *J. Chem. Phys.*, 50, 4125 (1969); A. G. Marshall and S. E. Buttrill, Jr., *J. Chem. Phys.*, 52, 2752 (1970).
22. T. B. McMahon, R. J. Blint, D. P. Ridge, and J. L. Beauchamp, submitted for publication.
23. J. L. Beauchamp and M. C. Caserio, *J. Amer. Chem. Soc.*, 94, 2638 (1972).
24. H. Budzikiewicz, C. Djerassi, and D. H. Williams, Mass Spectrometry of Organic Compounds, Holden-Day, San Francisco, 1967.
25. F. W. McLafferty in A. L. Burlingame, ed., Topics in Organic Mass Spectrometry, *Adv. Anal. Chem.*, 8, Wiley, New York, 1970, p. 223.

26. M. Sheehan, R. J. Spangler, and C. Djerassi, *J. Org. Chem.*, 36, 3526 (1971), and references therein.
27. J. H. Bowie, R. Grigg, D. H. Williams, S.-O. Lawesson, G. Scholl, *Chem. Comm.*, 409 (1965); J. H. Bowie, R. Grigg, S.-O. Lawesson, P. Madsen, G. Scholl, and D. H. Williams, *J. Amer. Chem. Soc.*, 88, 1699 (1966).
28. J. Winkler and H.-F. Grutzmacher, *Org. Mass Spec.* 3, 295 (1970); 3, 1117 (1970); 3, 1139 (1970).
29. E. V. White, S. Tsuboyama, and J. A. McCloskey, *J. Amer. Chem. Soc.*, 93, 6340 (1971).
30. J. H. Bowie and P. Y. White, *Org. Mass Spec.*, 6, 317 (1972).
31. J. R. Dias and C. Djerassi, *Org. Mass Spec.*, 6, 385 (1972).
32. G. Horvath and J. Kuszmann, *Org. Mass Spec.*, 6, 447 (1972).
33. S. M. Schildcrout and C. G. Gebelein, *Org. Mass Spec.*, 6, 485 (1972).
34. F. Benoit and J. L. Holmes, *Org. Mass Spec.* 6, 541 (1972); 6, 549 (1972).
35. D. G. I. Kingston, "Functional Group Interactions in Mass Spectrometry," Paper # 77 presented before the Organic Section, 163rd National Meeting of the American Chemical Society, 12 April 1972.
36. R. Breslow and M. A. Winnik, *J. Amer. Chem. Soc.*, 91, 3083 (1969).
37. R. Breslow and S. Baldwin, *J. Amer. Chem. Soc.*, 92, 732 (1970).

38. S. Meyerson and L. C. Leitch, *J. Amer. Chem. Soc.*, 93, 2244 (1971).
39. M. M. Green, J. G. McGrew II, and J. M. Moldowan, *J. Amer. Chem. Soc.*, 93, 6700 (1971).
40. T. H. Morton and J. L. Beauchamp, "Interaction of remote functional groups; an ICR examination of the mass spectrometry and ion-molecule reactions of dialkoxyalkanes," Paper # 78, presented before the Organic Section, 163rd National Meeting of the American Chemical Society, 12 April 1972.
41. F. W. McLafferty, *Anal. Chem.* 29, 1782 (1957).
42. W. G. Dauben, J. H. Smith, and J. Saltiel, *J. Org. Chem.*, 34, 261 (1969).
43. G. W. Klein and V. F. Smith, Jr., *J. Org. Chem.*, 35, 52 (1970).
44. C. Djerassi and C. Fenselau, *J. Amer. Chem. Soc.*, 87, 5747 (1965).
45. J. K. MacLeod and C. Djerassi, *J. Amer. Chem. Soc.*, 88, 1840 (1966).
46. S. L. Bernasek and R. G. Cooks, *Org. Mass Spec.*, 3, 127 (1970).
47. H. M. Rosenstock and M. Krauss, "Quasi-Equilibrium Theory of Mass Spectra," in Mass Spectrometry of Organic Molecules, F. W. McLafferty, ed., Academic Press, New York (1963), pp. 1-64; D.H. Williams and R.G. Cooks, *Chem. Commun.* 663 (1968).
48. F. P. Lossing, private communication.
49. S. W. Benson, Thermochemical Kinetics, Wiley, New York, 1968.

50. F. H. Field and J. L. Franklin, Electron Impact Phenomena, Academic Press, New York, 1970.
51. J. L. Beauchamp, Ph.D. Thesis, Harvard University, 1967.
52. L. F. Loucks and K. J. Laidler, *Can. J. Chem.*, 45, 2785 (1967).
53. Instrument of the type described in J. Berkowitz and W. A. Chupka, *J. Chem. Phys.*, 45, 1287 (1966).
54. Spectra, courtesy of Dr. P. R. Le Breton, taken on joint Caltech-JPL Photoionization Mass Spectrometer.
55. M. L. Gross, *J. Amer. Chem. Soc.*, 94, 3744 (1972).
56. T. B. McMahon and J. L. Beauchamp, *Rev. Sci. Instr.*, 43, 509 (1972).
57. R. P. Clow and J. H. Futrell, *Int. J. Mass Spectrom. Ion Phys.*, 4, 165 (1970).
58. R. P. Clow and J. H. Futrell, *J. Amer. Chem. Soc.*, 94, 3748 (1972).
59. F. H. Field, J. L. Franklin, and M. S. B. Munson, *J. Amer. Chem. Soc.*, 85, 3575 (1963).
60. S. N. Vinogradov and R. H. Linnell, Hydrogen Bonding, Van Nostrand, New York, 1971, pp. 134-138.
61. 70 eV ionization cross section calculated from the expression  $Q_{\text{ethers}} = 1.2 (2.2 n_{\text{C}} + 0.3 n_{\text{H}} + 1.6 n_{\text{O}}) \text{Å}^2$ , where  $n_{\text{C}}$ ,  $n_{\text{H}}$ , and  $n_{\text{O}}$  are the number of carbon, hydrogen, and oxygen atoms, respectively. J. A. Beran and L. Kevan, *J. Phys. Chem.*, 73, 3866 (1969).

62. R.G. Azrak and E.B. Wilson, Jr., *J. Chem. Phys.*, 52, 5299 (1970).
63. J.K. Kim, M.C. Findlay, W.H. Henderson, and M.C. Caserio, "Ion Cyclotron Resonance Spectroscopy: Neighboring Group Effects in the Gas Phase Ionization of  $\beta$ -Substituted Alcohols", manuscript submitted for publication.
64. D.A. Sweigart and D.W. Turner, *J. Amer. Chem. Soc.*, 94, 5599 (1972).
65. S. Meyerson and J.D. McCollum, *Adv. Anal. Chem. and Inst.*, 2, 179 (1963).
66. M.T. Bowers and J.B. Laudenslager, *J. Chem. Phys.*, 56, 4711 (1972); M.T. Bowers, private communication.
67. A.G. Marshall and S.E. Buttrill, Jr., *J. Chem. Phys.*, 52, 2752 (1970); program courtesy of S.L. Patt and T.B. McMahon.
68. D.F. Eggers, Jr., N.W. Gregory, G.D. Halsey, Jr., and B.S. Rabinovitch, Physical Chemistry, Wiley, New York, 1964, p.429.
69. H.A. Stuart in Landolt-Bornstein, Zahlenwerten und Functionen, 6<sup>th</sup> Edition, Vol. I, Part 3, Springer-Verlag, Berlin, 1951, pp. 509-513.
70. J.O. Hirschfelder, C.F. Curtiss, and R.B. Bird, The Molecular Theory of Gases and Liquids, Wiley, New York, 1954, pp. 947-951.
71. G. Gioumousis and D.P. Stevenson, *J. Chem. Phys.*, 29, 294 (1958).
72. D. Holtz, J.L. Beauchamp, and J.R. Eyler, *J. Amer. Chem. Soc.*, 92, 7045 (1970).

73. D.H. Aue and M.T. Bowers, private communication.
74. F. Klages, J.E. Gordon, and H.A. Jung, Chem. Ber., 98  
3748 (1965).
75. M.J. Caserio, W.H. Graham, and J.D. Roberts, Tetrahedron,  
11, 171 (1960).
76. R. Fittig, Ann., 267, 186 (1891).